universität wien

DISSERTATION

Titel der Dissertation

„Natural Products as Scaffold for the Development of $GABA_A$ Receptor Ligands“

Verfasserin

Mag. pharm. Angela Johanna Schöffmann

angestrebter akademischer Grad

Doktorin der Naturwissenschaften (Dr. rer. nat.)

Wien, 2015

Studienkennzahl lt. Studienblatt:	A 791 449
Dissertationsgebiet lt. Studienblatt:	Pharmazie
Betreuer:	Univ.-Prof. Dr. Steffen Hering

Für meine Eltern.

„Man sieht nur mit dem Herzen klar.
Das Wesentliche ist für die Augen unsichtbar.“

Der Kleine Prinz, Antoine de Saint-Exupéry

In liebevoller Erinnerung an meine Großväter

Walter, Hermann

Danksagung

Ich bedanke mich bei Univ.-Prof. Dr. Steffen Hering für die Möglichkeit meine Dissertation am Department für Pharmakologie und Toxikologie der Universität Wien durchzuführen. Weiters gilt mein besonderer Dank dem österreichischen Fonds zur Förderung der wissenschaftlichen Forschung (FWF) für die finanzielle Ermöglichung meiner Studien. Darüber hinaus möchte ich mich vor allem bei folgenden KollegInnen bedanken: Laurin Wimmer (Technische Universität Wien) und Thomas Schwarz (vorm. Universität Wien) für die Synthese der untersuchten Piperinderivate; Marketa Bernaskova (Karl Franzens Universität Graz) für die Synthese der Honokiolderivate; Juliane Hintersteiner und Sophia Khom (Universität Wien) für die Durchführung und Auswertung der *in vivo* Experimente; Daria Goldmann (Universität Wien) für ihre Arbeit *in silico*.

Ich möchte mich bei allen meinen Weggefährten für ihre fortwährende Unterstützung, für die unzähligen unvergesslichen Momente und ihre Freundschaft bedanken, ohne die diese Arbeit nicht in der vorliegenden Form möglich gewesen wäre; dabei gilt mein besonderer Dank: Christina Rinne, Annette Hochhaus, Denise Luger, Barbara Strommer, Priyanka Saxena, Yvonne Kosch, Beata Gaisbauer, Peter Höflich, meinen Diplomandinnen Mihaela Coner und Verena Hiebl, Lisa Holler, sowie Andressa Gazola und Diana Rueda. Ich bedanke mich außerdem ganz besonders bei Xueyan Wang und Martin Schepelmann für ihre Freundschaft, ihre unermüdliche Unterstützung und Hilfe, und ihren guten Rat.

Allen voran und von ganzem Herzen danke ich jedoch den Menschen, die mich auf diesem langen und nicht immer leichten Weg begleitet und motiviert und mir stets den Rücken gestärkt haben: *Stefan, meinen Eltern, meinen Geschwistern und meiner Oma*. Ohne euch hätte ich es nicht geschafft.

Stockerau, 2015

Table of Contents

List of Figures

List of Tables

1 Abstract

In the course of this thesis, novel γ-aminobutyric acid type A ($GABA_A$) receptor modulators from plant origin belonging to different classes of secondary metabolites – alkaloids, stilbenoids, abietan diterpenes and (neo)lignans – were identified. In order to evaluate the potential medical use of these natural products and their derivatives, $GABA_A$ receptors of different subunit composition and transient receptor potential vanilloid type 1 (TRPV1) channels were expressed in *Xenopus laevis* oocytes and their interaction with these natural products or derivatives was studied by means of two-microelectrode voltage-clamp technique.

Derivatisation of piperine [1-[5-(1,3-Benzodioxol-5-yl)-1-oxo-2,4-pentadienyl]piperidine] and honokiol [2-(4-hydroxy-3-prop-2-enyl-phenyl)- 4-prop-2-enyl-phenol] led to the development of more potent, more efficacious and more selective $GABA_A$ receptor ligands. Structural modifications of piperine diminished interaction with TRPV1 channels and thereby prevented the heat and pain inducing effects of this natural product. **Piperine derivative 24** [(*2E,4E*)-5-(*1,3*-benzodioxol-5-yl))-*N,N*-diisopropyl-2,4-pentadienamide] inhibited capsaicin-induced activation of TRPV1 receptors (95 % reduction of current amplitude; IC_{50} = 39.3±3.0 µM), and modulated $GABA_A$ receptors more efficaciously and more potently than piperine ($\alpha_1\beta_2\gamma_{2S}$: E_{max} = 359±4 %; EC_{50} = 21.5±1.7 µM). **Piperine derivative 6** [(*2E,4E*)-*N,N*-dibutyl-5-(4-methoxyphenyl)penta-2,4-dienamide] displayed a higher efficacy than piperine ($\alpha_1\beta_2\gamma_{2S}$: E_{max} = 1363±57 %; EC_{50} = 7.5±1.0 µM) as well as $\beta_{2/3}$ $GABA_A$ receptor subunit selectivity, and also did not activate TRPV1 channels. **Batatasin III** ($\alpha_1\beta_2\gamma_{2S}$: E_{max} = 1513±177 %; EC_{50} = 52.5±17.0 µM), a dihydrostilbene derived from the orchid species *Pholidota chinensis*, and **dehydroabietic acid** ($\alpha_1\beta_2\gamma_{2S}$: E_{max} = 682±45 %; EC_{50} = 8.7±1.3 µM) found in *Olibanum*, were identified as novel $GABA_A$ receptor modulators. Seven **nitrogenated honokiol derivatives** (e.g. **5**: 3-acetamido-4'-ethoxy-3',5-dipropylbiphenyl-2-ol) were characterized as highly efficacious and potent $GABA_A$ receptor modulators (e.g. **5**, $\alpha_1\beta_2\gamma_{2S}$: E_{max} = 1975±218 %; EC_{50} = 2.1±1.2 µM) with partial agonist activity.

I conclude that these natural products and derivatives represent promising scaffolds for the development of novel $GABA_A$ receptor modulators for the treatment of anxiety disorders, epilepsy and various other disease states.

1.1 Zusammenfassung

Im Rahmen dieser Arbeit wurden neue, zu verschiedenen Klassen sekundärer Metabolite – Alkaloide, Stilbenoide, Diterpene und (Neo-)Lignane – zählende $GABA_A$ Rezeptormodulatoren pflanzlichen Ursprungs identifiziert. Die Effekte dieser Substanzen wurden an $GABA_A$ Rezeptoren unterschiedlicher Untereinheitenkomposition sowie *transient receptor potential vanilloid type 1* (TRPV1) Kanälen, die in Oozyten des *Xenopus laevis* exprimiert wurden, mittels Zwei-Mikroelektroden-Spannungsklemmtechnik untersucht.

Die Derivatisierung von Piperin und Honokiol ermöglichte die Entwicklung noch potenterer, effizienterer und stärker untereinheitenselektiver $GABA_A$ Rezeptormodulatoren. Die an Piperin vorgenommenen strukturellen Veränderungen hoben die Interaktion der Substanzen mit TRPV1 Kanälen auf und verhinderten so die schmerz- und wärmeinduzierenden Effekte dieses Naturstoffs.

Das **Piperinderivat 24** [(*2E,4E*)-5-(*1,3*-Benzodioxol-5-yl))-*N,N*-diisopropyl-2,4-pentadienamid] inhibierte die Capsaicin-induzierte Aktivierung von TRPV1 Kanälen (95%ige Reduktion der Stromamplitude; IC_{50} = 39.3±3.0 µM) und erwies sich als effizienterer und potenterer Modulator von $GABA_A$ Rezeptoren als Piperin ($\alpha_1\beta_2\gamma_{2S}$: E_{max} = 359±4 %; EC_{50} = 21.5±1.7 µM). Das **Piperinderivat 6** [(*2E,4E*)-*N,N*-Dibutyl-5-(4-methoxyphenyl)penta-2,4-dienamid] zeigte bessere Wirksamkeit im Vergleich zu Piperin ($\alpha_1\beta_2\gamma_{2S}$: E_{max} = 1363±57 %; EC_{50} = 7.5±1.0 µM) sowie $\beta_{2/3}$ $GABA_A$ Rezeptoruntereinheitenselektivität, ohne TRPV1 Kanäle zu aktivieren. **Batatasin III** ($\alpha_1\beta_2\gamma_{2S}$: E_{max} = 1513±177 %; EC_{50} = 52.5±17.0 µM), ein Dihydrostilben aus der Orchideenspezies *Pholidota chinensis*, und **Dehydroabietansäure** ($\alpha_1\beta_2\gamma_{2S}$: E_{max} = 682±45 %; EC_{50} = 8.7±1.3 µM), eine Komponente des Weihrauchs (*Olibanum*), wurden erstmalig als

$GABA_A$ Rezeptormodulatoren identifiziert. Sieben **Stickstoffderivate des Honokiols** wurden als hocheffiziente und potente $GABA_A$ Rezeptormodulatoren (z.B. **5**, 3-Acetamido-4'-ethoxy-3',5-dipropylbiphenyl-2-ol; $\alpha_1\beta_2\gamma_{2S}$ (E_{max} = 1975±218 %; EC_{50} = 2.1±1.2 µM) mit partiell agonistischer Wirkung identifiziert.

Abschließend bin ich der Überzeugung, dass diese Naturstoffe und Derivate interessante Modellsubstanzen für die Entwicklung neuartiger $GABA_A$ Rezeptormodulatoren zur Behandlung von Angststörungen, Epilepsie und anderen Krankheitsbildern darstellen.

2 Aims

General Aims

$GABA_A$ receptors are the target for many clinically important drugs such as benzodiazepines (BDZ), barbiturates, neuroactive steroids, anaesthetics, and other depressants of the central nervous system (CNS)[4]. Their use however, is accompanied by a number of adverse side effects. For instance, BDZ may cause daytime sedation, hangover, and ataxia, loss of motor coordination, memory and cognitive impairment, and development of tolerance[5]. A reduced number of side effects may be expected from ligands targeting a certain $GABA_A$ receptor subtype expressed in a restricted brain area[6]. The search for and the development of subtype-selective $GABA_A$ receptor modulators devoid of these side effects is, thus, an unmet medical need. Traditional folk medicines such as the Traditional Chinese Medicine (TCM) and other Asian or African folk medicines represent a plentiful source for the search for new $GABA_A$ receptor ligands.

In this work, I have studied constituents derived from four different plant families – *Piperaceae* (*Piper nigrum*), *Magnolidaceae* (*Magnolia officinalis*), *Orchidaceae* (*Pholidota chinensis*), and *Burseracea* (*Boswellia thurifera*) – and synthetic derivatives thereof for their effects on $GABA_A$ receptors of different subunit composition ($\alpha_{1\text{-}5}\beta_2\gamma_{2S}$, and $\alpha_1\beta_{2/3}\gamma_{2S}$), and – for piperine derivatives – for their effects on TRPV1 channels.

Specific Aims

In order to evaluate the potential medical use of these natural products and their derivatives, the following specific aims were defined:

1) To analyse the modulation of $GABA_A$ receptors by **piperine derivatives** and the effect of these derivatives on activation of TRPV1 channels. The following structural modifications of the parent molecule (**Figure 1**) were analysed:

a) **Systematic modifications of the amide nitrogen;**

b) **Rigidification of the linker**; and

c) **Modifications of the aromatic core**.

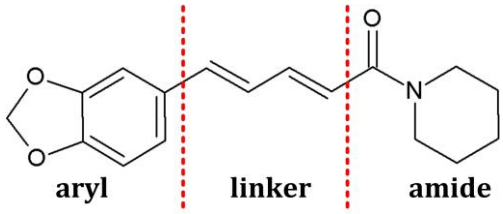

Figure 1 *Strucutral key features of the piperine molecule.*

2) To analyse the modulation of $GABA_A$ receptors by **honokiol derivatives**. The following structural modifications of the molecule (**Figure 2**) were analysed:

a) **Nitrogenation of the aromatic ring**, and

b) **Substitution of the free hydroxy groups.**

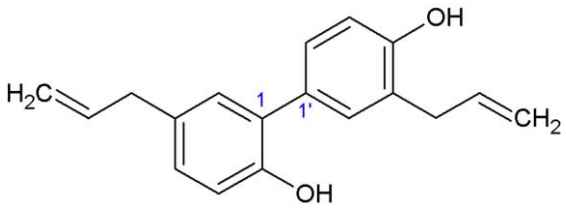

Figure 2 *Structure of honokiol.*

3) To identify **novel $GABA_A$ receptor modulators derived from plant sources.** A dicholoromethane extract of stems and roots of *Pholidota chinensis* and a petroleum ether extract of the resin of *Boswellia thurifera,* two plants being used in folk medicines and TCM[7] for their, amongst others, sedative properties, were investigated.

3 Introduction

3.1 The $GABA_A$ Receptor

$GABA_A$ receptors are assigned to the superfamily of Csy-loop pentameric ligand-gated ion channels (LGIC), which also includes nicotinic acetylcholine receptors, inhibitory glycine receptors, ionotropic serotonin (5-HT3) receptors and Zn^{2+} activated ion channels[8-13]. These four receptors differ in structure from two further members of the LGIC superfamily, the tetrameric glutamate receptors and the trimeric purine receptors[14-16]. The members of the superfamily share 30 % sequence homology, and show even greater similarity on the level of secondary and tertiary structures[10,17-21].

All mammalian $GABA_A$ receptors are anion-selective. Upon binding of γ-aminobutyric acid (GABA), they lead to an increased chloride (Cl^-) permeability of the membrane and thus hyperpolarisation. In general, the Cl^- membrane potential in most neurons is close to the membrane resting potential, while the intracellular Cl^- concentration ($[Cl^-]_i$) is much lower than the concentration in the extracellular liquid ($[Cl^-]_o$)[22]. However, especially in early development[23] conditions such as altered $GABA_A$ receptor expression and increased $[Cl^-]_i$ may occur. These conditions lead to a Cl^- equilibrium potential more negative than the membrane resting potential, where the binding of GABA can cause efflux of Cl^- rather than influx. This Cl^- efflux is possibly sufficient for membrane depolarisation, and thus the binding of GABA can paradoxically cause excitation. Apart from conducting Cl^-, $GABA_A$ receptors also are permeable for bicarbonate (HCO_3^-) ions[24].

3.1.1 γ-Aminobutyric Acid

The neutral amino acid GABA is the major inhibitory neurotransmitter in the CNS. GABA can be found in the pancreatic and muscle tissue in small amounts, while significant levels can be detected only in tissues of the nervous system[25]. *In vivo*, glucose is the principal precursor for the synthesis of GABA. In the *Krebs*

cycle, glucose is metabolised to α-ketoglutarate, which subsequently is transaminated to L-glutamic acid via the enzyme GABA α-oxoglutarate transaminase (GABA-T). GABA then is synthesised in a single step of decarboxylation from the major excitatory neurotransmitter, glutamate, by the enzyme glutamic acid decarboxylase (GAD). GABA is metabolised by GABA-T to succinic semialdehyde, which is oxidised to succinic acid. The GABA shunt is closed upon re-entry of succinic acid into the *Krebs cycle*[26] (**Figure 3**).

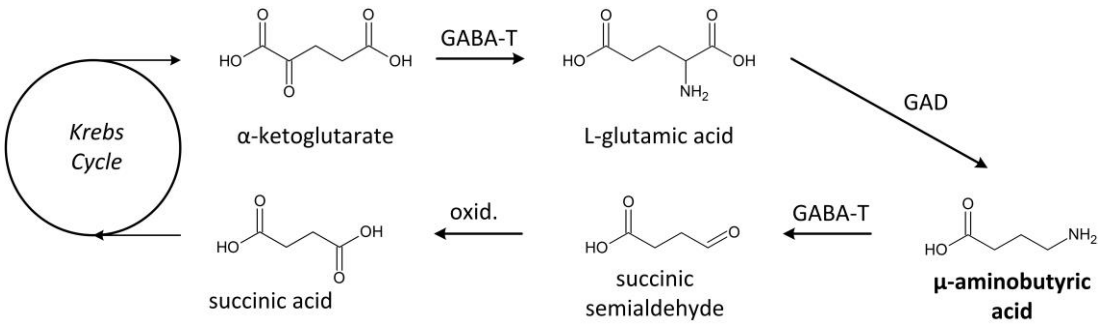

Figure 3 *The GABA shunt.*

GABA exerts its action via $GABA_A$ and γ-aminobutyric acid type B ($GABA_B$) receptors. $GABA_A$ receptors are the major inhibitory receptors in the CNS, and are pharmacologically characterised as being activated by muscimol, blocked by picrotoxin and bicuculline, and modulated by BDZ, barbiturates, and other CNS depressants[27,28]. $GABA_A$ receptors mediate rapid phasic inhibitory synaptic transmission and tonic inhibition, as they produce currents in extrasynaptic and perisynaptic locations[29-31]. In contrast, $GABA_B$ receptors are activated by baclofen, but insensitive to muscimol and bicuculline. $GABA_B$ receptors are metabotropic, G-protein ($G_{i/0}$) coupled 7-helix receptors, which connect to different effector systems. Upon binding of GABA, they activate inwardly rectifying K^+ channels or inhibit voltage-gated Ca^{2+} channels[32,33].

3.1.2 GABA and Benzodiazepine Binding Sites

The $GABA_A$ receptor provides two binding sites for the endogenous ligand GABA, which are located at the interface of its α and β subunits (**Figure 4**)[34-37]. The binding pockets are formed by six so-called "loops": loop A, B and C from the β+ ("principal") side, and "loops" D, E and F from the α- ("complementary") side[38]. These "loops" contain clusters of binding site residues: in the α_1 subunit Phe64, Arg66, Ser68 (loop D), and Arg119 and Ile120 (loop E)[34,37,39-41]; in the β_2 subunit Tyr157, Thr160 (loop B), and Thr202, Ser204, Tyr205, Arg207, and Ser209 (loop C)[35,42].

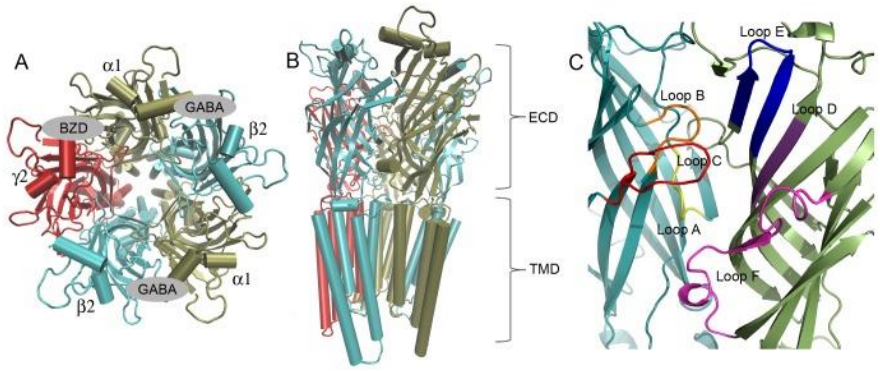

Figure 4 *GABA and benzodiazepine (BZD) binding sites at the $GABA_A$ receptor (top view)* ***(A)*** *and side view* ***(B)****. Loops contributing to the GABA binding pocket* ***(C)****. Adapted from Bergmann:* [43].

The benzodiazepine (BDZ) binding site is located on the interface of the α and γ subunit, and involves residues homologous to the agonist binding "loops" at the α/β interface: "loops" A, B and C from the α+ side, and "loops" D, E and F from the γ- side[38]. In all members of the superfamily (see below), these residues have been found to be homologous[10,21,40].

3.1.3 Subunits

Nineteen genes encoding for different subunits have been identified in the human genome. These comprise of 16 subunits assembling $GABA_A$ receptors (α_{1-6}, β_{1-3}, γ_{1-3}, δ, ε, θ, and π), including splice variants (e.g. γ_{2S} and γ_{2L},[44]), and three subunits (ρ_{1-3}) forming what has previously been called "$GABA_C$ receptor"[3,45]. "$GABA_C$ receptors" are homopentameric $GABA_A$ receptors formed exclusively of ρ subunits, and are closely related to $GABA_A$ receptors in

structure, function and sequence. Following the Nomenclature Committee of IUPHAR, they are now being referred to as $GABA_{A\rho}$ receptors[31,46,47]. Each receptor subunit consists of a large extracellular N-terminus, four membrane spanning domains (M1-M4) – of which domain M2 forms the lining of the central pore – and a comparably small extracellular C-terminus[10,17].

The existence of 19 subunits (**Figure 5**) theoretically allows more than 800 possible combinations[45]; however, so far there is conclusive evidence only for 11 functional $GABA_A$ receptors[31]. In the last decades of GABA research, great efforts have been made to identify native $GABA_A$ receptors by their regional and cellular distribution using immunohistochemistry and in situ hybridisation[48-51]. Immunocytochemical and electron microscopic studies[48,52-54] revealed that the majority of $GABA_A$ receptors is likely to consist of α, β and γ subunits, supporting the conclusion that the $\alpha_1\beta_2\gamma_2$ receptor subtype is the most abundantly expressed subunit combination in the brain[45,51].

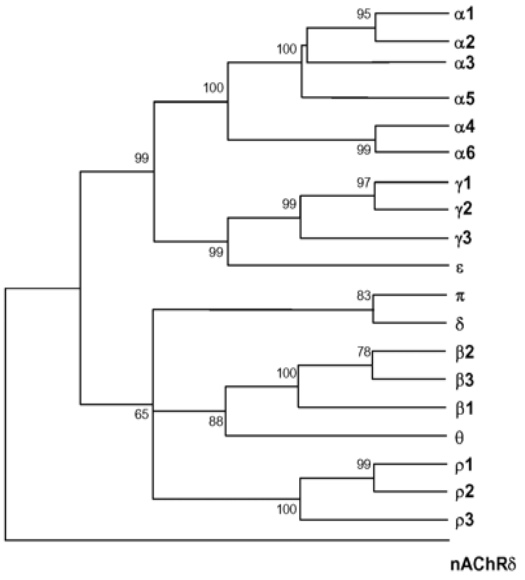

Figure 5 *Dendrogram showing the sequence identity of 19 genes encoding for $GABA_A$ receptor subunits. Greek letters show in total 8 homologous subunit families (α, β, γ, δ, ε, π, ρ, θ) which share >70 % sequence identity. The scale bar indicates 20 % sequence divergence. nAChRδ is given as distantly related outgroup marker. Adapted from Simon et al.[3].*

The α_1 subunit is the most prevalent of the α subunits, and is frequently co-localised with its chromosomal partners, β_2 and γ_2[55]. A knock-out of the α_1 subunit leads to a 50 % decrease in $GABA_A$ receptors in the mouse brain, and similar effects are observed upon β_2 knock-out[56]. In comparison, α_2 and α_3 subunits are of moderate abundance and α_5 is relatively rare, except in the hippocampus[51,55]. Amongst the β subunits, β_2 is predominantly expressed,

followed by β_3, while β_1 is rarely expressed. However, the identity of the β subunit often is difficult to determine since all three of them are likely to coprecipitate with α, γ or δ subunit specific antibodies[31]. There are three γ subunits, of which γ_2 is required for synaptic localisation of the receptor and which is usually associated with $\alpha_{1\text{-}3}$. However, due to the larger area of extrasynaptic membranes, the majority of γ_2 subunits can be found in extrasynaptic locations, again including the above mentioned α subunits plus $\alpha_{4\text{-}6}$. In contrast, combinations with δ or ε subunits are exclusively found in extrasynaptic locations. The "minor" subunits, i.e. δ, ε, ρ, π and θ, are generally thought to be able to replace the γ subunit in the pentamere, first and foremost the δ subunit[57]. The δ subunit seems to be located predominantly extrasynaptically/perisynaptically[58-60]. The ε subunit can substitute for γ or δ, while π and θ are only vaguely characterised in both localisation and function[55,61].

$GABA_A$ receptors can be subdivided into receptors sensitive for traditional BDZ site ligands, such as diazepam, and those insensitive to modulation by classical BDZ. Apart from the γ_2 subunit[62], the sensitive receptors contain one of the β subunits and $\alpha_{1/2/3/5}$[28]. Furthermore, these BDZ sensitive receptors can be sub-classified by their affinity for the BDZ quazepam and cinolazepam[63], non-BDZ such as the imidazopyridine zolpidem, and other compounds including the triazolopyridazine CL218-872, zaleplon, indiplon, and the β-carboline abecarnil[64]. Receptors incorporating α_4 or α_6 subunits, however, are insensitive to modulation by classical BDZ site ligands as well as zolpidem. Depending on the nature of the respective α subunit, BDZ sensitive $GABA_A$ receptors show significant sensitivity to ligands such as imidazobenzodiazepines (i.e. flumazenil, Ro15-4513 or bretazenil)[61].

The β subunit, even though it is necessary for the formation of functional receptors, does not greatly affect BDZ sensitivity[65]. The γ subunit, in contrast, does influence BDZ binding: Compared to γ_2 incorporating receptors, such containing either γ_1 or γ_3 subunits are less sensitive to BDZ or are modulated with altered selectivity[28,66].

Apart from influencing BDZ sensitivity, the existence of six α subunits plays a major role in the determination of the receptors' physiological functions. Barnard *et al.*[45] showed that some of these α subunit containing receptors can be distinguished using BDZ binding site ligands. Triazolopyridazine anxiolytics based on substance CL218-872 (L838,417; TPA003; or TPA023[67-69]) were shown to selectively affect the $\alpha_{2/3}$ receptors *in vitro*. Consequently, great efforts have been made to further study subtype selectivity for drugs *in vivo* using genetically engineered mice[68,70,71]: a histidine (H) to arginine (R) point mutation was introduced into $\alpha_{1/2/3/5}\beta\gamma$ receptors [α_1(H101R), α_2(H101R), α_3(H126R), α_5(H105R)], rendering each of these receptors insensitive to allosteric modulation by diazepam. In so doing drug induced behavioural responses in mutant and wild-type mice could be compared, leading to the identification of α subunit-specific effects of diazepam: the α_1 subunit mediates sedative, anterograde amnestic and partially the anticonvulsant effects of diazepam[72,73]; the α_2[74], and in case of high receptor occupancy the α_3 subunit[75-77], was found to be involved into anxiolysis; in addition, the α_3-selective drug TP003 indicated anxiolytic[75] and anticonvulsant[78] functions of the α_3 subunit. A knock-out of the α_5 subunit improved spatial memory[79]. A similar effect can also be observed by using an α_5 selective inverse agonist which enhances cognitive function[68,80]. In contrast, a point-mutated α_5 knock-in led to facilitated trace-fear-conditioning[70,81].

It has been thought that β subunits do not influence drug selectivity[65,82,83]. However, Cestari *et al.*[84], and Rudolph and Antkowiak[85], found that mutations in the M2 domain of the β subunit do influence subunit selectivity of pharmacological agents. Additional evidence came from studies on the non-BDZ loreclezole and chemically related agents, such as the general anaesthetic etomidate. Etomidate showed tendencies for β_2 and β_3 over β_1 subunit incorporating receptors[86,87], where the 15' amino acid residue (counting from the intracellular N-terminal end of the pore forming second helix) in the β_2 M2 domain was found to be of great influence. A point mutation of this asparagine to a serine (N265S) eliminated the receptors' etomidate sensitivity *in vitro* and abolished the compound's sedative-hypnotic action in the mouse knock-in

model[88]. In contrast, an asparagine to methionine (N265M) point mutation in the β_3 subunit abolished the immobilising effects of etomidate and suppressed the loss of the righting reflex, a typical characteristic of general anaesthetics[89]. Furthermore, this distinctive amino acid residue in the pore domain also influenced selectivity and sensitivity of other $GABA_A$ modulators, such as propofol, barbiturates and volatile anaesthetics[84,85], and may contribute to the formation of the binding pocket of these drugs[90,91]. Apart from etomidate and loreclezole, subunit selectivity has also been reported for valerenic acid[92], plant substances of polyacetylene structure[93], tracazolate and mefenamic acid[61,83], and ethanol[94], pointing at the β_3 subunit's importance in drug selectivity.

3.1.4 $GABA_A$ Receptors in Pathophysiology

A deficit in the GABAergic transmission has been shown to be linked to anxiety, epilepsy, schizophrenia and sleeping disorders which are described in brief in the following section.

Anxiety

Anxiety is causally linked to dysfunctions of the GABAergic system. Pharmacologically, this can be demonstrated by the fact that blocking $GABA_A$ receptors using pentylenetetrazole results in avoidance behaviour, anxiety and traumatic memories[95], whereas enhancement of the GABAergic transmission using BZD causes anxiolysis[5]. Thus, a defective GABAergic system plays a vital role in the arousal of anxiety. Apart from that, reduced levels of $GABA_A$ receptor expression could be detected in anxiety patients as well as in an animal model[96]. Since the γ_2 subunit anchors the $GABA_A$ receptor protein in the synapse, a reduction in γ_2 gene expression resulted in reduced levels of functional $GABA_A$ receptors in, amongst other regions, the cerebral cortex, hippocampus and amygdala, all of which are involved in the processing of fear[96]. In conclusion, a $GABA_A$ receptor deficit is a predisposition for anxiety disorders, whose symptoms in turn are a manifestation of an impaired GABAergic system[96-99].

Epilepsy

Both the GABAergic system and glutamatergic circuits, are clearly connected to different epileptic syndromes and the *status epilepticus*: the GABA system has to give an appropriate response to the glutamatergic circuits' excessive excitatory drive associated with these disease states[1]. During seizures, an imbalance in both pre- and postsynaptic GABAergic transmission can occur. Presynaptically, a decrease in GABA synthesis, an increase in GABA breakdown or a decrease in

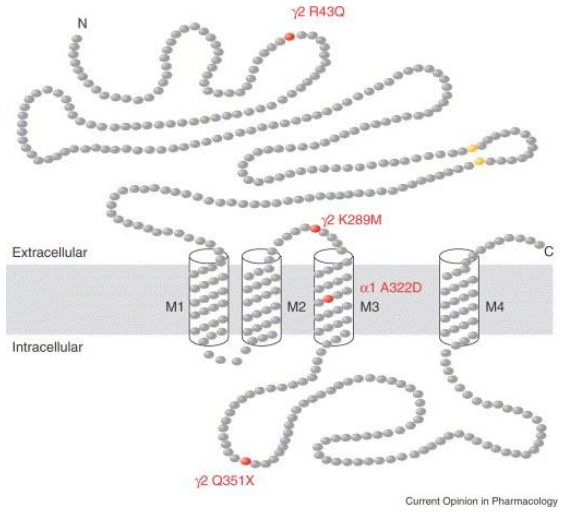

Figure 6 *Locations of four genetic mutations linked to epilepsy in a diagram of the putative membrane topology of the $GABA_A$ receptor. Reproduced with permission from Jones-Davis and McDonald[1].*

the amount of GABA released, reduced GABAergic firing and a decrease in the total number of GABAergic nerve terminals can be observed. Postsynaptically, alterations can include a decrease of total active $GABA_A$ receptors and structural as well as physical changes in the properties of the postsynaptic receptors[1].

Although most forms of epilepsy are idiopathic (only for approximately 1% of all cases an underlying genetic cause has been identified[100]), several studies could link disrupted GABAergic inhibition and seizure activity. Consequently, $GABA_A$ receptor agonists, i.e. compounds enhancing GABA-induced chloride currents (I_{GABA}), such as BDZ or barbiturates, act as potent anticonvulsant drugs[101], likewise drugs either reducing GABA reuptake (e.g. tiagabine), or drugs inhibiting GABA breakdown (e.g. vigabatrin[102]). In contrast, $GABA_A$ receptor blocking agents, such as bicuculline and picrotoxin, induce seizures[103].

Four mutations of GABA subunit genes involved in epilepsy have been identified (**Figure 6**). Baulac *et al.*[104] and Wallace *et al.*[105] identified the first two $GABA_A$ receptor subunit mutations involved in epilepsy: a K289M mutation in the

GABRG2 gene which encodes for the γ_2 subunit; and a R43Q mutation in the γ_{2L} subunit. However, the effects of these mutations have been disputed controversially (for review see Jones-Davis and McDonald[1]). Further research led to the identification of *(i)* a splice-donor site point mutation (IVS6 + 2T → G) resulting in a truncated γ_2 subunit protein; *(ii)* a Q351X mutation leading to a premature stop codon, the formation of non-functional $GABA_A$ receptors, trapping of the receptor protein in the endoplasmatic reticulum, and thus diminished surface expression[106]; and *(iii)* an A322D mutation in the GABRA1, which has been found to be involved in the development of juvenile myoclonic epilepsy[107].

Apart from that, the $GABA_A$ receptor is also involved in the development of the *Angelman Syndrom*, a disorder characterised by mental retardation, motor dysfunctions, sleeping disorders, and epilepsy. Studies in β_3 subunit knock-out mice revealed a disruption in the GABRB3 gene. This mutation could be linked to seizures and hypersensitivity, and to a lack of functional $GABA_A$ receptor formation[108].

Schizophrenia

Following the WHO's ICD-10 code system, section "mental and behavioural disorders", schizophrenia is characterised as "*fundamental and characteristic distortions of thinking and perception, and affects that are inappropriate or blunted*"[109]. Although intellectual capacity usually is maintained, the patient develops cognitive deficits in the course of the disease. Schizophrenia is characterised by psychopathological phenomena including thought echo, insertion or withdrawal; delusions of perception and control; passivity; hallucinatory voices; discussing the patient in the third person; and negative symptoms, such as anhedonia, apathy and affective flattening[110].

In the early 1970s, a connection between GABAergic deficits and schizophrenia has been proposed[111]. Alterations could be found in synaptic[112] and extrasynaptic $GABA_A$ receptors[113], as well as altered expression rates of several receptor subunits in the prefrontal cortex, including decreased levels of the δ

subunit[114] or elevated levels of the α_5[115,116] subunit. In addition, a lack in GAD67 expression[113] and decreased GABA levels[117] are implicated in the development of schizophrenia. Despite the evident involvement of $GABA_A$ receptors in this disease pattern, $GABA_A$ receptor agonists failed to be established as therapeutics for schizophrenia due to unwanted side effects, including sedation, dependence, amnesia, confusion, tolerance and memory deficits[113].

Sleeping Disorders

Sleeping disorders are subclassified into insomnia (primary and secondary), hypersomnia, parasomnias and other sleeping disorders, such as circadian rhythm disorders[118]. Insomnia can occur as single medical complaint or associated with other medical disorders, e.g. depression, anxiety or heart failure[119]. About 25 % of adults report sleeping difficulties, and 6–10 % meet the diagnostic criteria for an insomnia disorder[119].

Regular human sleep is divided into two states referred to as non-rapid eye movement (NREM) and rapid eye movement (REM) sleep. While NREM sleep is further divided into four phases, REM sleep classifies into a phasic and a tonic stage. NREM sleep accounts for 75–85 % of total sleep time, and is characterised by slow rolling eye movement, reduced muscle tone and electrocardiographic activity. REM sleep, in contrast, accounts for 20–25 % of total sleep time. Dreams arise during REM sleep[120]; thus it has formerly been called “dream sleep”.

The day-and-night rhythm is maintained by a master circadian clock, the suprachiasmatic nucleus (SCN)[121]. Within the SCN, GABA[122-125], its receptors[126-128], its enzymes[129-131] and transporters[132] can be found almost ubiquitously, rendering GABA a major determinant in the regulation of SCN neurons[121]. Besides GABA, histaminergic, serotonergic, melatoninergic and hypocretinergic (orexinergic) systems are involved in the control of sleep[133].

The sedative-hypnotic $GABA_A$ receptor modulators BDZ (e.g. diazepam, flunitrazepam, alprazolam, clonazepam and others), introduced in the 1960s, and the so-called “Z-drugs” (i.e. zolpidem, zaleplon, zopiclone and eszopiclone),

introduced in the 1980s, are the predominantly used drugs to treat sleeping disorders and insomnia[118,134]. Besides, various other drugs, including over-the-counter (OTC) medications, such as antihistamines (e.g. diphenhydramine, doxylamine succinate), melatonin and herbal preparations (e.g. valerian[132]), chronobiotic agents and also antidepressants with sedative effects (i.e. trazodone hydrochloride, mirtazapine, and tricyclic antidepressants, such as doxepin[135]) are used to treat sleeping disorders (reviewed in [119]).

3.1.5 $GABA_A$ Receptor Ligands

Benzodiazepines and Barbiturates

In 1955, Leo Henryk Sternbach (1908-2005) created the group of the so-called "benzodiazepines" by patenting the compound chlordiazepoxid, which was introduced to the market in 1960 under the name of Librium®. Shortly after, in 1963, the probably most famous BDZ, diazepam, was released named Valium® and thereafter became the most successful drug in pharmaceutical history[136]. The two compounds heralded four decades of innovating new BDZ, until by the 1990s more than 100 different BDZ containing preparations were marketed worldwide. Although they were classified as addictive and proved to have various undesired side effects, such as daytime sedation, hangover, ataxia, loss of motor coordination, memory and cognitive impairment and development of tolerance, the BDZ are still the most frequently prescribed class of drugs worldwide[5,136].

Barbiturates, such as pentobarbital, phenobarbital or secobarbital, also mediate sedative and hypnotic action via the $GABA_A$ receptor. They increase the average opening duration of the chloride conducting pore, while they do not influence opening frequency[27,137,138]. At concentrations beyond 50 mM barbiturates open the channel also in the absence of GABA, indicating at least two binding sites at the receptor protein[139,140].

Steroids

Steroids encompassing anaesthetic (alphaxalone) or sedative hypnotic, anxiolytic and anticonvulsant (3a-hydroxylated, 5α- or 5β-reduced metabolites of progesterone and deoxycorticosterone) properties modulate $GABA_A$ receptors at low concentrations between 30 – 300 nM[141,142]. At higher concentrations, like the barbiturates, they directly open the channel even in the absence of GABA[142,143]. In contrast to barbiturates, steroids active at $GABA_A$ receptors increase both frequency and duration of channel opening[144]. Compared to these GABA current enhancing steroids, pregnenolone sulphate and dehydroepiandrosterone sulphate (DHEAS) act as non-competitive antagonists at the receptor[142].

Divalent Cations

Divalent cations, such as Cd^{2+}, Ni^{2+}, Mn^{2+}, and Co^{2+}, but first and foremost Zn^{2+}, play a vital role in the regulation of $GABA_A$ receptors. These ions regulate multiple aspects in cellular biochemistry and membrane structure and have been found at considerable amounts in different tissues[28,145-147]. Zn^{2+} inhibits I_{GABA}, where the extent of inhibition seems to depend critically on the stage of neuronal development: embryonic and young postnatal neurons are more sensitive to Zn^{2+} compared to cells from adult mice[148,149]. While Zn^{2+} leaves single-channel conductance and mean open and shut times unaffected, it reduces the opening frequency of the $GABA_A$ receptor chloride channel[148].

General Anaesthetics

$GABA_A$ receptors are modulated by the structurally greatly diverse group of general anaesthetics, which include the volatile anaesthetics such as halothane, isoflurane, desfluran, sevofluran, enfluran, methoxyfluran and injection anaesthetics such as pentobarbital, propofol, nitrous oxide, ketamine, etomidate, alphaxalone, and ethanol[88,89,150-153]. At first, it was hypothesised that anaesthetics are non-selective agents acting via perturbation of the nerve cell's lipid bilayer[154]; however, later it has been found that membrane proteins, and

amongst them particularly ligand gated ion channels, are sensitive targets for modulation by anaesthetic agents[155]. Focussing on $GABA_A$ receptors, clinically relevant concentrations of all general anaesthetics strongly potentiate I_{GABA}, and, at higher concentrations, many of them even show GABA-mimetic effects[154,156-163]. The subunit composition of the $GABA_A$ receptor influences the allosteric effects of general anaesthetics, suggesting that the incorporated β subunit might play a vital role in anaesthetic binding to the receptor. For instance, it could be demonstrated that $\beta_{2/3}$-containing receptors are highly sensitive for etomidate, while β_1-incorporating receptors are only weakly affected[164].

Ethanol

Ethanol in particular has been demonstrated not to elicit its actions via perturbation of the lipid bilayer: evidence has been accumulating in still ongoing research for the involvement of LGIC as mediators of the effects of ethanol, with the $GABA_A$ receptor playing a central role. Apart from LGIC, ethanol interferes with voltage-gated calcium channels and alters the function of second-messenger proteins, such as protein kinase C[165] or cyclic adenosine 3',5'-monophosphate (cAMP) and the phosphoinositide (PI) pathway[166] (reviewed by M. Davies[167]). Ethanol is the most frequently abused drug worldwide, causing serious long-term effects including premature death and augmented proneness to serious illnesses, and causes the foetal alcohol syndrome (for review see[167]). It acts as CNS depressant of lower potency evoking disinhibition and euphoria at low concentrations; impairment of motor functions and speech; and at blood alcohol concentrations of 200 – 300 mg/dL sickness and stupor. At high concentrations ethanol causes coma and, above 500 mg/dL, respiratory failure and death[168]. Various studies have investigated the connection between different $GABA_A$ receptor subtype combinations and the effects of ethanol. The effects seem to be independent of the type of γ2-subunit (both γ_{2L} and γ_{2S}) and the receptor subtype being most sensitive to ethanol amongst every subtype tested so far proved to be the $\alpha_4\beta_1\delta$ $GABA_A$ receptor[169]. In 1997, Mihic *et al.* reported a putative binding site for ethanol on

the $GABA_A$ receptor, which involves TM2, TM3 and the extracellular loop between those domains[90].

3.2 TRP Channels

TRP channels were first discovered in a visually impaired mutant of the fruit fly *Drosophila melanogaster*. This mutant reacted to extended exposure to bright light with a transient influx of calcium ions instead of the sustained electro-retinogram recorded in the wild type[170]. This mutant was named transient receptor potential (trp) and, two decades later, in 1989, led to the identification of the trp gene[171]. Shortly after, the first homolog mammalian TRP channel was discovered[172,173].

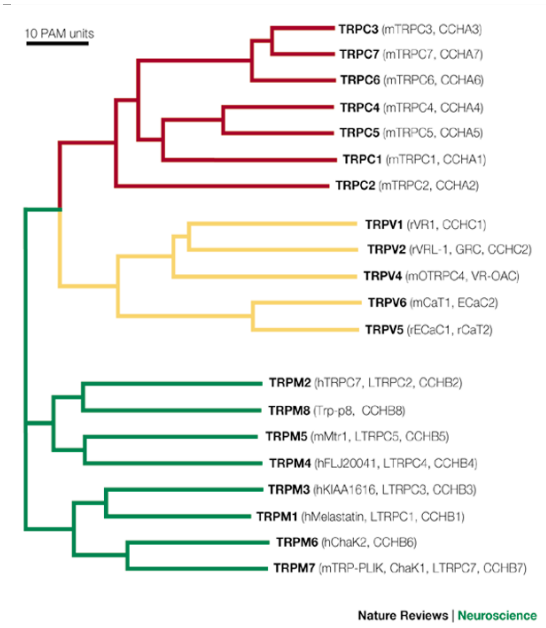

Figure 7 *Evolutionary tree of the TRP channel superfamily (Reproduced with permission from Clapham et al.[2]*

In total, the TRP channel superfamily comprises seven subfamilies: A (ankyrin, TRPA), C (canonic, TRPC1-7), L (mucolipin, TRPL), M (melastatin, TRPM), P (polycystin, TRPP), V (vanilloid, TRPV) and N (NO-mechano-potential-C like, TRPN)[2,174-177] (**Figure 7**). Apart from the TRPN family, the human genome comprises genes assigned to all TRP subfamilies, including 27 members in total[177]. Land plants, however, seem to have lost TRP channels after their divergence from the chlorophyte algae[178], and fungi only express a single subtype of TRP channels, TrpY1 (Yvc1, yeast vacuolar conductance)[179].

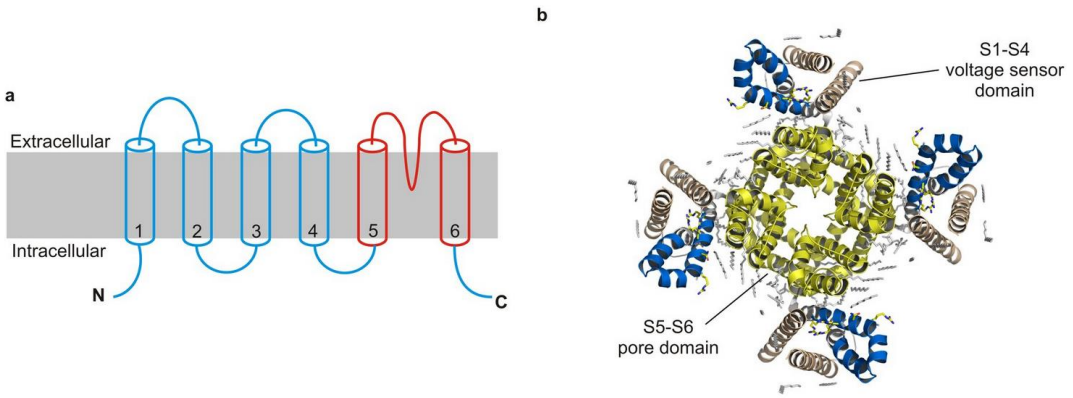

Figure 8 *Schematic representation of the transmembrane topology of TRP channel subunits (a) and crystal structure of the tetrameric assembly of the Kv1.2–Kv2.1 chimera viewed from the extracellular side (b). Modified from Kalia and Swartz [180].*

Due to the lack of X-ray crystallography data, the 3D structure of TRP channels is mostly based on *in silico* models and structure-function relationship studies. Most members form homotetramers as functional channels; however, heteromultimerisation is a commonly observed phenomenon[181]. TRP channels resemble voltage-dependent tetrameric potassium (K_V) channels in structure (**Figure 8**): each subunit consists of 6 transmembrane domains or segments (S1 – S6), where positively charged lysine and arginine residues in S4 and the S4-S5 linker are involved in voltage sensing. Amphipathic regions in domains S5 and S6 form the ion pore, and both N- and C-terminus are located intracellularly[177]. Distal to S6, the C-terminus (also called TRP domain) comprises a motif of 25 highly conserved amino acids, of which six are referred to as "TRP box". This motif, consisting of basic lysine and arginine residues[174], is thought to play a vital role in active channel formation[182].

Most TRP channels are non-selective cation channels[177] with low voltage dependence[182], and only a few are highly selective for Ca^{2+} [177]. Despite years of research, their mechanism of gating is still under discussion, and a number of theories have been established[174,183,184].

While TRPV1 is highly expressed in sensory neurons[185], where it mediates excitation followed by the typical desensitisation evoked by capsaicin and it's

even more potent analogue resiniferatoxin[186], only little is known about distribution patterns of TRP channels in general. TRPC channels, for instance, can be found more or less ubiquitously expressed[187]. Even though the varying distribution of the channels hampers the development of targeted substances, TRP channels compensate for this disadvantage by their low degree of homology[175], thus increasing chances to discover subtype selective ligands. This low degree of homology seems especially favourable with regard to the fact that activation or inhibition of TRP channels may have both beneficial and adverse effects depending on the targeted organ[188]. So far, this has challenged and stopped investigation and clinical development of first generation TRPV1 antagonists, as they were found to cause hyperthermia and elevation of the heat-pain-threshold in patients[189] (reviewed in Moran *et al.*[190]).

These difficulties aside, the members of the TRP family still appear as one of the most interesting future therapeutic targets. They act as cellular sensors involved in processes such as nociception[185], thermosensation[191], taste perception[192], and mechano and osmolarity sensing[193,194], and additionally play a vital role in signal transduction[175,195]. Consequently, their dysfunction results in various disease states including chronic pain, overactive bladder, obesity and diabetes[196,197], chronic cough and COPD, cardiac hypertrophy, Familial Alzheimer Disease, dermatological disorders, and also cancer[188]. TRPV1, in contrast, could so far not be linked to neuropathic pain[198], which this TRP family member has been associated with and which the whole TRP family is intensively studied for. So far, only some TRPV1 variants could be correlated with *modified* somatosensory function in neuropathic pain patients[198]. In other fields, research has been more successful, leading to six TRPV1 gene single nucleotide polymorphisms being linked to an increased risk of developing chronic cough[199]. Furthermore, both lack of activity and hyperactivity of TRP channels have pathogenic potential: while TRPC3 knock-out (-/-) mice show impaired motor coordination and walking behaviour[200], transgenic mice overexpressing cardiac TRPC6 developed massive cardiac hypertrophy[201]. All these discoveries highlight the importance of finding novel, TRP channel specific ligands.

Interestingly, despite years of intensive research, only few endogenous ligands of the TRP channel family could be identified up to now: diacylglycerol for TRPC channels[202]; the endocannabinoids anandamide (arachidonoyl ethanolamide) and palmitoylethanolamide, 12,15-(*S*)-hydroperoxy eicosatetraenoic acid and leukotriene B_4 for TRPV1[203,204]; 5´,6´-epoxieicosatrienoic acid for TRPV4[205]; and sphingosine for TRPM3[206]. In contrast, various natural products – including herbs and spices, venoms and toxins[207] – have been found to affect one or another subtype of the TRP channel superfamily (a comprehensive summary of ligands of different TRP channels can be found in Kaneko and Szallasi[188]). Temperature-sensitive TRP channels seem to be a preferred target for plant-derived chemicals, such as TRPV1 for capsaicin, derived from hot peppers[208]; resiniferatoxin, a compound of *Euphorbia resinifera*[209]; piperine, the hot compound of *Piper nigrum*[210]; or camphor, gained from *Cinnamomum camphora*[211]. Other plant substances include menthol (*Mentha piperita*) and eucalyptol (*Eucalyptus globulus*), which both directly activate the cold receptor TRPM8[212,213], or bisandrographolide (*Andrographis paniculata*), which activates TRPV4[214]. Apart from endogenous ligands and natural products, TRP channels can be modulated by a wide variety of chemical substances, which are useful pharmacological tools to study channel function: 2-aminoethyl diphenylborinate, for example, activates TRPV1-3[215,216], and icilin is used to activate TRPM8 and TRPA1[212,217]. More selectively activating compounds are e.g. olvanil for TRPV1[218], and 4α-phorbol-12,13-didecanoate (4α-PPD) for TRPV4[219].

3.2.1 The Vanilloid Receptor (TRPV1)

Of the described TRP channels, the vanilloid receptor TRPV1 deserves a more thorough introduction since piperine, the parent molecule of the piperine derivatives studied in this thesis, acts as TRPV1 antagonist, thereby causing heat sensation and pain[195]. In 1997, Caterina *et al.* identified a receptor responsible for the chili peppers' burning sensation in taste and named it capsaicin receptor[208]. TRPV1 – or capsaicin or vanilloid receptor – characterises a distinct subset of nociceptive neurons whose somata are located in dorsal root

and trigeminal ganglia. They are distinct from other nociceptive neurons by their unique sensitivity to capsaicin[186]. Initial capsaicin evoked excitation of these channels is followed by a lasting refractory phase, which is commonly referred to as "desensitisation". In this state, cells remain unresponsive to various incoming stimuli, for instance caused by heat[186]; thus, this effect of capsaicin suggests a substantial role of TRPV1 channels in pain sensation, and holds significant therapeutic potential[220]. Apart from the insights gained concerning the mechanism of vanilloid action, at present, the vanilloid ligand recognition site has not yet been conclusively identified. A first suggestion for its location was proposed by Humphrey H. Rang: he suggested the vanilloid binding site to be located intracellularly (Spring Pain Conference, Grand Cayman, BWI, 1998; reviewed in[186]). Since then, comprehensive research from other groups combining findings from capsaicin-insensitive mice, site-directed mutagenesis and the analysis of structural data suggested that residues found in the S4-S5 linker, as well as residues Y511 and S512 in S3 might be involved in capsaicin binding. These residues may stabilise capsaicin binding via hydrophobic and polar interactions[221,222]. Also, residues located in S4 (M547 and T550) have been proposed to be part of the vanilloid binding mechanism[222,223].

Apart from capsaicin, TRPV1 channels can be activated by different painful stimuli, such as noxious heat, other pungent compounds (e.g. venoms), and protons (i.e. acids)[183]. Additionally, Pingle *et al.* identified voltage, lipids and phosphorylation as activators of TRPV1 channels[224]. A deficiency in TRPV1 expression in mice resulted in reduction of thermal hyperalgesia in response to inflammatory mediators, such as bradykinin or neuronal growth factor[225-227]. In contrast to their wild type counterparts, TRPV1 knock out (-/-) mice did not display oleoylethanolamide induced visceral pain-related behaviour, which can also be inhibited by the TRPV1 antagonist capsazepine in wild type mice[228,229]. These observations could be reproduced by pharmacological blockade or knock-down of TRPV1: both approaches resulted in analgesic activity in numerous preclinical pain models, amongst others for arthritic[230,231] and cancer pain[232].

Based on capsaicin's capability to first activate and then desensitise TRPV1 channels, capsaicin-containing ointments have been used for decades to treat painful conditions, such as diabetic neuropathy[233], lumbago or muscle ache of different causes. Still, and despite their widespread acceptance and use, none of these preparations proved superior analgesic properties compared to placebo (reviewed by Szallasi and Sheta[234]). In contrast, resiniferatoxin led to long lasting pain relief and restored ambulation in dogs suffering from severe osteosarcoma pain when applied intrathecally[235,236]. This finding raises the hopes to develop an alternative treatment to narcotic analgesics for such pain conditions.

3.3 *Xenopus laevis* and Two-Microelectrode Voltage-Clamp (TEVC)

To study the effect of various GABAergic drugs and their potential effects on TRPV1 channels *Xenopus laevis* (*X. leavis*) oocytes were used in the course of this thesis. The wild African clawed frog, *X. laevis*, naturally inhabits ponds and dead river arms. Due to its resistant and easy-to-handle oocytes, *X. laevis* has been kept as laboratory animal for decades. In 1971, Gurdon *et al.*[237] discovered the frogs' oocytes as expression system for proteins. Microinjection of mRNA coding for the human protein globin resulted in the expression of the functional human protein[237]. Ten years later, the acetylcholine receptor could be expressed[238], and it was verified that protein expression could be obtained by both mRNA and cDNA injection[239]. In 1995, Marsal *et al*. found that not only mRNA or cDNA, but also injection of the mature protein results in functional plasma membrane proteins[240]. Ever since, *X. laevis* oocytes are an often-used functional expression system, first and foremost for studying plasma membrane proteins[241]. The major applications, which are structure-function studies of proteins, are extended by the possibility of investigating the influence of the introduction of unnatural amino acid residues, and the contribution to a better understanding of genetic diseases[241-243].

During *X. laevis* oogenesis, six stages (I-VI) of oocyte development occur simultaneously. The fully grown stages V and VI account for the major amount of oocytes in the ovaries[243], and they are the cells preferably used for electrophysiological studies[241]. The oocyte itself is divided into an animal (dark) and vegetal (light) pole, where the animal pole contains the nucleus. The cell is surrounded by cellular and non-cellular tissues, including the vitelline membrane, a non-cellular fibrous layer, and a layer of follicle cells, a tissue layer and an epithelial cell layer[241]. To collect oocytes for TEVC experiments, parts of the ovaries of anaesthetised female frogs were removed (**Figure 9, left**). The cells were defolliculated using collagenase, and consequently stage V – IV oocytes (**Figure 9, right**) were selected for injection with the respective cRNA (i.e. $GABA_A$ or TRPV1).

Figure 9 *Female X. laevis frog undergoing surgery for partial removal of ovaries (left). Stage V-IV oocytes which have been defolliculated using collagenase and selected for cRNA injection (right).*

After *X. laevis* oocytes had first been used to express ion channels and receptors[244,245], they became a popular expression system for ion channels, receptors and transporters[246]. The simplest approach to obtain whole-cell measurements of ion channels expressed in oocytes is the two-microelectrode voltage-clamp technique (TEVC)[247] (**Figure 10**).

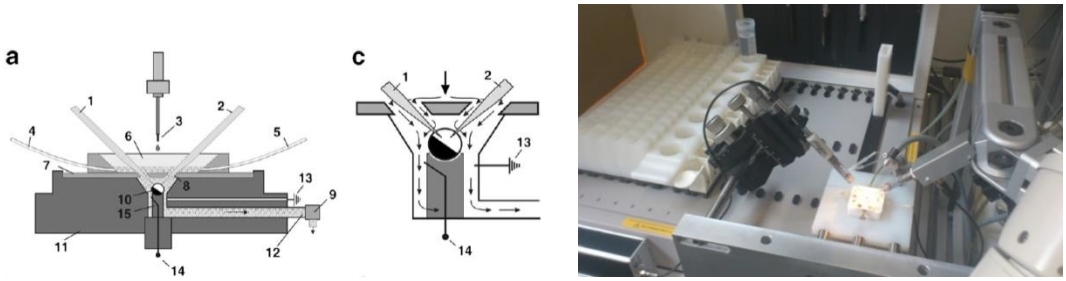

Figure 10 Left: *Schematic view of the two-microelectrode voltage-clamp and "fast perfusion" set up used for investigation of GABA and TRPV1 channels (modified with permission from Baburin et al. [248]).* ***Right****: Two-microelectrode voltage-clamp setup with automated probe application.*

The cell's membrane is penetrated with two microelectrodes for voltage sensing (voltage electrode) and for current injection (current electrode). The membrane potential, which is determined by the voltage electrode, is compared with a command voltage (holding potential); the difference between the actual voltage and the command voltage is set to zero by a control amplifier. Simultaneously, the injected current is monitored to measure total membrane current[246,249]. Opening or closing of the ion channel alters the transmembrane current and is immediately followed by a change in the current the amplifier detects. This change in current is equal in amplitude, but opposite in sign[249]. I_{GABA} and cationic currents through TRPV1 channels were measured at ambient room temperature (+20–22 °C) by means of the TEVC technique and were elicited at a holding potential of –70 mV.

The reader may refer to Schöffmann *et al.*[250] for a detailed description of materials and methods.

4 Results and Discussion

4.1 Piperine Derivatives as New $GABA_A$ Receptor Ligands

4.1.1 $GABA_A$ Receptor Modulation by Piperine and a non-TRPV1 activating Derivative

Biochem Pharmacol. 2013 Jun 15;85(12):1827-36. doi: 10.1016/j.bcp.2013.04.017. Epub 2013 Apr 25.

Sophia Khom[a], Barbara Strommer[a], Angela Schöffmann[a], Juliane Hintersteiner[a], Igor Baburin[a], Thomas Erker[b], Thomas Schwarz[b], Christoph Schwarzer[c], Janine Zaugg[d], Matthias Hamburger[d], Steffen Hering[a,*]

[a] Department of Pharmacology and Toxicology, University of Vienna, Althanstraße 14, A-1090 Wien, Austria

[b] Department of Medicinal Chemistry, University of Vienna, Althanstraße 14, A-1090 Wien, Austria

[c] Institute of Pharmacology, Innsbruck Medical University, Peter-Mayr-Str., A-6020 Innsbruck, Austria

[d] Institute of Pharmaceutical Biology, University of Basel, Klingelbergstrasse 50, CH-4056 Basel, Switzerland

Contribution Statement: *Measurement of SCT-66 (**24**) modulatory effect through $\alpha_1\beta_2\gamma_{2S}$ $GABA_A$ receptors and activation of TRPV1 channels, measurement of activation of TRPV1 channels by piperine, preparation of chemical structures and figures were my contributions to this work.*

Biochemical Pharmacology 85 (2013) 1827–1836

Contents lists available at SciVerse ScienceDirect

Biochemical Pharmacology

journal homepage: www.elsevier.com/locate/biochempharm

$GABA_A$ receptor modulation by piperine and a non-TRPV1 activating derivative

Sophia Khom [a,1], Barbara Strommer [a,1], Angela Schöffmann [a], Juliane Hintersteiner [a], Igor Baburin [a], Thomas Erker [b], Thomas Schwarz [b], Christoph Schwarzer [c], Janine Zaugg [d], Matthias Hamburger [d], Steffen Hering [a,*]

[a] Department of Pharmacology and Toxicology, University of Vienna, Althanstraße 14, A-1090 Wien, Austria
[b] Department of Medicinal Chemistry, University of Vienna, Althanstraße 14, A-1090 Wien, Austria
[c] Institute of Pharmacology, Innsbruck Medical University, Peter-Mayr-Str., A-6020 Innsbruck, Austria
[d] Institute of Pharmaceutical Biology, University of Basel, Klingelbergstrasse 50, CH-4056 Basel, Switzerland

ARTICLE INFO

Article history:
Received 28 January 2013
Accepted 17 April 2013
Available online 25 April 2013

Keywords:
$GABA_A$ receptors
TRPV1 channels
2-Microelectrode voltage clamp technique
Behavioural pharmacology
Piperine

ABSTRACT

The action of piperine (the pungent component of pepper) and its derivative SCT-66 ((2E,4E)-5-(1,3-benzodioxol-5-yl))-*N*,*N*-diisobutyl-2,4-pentadienamide) on different gamma-aminobutyric acid (GABA) type A ($GABA_A$) receptors, transient-receptor-potential-vanilloid-1 (TRPV1) receptors and behavioural effects were investigated.

$GABA_A$ receptor subtypes and TRPV1 receptors were expressed in *Xenopus laevis* oocytes. Modulation of GABA-induced chloride currents (I_{GABA}) by piperine and SCT-66 and activation of TRPV1 was studied using the two-microelectrode-voltage-clamp technique and fast perfusion. Their effects on explorative behaviour, thermoregulation and seizure threshold were analysed in mice. Piperine acted with similar potency on all $GABA_A$ receptor subtypes (EC_{50} range: 42.8 ± 7.6 μM ($\alpha_2\beta_2$)–59.6 ± 12.3 μM ($\alpha_3\beta_2$)). I_{GABA} modulation by piperine did not require the presence of a γ_{2S}-subunit, suggesting a binding site involving only α and β subunits. I_{GABA} activation was slightly more efficacious on receptors formed from $\beta_{2/3}$ subunits (maximal I_{GABA} stimulation through $\alpha_1\beta_3$ receptors: 332 ± 64% and $\alpha_1\beta_2$: 271 ± 36% vs. $\alpha_1\beta_1$: 171 ± 22%, $p < 0.05$) and α_3-subunits ($\alpha_3\beta_2$: 375 ± 51% vs. $\alpha_5\beta_2$:136 ± 22%, $p < 0.05$). Replacing the piperidine ring by a *N*,*N*-diisobutyl residue (SCT-66) prevents interactions with TRPV1 and simultaneously increases the potency and efficiency of $GABA_A$ receptor modulation. SCT-66 displayed greater efficacy on $GABA_A$ receptors than piperine, with different subunit-dependence. Both compounds induced anxiolytic, anticonvulsant effects and reduced locomotor activity; however, SCT-66 induced stronger anxiolysis without decreasing body temperature and without the proconvulsive effects of TRPV1 activation and thus may serve as a scaffold for the development of novel $GABA_A$ receptor modulators.

1. Introduction

Piperine (1-piperoylpiperidine) is the pungent component of several pepper species and activates transient receptor potential of the subfamily V member 1 (TRPV1) receptors [1,2]. We have recently shown that piperine modulates γ-aminobutyric acid (GABA) type A ($GABA_A$) receptors [3]. Via TRPV1-activation, piperine affects pain signalling and regulation of the body temperature [4,5], while $GABA_A$ receptor modulation is expected to induce fast inhibitory synaptic neurotransmission in the mammalian brain, resulting in, for example, anxiolysis, sedation, hypnosis, muscle relaxation, analgesia and anticonvulsant effects [6–11].

Piperine complies in all respects with Lipinski's "rule of five" and could therefore be a scaffold for the development of novel $GABA_A$ receptor modulators [3,12]. However, it is currently unknown whether piperine interacts preferentially with specific $GABA_A$ receptor subtypes. Moreover, simultaneous activation of TRPV1 receptors may cause unwanted side effects including changes in pain sensation and body temperature that would be an obstacle to its therapeutic use [5]. Here we analyse the action of piperine and its derivative SCT-66 ((2E,4E)-5-(1,3-benzodioxol-5-yl))-*N*,*N*-diisobutyl-2,4-pentadienamide) on nine $GABA_A$ receptor subtypes and on TRPV1 receptors. Unlike piperine, SCT-66 did not activate TRPV1 receptors. This compound increased I_{GABA} more potently and more efficaciously than piperine, although with altered subunit dependence. In vivo studies in mice revealed that

* Corresponding author. Tel.: +43 1 4277 55301/10; fax: +43 1 4277 9553.
E-mail address: steffen.hering@univie.ac.at (S. Hering).
[1] Both authors contributed equally to this work.

0006-2952
http://dx.doi.org/10.1016/j.bcp.2013.04.017

only piperine affects thermoregulation; that both piperine and SCT-66 have anticonvulsant and anxiolytic effects and reduce locomotor activity; and that SCT-66 has a stronger anxiolytic effect than piperine.

2. Materials and methods

All procedures involving animals were approved by the Austrian Animal Experimentation Ethics Board in compliance with the European Convention for the Protection of Vertebrate Animals used for Experimental and Other Scientific Purposes (ETS No. 123). Every effort was made to minimize the number of animals used.

2.1. Reagents

Piperine was obtained from Sigma™ (Vienna, Austria) and the piperine derivative SCT-66 (2E,4E)-5-(1,3-benzodioxol-5-yl))-*N*,*N*-diisobutyl-2,4-pentadienamide) was synthesized as described below (for structural formulae see Fig. 1): To a solution of piperic acid chloride (3 mmol, 0.71 g) in 10 mL dry THF, diisobutylamine (10.5 mmol; 1.357 g) was added and stirred overnight. The reaction mixture was evaporated and purified by column chromatography (toluene/ethyl acetate 20:3) to give the compound SCT-66 (0.661 g, 67%) as oil.

^{1}H NMR (200 MHz, $CDCl_3$): δ 7.,54–7.34 (m, 1H), 7,00 (d, J = 1.4 Hz, 1H), 6.90 (dd, J = 8.0, 1.6 Hz, 1H), 6.84–6.71 (m, 3H), 6.39 (d, J = 14.6 Hz, 1H), 5.97 (s, 2H), 3.28 (d, J = 7.5 Hz, 2H), 3.19 (d, J = 7.5 Hz, 2H), 2.12–1.88 (m, 2H), 0.98–0.82 (m, 12H). ^{13}C NMR (50 MHz, $CDCl_3$): δ 167.0, 148.4, 148.3, 142.5, 138.5, 131.2, 125.6, 122.7, 120.8, 108.7, 105.9, 101.5, 56.2, 54.9, 29.2, 27.2, 20.5, 20.3. MS m/z: 329 (12%, M^+), 201 (100%), 115 (39%), 57 (17%), 43 (23%). CHN for $C_{20}H_{27}NO_3$: calc.: C 72.92, H 8.26, N 4.25; found: C 72.78, H 8.13, N 4.16.

Stock solutions of piperine and SCT-66 were prepared in 100% DMSO (100 mM for oocyte experiments, 10 mg/μl for animal experiments; Dimethyl Sulfoxide). All chemicals were purchased from Sigma™, Vienna, Austria except where stated otherwise.

2.2. Expression and functional characterization of $GABA_A$ receptors and TRPV1 channels

Preparation of stage V-VI oocytes from *Xenopus laevis* and synthesis of capped off run-off poly(A^+) cRNA transcripts from linearized cDNA templates (pCMV vector) were performed as previously described [13]. Briefly, female *X. laevis* (NASCO™, Fort Atkinson, WI, USA) were anaesthetized by exposing them for 15 min to a 0.2% solution of MS-222 (methane sulfonate salt of 3-aminobenzoic acid ethyl ester) before surgically removing parts of the ovaries. Follicle membranes from isolated oocytes were digested with 2 mg/ml collagenase (Type 1A). Selected stage V-VI oocytes were injected with about 10–50 nl of DEPC- treated water (diethyl pyrocarbonate) containing the different cRNAs at a concentration of approximately 300–3000 pg/nl. The amount of cRNA was determined by means of a NanoDrop ND-1000 (Kisker-biotech™, Steinfurt, Germany).

$GABA_A$ receptors: To ensure expression of the gamma-subunit in rat $GABA_A$ receptors, cRNAs for expression of $\alpha_1\beta_2\gamma_{2S}$, $\alpha_2\beta_2\gamma_{2S}$, $\alpha_3\beta_2\gamma_{2S}$ and $\alpha_5\beta_2\gamma_{2S}$ receptors were mixed in a ratio of 1:1:10. For receptors comprising only α and β subunits ($\alpha_1\beta_2$, $\alpha_2\beta_2$, $\alpha_1\beta_3$, $\alpha_2\beta_2$, $\alpha_3\beta_2$, $\alpha_5\beta_2$), the cRNAs were mixed in a ratio 1:1. cRNAs for

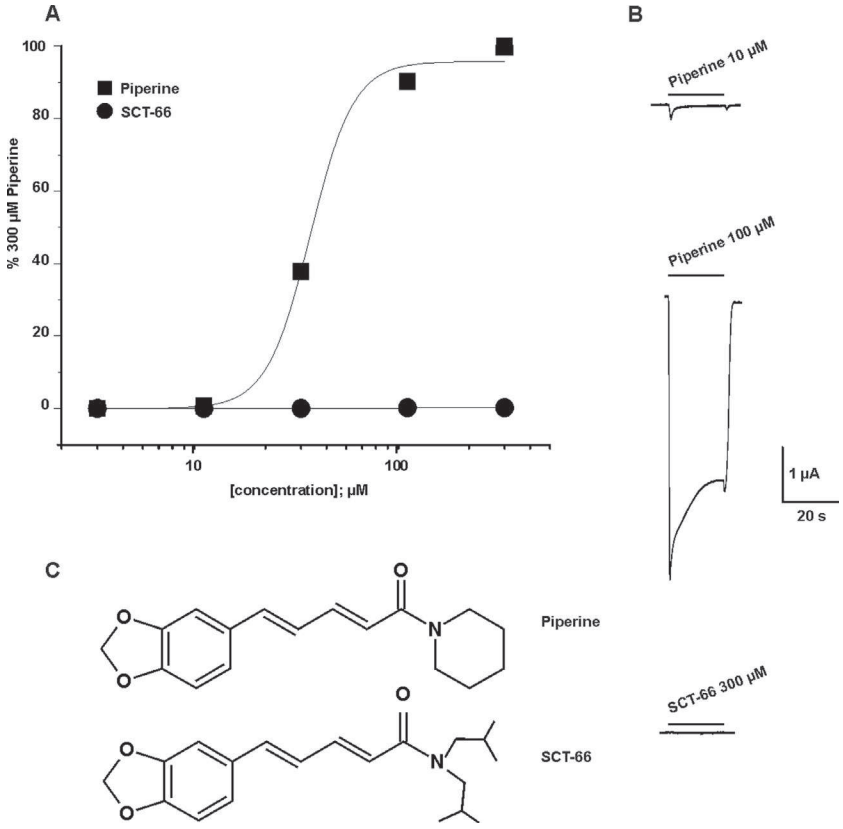

Fig. 1. Comparison of TRPV1 activation by piperine and SCT-66. (A) The concentration–response relationship for piperine (■; 3–300 μM) and SCT-66 (●, 3–300 μM) are shown. These normalized data were generated by measuring the net currents evoked in response to a test concentration of agonist and are expressed as a percentage of a preceding 300 μM piperine control response recorded in the same cell. Data are expressed as the mean ± S.E.M with n = 3–10 individual cells. The EC_{50} for piperine was 33.3 ± 0.1 μM (Hill coefficient of 4.1 ± 0.1; n = 3–10 per concentration). The EC_{50} value of piperine agrees with [2]. (B) Typical traces showing activation of TRPV1 channels by piperine and the lack of TRPV1 activation by SCT-66 at the indicated concentrations. (C) Structural formulae of piperine and its derivative SCT-66.

$\alpha_1\beta_1$ channels were injected in a ratio 3:1 to avoid formation of β_1 homomeric $GABA_A$ receptors [14,15].

TRPV1 channels: The rat TRPV1 clone was a gift from Prof. David Julius (Department of Cellular and Molecular Pharmacology, University of California, San Francisco).

After injection, oocytes were stored at 18 °C for 24–48 h in ND96 solution containing penicillin G (10 000 IU/100 ml) and streptomycin (10 mg/100 ml) [16]. Electrophysiological experiments on $GABA_A$ receptors and TRPV1 channels were performed using the two-microelectrode-voltage-clamp method at a holding potential of −70 mV ($GABA_A$ receptors) and −60 mV (TRPV1), respectively, making use of a TURBO TEC 01 C amplifier (npi electronic™, Tamm, Germany) and an Axon Digidata 1322A interface (Molecular Devices™, Sunnyvale, CA). Data acquisition was done using pCLAMP v.9.2. The bath solution contained 90 mM NaCl, 1 mM KCl, 1 mM $MgCl_2 \cdot 6H_2O$, 1 mM $CaCl_2$ and 5 mM HEPES (pH 7,4). Microelectrodes were filled with 2 M KCl.

2.3. Perfusion system

GABA, piperine and SCT-66 were applied by means of a fast perfusion system [17, ScreeningTool, npi electronic™, Tamm, Germany] to study I_{GABA} modulation and TRPV1 activation. To elicit I_{GABA}, the chamber was perfused with 120 μl of GABA-containing solution at a volume rate between 300 and 1000 μl/s. The I_{GABA} rise time ranged from 100 to 250 ms [13].

To account for possible slow recovery from increasing levels of desensitization in the presence of high GABA or piperine/SCT-66 concentrations, the duration of washout periods was extended from 1.5 min (for 1–10 μM GABA, <10 μM piperine/SCT-66) to 30 min (for ≥30 μM GABA, ≥10 μM piperine/SCT-66). To exclude voltage-clamp errors, oocytes with maximal current amplitudes >3 μA were discarded.

Because of low solubility in the bath solution, piperine and SCT-66 were used up to a concentration of 300 μM. Equal amounts of DMSO were present in all testing solutions. The maximum DMSO concentration in the bath (0.3%) had no observable effects on I_{GABA} or TRPV1.

2.4. Analysing concentration–response curves

Stimulation of chloride currents by modulators of the $GABA_A$ receptor was measured at a GABA concentration eliciting between 3 and 7% of the maximal current amplitude (EC_{3-7}). The EC_{3-7} was determined at the beginning of each experiment.

Enhancement of the chloride current was defined as $(I_{(GABA+Comp)}/I_{GABA}) - 1$, where $I_{(GABA+Comp)}$ is the current response in the presence of a given compound and I_{GABA} is the control GABA current. Concentration–response curves for activation of TRPV1 channels were generated by comparing the peak response evoked by a test concentration of the compounds at the different concentrations to that evoked by a previous control current recorded in response to 300 μM piperine.

Data were fitted by non-linear regression analysis using Origin software (OriginLab Corporation, USA). Data were fitted to the equation: $1/(1 + (EC_{50}/[Comp])^{n_H})$, where n_H is the Hill coefficient. Each data point represents the mean ± S.E.M. from at least 3 oocytes and ≥2 oocyte batches.

2.5. Behavioural analysis

2.5.1. Animals

Male mice (C57BL/6N) were obtained from Charles River Laboratories™ (Sulzfeld, Germany). For maintenance, mice were group-housed (maximum 5 mice per type IIL cage) with free access to food and water. At least 24 h before the commencement of experiments, mice were transferred to the testing facility, where they were given free access to food and water. The temperature in the maintenance and testing facilities was 23 ± 1 °C; the humidity was 40–60%; a 12 h light–dark cycle was in operation (lights on from 07:00 to 19:00). Only male mice aged 3–6 months were tested. Compounds were applied by intraperitoneal (i.p.) injection of aqueous solutions (either control or compound) 30 min before each test, except for body temperature, which was measured 3 h after injection. Testing solutions were prepared in a solvent composed of saline 0.9% NaCl solution with 10% DMSO and 3% Tween 80. The final DMSO concentration did not exceed 10% (see [18] for effects of DMSO on blood-brain barrier penetration). 1 M NaOH was used to adjust the pH to 7.4. All solutions were prepared freshly on the day of the experiment. Application of the solvent alone did not influence animal behaviour.

2.5.2. Measurement of body temperature

A temperature probe (Type T Thermocouple probe RET-3 connected to a Type T Thermometer, Physitemp Instruments Inc™; Clifton, USA), lubricated with glycerol, was inserted into the rectum of the mouse for a depth of up to 1 cm. The temperature probe remained in the animal till a stable temperature was reached (maximum 10 s).

2.5.3. Open Field Test (OF)

Ambulation was tested over 10 min in a 50 cm × 50 cm × 50 cm field box equipped with infrared rearing detection. Illumination was set to 150 lx. The explorative behaviour of C57BL/6N mice was analysed using the Actimot2 equipment and software (TSE-systems™, Bad Homburg, Germany). Areas were subdivided into border (up to 8 cm from wall), centre (20 cm × 20 cm, i.e. 16% of total area), and intermediate areas according to the recommendations of EMPRESS (European Mouse Phenotyping Resource of Standardized Screens; http://empress.har.mrc.ac.uk). The test was automatically started when the mouse was placed in the centre area.

2.5.4. Elevated Plus Maze Test (EPM)

The animal's behaviour was tested over 5 min on an elevated plus maze 1 m above ground consisting of two closed and two open arms, each 30 cm × 5 cm in size. The height of the closed arm walls was 20 cm. Illumination was set to 180 lx. Animals were placed in the centre, facing an open arm. Analysis was done automatically with Video-Mot2 equipment and software (TSE-systems™, Bad Homburg, Germany) [19].

2.5.5. Seizure threshold

Seizure threshold was determined by pentylentetrazole (PTZ)-tail-vein infusion on freely moving animals at a rate of 100 μl/min (100 mg/ml PTZ in saline). Infusion was stopped when animals displayed generalized clonic seizures. Animals were killed by cervical displacement immediately after the first generalized seizure. The seizure threshold dose was calculated from the infused volume in relation to body weight [20]. Piperine and SCT-66 were applied 30 min before PTZ infusion. Control animals were pre-treated with 10% DMSO in saline containing 3% Tween 80. At the infusion rate of 100 μl/min, generalized seizures are induced within 2 min after beginning infusion of PTZ.

2.5.6. Statistical analysis

Statistical significance of electrophysiological data was calculated using a paired Student *t*-test with a confidence interval of $p < 0.05$; for in vivo experiments, one-way ANOVA (Bonferroni Adjustment) was used. Statistical analysis was done with Origin software (OriginLab Corporation; USA). *p*-values of <0.05 were accepted as statistically significant. All data are given as mean ± S.E.M. (*n*).

3. Results

3.1. Replacing the piperidine ring by a N,N-diisobutyl-residue prevents activation of TRPV1 receptors

In line with previous studies piperine induced marked inward currents when applied to oocytes expressing TRPV1 receptors (Fig. 1A and B, [2]). A simple structural modification (replacing the piperidine ring by a *N,N*-diisobutyl residue; Fig. 1C) completely eliminated activation of TRPV1 receptors by SCT-66 (300 μM, Fig. 1A and B).

3.2. Different γ_2 subunit dependence of piperine and SCT-66

In order to analyse the interaction of piperine and SCT-66 with different $GABA_A$ receptor subtypes, receptors composed of different subunits were heterologously expressed in *Xenopus* oocytes and I_{GABA} modulation by both compounds was studied by means of the 2-microelectrode voltage-clamp technique and a fast-perfusion system (see Section 2).

First the enhancement of I_{GABA} by piperine and SCT-66 through $\alpha_1\beta_2$ and $\alpha_1\beta_2\gamma_{2S}$ receptors was compared. As illustrated in Fig. 2A, omitting the γ_{2S} subunit had no significant effect on I_{GABA} enhancement ($I_{GABA,max}$) or on the potency (EC_{50}) of piperine ($\alpha_1\beta_2$: $EC_{50} = 50.0 \pm 7.9$ μM, $I_{GABA,max} = 271 \pm 36\%$, $n = 13$ vs. $\alpha_1\beta_2\gamma_{2S}$: $EC_{50} = 52.4 \pm 9.4$ μM, $I_{GABA,max} = 302 \pm 27\%$; $n = 6$; $p > 0.05$; data for modulation of I_{GABA} through $\alpha_1\beta_2\gamma_{2S}$ receptors by piperine taken from [3]). This finding suggests that piperine interacts with a binding site located on α and/or β subunits or the α/β interface. In contrast, co-expression of a γ_{2S} subunit resulted in significant reduction of I_{GABA} enhancement by SCT-66 ($\alpha_1\beta_2$: $1256 \pm 292\%$; $n = 4$; $p < 0.05$; $\alpha_1\beta_2\gamma_{2S}$: $378 \pm 15\%$, $n = 6$; $\alpha_2\beta_2\gamma_{2S}$: $572 \pm 51\%$, $n = 5$; $\alpha_3\beta_2\gamma_{2S}$: 584 ± 20, $n = 5$ and $\alpha_5\beta_2\gamma_{2S}$: $398 \pm 26\%$, see Fig. 2D, Tables 1 and 2) suggesting a role of γ_2 in receptor modulation. Co-expression of a γ_{2S}-subunit did, however, not significantly affect the potency of SCT-66 (see Tables 1 and 2).

3.3. Piperine potentiates $GABA_A$ receptors composed of $\alpha_{1/2/3/5}$ and $\beta_{1/2/3}$ subunits

In order to investigate a potential subunit dependent action of piperine and SCT-66, we studied their interaction with 8 different receptor subtypes ($\alpha_1\beta_1$, $\alpha_1\beta_2$, $\alpha_1\beta_3$, $\alpha_2\beta_2$, $\alpha_3\beta_2$ and $\alpha_5\beta_2$) (Fig. 2A, B, D and E, Table 1). The highest efficacy of piperine was observed for receptors containing α_3 subunits, with maximal I_{GABA} potentiation (EC_{3-7}) of $375 \pm 51\%$ ($n = 6$), followed by $GABA_A$ receptors composed of α_1 and β_2 subunits ($271 \pm 36\%$, $n = 13$) and α_2 and β_2 subunits, respectively (248 ± 48; $n = 6$) (see also Table 1). Piperine was significantly less efficacious on $\alpha_5\beta_2$ receptors ($I_{GABA,max} = 136 \pm 22\%$, $n = 6$, Fig. 2A, Tables 1 and 2). The potencies of I_{GABA} modulation, however, did not significantly differ with EC_{50} values ranging from 42.8 ± 17.6 μM ($\alpha_2\beta_2$) to 59.6 ± 12.3 μM ($\alpha_3\beta_2$), Fig. 2B illustrates the effect of piperine on $GABA_A$ receptors with three different β-subunits. $\alpha_1\beta_2$ and $\alpha_1\beta_3$ receptors were more efficaciously modulated by piperine than $\alpha_1\beta_1$ receptors (maximal I_{GABA} modulation of $\alpha_1\beta_2$ receptors: $271 \pm 36\%$, $\alpha_1\beta_3$ $332 \pm 64\%$ vs. $\alpha_1\beta_1$ receptors: $171 \pm 22\%$; (see Fig. 2 C for representative I_{GABA} through $GABA_A$ receptors composed of α_3 and β_2 subunits in the absence and presence of 30 μM piperine).

3.4. Higher potency and different subunit dependence of SCT-66

SCT-66 displayed a higher potency on all subunit compositions tested (Fig. 2E and F, Tables 1 and 2 e.g. on $\alpha_1\beta_2\gamma_{2S}$ receptors: EC_{50}(SCT-66): 21.5 ± 1.7 μM, $n = 6$ compared to EC_{50}(piperine):57.6 ± 4.2 μM, $n = 6$, $p < 0.01$ and I_{GABA} was more efficaciously modulated by SCT-66 than by piperine. Stronger maximal I_{GABA} enhancement by SCT-66 ranged from 1.2-fold ($\alpha_1\beta_2\gamma_{2S}$ receptors) to 6.5-fold ($\alpha_1\beta_{1)}$ (Tables 1–2). Taken together, the stronger I_{GABA} enhancement by SCT-66 was accompanied by an apparent change in receptor subtype dependence (SCT-66 was e.g. equally efficacious on receptors comprising different β-subunits compared to piperine that was more efficacious on $\beta_{2/3}$ incorporating receptors, compare Fig. 2B to Fig. 2E).

3.5. Piperine and SCT-66 shift the GABA concentration–response curve

GABA concentration–response curves in the presence of piperine and SCT-66 for $\alpha_3\beta_2$ receptors are compared in Fig. 3. Almost-saturating concentrations of piperine and SCT-66 (100 μM, Fig. 2A, B, D and E) shifted the curves to the left (5.7 ± 1.9 μM and $n_H = 1.1 \pm 0.1$ (control); 2.7 ± 0.8 μM and $n_H = 1.1 \pm 0.2$ (piperine), and 1.9 ± 0.4 μM and $n_H = 1.1 \pm 0.1$ (SCT-66). Enhancement of $I_{GABA,max}$ by piperine and SCT-66 was statistically not significant ($I_{GABA;\ max\text{-}piperine} = 123 \pm 3$; $n = 4$ and $I_{GABA;\ max\text{-}SCT\text{-}66} = 129 \pm 6\%$, $n = 3$; $p > 0.05$). Neither piperine nor SCT-66 (up to 300 μM) activated $GABA_A$ receptors when applied in the absence of GABA.

3.6. Effects of piperine and SCT-66 on thermoregulation

Changes in body temperature might indicate activation of TRPV1 channels in vivo [21]. Core body temperature of male C57BL/6N mice was measured rectally shortly before application of saline, piperine or SCT-66. Basal values did not differ between the groups, averaging 36.80 ± 0.04 °C ($n = 184$). This temperature measurement was repeated 3 hours after injection of compound (to avoid interference from stress-induced hyperthermia early after injection). As illustrated in Fig. 4, a dramatic drop of body temperature was observed after injection of piperine at doses higher than 3 mg/kg bodyweight: application of 10 mg/kg bodyweight piperine significantly ($p < 0.01$) reduced body temperature of mice (Control: 36.10 ± 0.10 °C; $n = 38$ vs. 10 mg/kg bodyweight piperine 34.86 ± 0.29 °C; $n = 16$). An even more pronounced effect was observed upon application of 30 mg/kg bodyweight: body temperature was lowered to 30.37 ± 0.84 °C ($n = 9$; $p < 0.01$). In contrast, no significant changes in body temperature were observed after application of SCT-66 at all tested doses (see Fig. 4), thereby resulting in a statistically significant difference between the two drugs as analysed by one-way ANOVA ($p < 0.01$).

3.7. Piperine and SCT-66 reduce locomotor activity

In the Open-Field-Test (OF, see Section 2), control mice covered a distance of 39.3 ± 1.9 m, ($n = 20$; Fig. 5; white bar). Injection of piperine resulted in a dose-dependent reduction of ambulation: significant reductions were apparent from doses ≥3 mg/kg bodyweight, and the highest dose of 30 mg/kg reduced ambulation by approximately 50% compared to control littermates (control: 39.3 ± 1.9 m; $n = 20$ vs. 30 mg/kg bodyweight piperine 21.0 ± 3.7 m; $n = 13$; $p < 0.01$; see Fig. 5A; black bars for piperine). Unlike piperine, SCT-66 did not affect ambulation over a broad range (0.3–10 mg/kg bodyweight; see Fig. 5A, SCT-66 shaded bars). Only at a dose of 30 mg/kg bodyweight SCT-66 significantly reduced locomotor activity (Control: 39.3 ± 1.9 m; $n = 20$ vs. 30 mg/kg bodyweight SCT-66: 28.6 ± 2.5 m, $n = 10$, $p < 0.01$), however, this effect was still weaker than with piperine at the same dose.

3.8. Piperine and SCT-66 influence anxiety-related behaviour in the OF test

The marked influence of even low doses of piperine (≥3 mg/kg) on the locomotor activity of mice makes it difficult to analyse

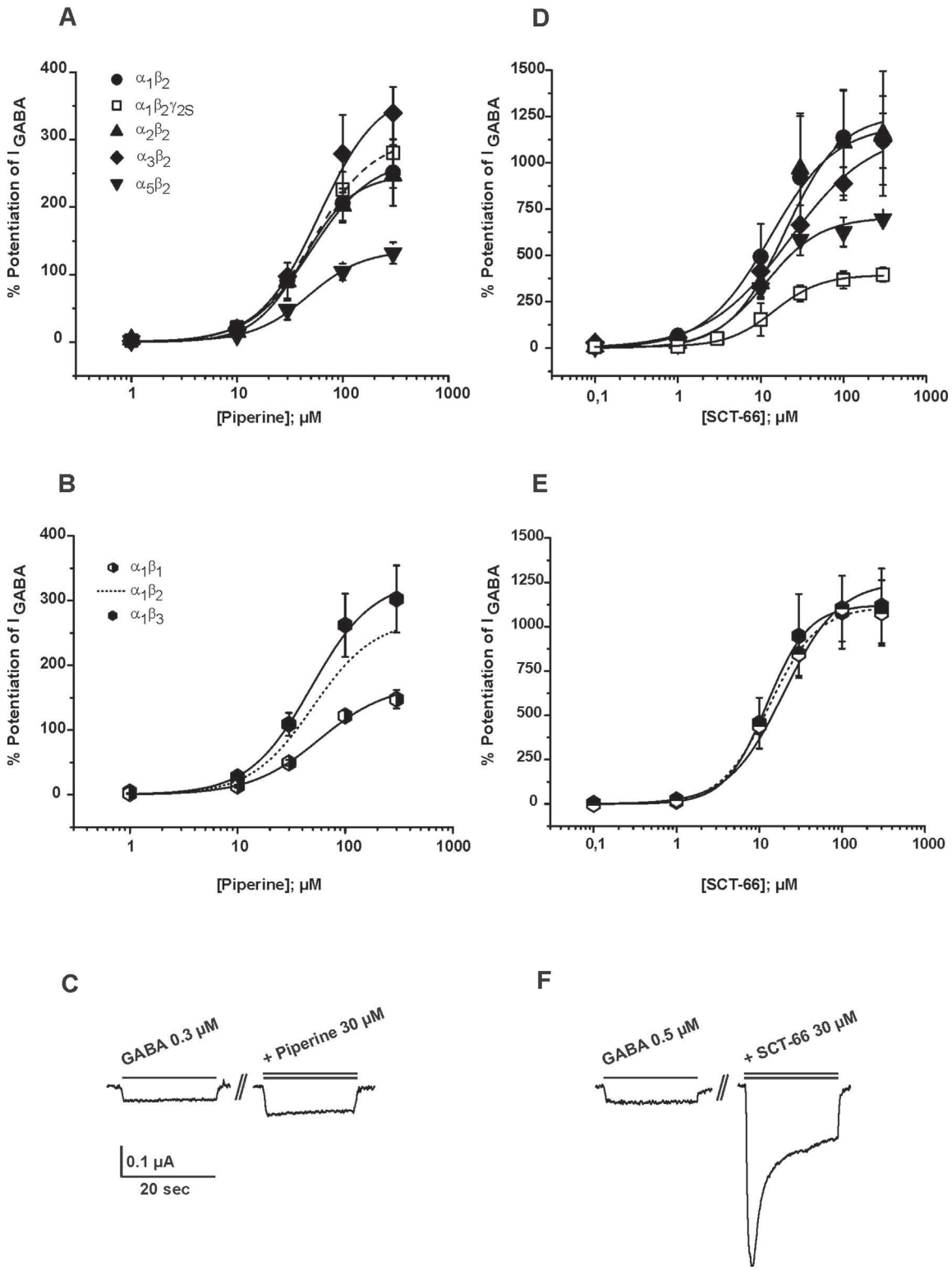

Fig. 2. I_{GABA} modulation by piperine and SCT-66 concentration–response curves for I_{GABA} modulation through $GABA_A$ receptors of the indicated subunit combinations by piperine (A and B) and SCT-66 (D and E) at a GABA concentration eliciting 3–7% of the maximal GABA response (EC_{3-7}). The enhancement of I_{GABA} by piperine trough $\alpha_1\beta_2\gamma_{2S}$ receptors (dashed line) receptors is taken from [3]. Each data point represents the mean ± S.E.M. from at least five oocytes and at least two oocyte batches. (C and F) Typical traces illustrating I_{GABA} enhancement by 30 μM compound. Control currents (GABA, single bar) and corresponding currents elicited by co-application of GABA and 30 μM piperine/SCT-66 (double bar) are shown.

anxiolytic properties in activity-based testing conditions. At lower doses, the only difference observed was an increase in distances travelled in the centre area (control: 8.8 ± 0.6%, $n = 20$ vs. SCT-66 0.3 mg/kg bodyweight: 10.7 ± 1.1%, $n = 12$; $p < 0.05$) in mice treated with SCT-66 at a dose of 0.3 mg/kg bodyweight.

3.9. Piperine and SCT-66 reduce anxiety-related behaviour in the EPM test

In order to analyse the impact of piperine and SCT-66 on anxiety-related behaviour, male C57BL/6N mice were tested

Table 1
Potency and efficiency of piperine/SCT-66 enhancement of $GABA_A$ receptors with different subunit compositions.

Subunit combination	EC_{50} (μM)	Maximum stimulation of-I_{GABA} at EC_{3-7}	Hill coefficient (n_H)	Number of experiments (n)
Piperine				
$\alpha_1\beta_1$	57.6 ± 4.2	171 ± 22	1.4 ± 0.2	10
$\alpha_1\beta_2$	50.0 ± 7.9	271 ± 36	1.5 ± 0.3	13
$\alpha_1\beta_3$	48.3 ± 7.3	332 ± 64	1.5 ± 0.3	7
$\alpha_2\beta_2$	42.8 ± 17.6	248 ± 48	1.9 ± 0.5	6
$\alpha_3\beta_2$	59.6 ± 12.3	375 ± 51	1.4 ± 0.2	6
$\alpha_5\beta_2$	47.5 ± 17.9	136 ± 22	1.7 ± 0.4	6
SCT-66				
$\alpha_1\beta_1$	13.3 ± 2.9	1112 ± 136	1.5 ± 0.2	4
$\alpha_1\beta_2$	19.8 ± 9.7	1256 ± 292	1.3 ± 0.4	4
$\alpha_1\beta_3$	12.3 ± 4.5	1128 ± 155	1.5 ± 0.3	3
$\alpha_1\beta_2\gamma_{2S}$	21.5 ± 1.7	378 ± 15	1.8 ± 0.2	6
$\alpha_2\beta_2$	13.1 ± 9.0	1204 ± 233	1.1 ± 0.3	4
$\alpha_2\beta_2\gamma_{2S}$	24.1 ± 7.5	572 ± 51	1.3 ± 0.3	5
$\alpha_3\beta_2$	22.2 ± 12.1	1169 ± 195	0.9 ± 0.2	3
$\alpha_3\beta_2\gamma_{2S}$	15.1 ± 1.8	584 ± 20	1.6 ± 0.2	5
$\alpha_5\beta_2$	11.5 ± 2.7	705 ± 24	1.3 ± 0.2	3
$\alpha_5\beta_2\gamma_{2S}$	14.2 ± 1.4	398 ± 26	2.0 ± 0.3	5

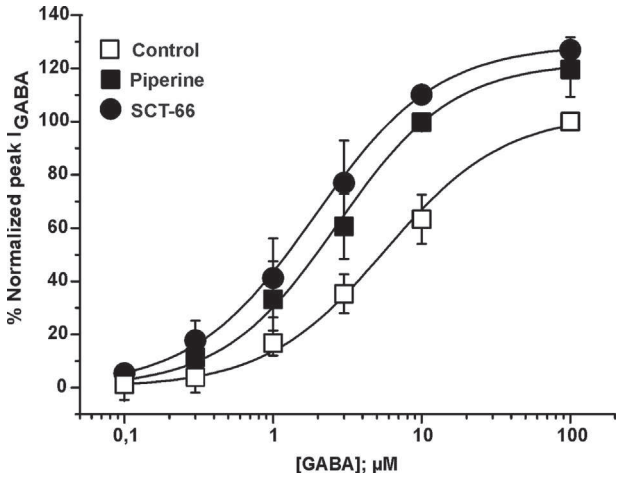

Fig. 3. Piperine and SCT-66 shift the GABA concentration–response curve towards higher GABA sensitivity GABA concentration–response curves for $\alpha_3\beta_2$ $GABA_A$ receptors in the absence (control, □) and in the presence of 100 μM piperine (■), and 100 μM SCT-66 (●) are compared. The corresponding EC_{50} values and Hill-coefficients were 5.7 ± 1.9 μM and n_H = 1.1 ± 0.1 (control) and 2.7 ± 0.8 μM and n_H = 1.1 ± 0.2 (piperine), and 1.9 ± 0.4 μM and n_H = 1.1 ± 0.1 (SCT-66), respectively. Each data point represents the mean ± S.E.M. from at least four oocytes and at least two oocyte batches.

30 min after i.p. injection in the Elevated-Plus-Maze-test (EPM, see Materials and Methods section). As illustrated in Fig. 6A, control mice (treated with saline; white bar) spent 28.6 ± 2.1% of the total test time in the open arms (OA) of the EPM (n = 27). While the behaviour of mice treated with 0.1 mg/kg bodyweight of piperine did not significantly differ from saline-treated control littermates, upon application of higher doses (i.e. 0.3 and 1 mg/kg bodyweight) mice spent significantly ($p < 0.01$) more time in the OA (0.3 mg/kg bodyweight: 43.0 ± 4.2%, n = 22 and 1 mg/kg bodyweight: 45.7 ± 6.3%, n = 16, black bars). At a dose of 1 mg/kg bodyweight piperine significantly reduced ambulation (see Fig. 6D), thus, higher doses were not investigated. Unlike piperine, SCT-66 did not significantly influence overall ambulation at the tested doses (0.3–10 mg/kg bodyweight; see Fig. 6D shaded bars). As shown in Fig. 6A, a significant increase in the time spent in the OA was observed with increasing doses of SCT-66, reaching a maximum at a dose of 1 mg/kg bodyweight (control: 28.6 ± 2.1, n = 27 vs. 1 mg/kg bodyweight SCT-66: 45.1 ± 5.7%, n = 14, $p < 0.01$). This effect remained stable and did not change even when applying higher doses (3–10 mg/kg bodyweight). Moreover, mice treated with 0.3 mg/kg bodyweight SCT-66 visited the OA more frequently than control mice (control: 12.4 ± 0.9, n = 27 vs. 0.3 mg/kg bodyweight SCT-66: 13.7 ± 1.1, n = 22, $p < 0.05$), while the number of visits to the OA did not differ at the other doses of piperine and SCT-66, respectively (see Fig. 6B). Accordingly, the number of closed arm (CA) entries also dropped significantly at doses ≥0.3 mg/kg bodyweight piperine and SCT-66, respectively (Fig. 6 C).

3.10. Piperine and SCT-66 modulate seizure threshold

The seizure threshold as assessed using pentylentetrazole (PTZ) tail vein infusions was significantly increased 30 min after i.p. injection of piperine at 3 or 10 mg/kg bodyweight (Control: 39.4 ± 2.8 mg/kg bodyweight PTZ; n = 7; vs. 3 mg/kg bodyweight

Table 2
Comparison of efficiencies for $GABA_A$ receptors of different subunit compositions. (*) indicates statistically significant ($p < 0.05$) differences.

Piperine	$\alpha_1\beta_2$	$\alpha_1\beta_2$	$\alpha_1\beta_3$	$\alpha_1\beta_2\gamma_{2S}$[1]	$\alpha_2\beta_2$	$\alpha_3\beta_2$	$\alpha_5\beta_2$
$\alpha_1\beta_1$		*	*	*			
$\alpha_1\beta_2$	*						*
$\alpha_1\beta_3$	*						*
$\alpha_1\beta_2\gamma_{2S}$[a]	*						*
$\alpha_2\beta_2$							*
$\alpha_3\beta_2$							*
$\alpha_5\beta_2$		*	*	*	*	*	

SCT-66	$\alpha_1\beta_1$	$\alpha_1\beta_2$	$\alpha_1\beta_3$	$\alpha_1\beta_2\gamma_{2S}$	$\alpha_2\beta_2$	$\alpha_2\beta_2\gamma_{2S}$	$\alpha_3\beta_2$	$\alpha_3\beta_2\gamma_{2S}$	$\alpha_5\beta_2$	$\alpha_5\beta_2\gamma_{2S}$
$\alpha_1\beta_1$				*		*		*	*	*
$\alpha_1\beta_2$				*						*
$\alpha_1\beta_3$				*		*		*	*	*
$\alpha_1\beta_2\gamma_{2S}$	*	*	*		*	*	*	*	*	
$\alpha_2\beta_2$				*		*		*		*
$\alpha_2\beta_2\gamma_{2S}$	*		*	*	*		*			*
$\alpha_3\beta_2$				*		*		*		*
$\alpha_3\beta_2\gamma_{2S}$	*		*	*	*		*		*	*
$\alpha_5\beta_2$	*		*	*				*		*
$\alpha_5\beta_2\gamma_{2S}$	*	*	*		*	*	*	*	*	*

[a] E_{max} values for enhancement of I_{GABA} through $\alpha_1\beta_2\gamma_{2S}$ receptors by piperine are taken from [3].

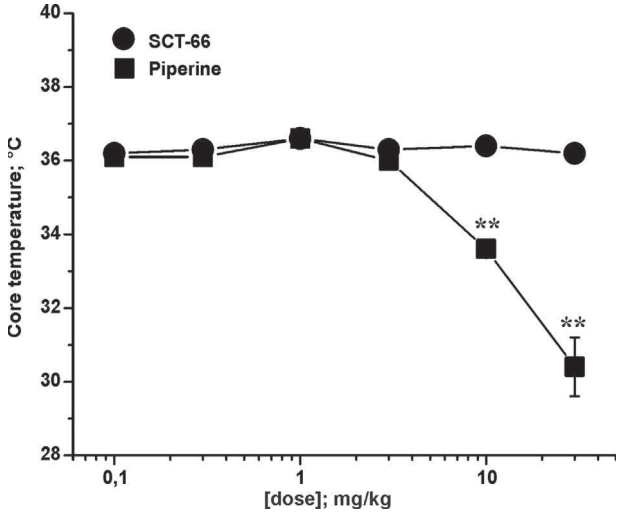

Fig. 4. SCT-66 does not reduce body temperature in mice Effects of piperine and SCT-66 on body temperature 3 h after injection of (■) piperine or (●) SCT-66 at the indicated doses (mg/kg bodyweight) are illustrated. Each data point represents the mean ± S.E.M. of at least 9 mice. (**) indicates statistically significant ($p < 0.01$) differences to control (ANOVA with Bonferroni).

piperine: 46.2 ± 5.4 mg/kg bodyweight PTZ; $n = 4$; $p < 0.05$ and 10 mg/kg bodyweight piperine, respectively: 48,7 ± 2.1 mg/kg bodyweight PTZ; $n = 4$; $p < 0.01$). A dose of 30 mg/kg bodyweight, however, resulted in a significant drop in seizure threshold (30.3 ± 3.4 mg/kg bodyweight PTZ; $n = 4$; $p < 0.01$; Fig. 7A). Doses below 3 mg/kg bodyweight did not affect seizure threshold.

Unlike piperine, SCT-66 did not display any observable effects on the seizure threshold up to 3 mg/kg bodyweight. Only higher doses significantly raised the seizure threshold (10 mg/kg bodyweight SCT-66: 47.6 ± 3.4 mg/kg bodyweight PTZ; $n = 4$; $p < 0.01$ and 30 mg/kg bodyweight SCT-66: 55.8 ± 2.8 mg/kg bodyweight PTZ, $n = 4$, $p < 0.01$; Fig. 7B).

4. Discussion

Natural products from distinct structural classes including flavonoids [22–25], terpenoids [26–28], sesquiterpenes [29–31], diterpenes [32], triterpene glycosides [33], polyacetylenes [34], (neo)lignans [28,35], alkaloids [3] or (furano)coumarins [36,37] have been shown to modulate $GABA_A$ receptors.

We have recently reported that besides activating TRPV1 receptors [2] piperine modulates $GABA_A$ receptors [3]. Here we report that replacing the piperidine ring by a *N,N*-diisobutyl-residue prevents activation of TRPV1 (Fig. 1A and B). In order to get insights into their therapeutic potentials we subsequently characterized the actions of piperine and its derivative SCT-66 in vitro and in vivo.

4.1. Subunit-dependent modulation of $GABA_A$ receptors by piperine

Comparable enhancement of I_{GABA} through $\alpha_1\beta_2$ receptors as through the $\alpha_1\beta_2\gamma_{2S}$ [3] and the similar potencies on the two receptor subtypes suggests that piperine interacts with a binding

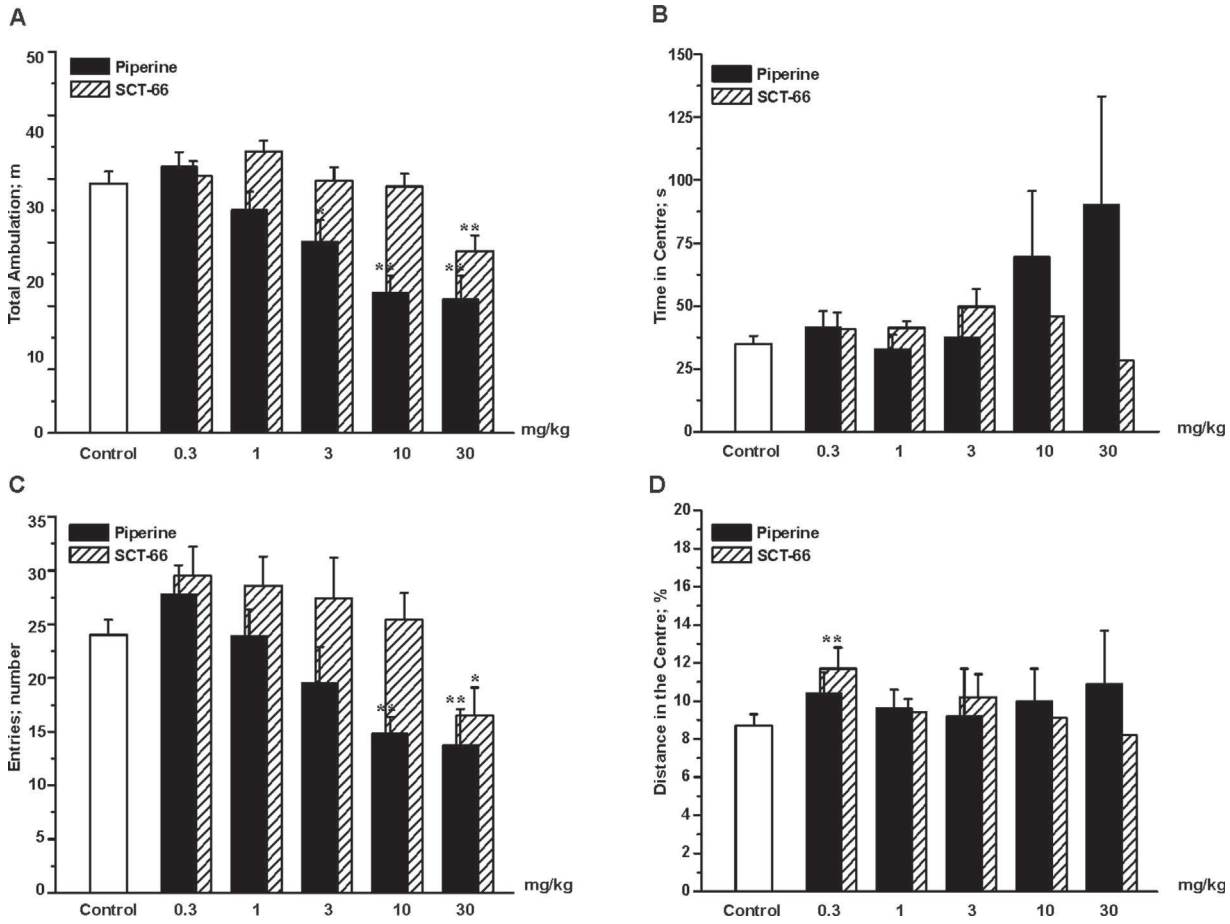

Fig. 5. Piperine and SCT-66 dose-dependently reduce locomotor activity in the OF test. Bars indicate in (A) the total distance travelled, in (B) the time spent in the centre, in (C) the number of entries to the centre and in (D) the distance travelled in the centre as % of the total distance after application of the indicated dose (mg/kg bodyweight) of piperine (black bars), SCT-66 (shaded bars) or control (white bars). Bars always represent means ± S.E.M. from at least 8 different mice. (*) indicates statistically significant differences with $p < 0.05$, (**) $p < 0.01$ to control (ANOVA with Bonferroni).

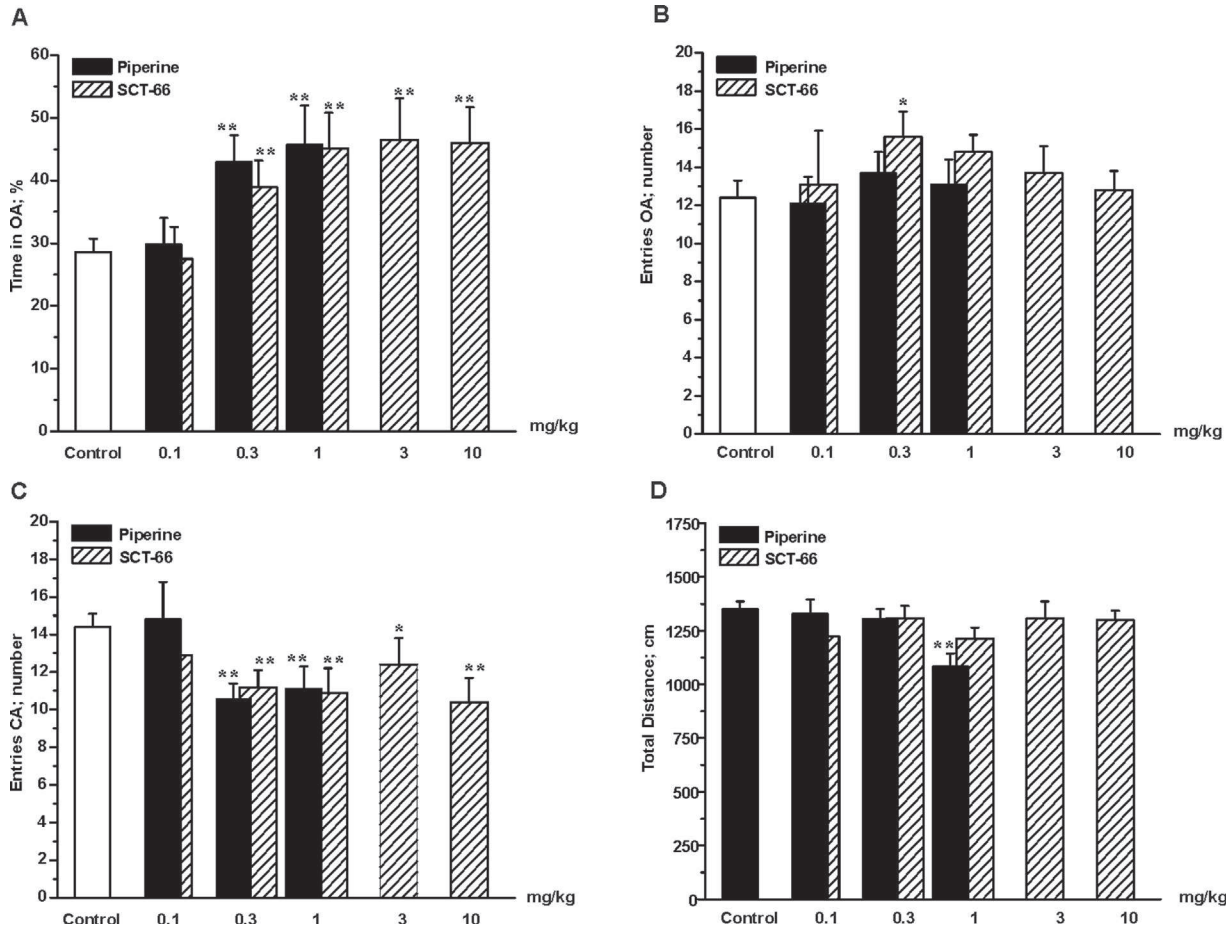

Fig. 6. Piperine and SCT-66 display anxiolytic-like effects in the EPM test. Bars indicate in (A) the time spent in the open arms (OA) in % of the total time, in (B) the number of OA entries, in (C) the number of closed arm (CA) entries and in (D) the total distance after application of the indicated dose in mg/kg bodyweight of either piperine (black bars) or SCT-66 (shaded bars), respectively. White bars illustrate the behaviour of control mice. Bars represent means ± S.E.M. from at least 9 different mice. (*) indicates statistically significant differences with $p < 0.05$, (**) $p < 0.01$ to control (ANOVA with Bonferroni).

site located on α and/or β subunits. This hypothesis is in line with our previous findings that $GABA_A$ receptor modulation by piperine is not blocked by flumazenil [3].

I_{GABA} enhancement by piperine was most efficacious for $GABA_A$ receptors with α_3 subunits, weakest for $GABA_A$ receptors incorporating α_5 subunits (Fig. 2A) and dependent on the β-subunit (Fig. 2B). While there was no significant difference in enhancement of I_{GABA} through $GABA_A$ receptors with either β_2 or β_3 subunits, incorporation of β_1 subunits reduced enhancement of I_{GABA} (see also Fig. 2B).

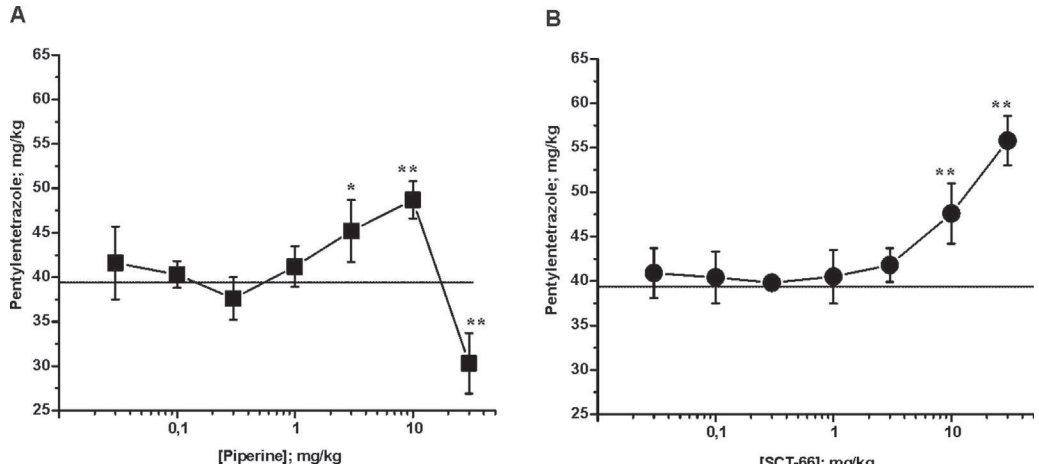

Fig. 7. Piperine and SCT-66 affect seizure threshold differently. Changes in seizure threshold upon PTZ-infusion of the indicated dose (mg/kg bodyweight) of piperine (A) and SCT-66 (B) are depicted. Each data point represents the mean ± S.E.M. of a least 3 mice. (*) indicates statistically significant differences with $p < 0.05$, (**) $p < 0.01$ to control (ANOVA with Bonferroni).

4.2. SCT-66 modulates $GABA_A$ receptors with higher potency and efficiency

A principle finding was that replacing the piperidine ring by a *N,N*-diisobutyl-residue did not only diminish interaction with TRPV1 receptors but additionally increased potency and efficacy of $GABA_A$ receptor modulation and affected subunit dependency (Figs. 2E, D and Table 1). Replacing the piperidine ring by a *N,N*-diisobutyl-residue not only diminished the $\beta_{2/3}$ subunit dependence (Fig. 2F), but also induced γ-subunit dependence. Hence, I_{GABA} stimulation in $\alpha_1\beta_2\gamma_{2S}$ receptors was about four times smaller than in $\alpha_1\beta_2$ receptors. These data suggest differences in the binding pockets of the two molecules and/or the existence of an additional binding site for SCT-66 involving the γ-subunit.

4.3. Consequences of different receptor specificity on anxiety, locomotor activity and seizure threshold

In order to analyse the consequences of the structural changes in the piperine scaffold we compared the in vivo action of piperine and SCT-66. However, before analyzing behavioural effects of piperine and SCT-66, the consequences of different TRPV1 activity were studied: since TRPV1 channels are involved in a variety of physiological processes including thermoregulation [38], measuring changes in body temperature is one way to detect their activation. In agreement with the literature, piperine at doses $\geq$ 10 mg/kg bodyweight drastically lowered body temperature of mice (compare to similar results in rats in [39]). In contrast, SCT-66 did not affect thermoregulation even at high doses (see Fig. 4). Our data derived on TRPV1 channels expressed on oocytes indicate that SCT-66, unlike piperine, does not interact with TRPV1 channels. While the in vivo effects of piperine are thus likely to include a TRPV1-related component, it seems that the in vivo effects of SCT-66 do not.

First insights into the behavioural effects of piperine and SCT-66 were obtained from the OF and the EPM test. Though both compounds reduced animals' locomotor activity, SCT-66 did so only at higher doses (see Fig. 5A). Considering the higher potency and efficiency of SCT-66 on $GABA_A$ receptors in vitro (Fig. 2D and E and Table 1) we speculate that the reduced locomotor activity induced by piperine at doses $\geq$10 mg/kg reflects interactions with vanilloid receptors. A plausible explanation would be that the alterations in pain sensation and thermoregulation result in depressed ambulation as discomfort and pain may well interfere with the exploratory drive. In contrast, reduced ambulation upon application of high doses of SCT-66 may indeed reflect sedation resulting from an enhancement of I_{GABA}. This is further supported by our finding of relatively subtype-independent, strong modulation of $GABA_A$ receptors by SCT-66 that did not differ between receptors containing α_1, α_2 or α_3 subunits, which is seen as a prerequisite for sedative actions of drugs [40,41].

As both tests depend on motor activity, potential anxiolytic effects of piperine could be observed only in one parameter of the EPM test, where mice treated with low doses of either piperine spent significantly more time in the open arms of the maze (see Fig. 6A). In contrast, clear anxiolytic effects were observed for SCT-66, which agrees with the stronger enhancement of I_{GABA} (see Fig. 2D and E) and the lack of TRPV1 activation observed in vitro.

Beside influences on emotional behaviour, positive allosteric modulators of $GABA_A$ receptors also influence the seizure threshold. Thus, enhancing GABAergic signalling was shown to significantly increase seizure threshold in mice. Importantly, the seizure threshold is independent of motor activity. Consistent with the data obtained from behavioural testing, the effects of piperine on the PTZ-induced seizure threshold suggest the involvement of more than just one receptor/target in vivo. Thus, piperine revealed a biphasic dose-response curve displaying increased thresholds at doses of 3–10 mg/kg bodyweight, which reverts to decreased thresholds at a dose of 30 mg/kg (Fig 7A). In contrast SCT-66 significantly increased the threshold at a dose of 10–30 mg/kg (Fig. 7B). Little information is available on the effects of TRPV1 activation on seizure threshold. The proposed effects of TRPV1 on epilepsy are controversial: while some groups suggest TRPV1 agonists as potential candidates for antiepileptics [42], others have shown increased glutamate release from hippocampal granule cells as a consequence of TRPV1 activation [43]. We can also not exclude the involvement of receptors other than $GABA_A$ and TRPV1. However, TRPV1 activation has been shown to cause vasodilation [44], and we observed vasodilatory effects during the PTZ tail-vein infusion experiments with piperine at doses of 10–30 mg/kg (data not shown), but not with SCT-66.

4.4. Conclusions and outlook

Replacing the piperidine ring by the *N,N*-diisobutyl residue of piperine diminished interaction with TRPV1 receptors, enhanced potency and efficacy of I_{GABA} modulation, diminished the higher efficacy of piperine on α_3-subunit and/or $\beta_{2/3}$-subunit containing receptors (compare Fig. 2A and B with Fig. 2D and E) and induced a γ_2 subunit dependence (Fig. 2 D). Piperine and SCT-66 induced anxiolytic-like, anticonvulsant action with SCT-66 and less depression of locomotor activity compared to piperine (Figs. 5–7). Its higher receptor specificity (lack of interaction with TRPV1) and higher potency and efficacy of I_{GABA} modulation and its in vivo action suggest that SCT-66 may represent a suitable scaffold for development of novel $GABA_A$ receptor modulators with anxiolytic and anticonvulsant potential. The addition of 2 extra methyl groups in SCT-66 significantly increased flexibility in the side chain and almost doubled the molecular volume of this part of the molecule. The generation of further piperine derivatives and studies on different $GABA_A$ receptor subtypes will help to clarify the structural basis of the receptor selectivity (TRPV1 vs. $GABA_A$) and changes in I_{GABA} modulation.

Conflict of interest

The authors declare no conflict of interests.

Acknowledgments

This work was supported by the Austrian Science Fund (FWF P21241, TRP10, P22395 and the doctoral programme "Molecular drug targets" W1232 to S.H.) and the Swiss National Science Foundation (Project 31600-113109 to M.H.)

References

[1] Szallasi A. Piperine: researchers discover new flavor in an ancient spice. Trends Pharmacol Sci 2005;26:437–9.
[2] McNamara FN, Randall A, Gunthorpe MJ. Effects of piperine, the pungent componentof black pepper, at the human vanilloid receptor (TRPV1). Br J Pharmacol 2005;144:781–90.
[3] Zaugg J, Baburin I, Strommer B, Kim HJ, Hering S, Hamburger M. HPLC based activity profiling: discovery of piperine as a positive GABA(A) receptor modulator targeting a benzodiazepine-independent binding site. J Nat Prod 2010;73:185–91.
[4] Di Marzo V, Gobbi G, Brain Szallasi A. TRPV1: a depressing TR(i)P down memory lane. Trends Pharmacol Sci 2008;29:594–600.
[5] Gunthorpe MJ, Chizh BA. Clinical development of TRPV1 antagonists: targeting a pivotal point in the pain pathway. Drug Discov Today 2009;14:56–67.
[6] Olsen RW, Sieghart W. International Union of Pharmacology. LXX. Subtypes of gamma-aminobutyric acid(A) receptors: classification on the basis of subunit composition, pharmacology, and function. Update. Pharmacol Rev 2008;60:243–60.
[7] Savic MM, Majumder S, Huang S, Edwankar RV, Furtmüller R, Joksimović S, et al. Novel positive allosteric modulators of GABAA receptors: do subtle

differences in activity at alpha1 plus alpha5 versus alpha2 plus alpha3 subunits account for dissimilarities in behavioral effects in rats. Prog Neuropsychopharmacol Biol Psychiatry 2010;34:376–86.
[8] Rudolph U, Knoflach F. Beyond classical benzodiazepines: novel therapeutic potential of GABAA receptor subtypes. Nat Rev Drug Discov 2011;10:685–97.
[9] Möhler H. The GABA system in anxiety and depression and its therapeutic potential. Neuropharmacology 2012;62:42–53.
[10] Trincavelli ML, Da Pozzo E, Daniele S, Martini C. The GABAA-BZR complex as target for the development of anxiolytic drugs. Curr Top Med Chem 2012;12:254–69.
[11] Knabl J, Witschi R, Hosl K, Reinold H, Zeilhofer UB, Ahmadi S, et al. Reversal of pathological pain through specific spinal GABAA receptor subtypes. Nature 2008;451:330–4.
[12] Lipinski CA, Lombardo F, Dominy BW, Feeney PJ. Experimental and computational approaches to estimate solubility and permeability in drug discovery and development settings. Adv Drug Deliv Rev 1997;23:3–25.
[13] Khom S, Baburin I, Timin EN, Hohaus A, Sieghart W, Hering S. Pharmacological properties of GABAA receptors containing gamma1 subunits. Mol Pharmacol 2006;69:640–9.
[14] Boileau AJ, Baur R, Sharkey LM, Sigel E, Czajkowski C. The relative amount of cRNA coding for gamma2 subunits affects stimulation by benzodiazepines in GABA(A) receptors expressed in Xenopus oocytes. Neuropharmacology 2002;43:695–700.
[15] Krishek BJ, Moss SJ, Smart TG. Homomeric beta 1 gamma-aminobutyric acid A receptor-ion channels: evaluation of pharmacological and physiological properties. Mol Pharmacol 1996;49:494–504.
[16] Methfessel C, Witzemann V, Takahashi T, Mishina M, Numa S, Sakmann B. Patch clamp measurements on *Xenopus laevis* oocytes: currents through endogenous channels and implanted acetylcholine receptor and sodium channels. Pflugers Arch 1986;407:577–88.
[17] Baburin I, Beyl S, Hering S. Automated fast perfusion of Xenopus oocytes for drug screening. Pflugers Arch 2006;453:117–23.
[18] Broadwell RD, Salcman M, Kaplan RS. Morphologic effect of dimethyl sulfoxide on the blood-brain barrier. Science 1982;217:164–6.
[19] Khom S, Strommer B, Ramharter J, Schwarz T, Schwarzer C, Erker T, et al. Valerenic acid derivatives as novel subunit-selective GABAA receptor ligands – in vitro and in vivo characterization. Br J Pharmacol 2010;161:65–78.
[20] Loacker S, Sayyah M, Wittmann W, Herzog H, Schwarzer C. Endogenous dynorphin in epileptogenesis and epilepsy: anticonvulsant net effectvia kappa opioid receptors. Brain 2007;130:1017–28.
[21] Rawls SM, Benamar K. Effects of opioids, cannabinoids, and vanilloids on body temperature. Front Biosci (Schol Ed) 2011;3:822–45.
[22] Hui KM, Huen MS, Wang HY, Zheng H, Sigel E, Baur R, et al. Anxiolytic effect of wogonin, a benzodiazepine receptor ligand isolated from *Scutellaria baicalensis* Georgi. Biochem Pharmacol 2002;64:1415–24.
[23] Huen MS, Hui KM, Leung JW, Sigel E, Baur R, Wong JT, et al. Naturally occurring 2′-hydroxyl-substituted flavonoids as high-affinity benzodiazepine site ligands. Biochem Pharmacol 2003;66:2397–407.
[24] Marder M, Viola H, Wasowski C, Fernandez S, Medina JH, Paladini AC. 6-methylapigenin and hesperidin: new valeriana flavonoids with activity on the CNS. Pharmacol Biochem Behav 2003;75:537–45.
[25] Yang X, Baburin I, Plitzko I, Hering S, Hamburger M. HPLC-based activity profiling for GABAA receptor modulators from the traditional Chinese herbal drug Kushen (Sophora flavescens root). Mol Divers 2011;15:361–72.
[26] Granger RE, Campbell EL, Johnston GA. (+)- And (−)-borneol: efficacious positive modulators of GABA action at human recombinant alpha1beta2gamma2L GABA(A) receptors. Biochem Pharmacol 2005;69:1101–11.
[27] Garcia DA, Bujons J, Vale C, Sunol C. Allosteric positive interaction of thymol with the GABAA receptor in primary cultures of mouse cortical neurons. Neuropharmacology 2006;50:25–35.
[28] Zaugg J, Ebrahimi SN, Smiesko M, Baburin I, Hering S, Hamburger M. Identification of GABA A receptor modulators in Kadsura longipedunculata and assignment of absolute configurations by quantum-chemical ECD calculations. Phytochemistry 2011;72:2385–95.
[29] Khom S, Baburin I, Timin E, Hohaus A, Trauner G, Kopp B, et al. Valerenic acid potentiates and inhibits GABA(A) receptors: molecular mechanism and subunit specificity. Neuropharmacology 2007;53:178–87.
[30] Benke D, Barberis A, Kopp S, Altmann KH, Schubiger M, Vogt KE, et al. GABA A receptors as in vivo substrate for the anxiolytic action of valerenic acid, a major constituent of valerian root extracts. Neuropharmacology 2009;56:174–81.
[31] Zaugg J, Eickmeier E, Ebrahimi SN, Baburin I, Hering S, Hamburger M. Positive GABA(A) receptor modulators from Acorus calamus and structural analysis of (+)-dioxosarcoguaiacol by 1D and 2D NMR and molecular modeling. J Nat Prod 2011;74:1437–43.
[32] Zaugg J, Khom S, Eigenmann D, Baburin I, Hamburger M, Hering S. Identification and characterization of GABA(A) receptor modulatory diterpenes from Biota orientalis that decrease locomotor activity in mice. J Nat Prod 2011;74:1764–72.
[33] Cicek SS, Khom S, Taferner B, Hering S, Stuppner H. Bioactivity-guided isolation of GABA(A) receptor modulating constituents from the rhizomes of Actaea racemosa. J Nat Prod 2010;73:2024–8.
[34] Baur R, Simmen U, Senn M, Sequin U, Sigel E. Novel plant substances acting as beta subunit isoform-selective positive allosteric modulators of GABAA receptors. Mol Pharmacol 2005;68:787–92.
[35] Taferner B, Schuehly W, Huefner A, Baburin I, Wiesner K, Ecker GF, et al. Modulation of GABAA-receptors by honokiol and derivatives: subtype selectivity and structure-activity relationship. J Med Chem 2011;54:5349–61.
[36] Zaugg J, Eickmeier E, Rueda DC, Hering S, Hamburger M. HPLC-based activity profiling of Angelica pubescens roots for new positive GABAA receptor modulators in Xenopus oocytes. Fitoterapia 2011;82:434–40.
[37] Singhuber J, Baburin I, Ecker GF, Kopp B, Hering S. Insights into structure-activity relationship of GABAA receptor modulating coumarins and furanocoumarins. Eur J Pharmacol 2011;668:57–64.
[38] Nieto-Posadas A, Jara-Oseguera A, Rosenbaum T. TRP channel gating physiology. Curr Top Med Chem 2011;11:2131–50.
[39] Jancso-Gabor A, Szolcsanyi J, Jancso N. Irreversible impairment of thermoregulation induced by capsaicin and similar pungent substances in rats and guinea-pigs. J Physiol 1970;206:495–507.
[40] Löw K, Crestani F, Keist R, Benke D, Brünig I, Benson JA, et al. Molecular and neuronal substrate for the selective attenuation of anxiety. Science 2000;290(5489):131–4.
[41] Dias R, Sheppard WF, Fradley RL, Garrett EM, Stanley JL, Tye SJ, et al. Evidence for a significant role of alpha 3-containing GABAA receptors in mediating the anxiolytic effects of benzodiazepines. J Neurosci 2005;25:10682–88.
[42] Fu M, Xie Z, Zuo H. TRPV1: a potential target for antiepileptogenesis. Med Hypotheses 2009;73:100–2.
[43] Bhaskaran MD, Smith BN. Effects of TRPV1 activation on synaptic excitation in the dentate gyrus of a mouse model of temporal lobe epilepsy. Exp Neurol 2010;223:529–36.
[44] Baylie RL, Brayden JE. TRPV channels and vascular function. Acta Physiol (Oxf) 2011;203:99–116.

4.1.2 Efficient Modulation of $GABA_A$ receptors by Piperine Derivatives

J Med Chem. 2014 Jul 10;57(13):5602-19. doi: 10.1021/jm5002277. Epub 2014 Jun 27. PMID: 24905252

Angela Schöffmann[†], Laurin Wimmer[‡], Daria Goldmann[§], Sophia Khom[†], Juliane Hintersteiner[†], Igor Baburin[†], Thomas Schwarz[§,▽], Michael Hintersteininger[§], Peter Pakfeifer[†], Mouhssin Oufir[∥], Matthias Hamburger[∥], Thomas Erker[§], Gerhard F. Ecker[§], Marko D. Mihovilovic[‡], and Steffen Hering[†]

[†]Department of Pharmacology and Toxicology and [§]Division of Drug Design and Medicinal Chemistry, Department of Pharmaceutical Chemistry, University of Vienna, Althanstrasse 14, A-1090 Vienna, Austria

[‡]Institute of Applied Synthetic Chemistry, Vienna University of Technology, Getreidemarkt 9, A-1060 Vienna, Austria

[∥]Pharmaceutical Biology, Department of Pharmaceutical Sciences, University of Basel, Klingelbergstrasse 50, CH-4056 Basel, Switzerland

[▽](T.S.) Institute of Medical Genetics Medical University of Vienna, Waehringerstrasse 10, 1090 Vienna, Austria

Contribution Statement: *Investigation of modulatory activity of all derivatives through $GABA_A$ receptors and preliminary studies of TRPV1 agonism and antagonism, writing of the manuscript (introduction, in vitro pharmacological results and discussion part) and preparation of figures were my contributions to this work.*

For Supporting Information see Appendix 7.1.

Journal of Medicinal Chemistry

Article

pubs.acs.org/jmc

Efficient Modulation of γ-Aminobutyric Acid Type A Receptors by Piperine Derivatives

Angela Schöffmann,[†,⊥] Laurin Wimmer,[‡,⊥] Daria Goldmann,[§,⊥] Sophia Khom,[†] Juliane Hintersteiner,[†] Igor Baburin,[†] Thomas Schwarz,[§,▽] Michael Hintersteininger,[§] Peter Pakfeifer,[†] Mouhssin Oufir,[∥] Matthias Hamburger,[∥] Thomas Erker,[§] Gerhard F. Ecker,[§] Marko D. Mihovilovic,[‡] and Steffen Hering*[,†]

[†]Department of Pharmacology and Toxicology and [§]Division of Drug Design and Medicinal Chemistry, Department of Pharmaceutical Chemistry, University of Vienna, Althanstrasse 14, A-1090 Vienna, Austria

[‡]Institute of Applied Synthetic Chemistry, Vienna University of Technology, Getreidemarkt 9, A-1060 Vienna, Austria

[∥]Pharmaceutical Biology, Department of Pharmaceutical Sciences, University of Basel, Klingelbergstrasse 50, CH-4056 Basel, Switzerland

Supporting Information

ABSTRACT: Piperine activates TRPV1 (transient receptor potential vanilloid type 1 receptor) receptors and modulates γ-aminobutyric acid type A receptors ($GABA_AR$). We have synthesized a library of 76 piperine analogues and analyzed their effects on $GABA_AR$ by means of a two-microelectrode voltage-clamp technique. $GABA_AR$ were expressed in *Xenopus laevis* oocytes. Structure−activity relationships (SARs) were established to identify structural elements essential for efficiency and potency. Efficiency of piperine derivatives was significantly increased by exchanging the piperidine moiety with either *N*,*N*-dipropyl, *N*,*N*-diisopropyl, *N*,*N*-dibutyl, *p*-methylpiperidine, or *N*,*N*-bis(trifluoroethyl) groups. Potency was enhanced by replacing the piperidine moiety by *N*,*N*-dibutyl, *N*,*N*-diisobutyl, or *N*,*N*-bistrifluoroethyl groups. Linker modifications did not substantially enhance the effect on $GABA_AR$. Compound **23** [(2*E*,4*E*)-5-(1,3-benzodioxol-5-yl)-*N*,*N*-dipropyl-2,4-pentadienamide] induced the strongest modulation of $GABA_A$ (maximal GABA-induced chloride current modulation ($I_{GABA\text{-}max}$ = 1673% ± 146%, EC_{50} = 51.7 ± 9.5 μM), while **25** [(2*E*,4*E*)-5-(1,3-benzodioxol-5-yl)-*N*,*N*-dibutyl-2,4-pentadienamide] displayed the highest potency (EC_{50} = 13.8 ± 1.8 μM, $I_{GABA\text{-}max}$ = 760% ± 47%). Compound **23** induced significantly stronger anxiolysis in mice than piperine and thus may serve as a starting point for developing novel $GABA_AR$ modulators.

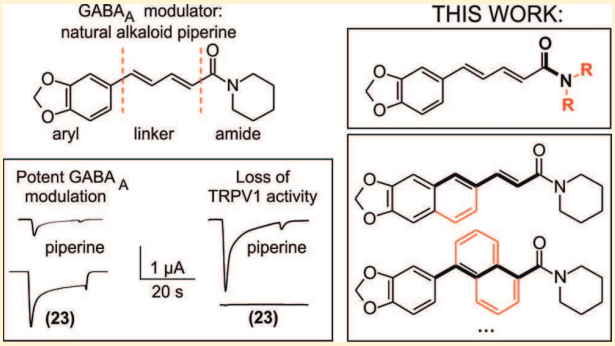

INTRODUCTION

γ-Aminobutyric acid type A ($GABA_A$) receptors are the major inhibitory neurotransmitter receptors in mammalian brain.[1−3] $GABA_A$ receptors belong to the superfamily of Cys loop ligand-gated ion channels. Five receptor subunits form a central chloride-conducting pore.[4−6] Nineteen genes encoding different subunits have been discovered in the human genome, comprising α_{1-6}, β_{1-3}, γ_{1-3}, δ, ε, θ, π, and ρ_{1-3}.[7,8] Different subunit combinations may theoretically form a vast number of receptor subtypes with different pharmacological properties (see ref 9 for review). There is consensus that the most abundantly occurring receptor subtype is formed of two α_1, two β_2, and one γ_2 subunits ($\alpha_1\beta_2\gamma_2$ receptor).[10−12]

Drugs that enhance chloride currents through $GABA_A$ receptors play an important role in the treatment of general anxiety, panic disorders, sleep disturbances, and epilepsy.[13−17] The most widely used benzodiazepines induce, however, a variety of side effects including dependence, unwanted sedation, and amnesia, complicating their long-term use.[18−20] Hence, there is high unmet medical need for $GABA_A$ receptor modulators lacking these unwanted effects.

Besides their modulation by clinically used drugs such as benzodiazepines, barbiturates, neurosteroids, and anesthetics,[3,9,15,21−27] $GABA_A$ receptors are modulated by numerous natural products that may provide lead structures for drug development.[28−30]

In this context, we[31] and others[32] have reported that piperine (1-piperoylpiperidine), the pungent component of several pepper species and activator of transient receptor potential vanilloid type 1 receptor (TRPV1),[33] also modulates $GABA_A$ receptors. We could establish that replacing the piperidine ring of piperine by a *N*,*N*-diisobutyl residue, resulting in (2*E*,4*E*)-5-(1,3-benzodioxol-5-yl))-*N*,*N*-diisobutyl-2,4-pentadienamide (SCT-66;[34] referred to as **24** in this work), diminishes the interaction with TRPV1 receptors. Furthermore, **24** enhanced

Received: February 15, 2014
Published: June 6, 2014

chloride currents through $GABA_A$ receptors more potently and more efficiently than piperine and displayed, concordantly, a stronger anxiolytic action.[34]

Based on these findings, a library of piperine derivatives was synthesized and investigated with respect to modulation of $\alpha_1\beta_2\gamma_{2S}$ $GABA_A$ receptors expressed in *Xenopus laevis* oocytes. Within this study we emphasized modifications at the amide functionality and on the diene motif within piperine in order to enhance the modulatory potential of analogue structures. Their structure−activity relationship on $GABA_A$ receptors was analyzed by establishing binary classification models.

RESULTS AND DISCUSSION

Modification of Amide Nitrogen. Starting with piperine as lead structure from prior biological assessment, the molecule can be structurally divided into three parts: the 1,3-benzodioxole or aromatic function, the olefinic linker region comprising four carbon atoms, and the amide function natively constituted by a piperidine ring (Figure 1). Within this study, we investigated modifications at the amide group as well as in the linker region.

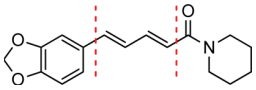

Figure 1. Piperine molecule can be structurally divided into three moieties: the 1,3-benzodioxole or aromatic function, the linker region comprising four carbon atoms, and the amide function natively constituted by a piperidine ring.

Modifications at the amide function were implemented in a straightforward fashion (Scheme 1). Piperic acid amides (**1**−**16**, **20**−**23**, and **25**−**43**) were synthesized by treating piperic acid chloride with the corresponding amine in the presence of triethylamine in tetrahydrofuran (THF). Compounds **17** and **18** were prepared in the same way from benzodioxolyl acryloyl chloride. Treatment of piperine with Lawesson's reagent[35] gave thioamide **44**. Reduction of the carbonyl group of piperine with lithium aluminum hydride afforded unsaturated amine **45** (Scheme 2).

First, we studied the effects of systematic modifications of the amide nitrogen on I_{GABA} modulation through $\alpha_1\beta_2\gamma_{2S}$ receptors. As illustrated in Figure 2A,B, 10 compounds (**22**, **23**, **25**, **28**, **33**, **34**, **35**, **38**, and **43**) at 100 μM induced stronger I_{GABA} modulation than piperine (≥220%)[31] and were classified as highly active. I_{GABA} potentiation of these compounds ranged between 294% ± 66% (**28**) and 1091% ± 257% (**23**, see Table 1). At this concentration, three derivatives (**17**, **30**, and **39**) were less efficient, while the other compounds did not significantly modulate I_{GABA} (see Figure 2A,B and Table 1).

Five derivatives of this first set (**22**, **23**, **25**, **35**, and **43**) with amide modifications enhanced I_{GABA} through $\alpha_1\beta_2\gamma_{2S}$ $GABA_A$ receptors with higher efficiency ($I_{GABA\text{-}max}$: **23** > **22** > **25** > **35**) and/or higher potency (EC_{50}: **25** < **43**) than piperine (Figure 2C,D and Table 2).

***N,N*-Dipropyl-Substituted Compounds 22 And 23 Display the Highest Efficiency.** Compounds **22** (*N*,*N*-dipropyl) and **23** (*N*,*N*-diisopropyl) modulated I_{GABA} most efficiently ($I_{GABA\text{-}max}$ for **22**, 1581% ± 74%; $I_{GABA\text{-}max}$ for **23**, 1673% ± 146%; $I_{GABA\text{-}max}$ for piperine, 302% ± 27%). Compounds **35** ($I_{GABA\text{-}max}$ 733% ± 60%) and **25** ($I_{GABA\text{-}max}$ 760% ± 47%) were less efficient, underscoring the important role of a noncyclic disubstituted amide motif (Figure 2C).

***N,N*-Dibutyl-Substituted Compound 25 Displays the Highest Potency.** Figure 2D illustrates I_{GABA} modulation by the most potent N-substituted piperine derivative (EC_{50} for **25**, 13.8 ± 1.8 μM < EC_{50} for **43**, 23.1 ± 3.3 μM < EC_{50} for piperine, 52.4 ± 9.4 μM[31]). Based on the modifications at the amide group, it can be concluded that installation of noncyclic substituents bearing 3−4 carbons each at the tertiary amide improves both efficacy and potency of the analogue compounds.

Rigidification of the Linker Region Has No Significant Effect on I_{GABA} Modulation. The influence of linker rigidity on I_{GABA} modulation was studied by means of a library comprising 32 linker derivatives. According to Zaugg et al.[31] and Pedersen et al.,[32] a carbon chain containing at least four carbons, a conjugated double bond adjacent to the amide group, and a bulky amine moiety seem to facilitate efficient receptor binding and/or I_{GABA} modulation.

Based on previous reports by Zaugg et al.,[31] we hypothesized that rigidification of the linker part of the structure may beneficially affect biological activity.[31] This assessment was based in particular on a decrease in modulatory capacity when partially saturated linkers were installed or when structural flexibility was increased by extending the linker length.

Three major structural modifications were envisaged (Scheme 1). (i) Replacement of the linker by an aryl ring (phenyl, heteroaryl, naphthyl): in this arrangement, both alkene groups of the diene system of the linker would be integrated into the rigid aromatic core. (ii) Integration of one linker double bond into a naphthyl ring: this compound class was expected to render more flexibility but still adopt a more rigidified system compared to the piperine diene structure; moreover, arrangement should allow for different angles of the aryl core relative to the amide anchoring group depending on the substitution site at the naphthyl system. (iii) "Ring closure" of the diene motif with the aryl part, consequently generating a carboxylate-substituted naphthyl lead structure: in this arrangement the double bond adopts a bent geometry, and again different angles of the aryl and amide parts can be obtained depending on the substitution site.

For the synthesis of aryl-bridged compounds, two different methods were utilized. For a number of products (**46**, **49**, **53**, and **58**−**64**) (Scheme 3), the corresponding bromo-substituted aromatic carboxylic acids were reacted with 3,4-(methylenedioxy)phenylboronic acid under Suzuki−Miyaura cross-coupling conditions.[36] The resulting bis(aryl)carboxylic acids were converted to the final amide products via the corresponding acid chloride intermediates. Alternatively, the corresponding bromobenzoic acid amides were prepared prior to the coupling step. Subsequent Suzuki−Miyaura coupling with 3,4-(methylenedioxy)phenylboronic acid afforded the final products **47**, **48**, **50**−**52**, and **54**−**57** (Scheme 3).

In order to access the 5-position of the naphtho[2,3-*d*]dioxole core, naphtho[2,3-*d*]dioxol-5-ol triflate was chosen as a precursor.[37] Heck coupling[38] employing methyl acrylate afforded **65a**, which gave acrylic acid **65b** after cleavage of the methyl ester (Scheme 4). Amide formation yielded the final products **65**−**67**.

Iridium-catalyzed direct borylation[39] of naphtho[2,3-*d*]-dioxole allowed direct access to the 6-position of the naphtho[2,3-*d*]dioxole core. Boronic acid ester **68a** obtained in this step was converted into the corresponding bromide[40]

dx.doi.org/10.1021/jm5002277 | J. Med. Chem. 2014, 57, 5602−5619

Scheme 1. Structural Modifications of the Piperine Scaffold

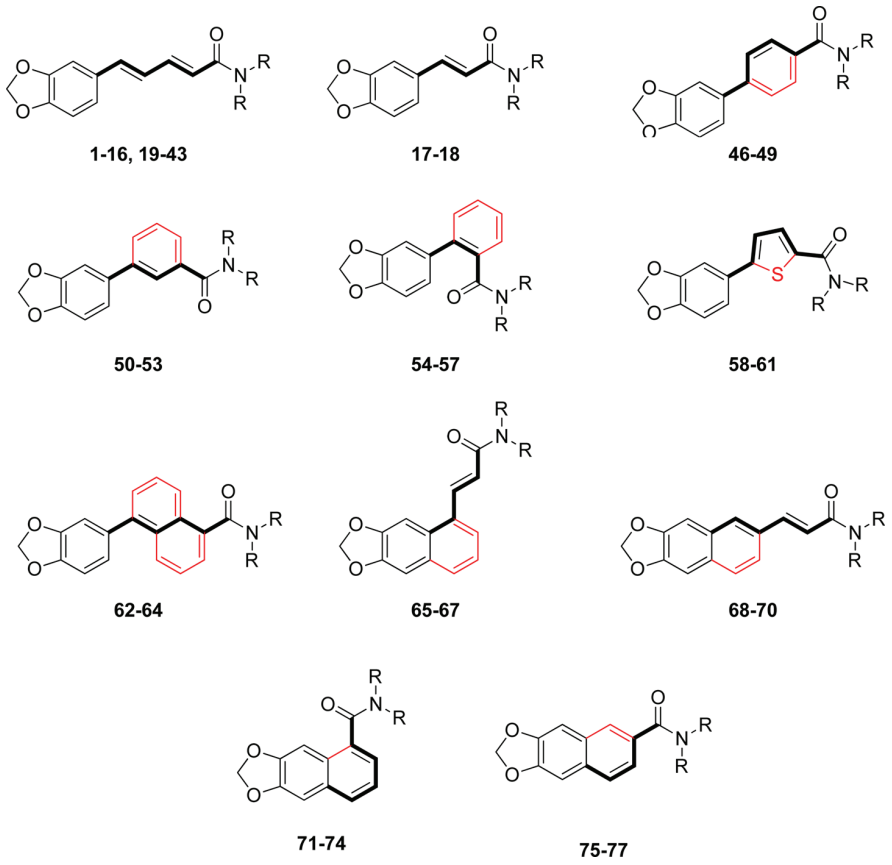

68b and coupled under standard Heck cross-coupling conditions to afford acrylate **68c** (Scheme 4). The methyl ester was hydrolyzed, and acid **68d** was converted into products **68**–**70** (Scheme 4).

Naphthodioxol-5-ol triflate was also used in a palladium-catalyzed hydroxycarbonylation reaction[41] to provide access to carboxylic acid **71a**, which was further converted to products **71**–**74** (Scheme 4). A different route was chosen to synthesize derivatives of naphtodioxole-6-carboxylic acid: By treating bis(bromomethyl)benzodioxole with iodide, a highly reactive diene was generated in situ,[42] which was intercepted with methyl acrylate in a Diels–Alder reaction. The resulting decaline derivative **75a** was oxidized with 2,3-dichloro-5,6-dicyano-1,4-benzoquinone (DDQ) to afford naphthaline **75b**. Saponification of the methyl ester gave carboxylic acid **75c**, which was further converted to final products **75**–**77** (Scheme 4).

At 100 μM, five compounds (**47**, **51**, **53**, **72**, and **73**) modulated I_{GABA} more efficiently than piperine (see Figure 3A,B and Table 2). I_{GABA} potentiation ranged from 280% ± 52% (**51**) to 514% ± 76% (**72**). I_{GABA} enhancement by **46**, **50**, **52**, **69**, **75**, **76**, and **77** was less pronounced compared to piperine [I_{GABA} potentiation range 42% ± 1% (**46**) to 178% ± 30% (**50**)]. None of the other derivatives induced significant I_{GABA} enhancement (see Figure 3A,B and Table 2).

Concentration–response curves of I_{GABA} modulation by linker-modified derivatives **47**, **53**, **56**, **72**, and **73** are illustrated in Figure 3C,D. The combination of *N*,*N*-dipropyl amide from the series **1**–**45** with the two most efficient modifications in the linker region (1,4-phenylene and naphthodioxol-5-yl) resulted in **47** ($I_{GABA\text{-}max}$ = 603% ± 87%, EC_{50} = 70.8 ± 21.1 μM), **72** ($I_{GABA\text{-}max}$ = 706% ± 58%, EC_{50} = 102.0 ± 11.2 μM), and **73** ($I_{GABA\text{-}max}$ = 480% ± 85%, EC_{50} = 31.8 ± 5.3 μM) inducing stronger I_{GABA} enhancement than piperine (Table 3). These findings underscore the general validity of favorable N,N-functionalization also for this series of linker-modified compounds. However, none of the modifications led to compounds with a higher activity than the initial parent compound **23**.

Selectivity Profile. Previously, we have shown that **24**[34] [(2*E*,4*E*)-5-(1,3-benzodioxol-5-yl)-*N*,*N*-diisobutyl-2,4-pentadienamide] similarly modulates $GABA_A$ receptors containing either $\beta_{2/3}$ or β_1 subunits, in contrast to the preferential modulation of $\beta_{2/3}$ receptors by piperine.[34]

In the present study, analysis of the most efficient piperine derivative (**23**) revealed that $GABA_A$ receptors composed of $\alpha_1\beta_2\gamma_{2S}$ ($I_{GABA\text{-}max}$ = 1673% ± 146%) and $\alpha_5\beta_2\gamma_{2S}$ ($I_{GABA\text{-}max}$ = 1624% ± 156%) subunits were more efficiently modulated than receptors containing $\alpha_3\beta_2\gamma_{2S}$ subunits ($I_{GABA\text{-}max}$ = 1284.6% ± 142%; see Table 4). Significantly weaker potentiation was observed for receptors composed of $\alpha_2\beta_2\gamma_{2S}$ ($I_{GABA\text{-}max}$ = 980% ± 129%) and $\alpha_4\beta_2\gamma_{2S}$ subunits ($I_{GABA\text{-}max}$ = 1316% ± 55%). Replacing the β_2 subunits by β_3 subunits did not significantly alter the strength of I_{GABA} potentiation, whereas modulation of $GABA_A$ receptors containing β_1 subunits was significantly less pronounced ($I_{GABA\text{-}max}$ = 1157% ± 69%; $p < 0.05$). In comparison with $\alpha_1\beta_2\gamma_{2S}$ receptors, **23** displayed an increased potency for $\alpha_2\beta_2\gamma_{2S}$ receptors, followed by $\alpha_1\beta_3\gamma_{2S}$, $\alpha_3\beta_2\gamma_{2S}$, and

dx.doi.org/10.1021/jm5002277 | *J. Med. Chem.* 2014, 57, 5602–5619

Scheme 2. Synthesis of Piperine Derivatives with Modification of the Amide Function and Truncated Alkene Spacer[a]

R = H

1	(4-methylthio)phenyl	7	2-(5-chloro)pyridyl	13	cyclopentyl
2	(3,4,5-trimethoxy)phenyl	8	(3-phenyl)propyl	14	benzyl
3	(2,4,6-trifluoro)phenyl	9	(2-hydroxy)phenyl	15	decyl
4	(2-dimethylamino)ethyl	10	(2-hydroxy-4-nitro)phenyl	16	adamantyl
5	(2-(3,4-dimethoxy)phenyl)ethyl	11	butyl		
6	3-pyridyl	12	(3,3-diphenyl)propyl		

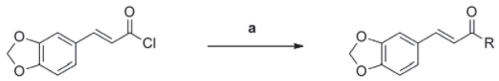

R =

17	piperidinyl	18	-N*i*Pr$_2$

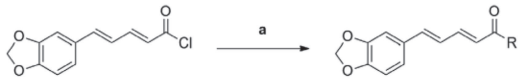

R =

19	piperidinyl	30	thiomorpholinyl	40	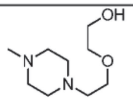
20	-NMe$_2$	31	(4-Me)piperazinyl		
21	-NEt$_2$	32	(4-Et)piperazinyl		
22	-N*i*Pr$_2$	33	(2-Me)piperidinyl	41	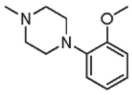
23	-NPr$_2$	34	(3-Me)piperidinyl		
24	-N*i*Bu$_2$	35	(4-Me)piperidinyl		
25	-N*n*Bu$_2$	36	(3-OH)piperidinyl		
26	-N(*n*-hexyl)$_2$	37	(4-OH)piperidinyl	42	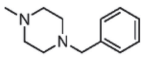
27	-N(cyclohexyl)$_2$	38	(*cis*-2,6-dimethyl)piperidinyl		
28	-N(CH$_2$)$_6$				
29	morpholinyl	39	(3-CF$_3$)piperidinyl	43	-N(CH$_2$CF$_3$)$_2$

X =

44	S	45	H

[a]Conditions: (a) Amine (3.5 equiv), dry THF, rt. (b) Lawesson's reagent, dry THF, rt. (c) $LiAlH_4$, THF, rt.

$\alpha_4\beta_2\gamma_{2S}$ receptors. EC_{50} values for the other receptor subtypes did not differ from those for $\alpha_1\beta_2\gamma_{2S}$ (see Figure 4A,B and Tables 4 and 5).

Like **23**, derivative **25** most efficiently enhanced I_{GABA} through $GABA_A$ receptors composed of $\alpha_1\beta_2\gamma_{2S}$ subunits ($I_{GABA\text{-}max}$ = 760% ± 47%; see Table 4 and Figure 4C,D). Replacing the α_1 subunit by $\alpha_{2/3/4/5}$ subunits significantly reduced I_{GABA} potentiation by **25** (see Table 4 and Figure 4C). Notably, **25** displayed a more pronounced $\beta_{2/3}$ preference compared to piperine or **23** [inducing a 3.9-fold ($\alpha_1\beta_3\gamma_{2S}$) to 5-fold ($\alpha_1\beta_2\gamma_{2S}$) stronger I_{GABA} enhancement compared to $\alpha_1\beta_1\gamma_{2S}$ receptors]. Compound **25** showed comparable potency for most of the tested receptor subtypes ranging from 13.8 ± 1.8 μM to 56.7 ± 21.0 μM; significantly higher EC_{50} values were estimated for $\alpha_1\beta_3\gamma_{2S}$ receptors (see Tables 4 and 6).

These data support the previous observation that when the cyclic piperidine residue is replaced by *N*,*N*-dialkyl moieties such as *N*,*N*-dipropyl (**23**), *N*,*N*-diisopropyl (**24**),[34] or *N*,*N*-dibutyl (**25**), efficiency and potency can be significantly enhanced. However, while **24**[34] lost its ability to distinguish between the β-subunit isoforms, preferential modulation of $\beta_{2/3}$ receptors by **23** was comparable to piperine, and it was even more pronounced for **25** (see Figure 4 B,D and Tables 4–6). Thus, **23** and **25** display—compared to classical $GABA_A$ receptor modulators such as benzodiazepines—a distinct subunit selectivity profile. Unlike benzodiazepines, **23** and **25** also modulate $GABA_A$ receptors containing α_4 subunits with high efficiency and are not dependent on the presence of a γ_{2S} subunit (data not shown). Whether this subunit selectivity profile has any pharmacological relevance has to be clarified in further studies.

dx.doi.org/10.1021/jm5002277 | *J. Med. Chem.* 2014, 57, 5602–5619

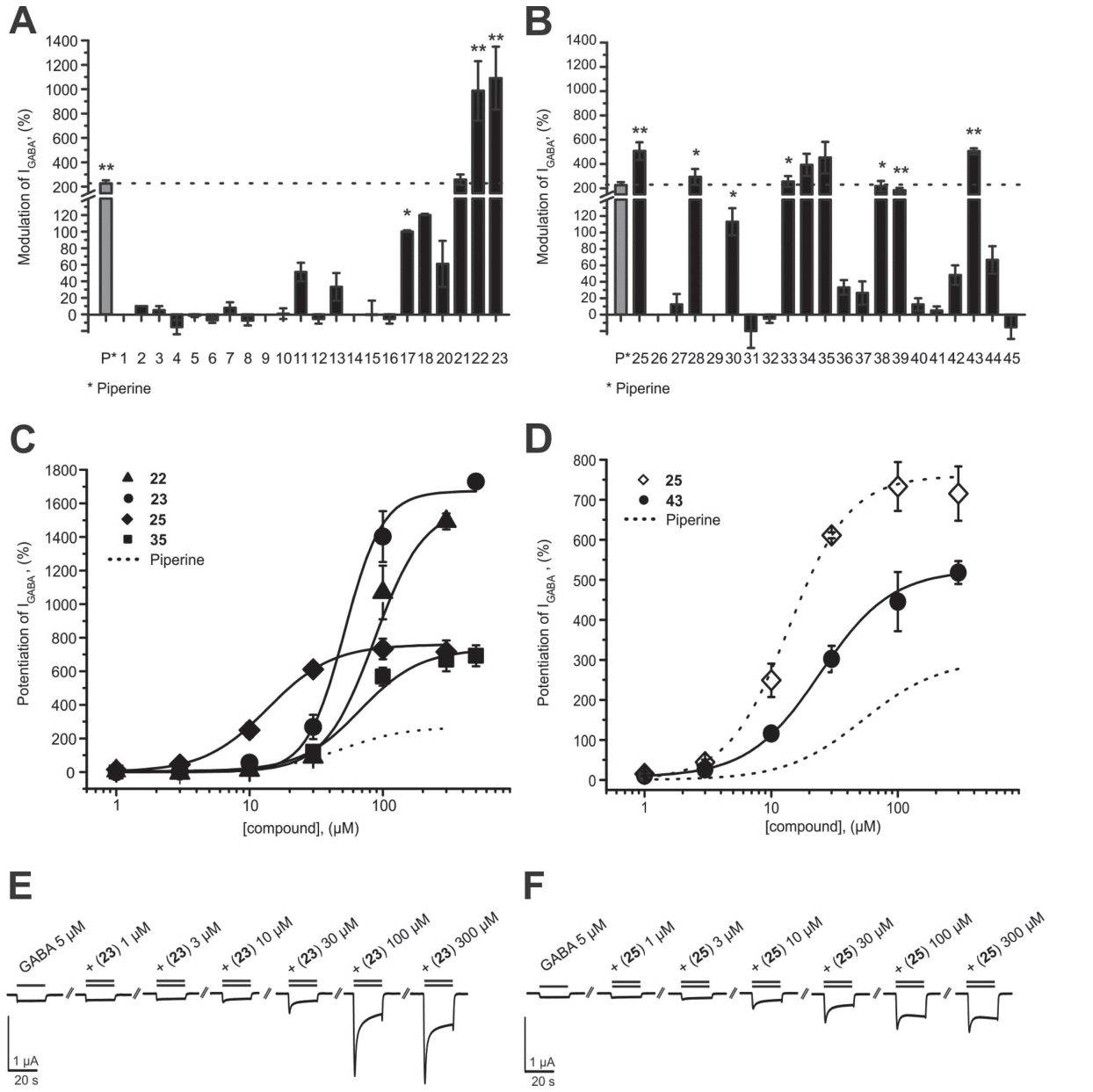

Figure 2. (A, B) Modulation of chloride currents through $GABA_A$ receptors composed of α_1, β_2, and γ_{2S} subunits by 100 μM piperine and the indicated derivatives (dotted line indicates cutoff for highly active compounds). (C, D) Concentration-dependent I_{GABA} (EC_{3-7}) enhancement through $\alpha_1\beta_2\gamma_{2S}$ $GABA_A$ receptors, (C) for **22** (▲), **23** (●), **25** (◆), and **35** (■), ranked by efficiency, and (D) for **25** (○) and **43** (●), ranked by potency, compared to piperine (dotted line). (E, F) Representative I_{GABA} modulated by (E) **23** and (F) **25**. Data represent mean ± SEM from at least three oocytes and two oocyte batches. Asterisks indicate statistically significant differences from zero: $*p < 0.05$, $**p < 0.01$. Data for piperine were taken from ref 31.

Structure–Activity Relationships: General Trends. When the whole data set was analyzed, several distinct SARs could be deduced. They are mostly related to the substitution pattern at the amide nitrogen atom, as this was the main point of variation in the data set. Thus, concerning *N,N*-dialkyl-substituted amides, there is evidence that I_{GABA} enhancement is related in a nonlinear (parabolic) function to the number of carbon atoms (Figure 5), with the optimum being dipropyl (**23**). This type of parabolic relationship is quite common, especially when it refers to a parameter that is linked to lipophilicity of the compounds and activity data obtained in a cellular assay. It has, for example, also been observed for a series of capsaicin analogues with respect to their TRPV1 activation.[43] Interestingly, whether the alkyl chains are linear or branched does not reverse the order: **20** (dimethyl) < **21** (diethyl) < **23** (dipropyl)/**22** (diisopropyl) < **25** (dibutyl)/**24**[34] (diisobutyl) < **26** (dihexyl)/**27** (dicyclohexyl). With respect to compounds where the amide nitrogen atom is part of a ring, methylpiperines **33**, **34**, and **35** induced the strongest I_{GABA} potentiation, followed by azepane amide **28** and piperine. Interestingly, the dimethylpiperine **38** was comparably active to the parent compound. Introduction of a second heteroatom

dx.doi.org/10.1021/jm5002277 | J. Med. Chem. 2014, 57, 5602–5619

Table 1. I_{GABA} Modulation through $\alpha_1\beta_2\gamma_{2S}$ $GABA_A$ Receptors by Indicated Compounds (100 μM)[a]

compd	modulation of I_{GABA} (%)	n	compd	modulation of I_{GABA} (%)	n
1	0 ± 0	3	**25**	506 ± 74**	3
2	10 ± 0	3	**26**	0 ± 0	3
3	5 ± 5	3	**27**	13 ± 13	3
4	−15 ± 9	3	**28**	294 ± 66*	3
5	−2 ± 2	3	**29**	0 ± 0	3
6	−7 ± 3	3	**30**	113 ± 17*	3
7	8 ± 7	3	**31**	−20 ± 20	3
8	−8 ± 6	3	**32**	−5 ± 5	3
9	0 ± 0	3	**33**	359 ± 50*	3
10	1 ± 7	3	**34**	439 ± 31*	3
11	51 ± 11	3	**35**	568 ± 54	3
12	−6 ± 6	3	**36**	33 ± 9	3
13	33 ± 17	3	**37**	26 ± 14	3
14	0 ± 0	3	**38**	218 ± 43*	3
15	−1 ± 17	3	**39**	183 ± 20**	3
16	−6 ± 6	3	**40**	12 ± 8	3
17	79 ± 8*	3	**41**	5 ± 5	3
18	66 ± 30	3	**42**	48 ± 12	3
20	61 ± 28	3	**43**	445 ± 74**	3
21	258 ± 28	3	**44**	17 ± 17	3
22	986 ± 244*	3	**45**	−16 ± 14	3
23	1091 ± 257*	3			

[a]All data are given as mean ± SEM. Asterisks indicate statistically significant differences from zero: *p < 0.05, **p < 0.01.

Table 2. I_{GABA} Modulation through $\alpha_1\beta_2\gamma_{2S}$ $GABA_A$ Receptors by Indicated Compounds (100 μM)[a]

compd	modulation of I_{GABA} (%)	n	compd	modulation of I_{GABA} (%)	n
46	42 ± 1**	3	**62**	13 ± 2	3
47	364 ± 55**	3	**63**	12 ± 4	3
48	49 ± 7	3	**64**	4 ± 4	3
49	30 ± 15	3	**65**	105 ± 18	3
50	178 ± 32*	3	**66**	67 ± 23	3
51	280 ± 52**	3	**67**	18 ± 9	3
52	63 ± 12*	3	**68**	−1 ± 12	3
53	298 ± 31**	3	**69**	74 ± 1*	3
54	34 ± 8	3	**70**	32 ± 12	3
55	79 ± 24	3	**71**	32 ± 10	3
56	114 ± 11	3	**72**	334 ± 23**	3
57	15 ± 15	3	**73**	514 ± 76**	3
58	−5 ± 12	3	**74**	60 ± 17	2
59	134 ± 39	3	**75**	58 ± 29*	3
60	51 ± 21	3	**76**	122 ± 26*	3
61	11 ± 2	3	**77**	138 ± 29*	3

[a]All data are given as mean ± SEM. Asterisks indicate significant differences from zero: *p < 0.05, **p < 0.01.

into the ring led to almost complete loss of I_{GABA} enhancement (*N*-alkylpiperazine amides **31**, **32**, **40**, **41**, and **42** and morpholine amide **29**).

Replacement of the tertiary nitrogen atom for a secondary one, irrespective of alkyl or aryl substitution, led to a complete loss of activity (aryl-substituted N, **1**−**3**, **5**−**7**, **9**, and **10**; alkyl-substituted N, **4**, **8**, and **11**−**16**). Reducing the H-bond acceptor strength of the amide by synthesizing the respective thioamide (**44**) abolished the modulatory activity. Reduction of the amide to the analogous amine changed the profile of the compound from potentiation (piperine at 100 μM, 226% ± 26%)[31] to inactive (**45** at 100 μM, −16% ± 14%; Table 1).

With respect to the linker region, shortening the distance by removing one vinylene unit significantly reduced I_{GABA} enhancement (piperine vs **17** and **22** vs **18**). All the other modifications, such as rigidification by inserting benzene, thiophene, or naphthalene moieties, reduced I_{GABA} potentiation by at least a factor of 5 compared to **23**. Interestingly, the modulatory activity did not seem to be related to distance of pharmacophoric substructures, such as the benzodioxole and the amide moiety. For naphthalene analogues **72** and **65**, an increase in distance led to a decrease of activity, whereas in the case of **22** and **18**, a decrease of distance led to a decrease of activity. Comparing **23** and **70**, which show identical distance of these two moieties, **70** completely lacks activity (32% ± 12%, Table 1). In conclusion, the best compounds achieved in terms of efficiency were the piperine analogues **22** and **23**.

Computational Analysis. In order to rationalize the trends observed in the SAR with respect to physicochemical properties and chemical substructures, we explored the possibility to apply quantitative structure−activity relationship (QSAR) methods. As I_{GABA} potentiation does not allow classical QSAR analysis, binary classification models were built from five methods and three descriptor sets. For these studies, all 76 piperine derivatives described above were employed. Sixteen compounds showing ≥200% I_{GABA} potentiation were assigned to an active class, since they were at least as active as the lead compound piperine. The remaining 60 ligands were assigned to an inactive class. Classification methods comprised instance-based classifier (IBk), J48 decision tree (J48), naïve-Bayes classifier (NB), random forest (RF), and support vector machine (SMO) implemented in the software package WEKA.[44] The software package Molecular Operating Environment (MOE) was used for calculation of 2D descriptors and fingerprints. The three descriptor sets used comprised six 2D descriptors obtained after applying a feature selection algorithm on the whole panel of 125 2D MOE descriptors (6D), 11 physical chemical properties (PHYSCHEM), and MACCS fingerprints (MACCS).

The statistical parameters obtained for the 15 best classification models are listed in Table 7. Most of the models possess reliable quality (except models 11 and 13); that is, values of the Matthews correlation coefficient (MCC) are higher than 0.4 and total accuracy varies from 0.7 to 0.9.

Models 3 and 4, although possessing the best statistical performance parameters, are not discussed further, as they are difficult to interpret. Instead, models 7 and 12 are discussed in more detail, because these models (i) show almost equal performance, (ii) were built using descriptors of physical chemical properties and MACCS fingerprints, (iii) provide clear separation between active and inactive instances, and (iv) allow us to trace back the decisive chemical and structural descriptors for the data set.

The decision tree obtained in model 7 with PHYSCHEM descriptors (Figure 6) uses as a first criterion for separation of active and inactive piperine derivatives: the topological polar surface area. By applying a threshold of 39, 25 inactive ligands exhibiting polar substituents at the amide nitrogen were filtered out. These include compounds **1**−**16** with monosubstituted amide function and compounds **29**, **31**, **32**, **36**, **37**, **40**−**42**, and **44** containing several heteroatoms (e.g., OH groups or an additional nitrogen as in piperazines or both). Thus, application of a single filter decreased the number of inactive ligands in the

Scheme 3. Synthesis of Piperine Analogues Containing an Aryl Spacer[a]

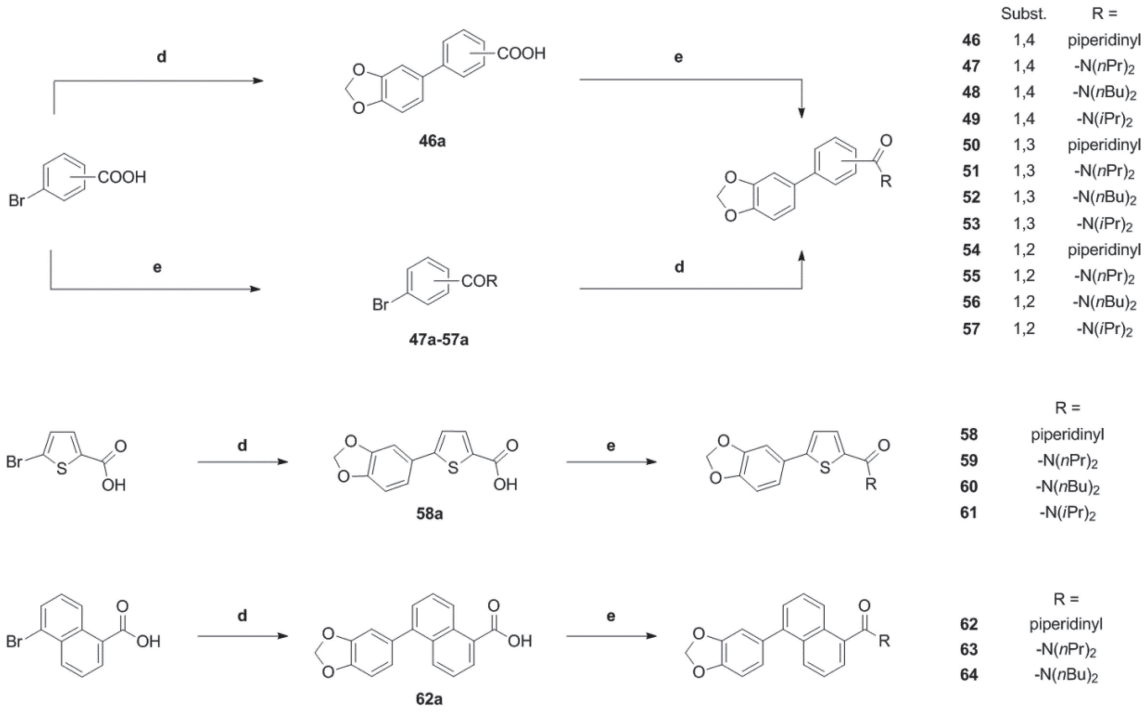

	Subst.	R =
46	1,4	piperidinyl
47	1,4	-N(*n*Pr)$_2$
48	1,4	-N(*n*Bu)$_2$
49	1,4	-N(*i*Pr)$_2$
50	1,3	piperidinyl
51	1,3	-N(*n*Pr)$_2$
52	1,3	-N(*n*Bu)$_2$
53	1,3	-N(*i*Pr)$_2$
54	1,2	piperidinyl
55	1,2	-N(*n*Pr)$_2$
56	1,2	-N(*n*Bu)$_2$
57	1,2	-N(*i*Pr)$_2$

	R =
58	piperidinyl
59	-N(*n*Pr)$_2$
60	-N(*n*Bu)$_2$
61	-N(*i*Pr)$_2$

	R =
62	piperidinyl
63	-N(*n*Pr)$_2$
64	-N(*n*Bu)$_2$

[a]Conditions: (d) Boronic acid, $Pd(PPh_3)_4$ 2 mol %, K_2CO_3, DME/EtOH/water, 140 °C, mw, 1 h. (e) Either $(COCl)_2$, cat. DMF, and DCM or EDCI·HCl, HOBt, and dry DCM, followed by amine.

data set almost by half, from 60 to 35 compounds. In the next branch of the decision tree, 10 compounds with less than four rotatable bonds were excluded from the data set. These included highly rigid piperine derivatives with linker regions modified to either a single double bond (**17**) or to an aromatic system (**46**, **50**, **54**, **58**, **62**, **65**, **68**, **71**, and **75**). Furthermore, 11 compounds with high lipophilicity (log P > 5.2) were filtered out: **26** and **27** with *n*-hexyl and cyclohexyl sustituents at the amide nitrogen, as well as **48**, **52**, **56**, **60**, **64**, **67**, **70**, **77**, and **63**, which have dibutyl and dipropyl substituents in the same region. The fact that the top-ranked compounds are either *N*,*N*-dipropyl-, *N*,*N*-dibutyl-, or *N*,*N*-diisobutyl-substituted is reflected in the next leaf, which assigns five compounds (**23**, **24**,[34] **25**, **43**, and **73**) with more than seven rotatable bonds to the active class. The last two branches of the decision tree filter out compounds on the basis of their molecular weight and refractivity.

The decision tree obtained for model 12 with MACCS fingerprints (Figure 7) is fully in line with the one based on the PHYSCHEM descriptor set. The first filtering criterion was presence or absence of an NH group. It filtered 21 derivatives (**1**−**16**, **31**, **32**, **40**, **42**, and **45**), most of which were those showing high polar surface area (TPSA). The next branching filter was presence of a sulfur atom, which removes six inactive ligands (**30**, **44**, and **58**−**61**) from the data set. The next leaf separates compounds that do not have a six-membered ring as in piperidinyl, cyclohexyl, and morpholinyl, which led to seven correctly classified active ligands (**21**−**23**, **24**,[34] **25**, **28**, and **43**) and three missclassified inactives (**18**, **20**, and **26**). This criterion is in line with the filter "b_rotN > 7" for active compounds in the PHYSCHEM model.

To summarize, active piperine analogues are mainly characterized by a topological polar surface smaller than 39, have at least three rotatable bonds (better more than 7), and show a log P value smaller than 5.2.

Compounds 25 and 23 Induce Anxiolysis in Mice. Activation of TRPV1 by piperine and its derivatives may cause unwanted side effects, including changes in pain sensation and body temperature and induction of fear that would interfere with $GABA_A$-mediated effects[45,46] (for review see ref 47). In order to rule out potential activation of TRPV1, selected compounds were studied in *X. laevis* oocytes for interaction with TRPV1 prior to in vivo characterization. The most potent (**25**) and most efficient (**23**) piperine analogues (Table 3, Figure 2C,D) did not activate TRPV1 expressed in *Xenopus* oocytes (upon application of 100 μM, data not shown). Both compounds were further characterized concerning their anxiolytic activity (see also ref 34).

As illustrated in Figure 8A, male C57BL/6N mice treated with **23** at doses ≥0.3 mg/kg body weight spent significantly more time in the open arms (OA) of the elevated plus maze (EPM) test compared to a saline-treated control group (control, 28.7% ± 2.7% for n = 41; **23** at 0.3 mg/kg, 45.6% ± 3.2% for n = 17; p < 0.01). This effect was dose-dependent and reached its maximum at a dose of 3 mg/kg body weight, indicating strong anxiolytic effects of **23**. Similarly, mice treated with **25** also spent significantly more time in the OA of the EPM test at doses ≥0.3 mg/kg body weight compared to saline-treated control littermates (control, 28.7% ± 2.7% for n = 41; **25** at 0.3 mg/kg, 39.8% ± 4.1% for n = 23; p < 0.05; Figure 8B). The anxiolytic effect of **25** reaching its maximum at a dose of 3 mg/kg body weight (**25** at 3 mg/kg, 43.9% ± 4.3% for n = 12), however, was less pronounced compared to **23**.

Application of doses ≥10 mg/kg of **23** or **25** did not further increase the anxiolytic effect in the EPM, which is presumably due to the concomitant occurring/developing of reduced

dx.doi.org/10.1021/jm5002277 | J. Med. Chem. 2014, 57, 5602−5619

Scheme 4. Synthesis of Piperine Analogues with (Partial) Integration of the Spacer Motif into an Aryl Core[a]

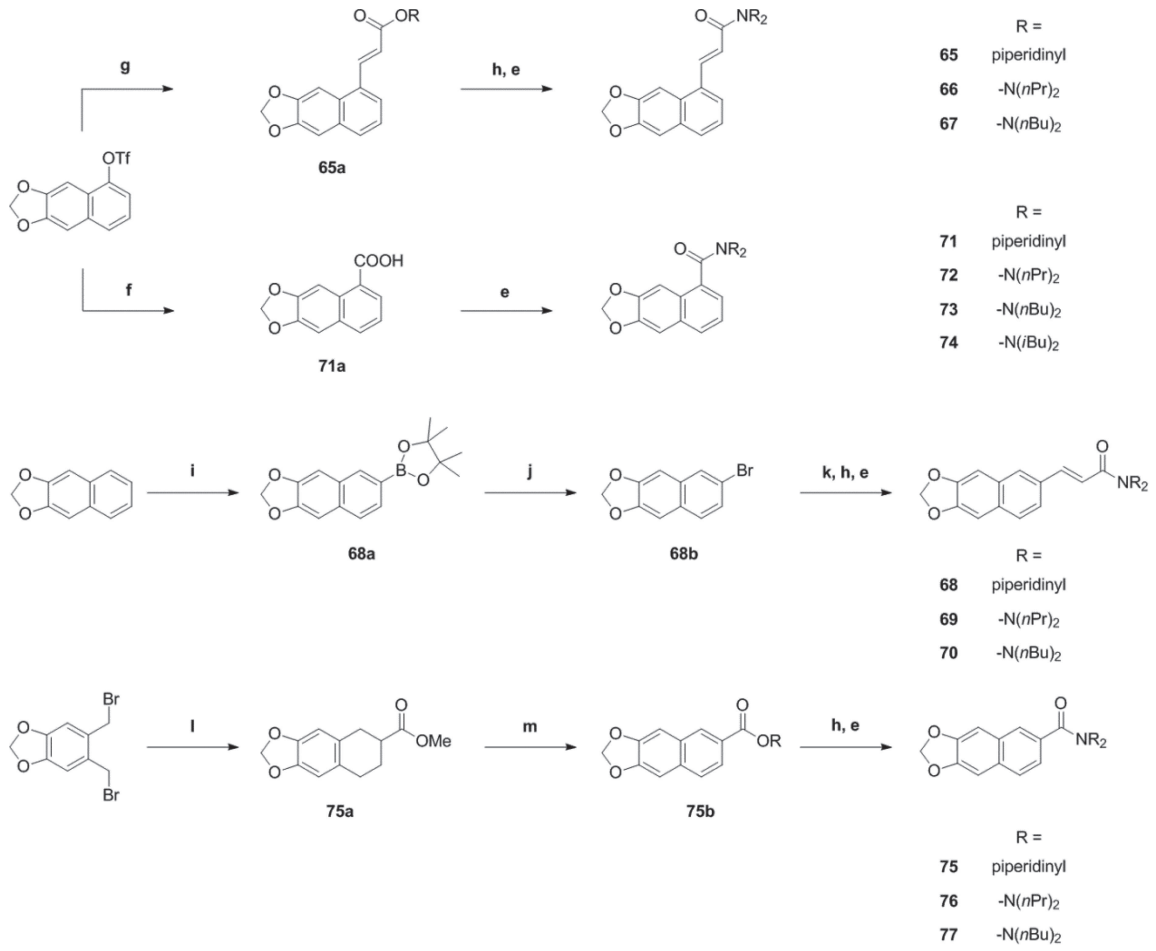

[a]Conditions: (e) Either $(COCl)_2$, cat. DMF, and DCM or EDCI·HCl, HOBt, and dry DCM, followed by amine. (f) CO, $Pd(OAc)_2$, dppp, Hünig's base, DMF/water, 70 °C. (g) Methyl acrylate, $Pd(OAc)_2$ 5 mol %, phenanthroline monohydrate 5.5 mol %, NEt_3, dry DMF. (h) LiOH, THF/water, rt. (i) B_2pin_2, $[Ir(OMe)cod]_2$ 1.5 mol %, 4,4′-di-*tert*-butyl-2,2′-bipyridine 3 mol %, cyclohexane, reflux. (j) $CuBr_2$, MeOH/water. (k) Methyl acrylate, $Pd(OAc)_2$ 3 mol %, (*o*-tolyl)$_3$P 6 mol %, NEt_3, 80 °C. (l) Methyl acrylate, NaI, dry DMF, 90°C. (m) DDQ, benzene, 80 °C.

locomotor activity (see Figure 8C,D for sedative effects in the open field test). Compared to piperine and the previously studied **24**[34] (Figure 8A, shaded bars taken from ref 34), anxiolysis induced by **23** was significantly ($p < 0.05$) more enhanced, which might reflect the stronger I_{GABA} potentiation by **23** and/or the higher potency of **23** on receptors containing $\alpha_{2/3}$ and β_3 subunits. Interestingly, the anxiolytic effect of the most potent and also more efficient derivative **25** did not differ from that of piperine and **24**.[34] It has, thus, to be clarified in further studies to what extent derivatization of the amide moiety affects the anxiolytic properties of piperine derivatives and whether receptors/channels other than $GABA_A$ receptors are targeted in vivo by these compounds.

Significant amounts of **23** and **25** were detected in mouse plasma after intraperitoneal (ip) application (see Table 8). The estimated plasma concentrations were below the micromolar concentrations required for significant I_{GABA} potentiation of $GABA_A$ receptors expressed in *Xenopus* oocytes. However, drugs are commonly less potent on ion channels expressed in *Xenopus* oocytes as compared to channels expressed in either mammalian cells or even native tissues.[48] The metabolite formation of **23** and **25** is currently unknown. At the current stage of our research, we cannot exclude that the observed anxiolytic and sedative effects are induced by more active metabolites. Furthermore, the currently unknown brain-barrier penetration of **23** and **25** and possible tissue accumulation warrants further research.

CONCLUSIONS

Piperine analogues modulating $GABA_A$ receptor with the highest efficiency show a tertiary amide nitrogen, substituted with flexible alkyl chains with a total of 6−8 carbon atoms. Polar substituents as well as rigid substituents give rise to a decrease of activity. Modifications of the linker region that lead to rigidification of the molecules also did not improve efficacy.

Compound **23** [(2*E*,4*E*)-5-(1,3-benzodioxol-5-yl))-*N*,*N*-dipropyl-2,4-pentadienamide] induced the strongest modulation of $GABA_A$ receptors (maximal GABA-induced chloride current enhancement $I_{GABA\text{-}max}$ = 1673.0% ± 146.3% and EC_{50} = 51.7 ± 9.5 μM, vs piperine, $I_{GABA\text{-}max}$ = 302% ± 27% and EC_{50} = 52.4 ± 9.4 μM), while **25** [(2*E*,4*E*)-5-(1,3-benzodioxol-5-yl))-*N*,*N*-dibutyl-2,4-pentadienamide] displayed the highest potency (EC_{50} = 13.8 ± 1.8 μM) but was less efficient than **23** ($I_{GABA\text{-}max}$ = 760% ± 47%). Both piperine analogues did not

dx.doi.org/10.1021/jm5002277 | J. Med. Chem. 2014, 57, 5602−5619

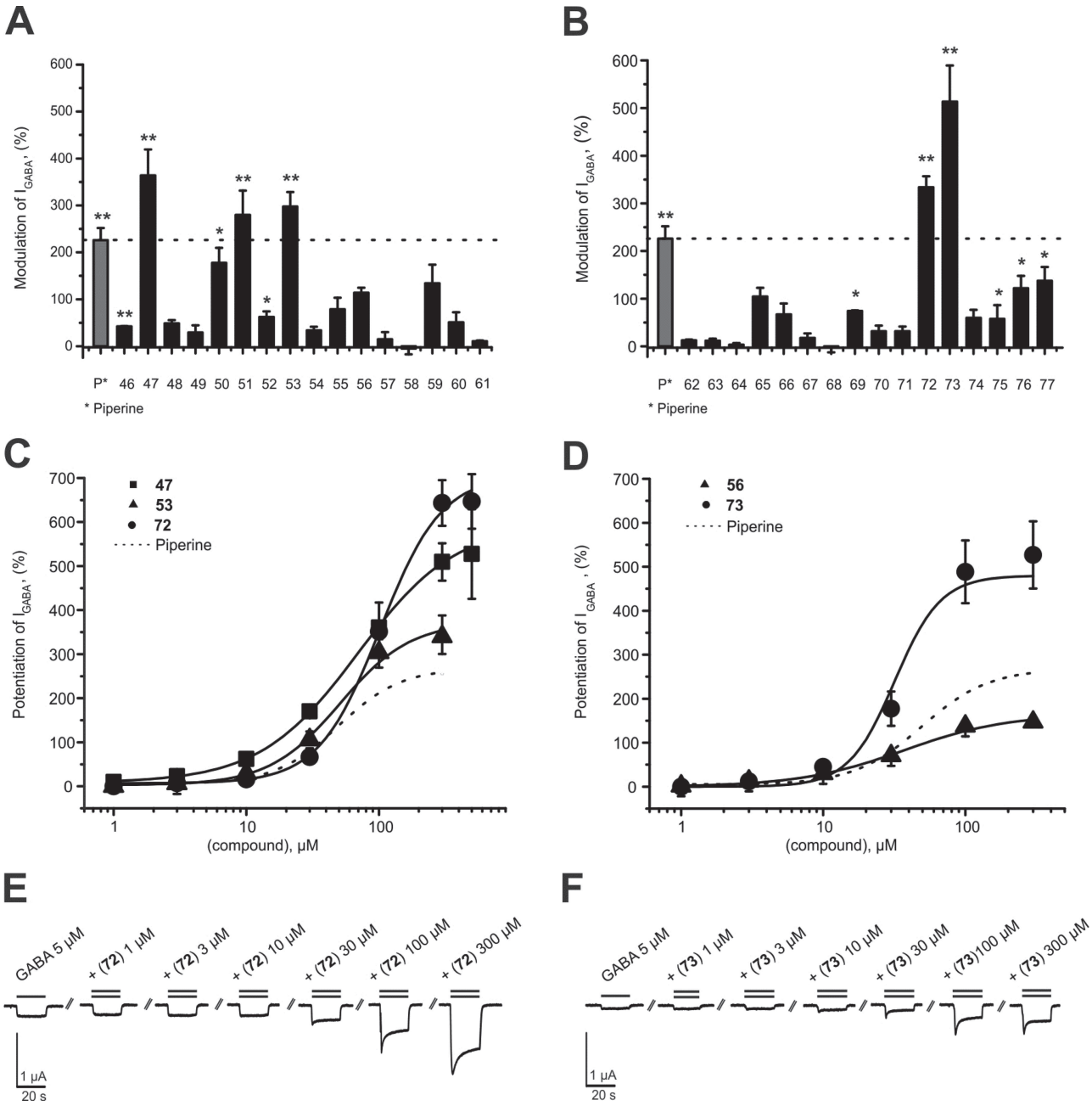

Figure 3. (A, B) Modulation of chloride currents through $GABA_A$ receptors composed of α_1, β_2, and γ_{2S} subunits by 100 μM piperine and the indicated derivatives (dotted line indicates cutoff for highly active compounds). (C, D) Concentration-dependent I_{GABA} (EC_{3-7}) enhancement through $\alpha_1\beta_2\gamma_{2S}$ $GABA_A$ receptors: (C) by **47** (■), **53** (▲), and **72** (●), ranked by efficiency, and (D) by **56** (▲) and **73** (●), ranked by potency, compared to piperine (dotted line). (E, F) Representative I_{GABA} modulated by (E) **72** and (F) **73**. Data represent mean ± SEM from at least three oocytes and two oocyte batches. Asterisks indicate statistically significant differences from zero: $*p < 0.05$, $**p < 0.01$. Data for piperine were taken from ref 31.

activate TRPV1 and induced pronounced anxiolytic action with little sedation, suggesting their potential use as scaffolds for drug development. The established determinants of efficacy may be used for future synthesis of improved $GABA_A$ modulators.

■ EXPERIMENTAL SECTION

Biological Activity. All experiments on animals were carried out in accordance with the Austrian Animal Experimental Law, which is in line with EU Directive 2010/63/EU. Every effort was made to minimize the number of animals used.

Expression of $GABA_A$ Receptors in *Xenopus laevis* Oocytes and Two-Microelectrode Voltage-Clamp Experiments. Preparation of stage V–VI oocytes from *X. laevis* and synthesis of capped runoff poly(A) cRNA transcripts from linearized cDNA templates (pCMV vector) was performed as previously described.[49] Female *X. laevis* frogs (Nasco) were anesthetized by 15 min incubation in a 0.2% MS-222 (methanesulfonate salt of 3-aminobenzoic acid ethyl ester; Sigma–Aldrich, Vienna, Austria) solution before removal of parts of

dx.doi.org/10.1021/jm5002277 | J. Med. Chem. 2014, 57, 5602–5619

Table 3. Efficiency and Potency of Further Characterized Piperine Derivatives and Piperine[a]

compd	$I_{GABA\text{-}max}$ (%)	EC_{50} (μM)	n_H	n
piperine	302 ± 27	52.4 ± 9.3	1.5 ± 0.2	3
22	1581 ± 74**	86.7 ± 13.9	2.3 ± 0.2	6
23	1673 ± 146**	51.7 ± 9.5	3.1 ± 0.8	6
25	760 ± 47**	13.8 ± 1.8**	1.8 ± 0.1	6
35	733 ± 60**	67.7 ± 11.0	1.9 ± 0.3	6
43	505 ± 24**	23.1 ± 3.3*	1.6 ± 0.2	6
47	603 ± 87*	70.8 ± 21.1	1.2 ± 0.2	3
53	388 ± 64	55.3 ± 17.6	1.5 ± 0.2	3
56	165 ± 4**	36.8 ± 2.0	1.2 ± 0.0	3
72	706 ± 58**	102.0 ± 11.2	1.9 ± 0.2	5
73	480 ± 85	31.8 ± 5.3	2.7 ± 0.2	6

[a]From ref 31, including number of experiments n. Asterisks indicate significant differences from piperine: *$p < 0.05$; **$p < 0.01$.

Table 4. Efficiency and Potency of 23 and 25 on $GABA_A$ Receptors of Different Subunit Compositions[a]

receptor subtype	$I_{GABA,max}$ (%)	EC_{50} (μM)	n_H	n
Compound **23**				
$\alpha_1\beta_1\gamma_{2S}$	1157 ± 69*	57.5 ± 7.3	1.8 ± 0.1	5
$\alpha_1\beta_2\gamma_{2S}$	**1673 ± 146**	**51.7 ± 9.5**	**3.1 ± 0.8**	**6**
$\alpha_1\beta_3\gamma_{2S}$	1240 ± 128	34.7 ± 5.7	1.9 ± 0.2	5
$\alpha_2\beta_2\gamma_{2S}$	980 ± 129**	26.4 ± 6.6	1.9 ± 0.4	6
$\alpha_3\beta_2\gamma_{2S}$	1285 ± 142	36.6 ± 7.2	1.9 ± 0.3	5
$\alpha_4\beta_2\gamma_{2S}$	1316 ± 55*	34.7 ± 3.8	1.7 ± 0.1	7
$\alpha_5\beta_2\gamma_{2S}$	1624 ± 156	61.9 ± 10.4	1.4 ± 0.1	7
Compound **25**				
$\alpha_1\beta_1\gamma_{2S}$	152 ± 30**	15.9 ± 4.9	1.3 ± 0.6	5
$\alpha_1\beta_2\gamma_{2S}$	**760 ± 47**	**13.8 ± 1.8**	**1.8 ± 0.1**	**8**
$\alpha_1\beta_3\gamma_{2S}$	587 ± 8**	29.5 ± 2.9**	1.5 ± 0.1	4
$\alpha_2\beta_2\gamma_{2S}$	512 ± 26**	14.8 ± 1.9	2.2 ± 0.3	4
$\alpha_3\beta_2\gamma_{2S}$	617 ± 42*	16.0 ± 2.7	1.8 ± 0.1	6
$\alpha_4\beta_2\gamma_{2S}$	419 ± 73**	56.7 ± 21.0	1.3 ± 0.3	4
$\alpha_5\beta_2\gamma_{2S}$	387 ± 20**	17.2 ± 1.4	1.7 ± 0.2	5

[a]Asterisks indicate significant differences from $\alpha_1\beta_2\gamma_{2S}$ receptor subtype as follows: *$p < 0.05$; **$p < 0.01$.

the ovaries. Follicle membranes from isolated oocytes were enzymatically digested with 2 mg/mL collagenase (type 1A, Sigma–Aldrich, Vienna, Austria).

Selected oocytes were injected with 10–50 nL of DEPC-treated water (diethyl pyrocarbonate, Sigma, Vienna, Austria) containing the different $GABA_A$ cRNAs at a concentration of approximately 300–3000 pg·nL^{-1}·$subunit^{-1}$.

To ensure expression of the γ_{2S} subunit in the case of $\alpha_{1/2/3/5}\beta_{2/3}\gamma_{2S}$ receptors, cRNAs were mixed in a ratio of 1:1:10. For expression of receptors composed of $\alpha_4\beta_2\gamma_{2S}$ and $\alpha_1\beta_1\gamma_{2S}$, cRNAS were mixed in a ratio of 3:1:10. The amount of cRNAs was determined by means of a NanoDrop ND-1000 (Kisker-Biotech, Steinfurt, Germany).

Oocytes were stored at +18 °C in modified ND96 solution (90 mM NaCl, 1 mM $CaCl_2$, 1 mM KCl, 1 mM $MgCl_2 \cdot 6H_2O$, and 5 mM HEPES [4-(2-hydroxyethyl)-1-piperazineethanesulfonic acid], pH 7.4, all from Sigma–Aldrich, Vienna, Austria).

Chloride currents through $GABA_A$ receptors (I_{GABA}) were measured at room temperature (+21 ± 1 °C) by means of a two-microelectrode voltage clamp technique making use of a Turbo TEC-05X amplifier (npi electronic, Tamm, Germany). I_{GABA} were elicited at a holding potential of −70 mV. Data acquisition was carried out by means of an Axon Digidata 1322A interface using pCLAMP v.10 (Molecular Devices, Sunnyvale, CA). The modified ND96 solution was used as bath solution. Microelectrodes were filled with 2 M KCl and had resistances between 1 and 3 MΩ.

Fast Perfusion System. GABA and the studied derivatives were applied by means of the ScreeningTool (npi electronic, Tamm, Germany) fast perfusion system as described previously.[50] To elicit I_{GABA}, the chamber was perfused with 120 μL of GABA- or compound-containing solution at a volume rate of 300 μL/s.[34] Care was taken to account for possible slow recovery from increasing levels of desensitization in the presence of high drug concentrations. The duration of washout periods was therefore extended from 1.5 min (<10 μM compounds) to 30 min (≥10 μM compounds). Oocytes with maximal current amplitudes >3 μA were discarded to exclude voltage clamp errors.

Data Analysis: $GABA_A$ Receptors. Stimulation of chloride currents by modulators of the $GABA_A$ receptor was measured at a GABA concentration eliciting between 3% and 7% of the maximal current amplitude (EC_{3-7}). The GABA EC_{3-7} was determined for each oocyte individually. Enhancement of the chloride current was defined as $(I_{GABA+compd}/I_{GABA}) - 1$, where $I_{GABA+compd}$ is the current response in the presence of a given compound and I_{GABA} is the control GABA current. $I_{GABA\text{-}max}$ reflects the maximal I_{GABA} enhancement. Concentration–response curves were generated and the data were fitted by nonlinear regression analysis using Origin Software (OriginLab Corp.). Data were fitted to the equation $1/(1 + (EC_{50}/[\text{compound}])^{nH})$, where n_H is the Hill coefficient. Each data point represents the mean ± SEM from at least three oocytes and ≥2 oocyte batches. Statistical significance was calculated by paired Student t-test with a confidence interval of <0.05.

Molecular Modeling and Quantitative Structure–Activity Relationships. *Data Set.* The 2D structures of 76 piperine derivatives and piperine were drawn in the InstantJChem package for Excel (www.chemaxon.com/products/jchem-for-excel) and exported in sdf format. The LigPrep tool provided by Schrödinger in the Maestro package (Maestro, version 9.2; Schrödinger LLC, New York, 2011) was used to generate low-energy 3D structures and protonated states. All possible stereoisomers per ligand were computed and one low-energy conformation was generated per each stereoisomer in MMFF force field. The protonated states were determined at pH 7.4 (pH used in the experiments). For compounds **33**, **34**, **36**, **38**, and **39**, several stereisomers were determined. Since these structures were not ionizable at this pH, the stereoisomers were considered equal in terms of 2D structure and duplicates were removed. Subsequently, the structures were imported into MOE, where partial atomic charges were calculated in the MMFF94 force field. Piperine (obtained from Sigma–Aldrich, Vienna, Austria) was used as a reference compound to determine the class labels of its derivatives. Potentiation of GABA current by piperine was 226% ± 26%;[31] therefore, compounds with potentiation ≥200% were assigned to the active class, otherwise to the inactive. This led to an unbalanced data set with 17 "active" and 60 "inactive" compounds.

Descriptor Sets. One hundred forty-three 2D descriptors implemented in MOE were calculated. The full list is provided in Supporting Information (Table S1A). Descriptors showing no variance were removed from the data set, and the remaining 125 descriptors (Supporting Information, Table S1B) underwent feature selection by the BestFirst algorithm implemented in the software package WEKA version 3.7.9. Consequently, the six descriptors left (set 6D) were used for further classification studies (Table 9). Additionally, as a reference descriptor set, we used 11 descriptors of physicochemical properties (set PHYSCHEM) from the list of 125 descriptors described above (Table 10). These descriptors allow us to trace molecular features important for biological activity and have previously shown good performance in application to ligand-based studies.[51] As an attempt to trace the structural features relevant to the activity of piperine derivatives, MACCS fingerprints (MACCS Keys; MDL Information Systems, Inc., San Leandro, CA) were computed in MOE. MACCS are a set of structural keys, where each key describes a small substructure consisting of up to 10 non-hydrogen atoms. A Python script (Supporting Information) was applied to divide the fingerprints into bit strings. The latter were further used in the classification studies as descriptor set "MACCS".

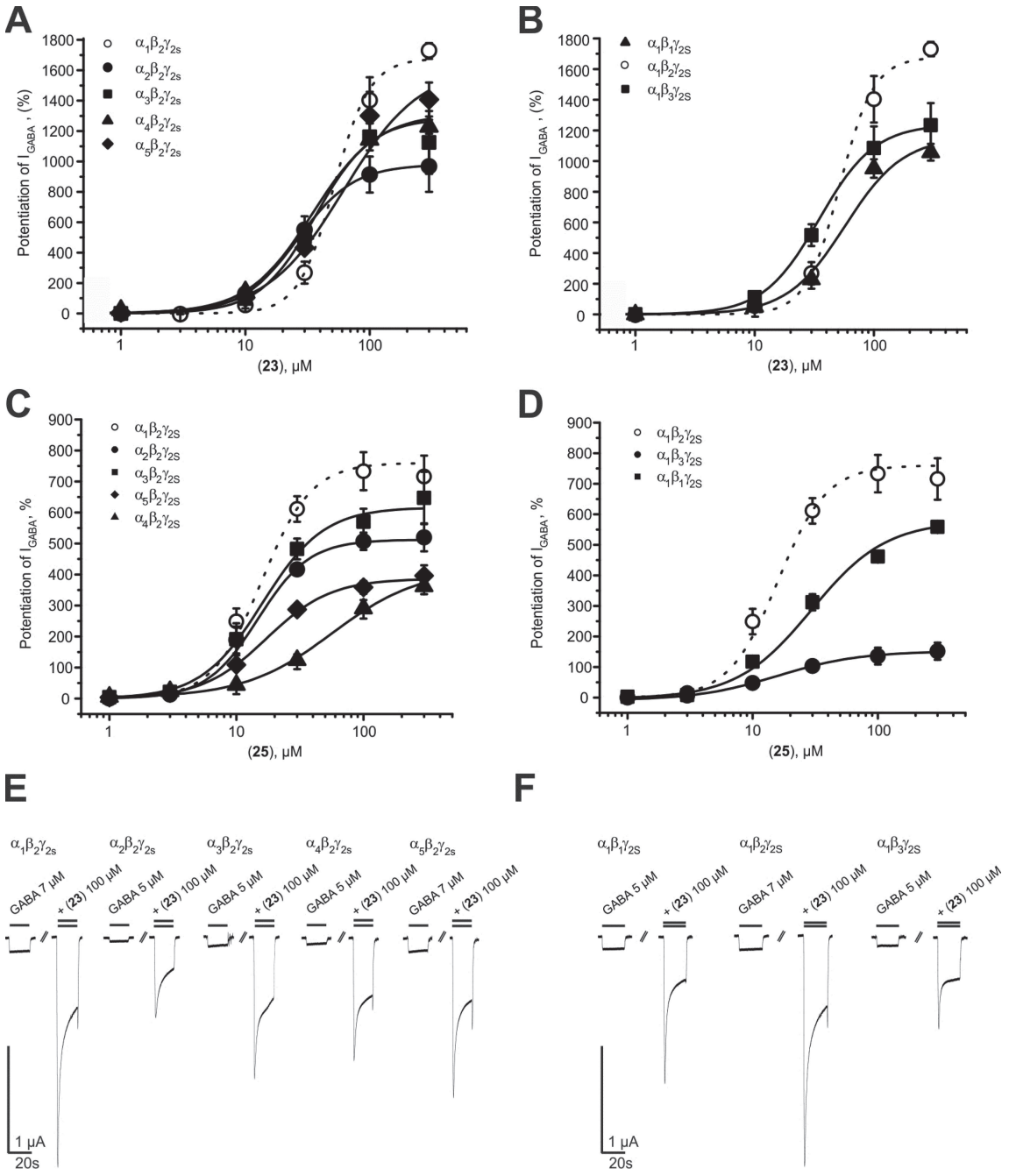

Figure 4. Analysis of subunit preferential I_{GABA} enhancement by (A, B) the most efficient (**23**) and (C, D) the most potent (**25**) piperine derivatives. (E, F) Representative I_{GABA} through seven $GABA_A$ receptor subtypes by **23** at 100 μM. Data represent mean ± SEM from at least three oocytes and two oocyte batches.

Computational Methods. As classification methods, instance-based classifier (IBk), J48 decision tree (J48), naïve-Bayes classifier (NB), random forest (RF), and Support vector machine (SMO) were used as implemented in Weka. All methods were used with the default parameter settings. Nevertheless, different costs were associated with misclassified compounds since the data set was unbalanced. The costs were evaluated by use of an in-house script (Supporting Information), which consequently built models with different costs of the false positive (FP) and false negative (FN) compounds (from 1 to 200 with step of 1 for FN and from 0 to 20 with step of 0.1 for FP). Moreover, inside the script the 10-fold cross-validation was applied and statistical parameters were computed. Subsequently, one model per method and descriptor set was selected on the basis of highest values of MCC, accuracy, sensitivity, and specificity and was taken for visual inspection and possible interpretation. The cost-sensitive parameters obtained for the best 15 models are listed in Table 11.

Statistical Parameters. The statistical parameters of every model were calculated on the basis of values from confusion matrix (for details see ref 52), where TP and TN stand for correctly classified active and inactive compounds and FP and FN for misclassified inactive and active ligands. The true-positive rates of active (sensitivity) and inactive (specificity) classes were calculated by the following formulas:

dx.doi.org/10.1021/jm5002277 | J. Med. Chem. 2014, 57, 5602−5619

Table 5. Comparison of Potency and Efficiency of 23 for $GABA_A$ Receptors of Different Subunit Compositions[a]

	$\alpha_1\beta_2\gamma_{2S}$		$\alpha_1\beta_1\gamma_{2S}$		$\alpha_1\beta_3\gamma_{2S}$		$\alpha_2\beta_2\gamma_{2S}$		$\alpha_3\beta_2\gamma_{2S}$		$\alpha_4\beta_2\gamma_{2S}$		$\alpha_5\beta_2\gamma_{2S}$	
	P	E	P	E	P	E	P	E	P	E	P	E	P	E
$\alpha_1\beta_2\gamma_{2S}$				*				**				*		
$\alpha_1\beta_1\gamma_{2S}$					**		*				*			*
$\alpha_1\beta_3\gamma_{2S}$													*	
$\alpha_2\beta_2\gamma_{2S}$												**	*	**
$\alpha_3\beta_2\gamma_{2S}$														
$\alpha_4\beta_2\gamma_{2S}$													*	
$\alpha_5\beta_2\gamma_{2S}$														

[a]Potency (P), expressed as EC_{50}, and efficiency (E), expressed as $I_{GABA\text{-}max}$, are compared. Asterisks indicate statistical significance as follows: *p < 0.05, **p < 0.01.

Table 6. Comparison of Potency and Efficiency of 25 for $GABA_A$ Receptors of Different Subunit Compositions[a]

	$\alpha_1\beta_2\gamma_{2S}$		$\alpha_1\beta_1\gamma_{2S}$		$\alpha_1\beta_3\gamma_{2S}$		$\alpha_2\beta_2\gamma_{2S}$		$\alpha_3\beta_2\gamma_{2S}$		$\alpha_4\beta_2\gamma_{2S}$		$\alpha_5\beta_2\gamma_{2S}$	
	P	E	P	E	P	E	P	E	P	E	P	E	P	E
$\alpha_1\beta_2\gamma_{2S}$				**	**	**		**		*		**		**
$\alpha_1\beta_1\gamma_{2S}$					*	**		**		**		*		**
$\alpha_1\beta_3\gamma_{2S}$							**	*	**				**	**
$\alpha_2\beta_2\gamma_{2S}$														**
$\alpha_3\beta_2\gamma_{2S}$												*		**
$\alpha_4\beta_2\gamma_{2S}$														
$\alpha_5\beta_2\gamma_{2S}$														

[a]Potency (P), expressed as EC_{50}, and efficiency (E), expressed as $I_{GABA\text{-}max}$, are compared. Asterisks indicate statistical significance as follows: *p < 0.05, **p < 0.01.

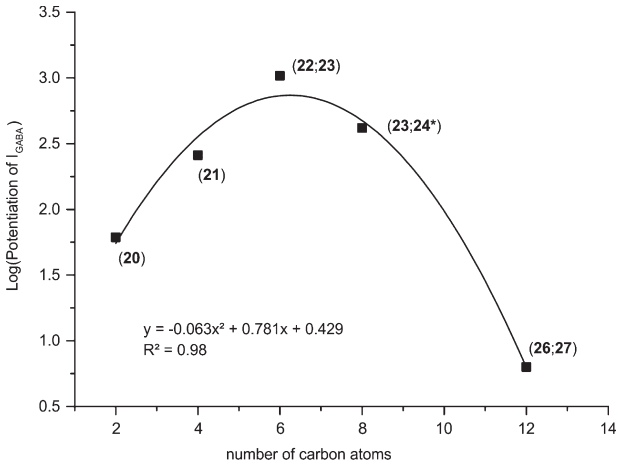

Figure 5. Relation between log(potentiation of I_{GABA}) of dialkyl-substituted piperine derivatives at the amide nitrogen and number of carbon atoms at this region. Data for **24*** were taken from ref 34.

$$\text{sensitivity} = \frac{TP}{TP + FN}$$

$$\text{specificity} = \frac{TN}{TN + FP}$$

The accuracy of the model was defined as the ratio of correctly predicted compounds to the total amount of compounds.

$$\text{accuracy} = \frac{TP + TN}{\text{total}}$$

Additionally, the Matthews correlation coefficient (MCC) was used to assess the quality of the obtained models. It was calculated from the formula

$$MCC = \frac{TP \cdot TN - FP \cdot FN}{\sqrt{(TP + FP)(TP + FN)(TN + FP)(TN + FN)}}$$

MCC is independent of the class sizes and therefore gives a rational evaluation of prediction in our case. It can return values from −1 to +1, where +1 determines perfect prediction, 0 means random classification, and −1 represents a total misclassification. The value of 0.4 was taken as a threshold to filter the best-performing models.

Behavioral Studies. Male mice (C57BL/6N) were obtained from Charles River Laboratories (Sulzfeld, Germany). For maintenance, mice were group-housed (maximum five mice per type IIL cage) with free access to food and water. At least 24 h before the commencement of experiments, mice were transferred to the testing facility, where they were given free access to food and water. The temperature in the maintenance and testing facilities was 23 ± 1 °C; the humidity was 40−60%; a 12 h light−dark cycle was in operation (lights on from 07:00 to 19:00). Only male mice aged 3−6 months were tested.

Compounds were applied by intraperitoneal (ip) injection 30 min before each test. Testing solutions were prepared in a solvent composed of 0.9% NaCl solution with 10% dimethyl sulfoxide (DMSO) and 3% Tween 80. Application of the solvent alone did not influence animal behavior. All doses are indicated as milligrams per kilogram of body weight of the animal.

Elevated Plus Maze Test. The animals' behavior was tested over 5 min on an elevated plus maze 1 m above ground consisting of two closed and two open arms, each 50 × 5 cm in size. The test instrument was built from gray PVC; the height of closed arm walls was 20 cm. Illumination was set to 180 Lux. Animals were placed in the center, facing an open arm. Analysis of open and closed arm entries and time on open arm was automatically done with Video-Mot 2 equipment and software (TSE Systems, Bad Homburg, Germany).[34]

Open Field Test. Ambulation was tested over 10 min in a 50 × 50 cm flexfield box equipped with infrared rearing detection. Illumination was set to 150 Lux. The animals' explorative behavior was analyzed by use of the ActiMot 2 equipment and software (TSE-systems, Bad Homburg, Germany). Arenas were subdivided into border (up to 8 cm from wall), center (20 × 20 cm, 16% of total area), and intermediate area according to the recommendations of EMPRESS (European

Table 7. Statistical Parameters of the 15 Best Models Obtained after 10-Fold Cross-Validation

model	classification method	TP, TN, FP, FN[a]	sensitivity	specificity	accuracy	MCC, ROC
		Descriptor Set 6D				
1	IBk	12, 52, 8, 5	0.706	0.867	0.831	0.542, 0.825
2	J48	15, 46, 14, 2	0.882	0.767	0.792	0.556, 0.818
3	NB	16, 49, 11, 1	0.941	0.817	0.844	0.659, 0.831
4	RF	13, 52, 8, 4	0.765	0.867	0.844	0.588, 0.838
5	SMO	16, 39, 21, 1	0.941	0.650	0.714	0.491, 0.796
		Descriptor Set PHYSCHEM				
6	IBk	10, 52, 8, 7	0.588	0.867	0.805	0.446, 0.749
7	J48	15, 46, 14, 2	0.882	0.767	0.792	0.556, 0.828
8	NB	15, 40, 20, 2	0.882	0.667	0.714	0.457, 0.828
9	RF	15, 46, 14, 2	0.882	0.767	0.792	0.556, 0.811
10	SMO	15, 36, 24, 2	0.882	0.600	0.662	0.400, 0.741
		Descriptor Set MACCS				
11	IBk	9, 45, 15, 8	0.529	0.750	0.701	0.250, 0.619
12	J48	12, 48, 12, 5	0.706	0.800	0.779	0.453, 0.797
13	NB	12, 42, 18, 5	0.706	0.700	0.701	0.345, 0.713
14	RF	13, 43, 17, 4	0.765	0.717	0.727	0.409, 0.730
15	SMO	10, 56, 4, 7	0.588	0.933	0.857	0.561, 0.761

[a]TP = true positive, TN = true negative, FP = false positive, FN = false negative.

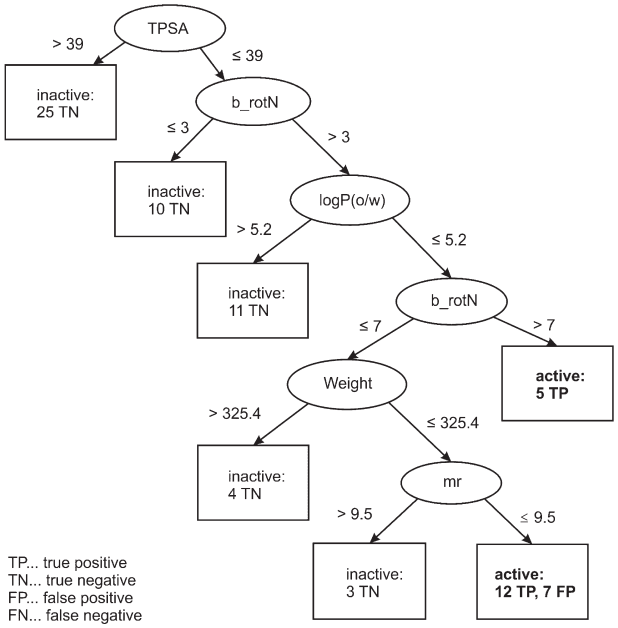

Figure 6. Decision tree obtained for the data set of 76 piperine derivatives with PHYSCHEM descriptor set.

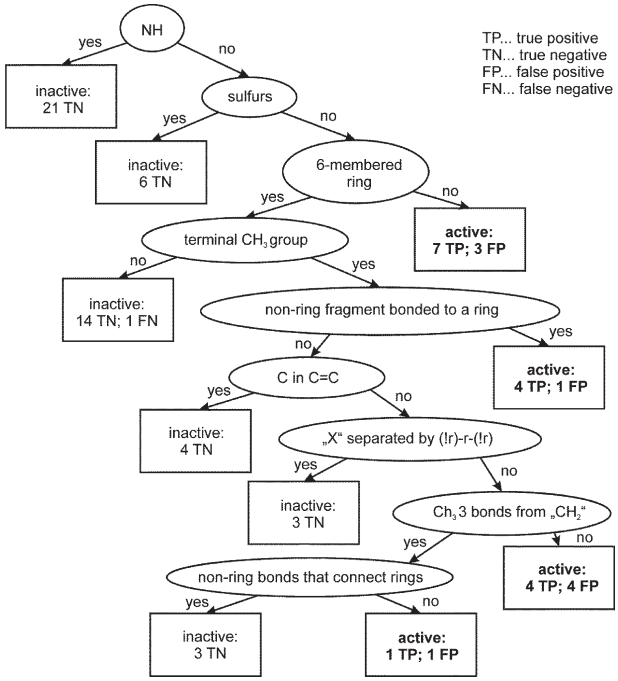

Figure 7. Decision tree obtained for the data set of 76 piperine derivatives with MACCS fingerprints.

Mouse Phenotyping Resource of Standardised Screens; http://empress.har.mrc.ac.uk).

Estimation of Plasma Levels. Trunk blood from male C57BL/6N (6 months) was taken 15, 30, and 60 min after ip application of **23** and **25** (doses 1, 3, and 10 mg/kg body weight; injection solutions were prepared as described for behavioral analysis). At each time point, mice were euthanized and blood samples (500−800 μL) were collected and compiled into ethylenediaminetetraacetic acid (EDTA)-coated microtubes (1.6 mg of EDTA/sample) and centrifuged at 12 000 rpm for 5 min at 4 °C. Plasma samples were transferred into 1.5 mL tubes and stored at −80 °C until analysis.

Materials. All solvents used were of UPLC grade. Acetonitrile and dimethyl sulfoxide (DMSO) were supplied by Scharlau (Barcelona, Spain). Methanol was from Lab-Scan (Gliwice, Poland). Ammonium formate, formic acid and trifluoroacetic acid (TFA) were purchased from BioSolve (Valkenswaard, Netherlands), and HPLC-grade water was obtained from an EASYpure II (Barnstead, Dubuque, IA) water purification system. Blank K_3EDTA C57BL/6N mouse plasma was collected for generating plasma calibrators and quality controls (QC).

Preparations of Calibrators and Quality Control Samples. Two separate sets of **23** and **25** stock solutions were prepared in DMSO for making calibrators and quality control (QC) samples. Plasma calibrators were prepared by spiking corresponding stock solutions into a blank plasma sample. The following **23** and **25** concentrations were added: 20, 50, 100, 250, 500, 1000, and 2000 ng/mL. The same blank plasma and both stock solutions (for QC) were used to generate three level plasma QC samples at 60, 1000, and 1600 ng/mL for both **23** and **25**.

dx.doi.org/10.1021/jm5002277 | J. Med. Chem. 2014, 57, 5602−5619

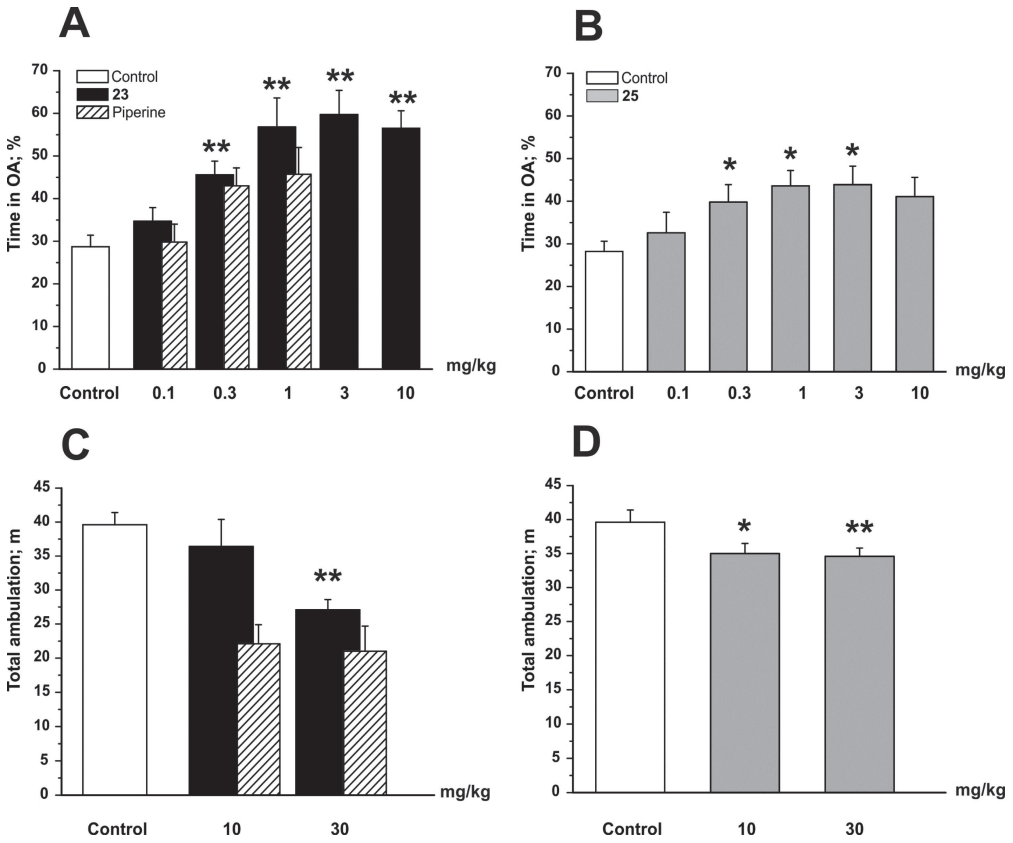

Figure 8. Compounds **23** and **25** display anxiolytic effects in the EPM test and little sedation in the OF test. Bars indicate time spent in open arms (OA) as a percentage of the total time 30 min after ip application of the indicated dose (in milligrams per kilogram of body weight) of (A) **23** and (B) **25** and the total ambulation after application of (C) **23** and (D) **25**. White bars illustrate the behavior of control mice. Bars represent means ± SEM from at least eight different mice. Asterisks indicate statistically significant differences to control $*p < 0.05$, $**p < 0.01$ [analysis of variance (ANOVA) with Bonferroni]. Shaded bars for the behavioral effects of piperine are taken from ref 34. Behavioral experiments comparing the sedative and anxiolytic potential of piperine, **23**, and **25** have been conducted in parallel.

Table 8. Estimated Plasma Levels of Derivatives 23 and 25 after Intraperitoneal Application[a]

applied dose (mg/kg body weight)	mean plasma concn (ng/mL)	*n*
Compound **23**		
1	60.6 ± 14.5	3
3	194.0 ± 50.2	3
10	593.0 ± 92.4	3
Compound **25**		
1	41.5 ± 8.7	3
3	172.0 ± 19.0	3
10	419.0 ± 37.2	3

[a]Data are given as mean ± SEM; *n* indicates the number of animals used.

Table 9. Set of Six 2D Descriptors Selected by BestFirst Algorithm for Classification Studies

name	definition
density	molecular mass density: weight divided by vdw_vol (amu/Å^3)
lip_don	no. of OH and NH atoms
opr_brigid	no. of rigid bonds[53]
PEOE_RPC+ numeric	relative positive partial charge: largest positive q_i divided by the sum of positive q_i
PEOE_VSA+3	sum of v_i where q_i is in the range [0.15, 0.20)
SMR	molecular refractivity (including implicit hydrogens)[a]

[a]This property is an atomic contribution model[54] that assumes the correct protonation state (washed structures). The model was trained on ∼7000 structures and results may vary from the mr descriptor.

Two internal standard (IS) stock solutions of **22** and **24** were prepared in DMSO in order to generate working solutions (WS) at 200 ng/mL in methanol.

Sample Preparation for UHPLC-MS/MS Analysis. Plasma proteins were precipitated by the addition of 50 μL of WS at 200 ng/mL of the corresponding IS: **22** (for **23**) or **24** (for **25**) and 500 μL of ice-cold acetonitrile to 20 μL of K_3EDTA mouse plasma. Samples were vortexed at 1400 rpm for 10 min and then centrifuged at 13200*g* for 20 min at 10 °C. The supernatant was transferred into a 96-deep-well plate for drying under nitrogen gas flow (Evaporex EVX-96, Apricot Designs, Monrovia, CA) and redissolved in 200 μL of injection solvent (65% 10 mM ammonium formate + 0.05% formic acid, 35% acetonitrile + 0.05% formic acid) before MS/MS analysis.

LC-MS/MS Analyses. Quantification was performed on a 1290 Infinity LC system coupled with a 6460 triple quadrupole mass spectrometer with Jet Stream Technology, and data was processed with a MassHunter Workstation Software version B.06.00 (Agilent; Waldbronn, Germany). The 1290 Infinity LC system was equipped with a binary capillary pump, degasser, autosampler, autosampler thermostat, thermostated column compartment, and FlexCube. Separation was performed at 55 °C on a Kinetex XB-C18 column, 100 × 2.1 mm, 1.7 μm particle size (Phenomenex; Torrance, CA); mobile phase of (A) 0.05% formic acid in 10 mM ammonium formate

dx.doi.org/10.1021/jm5002277 | J. Med. Chem. 2014, 57, 5602−5619

Table 10. Eleven Descriptors of Physical Chemical Properties Used in the Study

name	definition
a_acc	no. of hydrogen-bond acceptor atoms
a_don	no. of hydrogen-bond donor atoms
b_rotN	no. of rotatable bonds[a]
log_P(o/w)	log of octanol/water partition coefficient[b]
mr	molecular refractivity (including implicit hydrogens)[c]
PEOE_VSA_HYD	total hydrophobic van der Waals surface area
TPSA	polar surface area[d] (Å^2)
vsa_acc	approximate sum of VDW surface areas (Å^2) of pure hydrogen-bond acceptors
vsa_don	approximate sum of VDW surface areas (Å^2) of pure hydrogen-bond donors
vsa_hyd	approximate sum of VDW surface areas (Å^2) of hydrophobic atoms
Weight	molecular weight (including implicit hydrogens) (amu)

[a]A bond is rotatable if it has order 1, is not a ring, and has at least two heavy neighbors. [b]Calculated from a linear atom-type model with r^2 = 0.931. [c]Calculated from an 11-descriptor linear model with r^2 = 0.997. [d]Calculated from group contributions to approximate the polar surface area from connection table.

Table 11. Cost-Sensitive Parameters

method	cost FP	cost FN
	Descriptor Set 6D	
IBk	1	1
J48	6	1
NB	5	3
RF	9	5
SMO	52	19.1
	Descriptor Set PHYSCHEM	
IBk	1	1
J48	18	11
NB	1	1
RF	21	2
SMO	49	18.1
	Descriptor Set MACCS	
IBk	3	2
J48	29	12
NB	1	8
RF	4	1
SMO	3	2.2

and (B) 0.05% formic acid in ACN, gradient 40% B for 1 min, linear gradient to reach 88% B after 5.3 min, shifted to 100% B for 1 min, and back to equilibrium condition of 40% B for 0.7 min; flow rate of 0.5 mL/min; total run time of 7 min. Sample injected volume was 1 μL and autosampler was set at 10 °C. Needle wash solution was MeOH/ACN/IPA/H_2O (1:1:1:1 v/v/v/v). Flexible cube was set at a flow rate of 1 mL/min for 20 s.

MS parameters were manually optimized as follow: drying N_2 gas of 320 °C at a flow rate of 10 L/min, nebulizer pressure of 20 psi, sheath N_2 gas of 400 °C at a flow rate of 11 L/min, nozzle voltage of 0 V, capillary voltage of 2.5 kV, and delta EMV 0 V. Quantification was determined in multiple reaction monitoring (MRM) mode with an ESI-MS/MS system in positive ionization mode. The MRM transitions of both **23** and **25** and corresponding internal standard were as shown in Table S2 (Supporting Information).

Syntheses. Details of synthesis and characterization of selected products **25**, **51**, and **62** and key intermediates **65a**, **68a−c**, **71a**, and **75a,b** are described below. Synthetic procedures and characterization data for all other compounds are included in Supporting Information. Purity was determined either by elemental analysis or by HPLC and was >95%. Unless otherwise noted, chemicals were purchased from commercial suppliers and used without further purification. Microwave reactions were performed on a Biotage Initiator Sixty microwave unit (Biotage AB, Uppsala, Sweden). Flash column chromatography was performed on silica gel 60 from Merck (40−63 mm), whereas most separations were performed by using a Büchi Sepacore medium-pressure liquid chromatography (MPLC) system with a 9g column (Buchi Labortechnik AG, Flawil, Switzerland). For thin-layer chromatography (TLC), aluminum-backed silica gel was used. Melting points were determined by using a Kofler-type Leica Galen III micro hot stage microscope (Aigner-Unilab Laborfachhandel GmbH, Vienna, Austria) and are uncorrected. For compounds unknown in the literature, either high-resolution mass spectrometry (HR-MS) or combustion analysis was performed. HR-MS was performed by E. Rosenberg at the Institute for Chemical Technologies and Analytics, Vienna University of Technology; all samples were analyzed by liquid chromatography/ion trap time-of-flight mass spectrometry (LC/IT-TOF-MS) in positive or negative ion detection mode with the recording of MS and MS/MS spectra. Combustion analysis was carried out in the Microanalytical Laboratory, Institute of Physical Chemistry, University of Vienna. NMR spectra were recorded on a Bruker AC 200 (200 MHz), a Bruker Avance DP160 (200 MHz), or a Bruker Avance 400 (400 MHz) spectrometer (Bruker GmbH, Vienna, Austria) and chemical shifts are reported in parts per million (ppm). For assignment of ^{13}C multiplicities, standard ^{13}C distortionless enhancement by polarization transfer (DEPT) or attached proton test (APT) spectra were recorded. HPLC analyses were performed on a Agilent 1200 HP-LC system with a Kinetex XB-C18, 2.6 μm, 50 × 2.1 mm column (Agilent Technologies GmbH, Vienna, Austria). The mobile phase was composed of ACN/water (gradient 50:50 up to 95:5 v/v) with 0.1% AcOH added. GC−MS runs were performed on a Thermo Finnigan Focus GC/DSQ II with a standard capillary column BGB 5 (30 m × i.d. 0.32 mm; Fisher Scientific GmbH, Vienna, Austria).

*(2E,4E)-5-(1,3-Benzodioxol-5-yl)-N,N-dibutyl-2,4-pentadienamide (**25**).* Piperic acid chloride (218 mg, 1 mmol) was dissolved in 2.5 mL of dry THF. Dibutylamine (595 μL, 3.5 mmol) was added and the reaction mixture was stirred overnight at rt. After evaporation of the solvent, the residue was taken up in ethyl acetate (EtOAc; 40 mL) and washed two times each with 5% $NaHCO_3$ and 2 N HCl. The organic layer was separated, dried with sodium sulfate, filtered, and evaporated. The pure product was obtained after recrystallization from ethanol.

Yield 76% (746 mg, 2.26 mmol), light brown crystals, mp 88−90 °C. ^1H NMR ($CDCl_3$, 200 MHz) δ 0.85−1.05 (m, 6H, CH_3), 1.22−1.45 (m, 4H, CH_2), 1.46−1.71 (m, 4H, CH_2), 3.25−3.47 (m, 2H, CH_2), 5.98 (s, 2H, O−CH_2−O), 6.35 (d, J = 14.6 Hz, 1H, H2), 6.70−6.85 (m, 3H), 6.86−6.95 (m, 1H), 7.00 (d, J = 7.9 Hz, 1H), 7.36−7.54 (m, 1H). ^{13}C NMR ($CDCl_3$, 50 MHz) δ 14.1 (q, CH_3), 14.1 (q, CH_3), 20.3 (t, CH_2), 20.5 (t, CH_2), 30.3 (t, CH_2), 32.2 (t, CH_2), 46.8 (t, N−CH_2), 48.1 (t, N−CH_2), 101.5 (t, O−CH_2−O), 105.9 (d), 108.7 (d), 120.5 (d), 122.7 (d), 125.6 (d), 131.2 (s), 138.6 (d), 142.6 (d), 148.3 (s, C−O), 148.4 (s, C−O), 166.3 (s, CO−N). Anal. Found, C 71.96, H 7.91, N 3.95; Calcd (·0.23H_2O), C 72.01, H 8.30, N 4.20.

*3-(Benzo[d][1,3]dioxol-5-yl)-N,N-dipropylbenzamide (**51**).* Benzodioxol-5-boronic acid (138 mg, 0.83 mmol, 1 equiv), **51a** (237 mg, 0.83 mmol, 1 equiv), $Pd(PPh_3)_4$ (19 mg, 2 mol %), and sodium carbonate (615 mg, 5.81 mmol, 7 equiv) were charged into a microwave vial. Then a mixture of dimethyl ether (DME)/EtOH 5:1 (6.4 mL) and water (1.8 mL) was added, and the resulting suspension was degassed by passing through argon for 5 min. The vial was sealed and heated to 140 °C for 1 h in the microwave. After cooling to rt, the reaction mixture was extracted with dichloromethane (DCM), the solvent was evaporated, and the crude product was directly subjected to column chromatography with light petroleum (LP)/EtOAc mixture as eluent.

Yield 60% (163 mg, 0.50 mmol), colorless oil. TLC 0.24 (LP/EtOAc 4:1). ^1H NMR ($CDCl_3$, 200 MHz) δ 0.76−0.98 (br m, 6H, CH_3), 1.57−1.67 (br m, 4H, CH_2), 3.20−3.47 (br m, 4H, N−CH_2−), 6.00 (s, 2H, O−CH_2−O), 6.86−6.90 (m, 1H, ArH), 7.03−7.08 (m, 2H, ArH), 7.25−7.30 (m, 1H, ArH), 7.42 (t, J = 7.4 Hz, 1H, ArH), 7.48−7.54 (m, 2H, ArH). ^{13}C NMR ($CDCl_3$, 50 MHz) δ 11.1 (q, CH_3), 11.4 (q, CH_3), 20.7 (t, CH_2), 22.0 (t, CH_2), 46.3 (t, CH_2), 50.7

(t, CH_2), 101.2 (t, O−CH_2−O), 107.6 (d), 108.6 (d), 120.7 (d), 124.8 (d), 124.9 (d), 127.4 (d), 128.8 (d), 134.8 (s), 137.9 (s), 141.1 (s), 147.3 (s), 148.2 (s), 171.6 (s, −CO−N). HR-MS $[M + H]^+$ m/z (pred) = 326.1751, m/z (meas) = 326.1749, difference = −0.61 ppm.

*[5-(Benzo[d][1,3]dioxol-5-yl)naphthalen-1-yl](piperidin-1-yl)-methanone (**62**).* 1-Ethyl-3-(3-dimethylaminopropyl)carbodiimide hydrochloride (EDCI·HCl; 65 mg, 0.34 mmol, 2 equiv) was added to a suspension of **62a** (50 mg, 0.17 mmol, 1 equiv) and hydroxybenzotriazole (HOBt; 52 mg, 0.34 mmol, 2 equiv) in dry dichloromethane (2 mL) under argon at rt. After 2 h, the suspension was transformed into an opaque solution and TLC indicated full consumption of the starting material. Piperidine (0.5 mL) was added at rt and stirring was continued overnight. After full conversion was detected by TLC, the reaction mixture was diluted with EtOAc (30 mL); washed with 0.5 N HCl, saturated $NaHCO_3$, and brine (20 mL each); dried with sodium sulfate; and evaporated. The crude product was purified by column chromatography with LP/EtOAc mixture as eluent.

Yield 62% (0.11 mmol, 38 mg), colorless solid, mp 150−153 °C. TLC 0.09 (LP/EtOAc 4:1). ^{1}H NMR ($CDCl_3$, 200 MHz) δ 1.40−1.50 (m, 2H, CH_2), 1.66−1.80 (m, 4H, CH_2), 3.15−3.21 (m, 2H, N−CH_2), 3.87−3.93 (m, 2H, N−CH_2), 6.04 (s, 2H, O−CH_2−O), 6.93−6.95 (m, 3H, ArH), 7.39−7.56 (m, 4H, ArH), 7.84 (d, J = 8.3 Hz, 1H, ArH), 7.94 (dd, J^1 = 7.2 Hz, J^2 = 2.6 Hz, 1H, ArH). ^{13}C NMR ($CDCl_3$, 50 MHz) δ 24.6 (t, CH_2), 25.9 (t, CH_2), 26.7 (t, CH_2), 42.7 (t, N−CH_2), 48.3 (t, N−CH_2), 101.2 (t, O−CH_2−O), 108.2 (d), 110.6 (d), 123.3 (d), 123.4 (d), 124.4 (d), 125.3 (d), 126.2 (d), 126.9 (d), 127.4 (d), 120.9 (s), 131.9 (s), 134.3 (s), 135.2 (s), 140.3 (s), 147.0 (s), 147.5 (s), 169.4 (s, CO−N). HR-MS $[M + H]^+$ m/z (pred) = 360.1594, m/z (meas) = 360.1597, difference = 0.83 ppm.

*(E)-Methyl 3-(Naphtho[2,3-d][1,3]dioxol-5-yl)acrylate (**65a**).* For synthesis of **65a**, a modification of a previously published method[38] was employed. A 8-mL vial with magnetic stirrer, screw cap, and septum was charged with naphtho[2,3-*d*][1,3]dioxol-5-yl trifluoromethanesulfonate (synthesized according to ref 37) (480 mg, 1.5 mmol, 1 equiv), 1,10-phenanthroline monohydrate (16 mg, 0.083 mmol, 5.5 mol %), palladium(II) acetate (17 mg, 0.075 mmol, 5 mol %), and anhydrous *N*,*N*-dimethylformamide (DMF, 5 mL). Then triethylamine (250 μL, 1.8 mmol, 1.2 equiv) and methyl acrylate (680 μL, 7.5 mmol, 5 equiv) were added successively. The vial was flushed with argon and heated to 80 °C for 16 h. Reaction control by TLC showed full conversion. The solvent was evaporated, and the residue was taken up in DCM and adsorbed on silica. Column chromatography (45 g of SiO_2, eluent LP/EtOAc, 5% isocratic) yielded the pure product.

Yield 95% (364 mg, 1.425 mmol), colorless solid, mp 125−126 °C. TLC 0.44 (LP/EtOAc 4:1). ^{1}H NMR ($CDCl_3$, 200 MHz) δ 3.82 (s, 3H, CH_3), 5.99 (s, 2H, O−CH_2−O), 6.43 (d, J = 15.7 Hz, 1H, H3), 7.04 (s, 1H, ArH), 7.25 (t, J = 7.7 Hz, 1H, H7′), 7.38 (s, 1H, ArH), 7.52 (d, J = 7.1 Hz, 1H, ArH), 7.61 (d, J = 8.1 Hz, 1H, ArH), 8.29 (d, J = 15.7 Hz, 1H, H2). ^{13}C NMR ($CDCl_3$, 50 MHz) 51.7 (q, CH_3), 99.9 (d), 101.4 (t, O−CH_2−O), 104.4 (d), 119.9 (d), 123.5 (d), 124.0 (d), 128.7 (s), 129.5 (d), 130.7 (s), 130.9 (s), 142.1 (d), 147.6 (s), 148.6 (s), 167.3 (s, COOR). HR-MS $[M - MeOH]^+$ m/z (pred) = 225.0546, m/z (meas) = 225.0553, difference = 3.11 ppm.

*4,4,5,5-Tetramethyl-2-(naphtho[2,3-d][1,3]dioxol-6-yl)-1,3,2-dioxaborolane (**68a**).* For synthesis of **68a**, a modification of a procedure published by Ishyama et al.[39] was used. A three-necked flask with magnetic stirrer, septum, reflux condenser, and balloon was charged with naphtho[2,3-*d*][1,3]dioxole (1.72 g, 10 mmol, 1 equiv), bis(pinacolato)diboron (1.27 g, 5 mmol, 0.5 equiv), $[Ir(OMe)cod]_2$ (100 mg, 0.15 mmol, 1.5 mol %), and 4,4′-di-*tert*-butyl-2,2′-bipyridine (81 mg, 0.3 mmol, 3 mol %) and flushed with argon. Then cyclohexane (60 mL) was added and the reaction was heated to reflux and monitored with GC/MS. After 24 h the reaction did not proceed any further. After evaporation of the solvent, the residue was redissolved in DCM, adsorbed on silica, and directly subjected to column chromatography (45 g of SiO_2, eluent LP/EE 30:1), which yielded the pure product (683 mg of starting material could be reisolated in this step).

Yield 29% (48% based on recovered starting material, 874 mg, 2.9 mmol), colorless solid, mp 97−99 °C. TLC 0.18 (LP/EE 30:1). ^{1}H NMR ($CDCl_3$, 200 MHz) δ 1.38 (s, 12H, CH_3), 6.03 (s, 2H, O−CH_2−O), 7.10 (s, 1H), 7.64 (d, J = 8.2 Hz, 1H), 7.70 (d, J = 8.2 Hz, 1H), 8.16 (s, 1H, H5). ^{13}C NMR ($CDCl_3$, 50 MHz) 24.9 (q, 4C, CH_3), 83.8 (s, B−O−CR_3), 101.0 (t, O−CH_2−O), 103.8 (d), 104.4 (d), 126.2 (d), 129.3 (d), 129.8 (s), 132.5 (s), 134.9 (d), 147.4 (s), 148.4 (s); C6 signal could not be detected due to low signal intensity.

*6-Bromonaphtho[2,3-d][1,3]dioxole (**68b**).* For synthesis of **68b**, a modification of a published procedure[40] was used. In a three-necked flask with magnetic stirrer and reflux condenser, **68a** (700 mg, 2.35 mmol, 1 equiv) was dissolved in methanol. Copper(II) bromide (1.57 g, 7 mmol, 3 equiv) was dissolved in water (20 mL) and added. The reaction was heated to reflux for 18 h and checked with TLC. The reaction mixture was cooled, diluted with water (200 mL), and extracted with 3 × 50 mL of DCM. The combined organic extracts were washed with 50 mL each water and brine, dried with anhydrous sodium sulfate, and evaporated.

Yield 94% (555 mg, 2.21 mmol), colorless solid, mp 135−138 °C. TLC 0.40 (LP/EE 30:1). ^{1}H NMR ($CDCl_3$, 200 MHz) δ 6.04 (s, 2H, O−CH_2−O), 7.01 (s, 1H, ArH), 7.06 (s, 1H, ArH), 7.38 (dd, J^1 = 8.7 Hz, J^2 = 1.9 Hz, 1H, H7), 7.51 (d, J = 8.7 Hz, 1H, H8), 7.79 (d, J = 1.9 Hz, 1H, H5). ^{13}C NMR ($CDCl_3$, 50 MHz) 101.3 (t, O−CH_2−O), 103.0 (d), 103.8 (d), 118.1 (s), 127.5 (d), 128.5 (d), 128.9 (d), 131.8 (s), 148.0 (s), 148.3 (s). One signal could not be detected due to low signal intensity.

*(E)-Methyl 3-(Naphtho[2,3-d][1,3]dioxol-6-yl)acrylate (**68c**).* An 8-ml vial with magnetic stirrer, screw cap, and septum was charged with **68b** (300 mg, 1.2 mmol, 1 equiv), methyl acrylate (163 μL, 1.8 mmol, 1.5 equiv), palladium(II) acetate (8 mg, 0.036 mmol, 3 mol %), and tri-*o*-tolylphosphine (22 mg, 0.072 mmol, 6 mol %) and flushed with argon. Triethylamine (0.85 mL) was added via syringe and the reaction was heated to 80 °C. TLC monitoring (eluent LP/EE 30:1) showed full conversion after 8 h. The reaction mixture was diluted with diethyl ether (30 mL). Due to low solubility of the product in diethyl ether, it was necessary to add ethyl acetate (20 mL) and DCM (10 mL) to obtain a clear solution. The organic phase was washed with 3 × 10 mL of 0.5 N HCl and 30 mL of brine and dried with sodium sulfate. Evaporation of the solvent gave the pure product in quantitative yield.

Yield 100% (310 mg, 1.2 mmol), colorless solid, mp 151−152 °C. TLC 0.16 (LP/EE 30:1). ^{1}H NMR ($CDCl_3$, 200 MHz) δ 3.81 (s, 3H, CH_3), 6.06 (s, 2H, O−CH_2−O), 6.49 (d, J = 16.0 Hz, 1H, H3), 7.10 (s, 1H, ArH), 7.12 (s, 1H, ArH), 7.50 (dd, J^1 = 8.6 Hz, J^2 = 1.6 Hz, 1H, H7′), 7.64 (d, J = 8.6 Hz, 1H, H8′), 7.74−7.83 (m, 2H, H2, H5′). ^{13}C NMR ($CDCl_3$, 50 MHz) δ 51.7 (q, CH_3), 101.3 (t, O−CH_2−O), 103.9 (d), 104.4 (d), 116.9 (d), 127.6 (d), 128.7 (d), 130.3 (s), 130.4 (s), 131.7 (s), 145.1 (d), 148.2 (s), 148.7 (s), 167.6 (d, COOR). HR-MS $[M + H]^+$ m/z (pred) = 257.0808, m/z (meas) = 257.0807, difference = −0.39 ppm.

*Naphtho[2,3-d][1,3]dioxole-5-carboxylic acid (**71a**).* For synthesis of **71a**, a modification of a published procedure[41] was used. In a two-necked flask equipped with magnetic stirrer, septum, and balloon, naphtho[2,3-*d*][1,3]dioxol-5-yl trifluoromethanesulfonate[42] (96 mg, 0.3 mmol, 1 equiv), 1,3-bis(diphenylphosphino)propane (dppp; 7 mg, 0.018 mmol, 6 mol %), and palladium(II) acetate (2 mg, 0.009 mmol, 3 mol %) were suspended in DMF/water 3:1 (1 mL). A steel cannula reaching to the bottom of the flask was used to bubble carbon monoxide through the solution for 10 min; after that, the balloon was filled with CO gas in order to maintain its supply throughout the reaction time. Hünig's base (102 μL, 0.6 mmol, 2 equiv) was added via syringe and the reaction mixture was heated to 70 °C. After 3 h, reaction control with TLC indicated complete consumption of the starting material. The reaction mixture was diluted with ethyl acetate (10 mL) and extracted with 3 × 5 mL of saturated $NaHCO_3$. The combined aqueous extracts were acidified to pH = 2 with 2 N HCl and extracted with 3 × 10 mL of ethyl acetate. The combined organic extracts were washed with 10 mL each water and brine and dried with sodium sulfate. Evaporation of the solvent gave the pure product.

Yield 67% (116 mg, 0.54 mmol), colorless solid, mp 259−263 °C. TLC 0.60 ($CHCl_3$/MeOH 10%). ^{1}H NMR (acetone-d_6, 400 MHz) δ 6.17 (s, 2H, O−CH_2−O), 7.33 (s, 1H, ArH), 7.41−7.45 (m, 1H, H7), 8.00 (d, J = 8.0 Hz, 1H, ArH), 8.18 (dd, J^1 = 7.4 Hz, J^2 = 1.1 Hz, 1H, ArH), 8.49 (s, 1H, ArH). ^{13}C NMR (acetone-d_6, 100 MHz) δ 101.7 (t, O−CH_2−O), 102.2 (d), 104.1 (d), 123.1 (d), 125.7 (s), 128.9 (d), 129.2 (s), 131.6 (s), 132.4 (d), 147.6 (s), 149.5 (s), 168.2 (s, COOH).

*Methyl 5,6,7,8-Tetrahydronaphtho[2,3-d][1,3]dioxole-6-carboxylate (**75a**).* For synthesis of **75a**, a modification of a published method[42] was used. A three-necked flask with magnetic stirrer, septum, reflux condenser, and balloon was charged with 5,6-bis(bromomethyl)benzo[*d*][1,3]dioxole (2.0 g, 6.5 mmol, 1 equiv), methyl acrylate (2.94 mL, 32.5 mmol, 5 equiv), and anhydrous DMF (50 mL) and was flushed with argon. Sodium iodide (3.9 g, 26 mmol, 4 equiv) was added and the reaction was heated to 90 °C overnight (in previous experiments on a smaller scale, full conversion had been reached after 2 h). Above 70 °C the reaction mixture began to turn red. The reaction was quenched with 200 mL of water, and then, sodium thiosulfate 5% was added until the mixture became colorless. The aqueous mixture was extracted with 5 × 50 mL of methyl *tert*-butyl ether (MTBE). The organic phase was washed with 50 mL each water and brine, dried with anhydrous sodium sulfate, and evaporated.

Yield 89% (1.35 g, 5.79 mmol), colorless solid, mp 71−72 °C. TLC 0.15 (LP/EE 30:1). ^{1}H NMR ($CDCl_3$, 200 MHz) δ 1.75−1.91 (m, 1H), 2.10−2.22 (m, 1H), 2.61−2.78 (m, 3H), 2.88−2.91 (m, 2H), 3.71 (s, 3H, CH_3), 5.87 (s, 2H, O−CH_2−O), 6.53 (s, 1H, ArH), 6.55 (s, 1H, ArH). ^{13}C NMR ($CDCl_3$, 50 MHz) δ 25.9 (t, CH_2), 28.6 (t, CH_2), 31.6 (t, CH_2), 39.9 (d, C6), 51.8 (q, CH_3), 100.6 (t, O−CH_2−O), 108.5 (d), 108.6 (d), 127.6 (s), 128.5 (s), 145.7 (s), 145.9 (s), 175.8 (d, COOR)

*Methyl Naphtho[2,3-d][1,3]dioxole-6-carboxylate (**75b**).* Compound **75a** (100 mg, 0.43 mmol, 1 equiv) was dissolved in benzene (3 mL, p.a.) under argon. DDQ (242 mg, 1.07 mmol, 2.5 equiv) was added and the reaction mixture was heated to 80 °C for 2 h. TLC analysis was inconclusive due to very similar R_f values of starting material and product. Staining with cerium molybdophosphoric acid dip reagent indicated full conversion (The starting material is readily stained; the product only weakly). The reaction was quenched with 20 mL of 2 N NaOH and changed color to brown. The reaction was extracted with 3 × 10 mL of EtOAc. The organic phase was washed with water until the washings were colorless (5 × 10 mL) and subsequently washed with brine, dried over sodium sulfate, and evaporated.

Yield 73% (72 g, 0.31 mmol), colorless solid, mp 130−132 °C, sublimation above 105 °C. TLC 0.15 (LP/EE 30:1). ^{1}H NMR ($CDCl_3$, 200 MHz) δ 3.95 (s, 3H, CH_3), 6.06 (s, 2H, O−CH_2−O), 7.11 (s, 1H, ArH), 7.17 (s, 1H, ArH), 7.66 (d, J = 8.6 Hz, 1H, H8), 7.90 (dd, J^1 = 8.6 Hz, J^2 = 1.6 Hz, 1H, H7), 8.38 (d, J = 1.6 Hz, 1H, H5). ^{13}C NMR ($CDCl_3$, 50 MHz) δ 52.1 (q, CH_3), 101.4 (t, O−CH_2−O), 103.8 (d), 104.9 (d), 124.1 (d), 125.9 (s), 127.0 (d), 129.6 (s), 129.7 (d), 133.3 (s), 148.2 (s), 149.5 (s), 167.4 (d, COOR). HR-MS $[M + H]^+$ m/z (pred) = 231.0652, m/z (meas) = 231.658, difference = 2.60 ppm.

■ ASSOCIATED CONTENT

Ⓢ Supporting Information

Synthetic procedures and characterization data for piperine analogues; shell script for evaluation of costs; Python script to divide MACCS fingerprints into bite strings; parameters obtained for model 3; full composition of 10 trees in model 4; and a table with the full list of descriptors calculated. This material is available free of charge via the Internet at http://pubs.acs.org.

■ AUTHOR INFORMATION

Corresponding Author

*Phone +43-1-4277-55310; fax +43-1-4277-9553; e-mail steffen.hering@univie.ac.at.

Present Address

▽(T.S.) Institute of Medical Genetics Medical University of Vienna, Waehringerstrasse 10, 1090 Vienna, Austria.

Author Contributions

⊥A.S., L.W., and D.G. contributed equally.

Notes

The authors declare no competing financial interest.

■ ACKNOWLEDGMENTS

This work was supported by the Austrian Science Fund (FWF doctoral program "Molecular drug targets" W1232 to S.H., G.F.E., and M.D.M.). We thank Mihaela Coner for technical assistance.

■ ABBREVIATIONS USED

DEPC, diethyl pyrocarbonate; EtOAc, ethyl acetate; $GABA_A$, γ-aminobutyric acid type A receptor; I_{GABA}, γ-aminobutyric acid-induced chloride current; $I_{GABA\text{-}max}$, maximum aminobutyric acid-induced chloride current potentiation; LP, light petroleum; rt, room temperature; TRPV1, transient receptor potential vanilloid type 1 receptor; VR1, vanilloid receptor 1

■ REFERENCES

(1) Macdonald, R. L.; Olsen, R. W. GABAA Receptor Channels. *Annu. Rev. Neurosci.* **1994**, *17*, 569−602.

(2) Sieghart, W. Structure and Pharmacology of Gamma-Aminobutyric Acid A Receptor Subtypes. *Pharmacol. Rev.* **1995**, *47*, 181−234.

(3) Sigel, E.; Steinmann, M. E. Structure, Function, and Modulation of GABA(A) Receptors. *J. Biol. Chem.* **2012**, *287*, 40224−40231.

(4) Connolly, C. N.; Wafford, K. A. The Cys-Loop Superfamily of Ligand-Gated Ion Channels: The Impact of Receptor Structure on Function. *Biochem. Soc. Trans.* **2004**, *32*, 529−534.

(5) Sigel, E.; Kaur, K. H.; Luscher, B. P.; Baur, R. Use of Concatamers to Study GABAA Receptor Architecture and Function: Application to Delta-Subunit-Containing Receptors and Possible Pitfalls. *Biochem. Soc. Trans.* **2009**, *37*, 1338−1342.

(6) Smart, T. G.; Paoletti, P. Synaptic Neurotransmitter-Gated Receptors. *Cold Spring Harbor Perspect. Biol.* **2012**, *4*, No. a009662, DOI: 10.1101/cshperspect.a009662.

(7) Barnard, E. A.; Skolnick, P.; Olsen, R. W.; Möhler, H.; Sieghart, W.; Biggio, G.; Braestrup, C.; Bateson, A. N.; Langer, S. Z. International Union of Pharmacology. XV. Subtypes of Gamma-Aminobutyric Acid A Receptors: Classification on the Basis of Subunit Structure and Receptor Function. *Pharmacol. Rev.* **1998**, *50*, 291−313.

(8) Simon, J.; Wakimoto, H.; Fujita, N.; Lalande, M.; Barnard, E. A. Analysis of the Set of GABA(A) Receptor Genes in the Human Genome. *J. Biol. Chem.* **2004**, *279*, 41422−41435.

(9) Olsen, R. W.; Sieghart, W. International Union of Pharmacology. LXX. Subtypes of Gamma-Aminobutyric Acid(A) Receptors: Classification on the Basis of Subunit Composition, Pharmacology, and Function. Update. *Pharmacol. Rev.* **2008**, *60*, 243−260.

(10) Chang, Y.; Wang, R.; Barot, S.; Weiss, D. S. Stoichiometry of a Recombinant GABA Receptor. *J. Neurosci.* **1996**, *16*, 5415−5424.

(11) Tretter, V.; Ehya, N.; Fuchs, K.; Sieghart, W. Stoichiometry and Assembly of a Recombinant GABAA Receptor Subtype. *J. Neurosci.* **1997**, *17*, 2728−2737.

(12) Baumann, S. W.; Baur, R.; Sigel, E. Individual Properties of the Two Functional Agonist Sites in GABA(A) Receptors. *J. Neurosci.* **2003**, *23*, 11158−11166.

(13) Möhler, H. GABAA Receptors in Central Nervous System Disease: Anxiety, Epilepsy, and Insomnia. *J. Recept. Signal Transduction Res.* **2006**, *26*, 731−740.

(14) Macdonald, R. L.; Kang, J. Q.; Gallagher, M. J. Mutations in GABA Receptor Subunits Associated with Genetic Epilepsies. *J. Physiol.* **2010**, *588*, 1861−1869.

(15) Rudolph, U.; Knoflach, F. Beyond Classical Benzodiazepines: Novel Therapeutic Potential of GABAA Receptor Subtypes. *Nat. Rev. Drug Discovery* **2011**, *10*, 685−697.
(16) Engin, E.; Liu, J.; Rudolph, U. Alpha2-Containing GABA(A) Receptors: A Target for the Development of Novel Treatment Strategies for CNS Disorders. *Pharmacol. Ther.* **2012**, *136*, 142−152.
(17) Trincavelli, M. L.; Da Pozzo, E.; Daniele, S.; Martini, C. The GABA-BZR Complex as Target for the Development of Anxiolytic Drugs. *Curr. Trends Med. Chem.* **2012**, *12*, 254−269.
(18) Whiting, P. J. GABA-A Receptors: A Viable Target for Novel Anxiolytics? *Curr. Opin. Pharmacol.* **2006**, *6*, 24−29.
(19) Atack, J. R. The Benzodiazepine Binding Site of GABA(A) Receptors as a Target for the Development of Novel Anxiolytics. *Expert Opin. Invest. Drugs* **2005**, *14*, 601−618.
(20) Atack, J. R. GABAA Receptor Subtype-Selective Modulators. I. Alpha2/Alpha3-Selective Agonists as Non-Sedating Anxiolytics. *Curr. Top. Med. Chem.* **2011**, *11*, 1176−1202.
(21) Hosie, A. M.; Wilkins, M. E.; da Silva, H. M.; Smart, T. G. Endogenous Neurosteroids Regulate GABAA Receptors through Two Discrete Transmembrane Sites. *Nature* **2006**, *444*, 486−489.
(22) Li, G. D.; Chiara, D. C.; Sawyer, G. W.; Husain, S. S.; Olsen, R. W.; Cohen, J. B. Identification of a GABAA Receptor Anesthetic Binding Site at Subunit Interfaces by Photolabeling with an Etomidate Analog. *J. Neurosci.* **2006**, *26*, 11599−11605.
(23) D'Hulst, C.; Atack, J. R.; Kooy, R. F. The Complexity of the GABAA Receptor Shapes Unique Pharmacological Profiles. *Drug Discovery Today* **2009**, *14*, 866−875.
(24) Forman, S. A.; Miller, K. W. Anesthetic Sites and Allosteric Mechanisms of Action on Cys-Loop Ligand-Gated Ion Channels. *Can. J. Anaesth.* **2011**, *58*, 191−205.
(25) Gunn, B. G.; Brown, A. R.; Lambert, J. J.; Belelli, D. Neurosteroids and GABA(A) Receptor Interactions: A Focus on Stress. *Front. Neurosci.* **2011**, *5*, 131 DOI: 10.3389/fnins.2011.00131.
(26) Chiara, D. C.; Dostalova, Z.; Jayakar, S. S.; Zhou, X.; Miller, K. W.; Cohen, J. B. Mapping General Anesthetic Binding Site(S) in Human Alpha1beta3 Gamma-Aminobutyric Acid Type A Receptors with [(3)H]Tdbzl-Etomidate, a Photoreactive Etomidate Analogue. *Biochemistry* **2012**, *51*, 836−847.
(27) Richter, L.; de Graaf, C.; Sieghart, W.; Varagic, Z.; Morzinger, M.; de Esch, I. J.; Ecker, G. F.; Ernst, M. Diazepam-Bound GABAA Receptor Models Identify New Benzodiazepine Binding-Site Ligands. *Nat. Chem. Biol.* **2012**, *8*, 455−464.
(28) Johnston, G. A.; Hanrahan, J. R.; Chebib, M.; Duke, R. K.; Mewett, K. N. Modulation of Ionotropic GABA Receptors by Natural Products of Plant Origin. *Adv. Pharmacol. (San Diego, CA, U. S.)* **2006**, *54*, 285−316.
(29) Hanrahan, J. R.; Chebib, M.; Johnston, G. A. Flavonoid Modulation of GABA(A) Receptors. *Br. J. Pharmacol.* **2011**, *163*, 234−245.
(30) Nilsson, J.; Sterner, O. Modulation of GABA(A) Receptors by Natural Products and the Development of Novel Synthetic Ligands for the Benzodiazepine Binding Site. *Curr. Drug Targets* **2011**, *12*, 1674−1688.
(31) Zaugg, J.; Baburin, I.; Strommer, B.; Kim, H. J.; Hering, S.; Hamburger, M. HPLC-Based Activity Profiling: Discovery of Piperine as a Positive GABA(A) Receptor Modulator Targeting a Benzodiazepine-Independent Binding Site. *J. Nat. Prod.* **2010**, *73*, 185−191.
(32) Pedersen, M. E.; Metzler, B.; Stafford, G. I.; van Staden, J.; Jager, A. K.; Rasmussen, H. B. Amides from Piper Capense with CNS Activity: A Preliminary SAR Analysis. *Molecules* **2009**, *14*, 3833−3843.
(33) McNamara, F. N.; Randall, A.; Gunthorpe, M. J. Effects of Piperine, the Pungent Component of Black Pepper, at the Human Vanilloid Receptor (TRPV1). *Br. J. Pharmacol.* **2005**, *144*, 781−790.
(34) Khom, S.; Strommer, B.; Schöffmann, A.; Hintersteiner, J.; Baburin, I.; Erker, T.; Schwarz, T.; Schwarzer, C.; Zaugg, J.; Hamburger, M.; Hering, S. GABAA Receptor Modulation by Piperine and a Non-TRPV1 Activating Derivative. *Biochem. Pharmacol.* **2013**, *85*, 1827−1836.
(35) Thomsen, I.; Clausen, K.; Scheibye, S.; Lawesson, S. O. Thiation with 2,4-Bis(4-methoxyphenyl)-1,3,2,4-dithiadiphosphetane 2,4-Disulfide: N-Methylthiopyrrolidone (2-pyrrolidinethione, 1-methyl-). *Org. Synth.* **1984**, *62*, 158−164.
(36) Hayashi, K.; Yamazoe, A.; Ishibashi, Y.; Kusaka, N.; Oono, Y.; Nozaki, H. Active Core Structure of Terfestatin A, a New Specific Inhibitor of Auxin Signaling. *Bioorg. Med. Chem.* **2008**, *16*, 5331−5344.
(37) Blanchot, M.; Candito, D. A.; Larnaud, F.; Lautens, M. Formal Synthesis of Nitidine and Nk109 via Palladium-Catalyzed Domino Direct Arylation/N-Arylation of Aryl Triflates. *Org. Lett.* **2011**, *13*, 1486−1489.
(38) Cabri, W.; Candiani, I.; Bedeschi, A.; Santi, R. 1,10-Phenanthroline Derivatives: A New Ligand Class in the Heck Reaction. Mechanistic Aspects. *J. Org. Chem.* **1993**, *58*, 7421−7426.
(39) Ishiyama, T.; Takagi, J.; Hartwig, J. F.; Miyaura, N. A Stoichiometric Aromatic C-H Borylation Catalyzed by Iridium(I)/2,2′-Bipyridine Complexes at Room Temperature. *Angew. Chem., Int. Ed.* **2002**, *41*, 3056−3058.
(40) Thompson, A. L. S.; Kabalka, G. W.; Akula, M. R.; Huffman, J. W. The Conversion of Phenols to the Corresponding Aryl Halides under Mild Conditions. *Synthesis* **2005**, *2005*, 547−550.
(41) Grimm, J. B.; Wilson, K. J.; Witter, D. J. Suppression of Racemization in the Carbonylation of Amino Acid-Derived Aryl Triflates. *Tetrahedron Lett.* **2007**, *48*, 4509−4513.
(42) Plunkett, K. N.; Godula, K.; Nuckolls, C.; Tremblay, N.; Whalley, A. C.; Xiao, S. Expeditious Synthesis of Contorted Hexabenzocoronenes. *Org. Lett.* **2009**, *11*, 2225−2228.
(43) Klopman, G.; Li, J. Y. Quantitative Structure-Agonist Activity Relationship of Capsaicin Analogues. *J. Comput.-Aided Mol. Des.* **1995**, *9*, 283−294.
(44) Hall, M.; Frank, E.; Holmes, G.; Pfahringer, B.; Reutemann, P.; Witten, I. H. The Weka Data Mining Software: An Update. *SIGKDD Explorations* **2009**, *11* (1), 10−18.
(45) Gunthorpe, M. J.; Chizh, B. A. Clinical Development of Trpv1 Antagonists: Targeting a Pivotal Point in the Pain Pathway. *Drug Discovery Today* **2009**, *14*, 56−67.
(46) Marsch, R.; Foeller, E.; Rammes, G.; Bunck, M.; Kossl, M.; Holsboer, F.; Zieglgansberger, W.; Landgraf, R.; Lutz, B.; Wotjak, C. T. Reduced Anxiety, Conditioned Fear, and Hippocampal Long-Term Potentiation in Transient Receptor Potential Vanilloid Type 1 Receptor-Deficient Mice. *J. Neurosci.* **2007**, *27*, 832−839.
(47) Kaneko, Y.; Szallasi, A. Transient Receptor Potential (Trp) Channels: A Clinical Perspective. *Br. J. Pharmacol.* **2013**, DOI: 10.1111/bph.12414.
(48) Goldin, A. L. In *Expression and Analysis of Recombinant Ion Channels: From Structural Studies to Pharmacological Screening*; Clare, J. J., Trezise, D. J., Eds.; Wiley−VCH Verlag: Weinheim, Germany, 2006; pp 1−25.
(49) Khom, S.; Baburin, I.; Timin, E. N.; Hohaus, A.; Sieghart, W.; Hering, S. Pharmacological Properties of GABAA Receptors Containing Gamma1 Subunits. *Mol. Pharmacol.* **2006**, *69*, 640−649.
(50) Baburin, I.; Beyl, S.; Hering, S. Automated Fast Perfusion of Xenopus Oocytes for Drug Screening. *Pfluegers Arch.* **2006**, *453*, 117−123.
(51) Demel, M. A.; Kraemer, O.; Ettmayer, P.; Haaksma, E.; Ecker, G. F. Ensemble Rule-Based Classification of Substrates of the Human ABC-Transporter ABCB1 Using Simple Physicochemical Descriptors. *Mol. Inf.* **2010**, *29*, 233−242.
(52) Kohavi, R.; Provost, F. Glossary of Terms. *Mach. Learn.* **1998**, *30*, 271−274.
(53) Oprea, T. I. Property Distribution of Drug-Related Chemical Databases. *J. Comput.-Aided Mol. Des.* **2000**, *14*, 251−264.
(54) Wildman, S. A.; Crippen, G. M. Prediction of Physicochemical Parameters by Atomic Contributions. *J. Chem. Inf. Model.* **1999**, *39*, 868−873.

4.1.3 Aryl-modified Piperine Derivatives

4.1.3.1 Developing Piperine towards TRPV1 and $GABA_A$ Receptor Ligands - Synthesis of Piperine Analogs via Heck-Coupling of Conjugated Dienes

Org Biomol Chem. 2015 Jan 28;13(4):990-4. doi: 10.1039/c4ob02242d. Epub 2014 Dec 1.

Laurin Wimmer[a] David Schönbauer[a] Peter Pakfeifer[b] Angela Schöffmann[b], Sophia Khom[b] Steffen Hering[b] and Marko D. Mihovilovic[a]

[a]Institute of Applied Synthetic Chemistry, Vienna University of Technology, Getreidemarkt 9, 1060 Vienna, Austria.
[b]Department of Pharmacology and Toxicology, University of Vienna, Althanstr. 14, 1090 Vienna, Austria

Contribution Statement: *Investigation of modulatory activity of the derivatives on $GABA_A$ receptors and writing of the manuscript were my contributions to this work.*

Organic & Biomolecular Chemistry

COMMUNICATION

View Article Online
View Journal

Cite this: DOI: 10.1039/c4ob02242d

Received 22nd October 2014,
Accepted 10th November 2014

DOI: 10.1039/c4ob02242d

www.rsc.org/obc

Developing piperine towards TRPV1 and $GABA_A$ receptor ligands – synthesis of piperine analogs *via* Heck-coupling of conjugated dienes†

Laurin Wimmer,[a] David Schönbauer,[a] Peter Pakfeifer,[b] Angela Schöffmann,[b] Sophia Khom,[b] Steffen Hering[b] and Marko D. Mihovilovic*[a]

Piperine, the pungent alkaloid of black pepper, and several of its derivatives are modulators of γ-amino butyric acid type A ($GABA_A$) receptors. Concomitantly, this natural product has also been reported to activate transient receptor potential vanilloid type 1 (TRPV1) receptors. We have developed a Heck cross-coupling reaction of conjugated dienamides enabling the rapid assembly of piperine derivatives containing a modified aromatic core. Upon assessment of a focussed compound library, key aromatic substituents were identified selectively affecting either the $GABA_A$ or the TRPV1 receptor.

Piperine, the pungent alkaloid of *piper nigrum*, was recently identified as a positive allosteric modulator of γ-amino butyric acid type A ($GABA_A$) receptors.[1] Pharmaceutical compounds modulating this receptor and thus enhancing neuronal GABAergic inhibition, like benzodiazepines, are widely used as anxiolytics, sleep-inducing agents as well as for the treatment of convulsive disorders and other disease states.[2]

The pungency of piperine is caused by its ability to activate transient receptor potential vanilloid type 1 (TRPV1) receptors.[3] These receptors are non-selective cation channels which serve as sensors for pain-inducing stimuli like capsaicin, acidic conditions and heat and are also involved in temperature regulation of the human body.[4] Due to the receptors' involvement in pain processing, TRPV1 agonists and antagonists are currently under investigation as agents for the treatment of neuropathic pain and other diseases.[5] With regard to a further role of piperine derivatives in the formation of a prospective pharmacological lead compound, selectivity for either of these receptors would be highly desirable. However, the simultaneous interaction of piperine and (potentially) its derivatives with $GABA_A$ and TRPV1 receptors could lead to unwanted side effects.

In a most recent study[6] we have modified the amide functionality as well as the linker region of the natural product to investigate the effect of such structural modifications on its pharmacological activity. Analyzing the modulation of GABA-induced chloride currents through the $GABA_A$ activity of these derivatives has revealed a strong preference for di-*n*-butyl and di-*n*-propyl amide. The scaffold has proven to be highly sensitive to modifications of the linker region – all attempted modifications led to a significant loss of efficiency.

With the goal of synthesizing a library of aryl-modified piperine derivatives in mind, we required a robust synthetic method which would allow us to synthesize the desired aryldienamides in a minimum number of steps and a high level of modularity with respect to the aryl residues.

Although at present a plethora of methods for the assembly of 1-carbonyl-4-aryl substituted dienes exist, there is a demand for the development of modern and efficient methods,[7] including Wittig reactions,[8] metathesis,[9] transition-metal catalyzed ene–ene[10] and ene–yne[11] coupling reactions and C–H activation reactions.[12] These methods typically assemble the 1,3-diene from 2 + 2 or 3 + 1 carbon synthons with the requirement for pre-functionalization of both coupling partners. In this context, coupling reaction of suitably substituted dienoic acid derivatives with an aryl coupling partner is attractive. Such a reaction was recently reported by Maulide and coworkers:[13] they prepared 5-halodienoic derivatives from cyclobutene lactones and coupled these compounds in a Suzuki–Miyaura cross-coupling reaction with arylboronic acids.

In this project, we chose to employ a Heck cross-coupling reaction, which is appealing for several reasons: good atom economy, the diene coupling partner can be easily prepared in a single step from commercial material, substituted arylbromides are abundantly available and the reaction can be expected to be *E*-selective.[14]

From the arsenal of metal assisted C–C bond formation strategies, the Heck-cross coupling reaction, *i.e.* the palladium-

[a]*Institute of Applied Synthetic Chemistry, Vienna University of Technology, Getreidemarkt 9, 1060 Vienna, Austria. E-mail: marko.mihovilovic@tuwien.ac.at; Fax: +43 1 58801 154 99; Tel: +43 1 58801 163615*

[b]*Department of Pharmacology and Toxicology, University of Vienna, Althanstr. 14, 1090 Vienna, Austria*

†Electronic supplementary information (ESI) available. See DOI: 10.1039/c4ob02242d

catalyzed cross-coupling of olefins and aromatic or vinylic (pseudo)halides, has become an integral part of modern cross-coupling methods.[15] The palladium-catalyzed arylation[14] and vinylation[16] of conjugated dienes was first reported by Heck and coworkers in the late 1970s and early 1980s. In the case of arylation of pentadienoic acid it has been shown that the reaction occurs at the terminal olefinic position providing *E*,*E*-dienes as products.[14]

Given the importance of dienes as synthetic intermediates and final products, there are only a few precedents of direct coupling of dienes with suitable coupling partners in the literature. Arylation has been reported in the presence of silver or thallium salts,[17] in ionic liquids[18] or under C–H activation conditions with benzoxazole as a coupling partner[19] as well as in the total synthesis of galanthamine.[20] Vinylation has been reported under oxidative coupling conditions[10] or in rhodium(I) catalysis[21] using boron compounds as coupling partners and in a tandem hydrozirconation-coupling process.[22] Trapping of the intermediate Pd-π-allyl species by nucleophiles has been utilized for carbo- and heteroannulation reactions.[23]

The conditions for the arylation of dienes initially published by Heck were not suitable for our purpose: reactions are conducted without a solvent, which, on a small reaction scale, leads to impractically small volumes. In our hands, the diene substrate was also prone to polymerization under these conditions. In the present study we report the optimization of reaction conditions and the synthesis of a focused library of aryl-modified piperine derivatives. Demonstrating the potential of this facile access to a compound library for biological assessment, the modulation of currents through $GABA_A$ and TRPV1 receptors, expressed in *Xenopus laevis* oocytes by these compounds was analyzed by means of the 2-microelectrode clamp technique.

Results and discussion

Based on our previous findings and with the aim of further improving activity of the hit structure towards $GABA_A$ modulation,[6] we focused on the preparation of piperine derivatives bearing the non-natural dibutylamide function.

Pentadienoic acid[24] was readily converted into its acid chloride *in situ* by treatment with oxalylchloride/DMF, followed by the addition of dibutylamine. Attempts to isolate the acid chloride led to decomposition in our hands. Alternatively, pentadienoic acid was smoothly converted into the required amide in the presence of EDCI·HCl. When kept at −20 °C the amide displayed a storage stability of several months without significant degradation.

As a starting point for the optimization of the metal assisted C–C bond formation reaction, the coupling of 4-bromotoluene was conducted employing the standard Heck-reaction conditions ($Pd(OAc)_2$, (*o*-tolyl)$_3$P, NEt_3, MeCN, 70 °C).[25]

The reaction proceeded slowly, giving 52% yield after 72 hours (Table 1, entry 1). Throughout the screening process, reactions at temperatures at or below the boiling point of the

Table 1 Optimization of coupling conditions

Entry	Solvent	Base	Ligand	*T*/°C	Time	GC-yield
1	MeCN	NEt_3	(*o*-Tolyl)$_3$P	70	72 h	52%
2	MeCN	NEt_3	(*o*-Tolyl)$_3$P	140, mw	3 h	31%
3	MeCN	NEt_3	(*o*-Tolyl)$_3$P	160, mw	3 h	31%
3	MeCN	NEt_3	(*o*-Tolyl)$_3$P	160, mw	1 h	13%
4	MeCN	NaOAc	(*o*-Tolyl)$_3$P	160, mw	1 h	4%
5	MeCN	$NaHCO_3$	(*o*-Tolyl)$_3$P	160, mw	1 h	3%
6	MeCN	K_2CO_3	(*o*-Tolyl)$_3$P	160, mw	1 h	16%
7	PhMe	NEt_3	(*o*-Tolyl)$_3$P	160, mw	1 h	3%
8	PhMe	NaOAc	(*o*-Tolyl)$_3$P	160, mw	1 h	1%
9	PhMe	$NaHCO_3$	(*o*-Tolyl)$_3$P	160, mw	1 h	1%
10	PhMe	K_2CO_3	(*o*-Tolyl)$_3$P	160, mw	1 h	4%
11	THF	NEt_3	(*o*-Tolyl)$_3$P	160, mw	1 h	2%
12	THF	NaOAc	(*o*-Tolyl)$_3$P	160, mw	1 h	3%
13	THF	$NaHCO_3$	(*o*-Tolyl)$_3$P	160, mw	1 h	2%
14	THF	K_2CO_3	(*o*-Tolyl)$_3$P	160, mw	1 h	48%
15	DMF	NEt_3	(*o*-Tolyl)$_3$P	160	1 h	16%
16	DMF	NaOAc	(*o*-Tolyl)$_3$P	160	13 h	49%
17	DMF	$NaHCO_3$	(*o*-Tolyl)$_3$P	160	1 h	53%
18	DMF	K_2CO_3	(*o*-Tolyl)$_3$P	160	1 h	79%
19	DMF	K_2CO_3 + NEt_4Cl	(*o*-Tolyl)$_3$P	160	1 h	76%
20	DMF	K_2CO_3 + NEt_4Br	(*o*-Tolyl)$_3$P	160	1 h	75%
21	DMF	K_2CO_3	(*o*-Tolyl)$_3$P	140	1 h	77%
22	DMF	K_2CO_3	(2-Furyl)$_3$P	140	1 h	3%
23	DMF	K_2CO_3	(*p*-ClPh)$_3$P	140	1 h	8%
24	DMF	K_2CO_3	(1-Naphthyl)$_3$P	140	1 h	21%
25	DMF	K_2CO_3	$Pd(PPh_3)_4$	140	1 h	42%
26	DMF	K_2CO_3	Dppf	140	1 h	76%
27	DMF	K_2CO_3	Cy_3P	140	1 h	79%
28	DMF	K_2CO_3	Dppp	140	1 h	87%
29	DMF	K_2CO_3	JohnPhos	140	1 h	89%

reaction solvent were carried out in screw-cap vials heated in a metal block. Reactions which required higher temperatures were carried out in a microwave reactor, which facilitates automated and safe handling of pressurized vessels (an experiment comparing these heat-sources showed that they can be used interchangeably for this transformation). Increasing the temperature to 140 °C or 160 °C both gave 31% of GC-yield after only three hours (entries 2 and 3). An extension of the reaction time was not attempted in these cases, since the mass balance indicated significant decomposition of the starting materials. First, a set of four bases (NEt_3, $NaHCO_3$, K_2CO_3 and NaOAc) and four solvents (MeCN, toluene, THF and DMF) were evaluated (entries 3–18). While toluene and THF did not facilitate coupling in combination with most bases, the best results were obtained with DMF as the solvent (entries 15–18). Out of the set of bases tested, K_2CO_3 proved most effective in all solvents (entries 6, 10, 14, 18), particularly in DMF (79% GC yield, entry 18). Quaternary ammonium salts as additives, which can be beneficial in Heck-couplings,[26] did not improve the reaction (entries 19 and 20).

An improvement in the side-product profile as judged by GC was achieved by lowering the reaction temperature to 140 °C, while the reaction yield was unaffected (entries 18 and 21).

Finally, a set of eight mono- and bidentate phosphine ligands were tested in combination with palladium(II) acetate. The use of ($Pd(dba)_2$) as a palladium source was also investigated, but it gave generally lower conversions (see ESI†). With respect to the ligands the best results were obtained with JohnPhos and dppp (87–89% GC yield, Table 1, entries 28 and 29). Compared to JohnPhos, dppp has a lower price and was therefore selected for the final reaction protocol.

After establishing an optimized set of reaction parameters for the required reaction, the robustness of the protocol was investigated (Scheme 1). Coupling proceeded smoothly for a variety of aryl bromides bearing electron donating (**4**, **6–9**) or electron withdrawing substituents (**12–15**). In the reactions of bromochlorobenzenes the chloro-substituent was inert under the reaction conditions (**10** and **11**). In the case of 3-bromothiophene the product was obtained in a low yield of 35%. 3- and 4-bromopyridines were well accepted giving products **17** and **18** in 59% and 62% yield, respectively. However, 2-substituted heterocycles (aimed at compound **19**) failed to undergo coupling. The same was observed in the cases of 2-bromothiophene and 2-bromothiazole. This indicates that complexation by the neighboring heteroatom could be responsible for the detrimental effect on the reaction in these cases. Concerning regio- and stereoselectivity of the reaction, all final products were isolated as the 2*E*,4*E*-dienamides. However, GC-MS analysis of the crude reaction mixture typically showed several minor peaks with the same *m*/*z* ratio as the products, which are likely to be stereo- and regioisomers. These side products occurred only in trace amounts and we were therefore unable to isolate sufficient quantities for their characterization.

The effect of aryl-modifications on the enhancement of GABA-induced chloride currents (I_{GABA}) through $\alpha_1\beta_2\gamma_{2S}$ receptors was studied at 100 μM. Compared to the natural product piperine, compounds **4** (783 ± 72%, $p < 0.001$), **6** (883 ± 70%, $p < 0.001$), **15** (570 ± 113, $p < 0.05$), **16** (970 ± 244%, $p < 0.001$) and **18** (782 ± 62%, $p < 0.001$) displayed a significantly more pronounced I_{GABA} enhancement, while I_{GABA} modulation by the other prepared compounds did not significantly differ from that of piperine (226 ± 26% at 100 μM; data taken from ref. 1, see Fig. 1A).

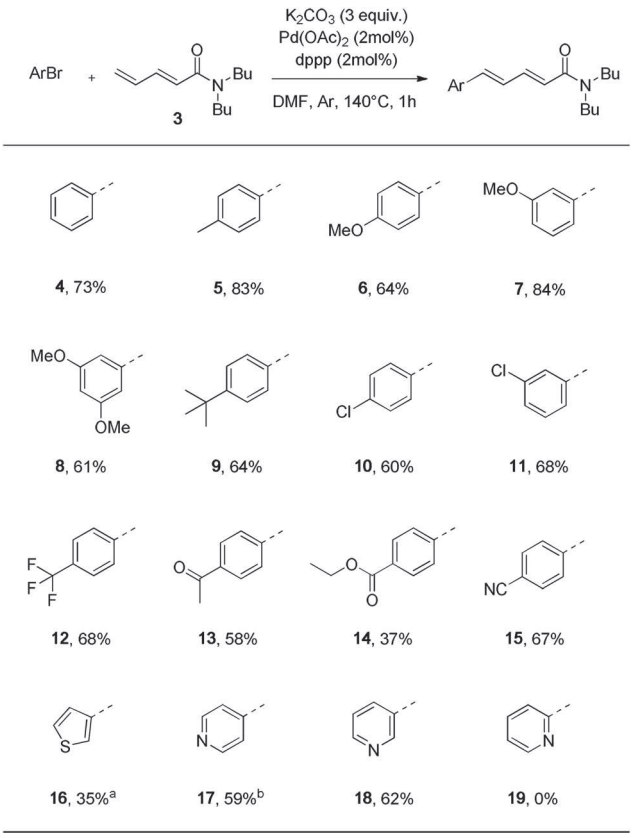

Scheme 1 Compound library. (a) 2 equiv. of 3-bromothiophene, 100 °C, 16 h; (b) 44 h, 2 mol% of catalyst added after 1 h, 1 equiv. of 4-bromopyridine added after 16 h.

Likewise, the effect on the modulation of capsaicin-induced currents through the TRPV1 receptors was studied at a concentration of 100 μM. As illustrated in Fig. 1B, compound **8** (80 ± 22%, $p < 0.001$) significantly enhanced the currents through TRPV1 channels, while compounds **4** (−90 ± 2%, $p < 0.0015$), **5** (−59 ± 6%; $p < 0.05$), **7** (−63 ± 16%; $p < 0.01$), **9** (−73 ± 10%; $p < 0.001$), **10** (65 ± 7%; $p < 0.01$) and **11** (87 ± 2%, $p < 0.001$) effectively inhibited them. Products **6**, **12**, **13**, **14**, **15**, **16**, **17** and **18** did not display any significant modulation of the TRPV1 receptors (representative traces for the modulation of GABA- and capsaicin-induced currents, respectively, by selected compounds, see Fig. 1C).

Collectively, these data indicate that slight modifications in the natural product piperine can lead to a high selectivity for either the $GABA_A$ or the TRPV1 channels.

Most strikingly, compound **8** significantly enhanced $I_{capsaicin}$ (80 ± 22%, $p < 0.001$), while it was nearly inactive on

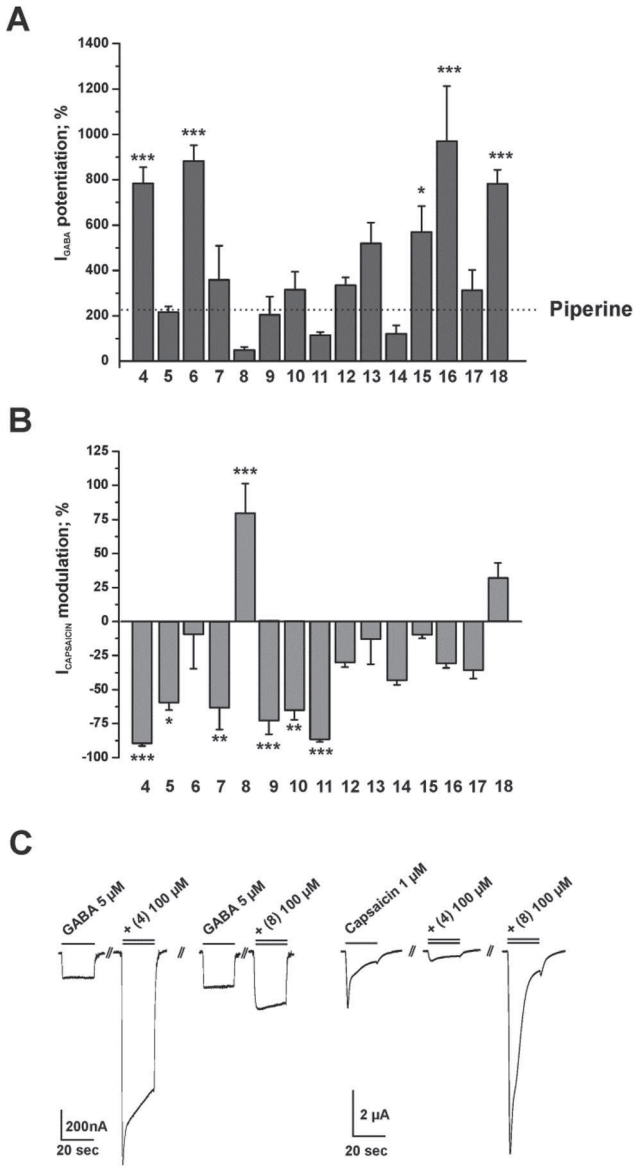

Fig. 1 (A) Modulation of GABA-induced currents through $\alpha_1\beta_2\gamma_{2s}$ $GABA_A$ receptors by 100 µM of the indicated compound. Dashed line represents the I_{GABA} enhancement by the natural product piperine 100 µM.[1a] Each data point represents a mean ± SEM; asterisks indicate statistical significance calculated by one-way ANOVA followed by a Dunnett mean comparison test. (B) Modulation of capsaicin-induced currents through TRPV1 receptors by 100 µM of the indicated compound. Each data point represents a mean ± SEM; asterisks indicate statistical significance calculated by one-way ANOVA followed by a Dunnett mean comparison test. (C) Representative currents for the modulation of GABA-induced currents (left panel) and capsaicin-induced currents (right panel), respectively, by co-application of 100 µM of the indicated derivative are illustrated.

the $GABA_A$ receptors. Likewise, products **11** and **14** displayed only weak I_{GABA} enhancement, however – in contrast to compound **8** – they significantly reduced capsaicin-induced currents through the TRPV1 receptors. The most effective inhibition of $I_{capsaicin}$ was observed for compound **4** (−90 ± 2%), however, this derivative also effectively modulated the $GABA_A$ receptors (783 ± 72%) and was thus not selective for either receptor type. Finally, compound **6** was identified as a novel piperine-derived effective $GABA_A$ receptor modulator (883 ± 70%), that did not affect the TRPV1 receptors (−10 ± 3%).

Conclusions

We have developed a facile protocol for the arylation of dienamides which facilitates rapid and stereoselective access to 2*E*,4*E*-products through operational simplicity and short reaction times. Compared to other protocols, the use of arylbromides instead of boronic acids,[13] alkynes,[11] alkenes[10] or aldehydes[8] comprises a significant advantage in terms of price and commercial availability. Applying this protocol we have synthesized a library of 15 compounds. Biological testing has revealed compounds with a high efficacy and selectivity for either the $GABA_A$ or the TRPV1 receptors. These results are very promising and a full pharmacological characterization of the test compounds is currently underway in our laboratories to be published in due course.

Experimental

The experimental procedures for compound synthesis and biological testing, as well as the compound characterization data can be found in the ESI.†

Acknowledgements

L. W. and A. S. were supported by the Austrian Science Fund (FWF doctoral program "Molecular drug targets" W1232).

Notes and references

1 (*a*) J. Zaugg, I. Baburin, B. Strommer, H.-J. Kim, S. Hering and M. Hamburger, *J. Nat. Prod.*, 2010, **73**, 185; (*b*) M. E. Pedersen, B. Metzler, G. I. Stafford, J. van Staden, A. K. Jager and H. B. Rasmussen, *Molecules*, 2009, **14**, 3833.
2 (*a*) P. J. Whiting, *Curr. Opin. Pharmacol.*, 2006, **6**, 24; (*b*) J. Riss, J. Cloyd, J. Gates and S. Collins, *Acta Neurol. Scand.*, 2008, **118**, 69; (*c*) U. Rudolph and H. Mohler, *Annu. Rev. Pharmacol. Toxicol.*, 2014, **54**, 483.
3 F. N. McNamara, A. Randall and M. J. Gunthorpe, *Br. J. Pharmacol.*, 2005, **144**, 781.
4 N. R. Gavva, A. W. Bannon, S. Surapaneni, D. N. Hovland Jr., S. G. Lehto, A. Gore, T. Juan, H. Deng, B. Han, L. Klionsky, R. Kuang, A. Le, R. Tamir, J. Wang, B. Youngblood, D. Zhu, M. H. Norman, E. Magal, J. J. S. Treanor and J.-C. Louis, *J. Neurosci.*, 2007, **27**, 3366.
5 M. J. Gunthorpe and A. Szallasi, *Curr. Pharm. Des.*, 2008, **14**, 32.
6 A. Schoeffmann, L. Wimmer, D. Goldmann, S. Khom, J. Hintersteiner, I. Baburin, T. Schwarz, M. Hintersteininger,

P. Pakfeifer, M. Oufir, M. Hamburger, T. Erker, G. F. Ecker, M. D. Mihovilovic and S. Hering, *J. Med. Chem.*, 2014, **57**, 5602.
7 M. De Paolis, I. Chataigner and J. Maddaluno, *Top. Curr. Chem.*, 2012, **327**, 87.
8 C. J. O'Brien, F. Lavigne, E. E. Coyle, A. J. Holohan and B. J. Doonan, *Chem. – Eur. J.*, 2013, **19**, 5854.
9 B. H. Lipshutz, S. Ghorai and Z. V. Boskovic, *Tetrahedron*, 2008, **64**, 6949.
10 J. H. Delcamp, P. E. Gormisky and M. C. White, *J. Am. Chem. Soc.*, 2013, **135**, 8460.
11 T. Schabel and B. Plietker, *Chem. – Eur. J.*, 2013, **19**, 6938.
12 Z.-K. Wen, Y.-H. Xu and T.-P. Loh, *Chem. Sci.*, 2013, **4**, 4520.
13 C. Souris, F. Frebault, A. Patel, D. Audisio, K. N. Houk and N. Maulide, *Org. Lett.*, 2013, **15**, 3242.
14 B. A. Patel, J. E. Dickerson and R. F. Heck, *J. Org. Chem.*, 1978, **43**, 5018.
15 (*a*) K. C. Nicolaou, P. G. Bulger and D. Sarlah, *Angew. Chem., Int. Ed.*, 2005, **44**, 4442; (*b*) I. P. Beletskaya and A. V. Cheprakov, *Chem. Rev.*, 2000, **100**, 3009.
16 W. Fischetti, K. T. Mak, F. G. Stakem, J. Kim, A. L. Rheingold and R. F. Heck, *J. Org. Chem.*, 1983, **48**, 948.
17 T. Jeffery, *Tetrahedron Lett.*, 1992, **33**, 1989.
18 L. Beccaria, A. Deagostino, C. Prandi, C. Zavattaro and P. Venturello, *Synlett*, 2006, 2989.
19 W.-C. Lee, T.-H. Wang and T.-G. Ong, *Chem. Commun.*, 2014, **50**, 3671.
20 J. Choi, H. Kim, S. Park and J. Tae, *Synlett*, 2013, 379.
21 G. De la Herran, C. Murcia and A. G. Csakye, *Org. Lett.*, 2005, **7**, 5629.
22 G. Wang, S. Mohan and E.-i. Negishi, *Proc. Natl. Acad. Sci. U. S. A.*, 2011, **108**, 11344.
23 (*a*) R. C. Larock and C. A. Fried, *J. Am. Chem. Soc.*, 1990, **112**, 5882; (*b*) R. C. Larock, N. Berrios-Pena and K. Narayanan, *J. Org. Chem.*, 1990, **55**, 3447.
24 K. Sparrow, D. Barker and M. A. Brimble, *Tetrahedron*, 2011, **67**, 7989.
25 R. F. Heck, *Org. React.*, 1982, **27**, 345.
26 T. Jeffery, *Tetrahedron*, 1996, **52**, 10113.

4.1.3.2 β-Subunit Specific Modulation of $GABA_A$ Receptors by Aryl-modified Piperine Derivatives – A Preliminary Study

Additional data.

Background

Di-*N*-butyl and di-*N*-propyl amide derivatives of piperine were shown to highly efficaciously modulate I_{GABA} through different $GABA_A$ receptors subtypes; for compound **23**, a tendency toward β-selective I_{GABA} modulation could be observed. In contrast, interference with the linker region of the piperine scaffold led to a significant loss of efficacy (**Chapter 4.1.1** and **Chapter 4.1.2**)[250,251]. Further studies on the influence of modification introduced to the aryl (*1,3*-benzodioxole or vanilloid) moiety of the derivatives revealed compounds with high efficacy and selectivity for either $GABA_A$ or TRPV1[252] (**Chapter 4.1.3.1**). Here, to study the impact of aryl modification on β subunit selective I_{GABA} modulation, a set of six piperine analogues (**6**, **16**, **17**, **4**[252] and **15**, please refer to, and **6a**) were investigated.

Materials and Methods

The reader may refer to Schöffmann *et al.*[250] for a detailed description of materials and methods.

Results

In a preliminary study on β subunit selective I_{GABA} modulation, six compounds (**6**, **6a**, **16**, **17**, **4** and **15**) were subjected to concentration-response measurements through $\alpha_1\beta_{1\text{-}3}\gamma_{2S}$ $GABA_A$ receptors. Derivative **6** [(*2E,4E*)-*N,N*-dibutyl-5-(4-methoxyphenyl)penta-2,4-dienamide] showed most efficacious modulation of $GABA_A$ receptors ($\alpha_1\beta_3\gamma_{2S}$: E_{max} = 2199±134 %, n=4, $p<0.01$), while **17** [(*2E,4E*)-*N,N*-dibutyl-5-(pyridin-4-yl)penta-2,4-dienamide] only

slightly more efficaciously enhanced I_{GABA} (highest efficacy observed for $\alpha_1\beta_3\gamma_{2S}$ receptors; E_{max} = 649±40 %, n=6, p<0.01) compared to piperine ($\alpha_1\beta_3$: 332±64 %, n=7)[253] (**Figure 11**). The derivatives were further subjected to concentration-response measurements through $\alpha_1\beta_{1\text{-}3}\gamma_{2S}$ $GABA_A$ receptors.

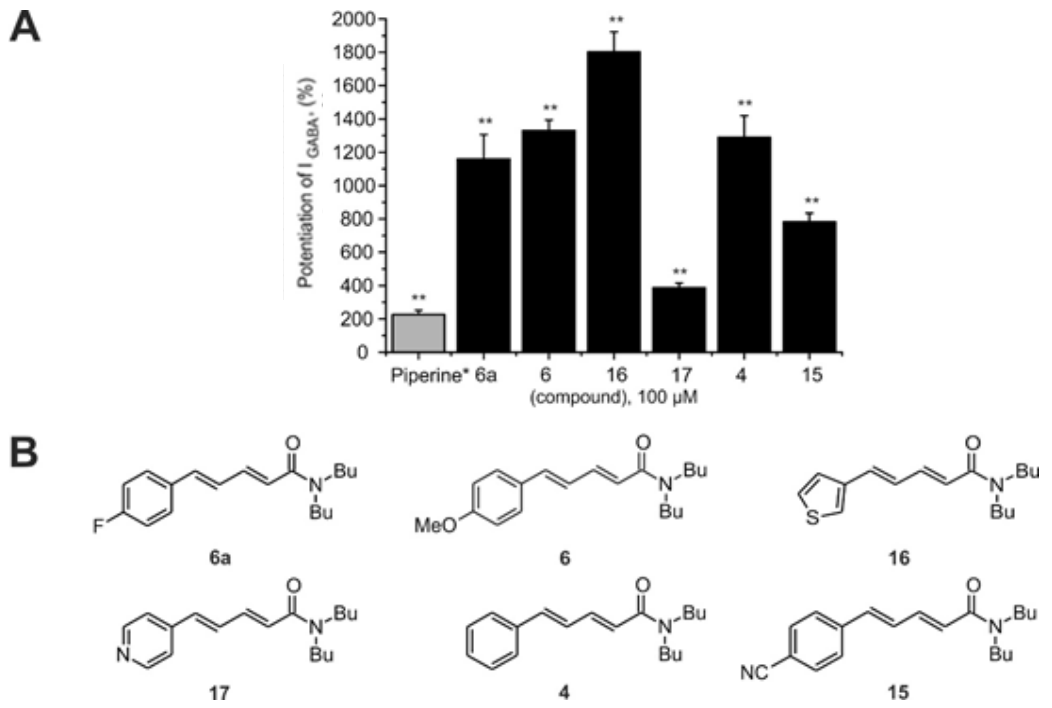

Figure 11 (A) *I_{GABA} modulation through $\alpha_1\beta_2\gamma_{2S}$ $GABA_A$ receptors by the piperine derivatives **6, 6a, 16, 17, 4** and **15** at a concentration of 100 µM, compared to piperine (grey bar). Asterisks indicate statistically significant difference to zero; ** = p<0.01 (paired Student's T-test). All values are given as mean±SE. Data are from at least 3 oocytes and 2 different frogs.* ***(B)*** *Chemical structures of derivatives **6, 6a, 16, 17, 4** and **15**. Data for piperine taken from Zaugg et al.[253].*

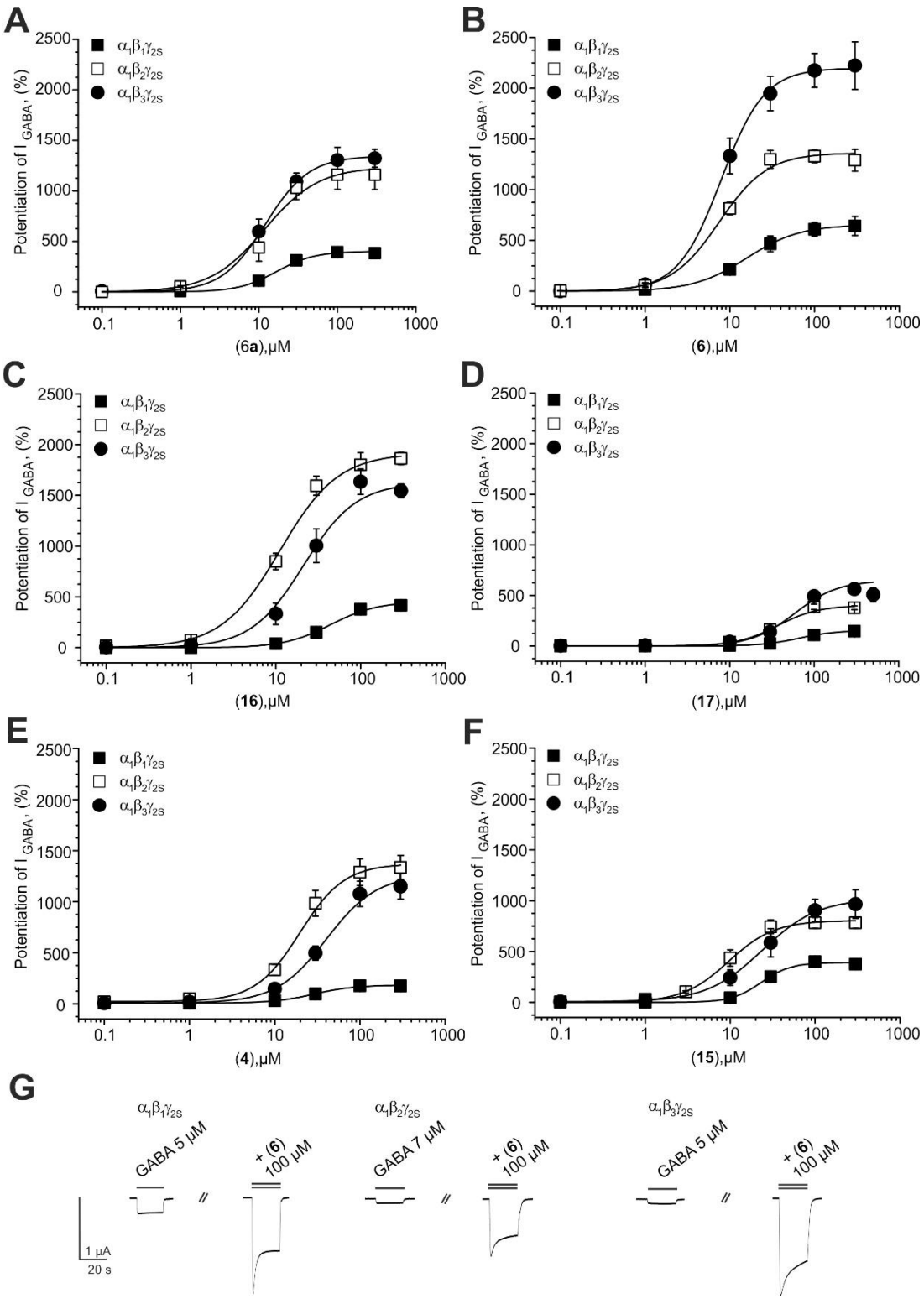

Figure 12 *Concentration dependent modulation of I_{GABA} through $\alpha_1\beta_1\gamma_{2S}$ (■), $\alpha_1\beta_2\gamma_{2S}$ (□) and $\alpha_1\beta_3\gamma_{2S}$ (●) $GABA_A$ receptors by* ***6a*** *(**A**),* ***6*** *(**B**),* ***16*** *(**C**),* ***17*** *(**D**),* ***4*** *(**E**), and* ***15*** *(**F**). Representative I_{GABA} modulated by* ***6*** *through $\alpha_1\beta_{1\text{-}3}\gamma_{2S}$ $GABA_A$ receptors (**G**). Each data point represents mean±SE from at least 3 oocytes and 2 different frogs.*

Derivative **6a** [**Figure 12 A**; (*2E,4E*)-*N,N*-dibutyl-5-(4-fluorophenyl)penta-2,4-dienamide)] modulated $\alpha_1\beta_{2/3}\gamma_{2S}$ $GABA_A$ receptors with similar efficacy (β_2: E_{max} = 1238±130 %, n=6, p<0.01; β_3: E_{max} = 1345±79 %, n=5, p<0.01), while showing a significant drop of I_{GABA} enhancement through β_1 containing receptor subtypes (E_{max} = 401±21 %, n=6, p<0.01). In contrast to this threefold drop in efficacy, comparable potency could be observed for all three subunit combinations. **6** (**Figure 12 B and G**) enhanced I_{GABA} through $\alpha_1\beta_3\gamma_{2S}$ (E_{max} = 2199±134 %, n=4, p<0.01) significantly more than through $\alpha_1\beta_2\gamma_{2S}$ $GABA_A$ receptors (E_{max} = 1363±57 %, n=3, p<0.01). Potentiation of I_{GABA} remained comparably low through β_1 containing receptor subtypes (E_{max} = 655±69 %, n=5, p<0.01). While the compound modulated β_2 and β_3 containing receptors with similar potency (β_2: EC_{50} = 7.5±1.0 µM, p<0.01; β_3: EC_{50} = 7.9±1.6 µM, p<0.01), a strong loss in potency was observed for $\alpha_1\beta_1\gamma_{2S}$ $GABA_A$ receptors (EC_{50} = 15.9±4.7 µM, p<0.01). **16** [**Figure 12 C**; (*2E,4E*)-*N,N*-dibutyl-5-(thiophen-3-yl)penta-2,4-dienamide)] led to comparable results on β_2 and β_3 containing receptors (β_2: E_{max} = 1916±63 %, EC_{50} = 11.2±1.5 µM, n=4, p<0.01; β_3: E_{max} = 1626±79 %, p<0.01, EC_{50} = 21.3±5.0 µM, p<0.05, n=4). Replacing β_2 or β_3 subunits with β_1 subunits decreased both efficacy (E_{max} = 454±51 %, n=5, p<0.01) and potency (EC_{50} = 44.2±11.0 µM, p<0.01). Comparable to **6**, **4** [**Figure 12 E**; (*2E,4E*)-N,N-dibutyl-5-phenylpenta-2,4-dienamide] enhanced I_{GABA} most efficaciously through $\alpha_1\beta_2\gamma_{2S}$ (E_{max} = 1371±112 %, n=4, p<0.01) and $\alpha_1\beta_3\gamma_{2S}$ $GABA_A$ receptors (E_{max} = 1265±155 %, n=4, p<0.01). In sharp contrast, I_{GABA} modulation through the β_1 containing receptor subtype was significantly decreased (E_{max} = 183±25 %, n=5). This effect, however, could not be observed in terms of potency (β_1: EC_{50} = 28.8±8.0 µM, p<0.01; β_2: EC_{50} = 19.7±4.2 µM, p<0.05; β_3: 40.6±10.9 µM). A similarly noticeable difference was detected for **15** [**Figure 12 F**; (*2E,4E*)-*N,N*-dibutyl-5-(4-cyanophenyl)penta-2,4-dienamide] in I_{GABA} modulation through $\alpha_1\beta_2\gamma_{2S}$ (E_{max} = 805±41 %, n=4, p<0.01) and $\alpha_1\beta_3\gamma_{2S}$ (E_{max} = 1021±138 %, n=8, p<0.01) compared to $\alpha_1\beta_1\gamma_{2S}$ $GABA_A$ receptors (E_{max} = 391±23 %, n=3, p<0.01). This compound most potently modulated I_{GABA} through $\alpha_1\beta_2\gamma_{2S}$ receptors (EC_{50} = 9.6±1.8 µM), whereas – interestingly and in contrast to all other compounds studied – no difference could be detected between β_1 and β_3 containing receptors (**Table 1**). In distinction from the other four

investigated derivatives, **17** [**Figure 12 D**; (*2E,4E*)-*N,N*-dibutyl-5-(pyridin-4-yl)penta-2,4-dienamide] did not reach saturating concentration at 300 µM; thus, concentration-response measurements were conducted including 500 µM. Overall, the results obtained for **17** lagged behind the other studied derivatives in regard of both efficacy and potency; **17** most efficaciously enhanced I_{GABA} through $\alpha_1\beta_3\gamma_{2S}$ receptors (E_{max} = 649±40 %, n=6, p<0.01).

Table 1 *Summary of efficacy and potency data collected for piperine derivatives* ***6, 6a, 16, 17, 4*** *and* ***15*** *through $\alpha_1\beta_{1/2/3}\gamma_{2S}$ $GABA_A$ receptors. Data for piperine were collected for $\alpha_1\beta_{1/3}$[a] and $\alpha_1\beta_2\gamma_{2S}$[b] receptors, respectively (see footnote). Asterisks indicated statistically significant (paired Student's T-test) differences when compared to piperine for the respective corresponding subunit combination, where: * = p<0.05. ** = p<0.01. All values are given as mean±SE. nH = Hill coefficient.*

Compound	Receptor subtype	E_{max} (%)	EC_{50} (µM)	n_H	n
Piperine[a.b]	$\alpha_1\beta_1$[a]	171±22	57.6±4.2	1.4±0.2	10
	$\alpha_1\beta_2\gamma_{2S}$[b]	302±27	52.4±9.4	1.5±0.2	6
	$\alpha_1\beta_3$[a]	332±64	48.3±7.3	1.5±0.3	7
6a	$\alpha_1\beta_1\gamma_{2S}$	401±21 **	11.8±4.3 **	1.3±0.2	6
	$\alpha_1\beta_2\gamma_{2S}$	1238±130 **	16.7±2.1 **	1.8±0.3	6
	$\alpha_1\beta_3\gamma_{2S}$	1345±79 **	12.2±2.5 **	1.6±0.1	5
6	$\alpha_1\beta_1\gamma_{2S}$	655±69 **	15.9±4.7 **	1.4±0.1	5
	$\alpha_1\beta_2\gamma_{2S}$	1363±57 **	**7.5±1.0 ****	1.5±0.1	3
	$\alpha_1\beta_3\gamma_{2S}$	**2199±134 ****	7.9±1.6 **	1.7±0.2	4
16	$\alpha_1\beta_1\gamma_{2S}$	454±51 **	44.2±11.0	1.6±0.3	5
	$\alpha_1\beta_2\gamma_{2S}$	1916±63 **	11.2±1.5 **	1.3±0.1	4
	$\alpha_1\beta_3\gamma_{2S}$	1626±79 **	21.3±5.0 *	1.4±0.2	4
17	$\alpha_1\beta_1\gamma_{2S}$	155±16	66.1±14.2	1.9±0.4	4
	$\alpha_1\beta_2\gamma_{2S}$	401±20 *	36.7±3.1	1.8±0.2	4
	$\alpha_1\beta_3\gamma_{2S}$	649±40 **	59.0±6.0	1.7±0.1	6
4	$\alpha_1\beta_1\gamma_{2S}$	183±25	28.8±8.0 **	1.8±0.6	5
	$\alpha_1\beta_2\gamma_{2S}$	1371±112 **	19.7±4.2 *	1.7±0.4	4
	$\alpha_1\beta_3\gamma_{2S}$	1265±155 **	40.6±10.9	1.5±0.2	4
15	$\alpha_1\beta_1\gamma_{2S}$	391±23 **	23.2±3.4 **	2.5±0.6	3
	$\alpha_1\beta_2\gamma_{2S}$	805±41 **	9.6±1.8 **	1.6±0.2	4
	$\alpha_1\beta_3\gamma_{2S}$	1021±138 **	23.9±9.7	1.3±0.2	8

[a]Khom *et al.*[251] (**Chapter 4.1.1**); Piperine does not show γ-subunit dependence. Data shown were consequently generated through $\alpha_1\beta_1$ and $\alpha_1\beta_3$ receptors, respectively. [b]Zaugg *et al.*[253].

Replacing the β_3 subunit with either β_2 (E_{max} = 401±20 %, $p<0.05$) or β_1 (E_{max} = 155±16 %) did not greatly enhance efficacy. **17** most potently modulated I_{GABA} through β_2 containing receptors (EC_{50} = 36.7±3.1 µM), whereas potency observed with β_1 (EC_{50} = 66.1±14.2 µM) and β_3 (EC_{50} = 59.0±6.0 µM) $GABA_A$ receptors remained in the range of the natural source compound piperine (**Table 1**).

Summary and Conclusions

Derivatives **6, 6a, 16, 17, 4 and 15** modulated I_{GABA} with efficacies ranging from 2199±134 % (**6**, n=4) to 155±16 % (**17**, n=4), while potency comprised values from 7.5±1.6 µM (**6**) to 66.1±14.2 µM (**17**). Methoxybenzyl derivative **6** enhanced I_{GABA} more efficaciously through all three studied receptor subtypes compared to the natural precursor piperine, and showed most efficacious I_{GABA} enhancement of all derivatives (E_{max} = 2199±134 %, n=4). In addition, a significant 3.4-fold decrease in efficacy could be observed for I_{GABA} modulation through β_1 receptors. Compared to piperine, efficacy of derivatives **6a** and **6, 16, 17, 4** and **15** through $\alpha_1\beta_{2/3}\gamma_{2S}$ receptors could consistently be enhanced by the introduced structural modifications. However, breakdown of the vanillyl moiety promoted I_{GABA} enhancement through $\alpha_1\beta_1\gamma_{2S}$ receptors only for **6a, 6 16,** and **15**, while **17** and **4** showed efficiencies comparable to the natural parent compound for this receptor subunit combination. Aside from the overall weaker I_{GABA} enhancement of **4** compared to the other five investigated derivatives, this compound generated the most pronounced subunit dependent difference in efficacy, showing a 7.5-fold decrease in efficacy comparing $\beta_{2/3}$ to β_1. In terms of potency, compound **6** displayed significantly lower EC_{50} values for all receptor subtypes than the natural parent compound, and $\beta_{2/3}$ preference could also be observed: EC_{50} values were two times lower for $\beta_{2/3}$ compared to β_1 receptors.

All derivatives displayed a clear tendency towards $\beta_{2/3}$ compared to β_1 containing receptor subtypes. However, no particular trend for either β_2 or β_3 receptors could be observed. In terms of potency, all derivatives – with the

exception of **17** – modulated I_{GABA} through $\alpha_1\beta_{2/3}\gamma_{2S}$ receptor subtypes significantly more potently than piperine. Particularly, and again apart from **17**, all derivatives showed lower EC_{50} values for β_2 than for β_3 incorporating receptors. The above observations suggest either a strong positive influence of the breakdown of the vanillyl moiety and installation of electronegative substituents, facilitated receptor binding due to reduced bulkiness of the molecule, or alleviated fitting in the binding pocket caused by higher flexibility of the modified rest.

4.1.4 Influence of Structural Modifications introduced to Piperine on Transient Receptor Potential Vanilloid Type 1 Receptor (TRPV1) Channels – A Preliminary Study

Additional data.

Background

Piperine is a known agonist of TRPV1, a characteristic which, for reasons such as piperine's potential to cause pain or deteriorations in thermoregulation[195], provides a challenge in the course of drug development. The aim of this study was to elucidate whether structural modifications introduced to the natural parent compound could influence the effect on TRPV1 or even eliminate it.

Materials and Methods

The reader may refer to Schöffmann *et al.*[250] for a detailed description of materials and methods.

Results and Discussion

Rat TRPV1 cRNA was expressed in *X. leavis* oocytes, which were subjected to TEVC studies conducted 1-3 days post injection. 78 compounds were studied for interaction with TRPV1 channels: only ten (**29 – 31** and **33** – **39**) out of 78 derivatives (please refer to Supporting Information of Schöffmann *et al.*[250], **Chapter 7.1**, for detailed compound information) evoked cationic currents through the channels, of which the majority at the same time elicited relatively low responses. As described in **Chapter 4.1.1** and **Chapter 4.1.2**, the modifications introduced to compounds **23** [(*2E,4E*)-5-(*1,3*-benzodioxol-5-yl))-*N,N*-dipropyl-2,4-pentadienamide], **24** [(*2E,4E*)-5-(*1,3*-benzodioxol-5-yl))-*N,N*-diisopropyl-2,4-pentadienamide] and **25** [(*2E,4E*)-5-(*1,3*-benzodioxol-5-yl))-*N,N*-dibutyl-2,4-pentadienamide] led to loss of direct TRPV1 channel activation.

The three derivatives were studied in more detail for modulatory effects on cationic currents through the channels evoked by capsaicin (8-methyl-*N*-vanillyl-6-nonenamide).

At a concentration of 100 µM, compound **24** (80% reduction of current amplitude) – and to a lower degree also **23** (30% reduction of current amplitude) – inhibited cationic currents. As shown in **Figure 13**, concentration-response experiments conducted for **24** revealed almost complete inhibition of capsaicin induced currents by **24** at a saturating concentration of 300 µM (95 % reduction of current amplitude; IC_{50} = 39.3±3.0 µM, n=6). In conclusion, piperine derivative **24** combines two interesting characteristics that need to be further investigated: replacing the piperidine moiety with a linear *N,N*-dipropyl substituent *(i)* enhanced efficacy of I_{GABA} modulation compared to the natural parent compound piperine; and *(ii)* evolved the compound from TRPV1 agonist to antagonist.

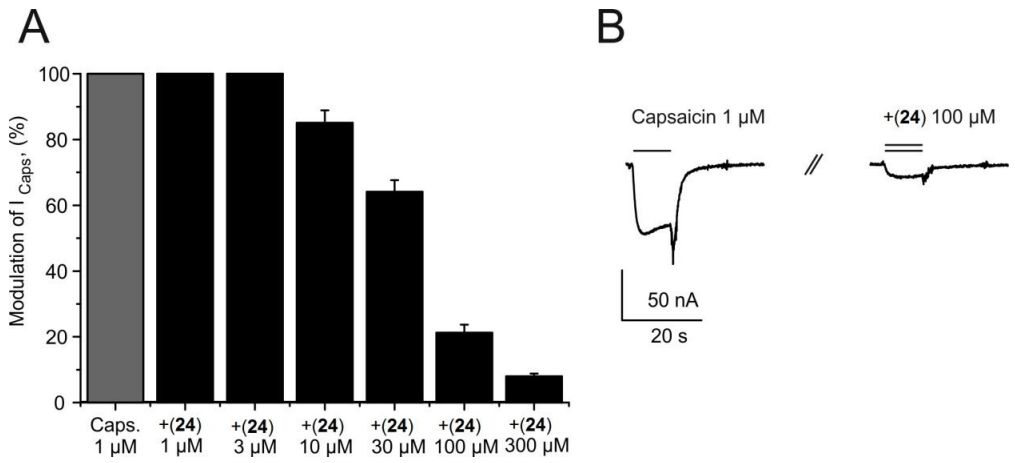

Figure 13 (A) *Concentration dependent inhibition of capsaicin induced currents (I_{Caps}) through TRPV1 channels by piperine derivative **24**. Each bar represents mean±SE from at least 3 oocytes derived from 2 different frogs. (**B**) Representative current of capsaicin (1 µM) and reduced current amplitude by **24** (100 µM).*

Summary and Conclusion

Compounds **23**, **24** and **25** were found to be efficacious $GABA_A$ receptor modulators antagonising capsaicin-evoked effects onTRPV1 channels. The

structural modifications introduced to the parent compound piperine led to inhibitory effects on TRPV1 channels with most pronounced effects for *N,N*-dipropyl derivative **24**. Despite this finding being an important interim success for drug development starting from the natural product piperine, the modes of action of these inhibitory effects remain unknown and need to be investigated in future studies.

4.2 Dihydrostilbenes, Dehydroabietic Acid and Honokiol Derivatives as $GABA_A$ Receptor Ligands

4.2.1 Identification of Dihydrostilbenes in *Pholidota chinensis* as New Scaffold for $GABA_A$ Receptor Modulators

Bioorg Med Chem. 2014 Feb 15;22(4):1276-84. doi: 10.1016/j.bmc.2014.01.008. Epub 2014 Jan 10. PMID: 24462176

Diana C. Rueda[a], Angela Schöffmann[b], Maria De Mieri[a], Melanie Raith[a], Evelyn A. Jähne[a], Steffen Hering[b], Matthias Hamburger[a]

[a] Division of Pharmaceutical Biology, University of Basel, Klingelbergstrasse 50, CH-4056 Basel, Switzerland

[b] Institute of Pharmacology and Toxicology, University of Vienna, Althanstrasse 14, A-1090 Vienna, Austria

Contribution Statement: *Investigation of Batatasin-III (2) modulatory effect through $\alpha_1\beta_2\gamma_{2S}$ $GABA_A$ receptors and preparation of figures were my contributions to this work.*

For Supporting Information see Appendix 7.2.

Bioorganic & Medicinal Chemistry 22 (2014) 1276–1284

Contents lists available at ScienceDirect

Bioorganic & Medicinal Chemistry

journal homepage: www.elsevier.com/locate/bmc

Identification of dihydrostilbenes in *Pholidota chinensis* as a new scaffold for $GABA_A$ receptor modulators

Diana C. Rueda [a], Angela Schöffmann [b], Maria De Mieri [a], Melanie Raith [a], Evelyn A. Jähne [a], Steffen Hering [b], Matthias Hamburger [a,*]

[a] Division of Pharmaceutical Biology, University of Basel, Klingelbergstrasse 50, CH-4056 Basel, Switzerland
[b] Institute of Pharmacology and Toxicology, University of Vienna, Althanstrasse 14, A-1090 Vienna, Austria

ARTICLE INFO

Article history:
Received 3 October 2013
Revised 20 December 2013
Accepted 3 January 2014
Available online 10 January 2014

Keywords:
Pholidota chinensis
HPLC-based activity profiling
$GABA_A$ receptor modulators
Dihydrostilbenes

ABSTRACT

A dichloromethane extract of stems and roots of *Pholidota chinensis* (Orchidaceae) enhanced GABA-induced chloride currents (I_{GABA}) by 132.75 ± 36.69% when tested at 100 μg/mL in a two-microelectrode voltage clamp assay, on *Xenopus laevis* oocytes expressing recombinant $\alpha_1\beta_2\gamma_{2S}$ $GABA_A$ receptors. By means of an HPLC-based activity profiling approach, the three structurally related stilbenoids coelonin (**1**), batatasin III (**2**), and pholidotol D (**3**) were identified in the active fractions of the extract. Dihydrostilbene **2** enhanced I_{GABA} by 1512.19 ± 176.47% at 300 μM, with an EC_{50} of 52.51 ± 16.96 μM, while compounds **1** and **3** showed much lower activity. The relevance of conformational flexibility for receptor modulation by stilbenoids was confirmed with a series of 13 commercially available stilbenes and their corresponding semisynthetic dihydro derivatives. Dihydrostilbenes showed higher activity in the oocyte assay than their corresponding stilbenes. The dihydro derivatives of tetramethoxy-piceatannol (**12**) and pterostilbene (**20**) were the most active among these derivatives, but they showed lower efficiencies than compound **2**. Batatasin III (**2**) showed high efficiency but no significant subunit specificity when tested on the receptor subtypes $\alpha_1\beta_2\gamma_{2s}$, $\alpha_2\beta_2\gamma_{2s}$, $\alpha_3\beta_2\gamma_{2s}$, $\alpha_4\beta_2\gamma_{2s}$, $\alpha_5\beta_2\gamma_{2s}$, $\alpha_1\beta_1\gamma_{2s}$, and $\alpha_1\beta_3\gamma_{2s}$. Dihydrostilbenes represent a new scaffold for $GABA_A$ receptor modulators.

1. Introduction

$GABA_A$ receptors are ligand-gated chloride channels physiologically activated by GABA, the major inhibitory neurotransmitter in the brain. Structurally, they are heteropentameric assemblies forming a central chloride-selective channel. Up to now 19 different subunits (α1–6, β1–3, γ1–3, δ, ε, θ, π, ρ1–3) have been identified. Depending on the nature, stoichiometry, and arrangement of these subunits, the receptor subtypes exhibit distinct pharmacological profiles providing the potential for rational drug therapy in several disorders related with impaired GABAergic function, such as epilepsy, insomnia, anxiety, and mood disorders.[1–3] $GABA_A$ receptors are the target for many clinically important drugs such as benzodiazepines (BDZs), barbiturates, neuroactive steroids, anesthetics, and certain other CNS depressants. Due to their lack of subunit specificity, these drugs show a number of adverse side effects. Hence, there is a need for subtype-selective drugs devoid of the side effects of the classical BDZs. Despite the availability of experimental subunit-specific GABAergic drugs for more than a decade, no subtype-selective $GABA_A$ receptor modulators have been introduced into clinical practice.[3,4]

In a search for new natural product-derived $GABA_A$ receptor modulators, we screened a library of 880 fungal and plant extracts in an automated functional two-microelectrode voltage clamp assay on *Xenopus* oocytes[5] transiently expressing $GABA_A$ receptors of the $\alpha_1\beta_2\gamma_{2S}$ subtype, the most abundant subunit combination in the human brain.[2] In this screening the dichloromethane extract of stems and roots of *Pholidota chinensis* LINDL (Orchidaceae) showed promising activity.

Orchidaceae is the largest family of flowering plants, with around 25,000 species in over 800 genera. The family shows worldwide distribution, with greatest diversity in tropical and subtropical climate zones. Apart from their ornamental value, many orchids have been used as medicinal plants. In traditional Chinese medicine we find the earliest written records for medicinal uses of orchids.[6–8] In Chinese folk medicine, the whole plant of *P. chinensis* (*shi xian tao*) has long been used in the treatment of diverse conditions, such as hypertension, headache, gastroenteritis, and bronchitis. Previous pharmacological studies on *P. chinensis* reported sedative and anticonvulsant activities.[9–12] The genus *Pholidota* comprises approximately 30 species distributed from tropical Asia to tropical

Abbreviations: BDZs, benzodiazepines; GABA, gamma-aminobutyric acid; $GABA_ARs$, gamma-aminobutyric acid type A receptors.

* Corresponding author. Tel.: +41 61 2671425; fax: +41 61 2671474.
E-mail address: matthias.hamburger@unibas.ch (M. Hamburger).

0968-0896/$ - see front matter © 2014 Elsevier Ltd. All rights reserved.
http://dx.doi.org/10.1016/j.bmc.2014.01.008

Australia. Phytochemical studies on the genus showed the presence of triterpenes, steroids, lignans, benzoxepines, and stilbenoids.[10] Stilbenoids exhibit a limited but heterogeneous distribution in the plant kingdom, and have been most widely reported from the Orchidaceae family. Dihydrostilbenes and 9,10-dihydrophenanthrenes have been previously identified in the genus *Pholidota*.[13–17]

In this study, batatasin III (**2**) isolated from a DCM extract of *P. chinensis* was identified as a positive $GABA_A$ receptor modulator by means of HPLC-based activity profiling,[18] a miniaturized approach for the rapid identification of new bioactive natural compounds,[19–22] that we have been successfully applying in the discovery of $GABA_A$ receptor ligands of natural origin.[23–27] The subunit selectivity of **2** was assessed at $GABA_A$ receptor subtypes $\alpha_2\beta_2\gamma_{2s}$, $\alpha_3\beta_2\gamma_{2s}$, $\alpha_4\beta_2\gamma_{2s}$, $\alpha_5\beta_2\gamma_{2s}$, $\alpha_1\beta_1\gamma_{2s}$, and $\alpha_1\beta_3\gamma_{2s}$. Furthermore, dihydrostilbenes were established as a new scaffold for $GABA_A$ receptor modulators, by comparison of the performance of a series of commercially available stilbenes and their semisynthetic dihydro derivatives on the oocyte assay.

2. Experimental

2.1. General procedures

1D and 2D NMR spectra were measured at room temperature on a Bruker Avance III 500 MHz spectrometer (Bruker BioSpin, Fällanden, Switzerland) operating at 500.13 MHz. Spectra were recorded at 291.2 K with a 1 mm TXI probe with z-gradient. The following settings were used: 128 scans for ^1H spectra; 8 scans for $^1H^1H$-COSY spectra (*cosygpqf* pulse program); 32 scans and 256 increments for HSQC experiments (*hsqcedetgp* pulse program); 64 scans and 128 increments for HMBC spectra (*hmbcgp* pulse program). Spectra were analyzed by TopSpin 3.0 software (Bruker). High resolution mass spectra (HPLC–ESITOFMS) were recorded in positive mode, *m*/*z* range 100–800, on a Bruker microTOF ESIMS system (Bruker Daltonics, Bremen, Germany) connected via a T-splitter (1:10) to an Agilent HP 1100 system consisting of a degasser, a binary mixing pump, autosampler, column oven, and a diode array detector (G1315B) (Agilent Technologies, Waldbronn, Germany). Nitrogen was used as a nebulizing gas at a pressure of 2.0 bar, and as drying gas at a flow rate of 9.0 L/min (dry gas temperature 240 °C). Capillary voltage was set at 45,000 V; hexapole at 230.0 Vpp. Instrument calibration was done with a reference solution of sodium formate 0.1% in 2-propanol/water (1:1) containing 5 mM NaOH. Data acquisition and processing was performed with Bruker Daltonics Hystar 3.0 software. Semi-preparative HPLC separations for activity profiling and purification were performed with an Agilent HP 1100 series system consisting of a quaternary pump, autosampler, column oven, and diode array detector (G1315B). Waters SunFire™ C18 (3.5 μm, 3.0 × 150 mm) and SunFire™ Prep C18 (5 μm, 10 × 150 mm) columns were used for analytical and semi-preparative HPLC analysis, respectively (Waters, Wexford, Ireland). Parallel evaporation of semi-preparative HPLC fractions was performed with a Genevac EZ-2 plus vacuum centrifuge (Genevac Ltd, Ipswich, United Kingdom). Flash chromatography was performed with pre-packed Buchi Sepacore® silica flash cartridges (40–63 μm, 40 × 150 mm) on a Buchi Sepacore® system consisting of two C-605 pumps, a C-620 control unit, and a C-660 fraction collector (Buchi, Flawil, Switzerland). Sample introduction was carried out with a Buchi Prep Elut adapter filled with the sample adsorbed onto silica gel. The separation was monitored by TLC. Preparative HPLC separations were performed with a Waters SunFire Prep C18 OBD column (5 μM, 30 × 150 mm) connected to a Shimadzu LC-8A preparative HPLC with SPD-M10A VP diode array detector. HPLC-grade MeOH (Scharlau Chemie S.A.), acetonitrile (Scharlau Chemie S.A.) and water were used for HPLC separations. For analytical separations, HPLC solvents contained 0.1% of HCO_2H. NMR spectra were recorded in methanol-d_4 (Armar Chemicals). For extraction and flash chromatography, distilled technical grade solvents were used. Silica gel (63–200 μm, Merck) was used for open column chromatography.

2.2. Plant material

Shi Xian Tao (dried stems/roots of *P. chinensis* Lindl.) was purchased in 2008 from a local herbal market in Kunming and authenticated by Dr. X. Yang (previously Pharmaceutical Biology, University of Basel, now Kunming Institute of Botany, Chinese Academy of Science, Kunming, PR China). A voucher specimen (463) is deposited at the Division of Pharmaceutical Biology, University of Basel.

2.3. Extraction

The plant material was frozen with liquid nitrogen and ground with a ZM1 ultracentrifugal mill (Retsch). The DCM extract for screening and HPLC-based activity profiling was prepared with an ASE 200 extraction system with solvent module (Dionex, Sunnyvale CA). Three extraction cycles (5 min each) were performed, at an extraction pressure of 120 bar and a temperature of 70 °C. For preparative isolation, 293 g of ground plant material was macerated with DCM (4 × 1 L, 3 h each, permanent magnetic stirring). The solvent was evaporated at reduced pressure to yield 10.3 g of extract. The extracts were stored at 2–8 °C until use.

2.4. Microfractionation for activity profiling

Time-based microfractionation for $GABA_A$ receptor activity profiling was performed as previously described,[23,27,28] with minor modifications: separation was done on a semi-preparative HPLC column with MeOH (solvent A) and water (solvent B), using a gradient from 50% A to 80% A in 30 min, followed by 80% A to 100% A in 2 min. The flow rate was 4 mL/min, and 10 mg of extract (in 200 μL of DMSO) were injected. A total of 24 microfractions of 90 s each were collected. After parallel evaporation of solvents, the dry films were redissolved in 1 mL of methanol, and aliquots of 0.5 mL were dispensed in two vials, dried under N_2 gas, and submitted to bioassay.

2.5. Isolation

An aliquot of the DCM extract (450 mg) was dissolved in $CHCl_3$ and adsorbed onto silica gel (3 g), prior to packing into a Buchi Prep Elut adapter. Separation was performed on a Sepacore® silica gel cartridge eluted with an *n*-hexane (solvent A) and EtOAc (solvent B) gradient: 0% B to 30% B in 90 min, followed by 30% B to 50% B in 30 min, and 50% B to 80% B in 30 min. The flow rate was set at 15 mL/min. Fractions of 15 mL were collected and later combined into 18 fractions (1–18) on the basis of a TLC analysis (detection at 254, 366, and at daylight after staining with anisaldehyde–sulfuric acid reagent). Fractions 1–18 were submitted to analytical HPLC–PDA–ESIMS with MeOH (solvent C) and water (solvent D), using a gradient from 50% C to 100% C in 30 min, hold for 15 min. The flow rate was 0.4 mL/min, and 10 μg of each fraction (in 10 μL of DMSO) were injected. Fractions 13 and 14 were found to contain the compounds of interest and were submitted to semi-preparative HPLC using solvents C and D as eluents. A gradient of 50% C to 60% C in 30 min was used for fraction 13, and isocratic conditions (50% C, 30 min) for fraction 14. The flow rate was 4 mL/min. Stock solutions in DMSO (50 mg/mL) were prepared and repeatedly injected in portions of 50–100 μL. A portion

(17 mg) of fraction 13 (25 mg) afforded compounds **1** (2.3 mg) and **2** (6.5 mg). Compound **3** (2 mg) was isolated from 10 mg of fraction 14 (16 mg).

Compounds **1**–**3** were identified by comparison of their physiochemical data (NMR, ESI-TOFMS, and UV–vis) with published values.[14,29–31] The purity was >95% (purity check by ^{1}H NMR).

2.5.1. Coelonin (1)

^{1}H NMR (methanol-d_4, 500.13 MHz) δ_H (ppm): 8.13 (1H, d, J = 8.4 Hz, H-5), 6.62 (1H, dd J = 8.3 and 2.7 Hz, H-6), 6.61 (1H, d, J = 2.6 Hz, H-8), 6.30 (1H, d, J = 2.5 Hz, H-3), 6.26 (1H, d, J = 2.5 Hz, H-1), 3.67 (3H, s, 4-OCH_3), 2.59 (4H, s, H-9 and H-10); ^{13}C shifts (derived from multiplicity-edited HSQC and HMBC spectra), δ_C (ppm): 158.3 (C, C-4), 155.4 (C, C-2), 154.8 (C, C-7), 139.8 (C, C-8a), 138.7 (C, C-10a), 128.6 (CH, C-5), 125.2 (C, C-4b), 114.8 (C, C-4a), 113.8 (CH, C-8), 112.2 (CH, C-6), 104.8 (CH, C-1), 100.1 (CH, C-3), 54.2 (4-OCH_3), 30.8 (CH_2, C-10) 30.1 (CH_2, C-9). HR-ESIMS m/z 243.1016 $[M+H]^+$ (calcd for $C_{15}H_{15}O_3$, 243.1016).

2.5.2. Batatasin III (2)

^{1}H NMR (methanol-d_4, 500.13 MHz) δ_H (ppm): 7.03 (1H, dd, J = 7.9 and 7.5 Hz, H-5′), 6.64 (3H, m, H-2′, H-4′, and H-6′), 6.29 (1H, br s, H-2), 6.23 (2H, m, H-4 and H-6), 3.63 (3H, s, 5-OCH_3), 2.75 (4H, m, H-α and H-β); ^{13}C shifts (derived from multiplicity-edited HSQC and HMBC spectra), δ_C (ppm): 160.9 (C, C-5), 157.6 (C, C-3), 156.7 (C, C-3′), 144.9 (C, C-1), 143.3 (C, C-1′), 129.0 (CH, C-5′), 119.8 (CH, C-6′), 115.3 (CH, C-2′), 112.4 (CH, C-4′), 108.1 (CH, C-2), 105.5 (CH, C-6), 98.7 (CH, C-4), 54.3 (CH_3, 5-OCH_3), 37.6 (CH_2, C-β), 37.0 (CH_2, C-α). HR-ESIMS m/z 245.1176 $[M+H]^+$ (calcd for $C_{15}H_{17}O_3$, 245.1172).

2.5.3. Pholidotol D (3)

^{1}H NMR (methanol-d_4, 500.13 MHz) δ_H (ppm): 7.17 (1H, dd, J = 7.9 and 7.8 Hz, H-5′), 7.00–6.95 (4H, m, H-2′, H-6′, H-α and H-β), 6.69 (1H, dd, J = 8.2 and 2.2 Hz, H-4′), 6.58 (2H, m, H-2 and H-6), 6.31 (1H, t, J = 2 Hz, H-4), 3.76 (3H, s, 5-OCH_3); ^{13}C shifts (derived from multiplicity-edited HSQC and HMBC spectra), δ_C (ppm): 160.8 (C, C-5), 157.7 (C, C-3), 156.0 (C, C-3′), 139.7 (C, C-1), 138.5 (C, C-1′), 129.4 (CH, C-5′), 128.6 (CH, C-β), 128.4 (CH, C-α), 117.8 (CH, C-6′), 114.4 (CH, C-4′), 112.4 (CH, C-2′), 105.8 (CH, C-2), 103.4 (CH, C-6), 100.3 (CH, C-4), 54.4 (CH_3, 5-OCH_3). HR-ESIMS m/z 243.1017 $[M+H]^+$ (calcd for $C_{15}H_{15}O_3$, 243.1016).

Further purification of compound **2** for subunit specificity tests was achieved by separating a portion of the extract (7.3 g) by open column chromatography (6 × 69 cm, 700 g of silica gel), using a step gradient of *n*-hexane–EtOAc (100:0, 95:5, 90:10, 85:15, 80:20, 75:25, 70:30, 65:35, 60:40, 55:45, 50:50, 40:60, 30:70, 20:80, 10:90, 0:100, 1 L each) and washing in the end with MeOH 100% (1.5 L). The flow rate was ca. 50 mL/min. The effluent was combined to 15 fractions (1–15) based on TLC patterns. After HPLC–PDA–MS analysis, fractions 7 and 8 were selected for isolation of compound **2** by preparative HPLC, with acetonitrile (solvent A) and water (solvent B), using a gradient from 40% A to 50% A in 30 min, followed by 50% A to 100% A in 5 min, hold for 10 min. The flow rate was 20 mL/min. Stock solutions in THF (100 mg/mL) were prepared and repeatedly injected in portions of 300–400 μL. The separation of fractions 7 (129 mg) and 8 (132 mg), yielded compound 10.8 mg of **2**.

2.6. Synthesis of dihydrostilbenes

2.6.1. Stilbenes

Compounds **4**–**7**, **9**, **11**, **13**, **15**, **17**, and **19** were purchased from TCI Europe N.V. Compounds **21** and **25** were purchased from Sigma–Aldrich Co. Compound **23** was purchased from Santa Cruz Biotechnology, Inc.

2.6.2. General procedure

Dihydro derivatives of compounds **7**, **9**, **11**, **13**, **15**, **17**, **19**, **21**, and **23** were prepared by hydrogenation of corresponding stilbenes. A standard protocol was followed,[32] with minor modifications. Solutions of each stilbene (10 mg) in absolute EtOH (5 ml) were stirred under H_2 for 3 h in the presence of 10% Pd/C. The reaction mixtures were filtered over Celite to remove the catalyst, and evaporated to dryness. The resulting residues were purified by flash column chromatography, using a hexane/EtOAc gradient, to afford target compounds **8**, **10**, **12**, **14**, **16**, **18**, **20**, **22**, and **24**, respectively, in yields of 85–95%. The spectroscopic data of compounds were in agreement with the literature, except for compound **24**, for which no report was found (^{1}H NMR spectrum is provided as Supporting information).[32–41]

2.6.3. *trans*-2-Fluoro-4′-methoxy-dihydrostilbene (24)

^{1}H NMR (chloroform-d_4, 500.13 MHz) δ_H (ppm): 7.26–7.08 (4H, m), 7.08–7.98 (2H, m), 6.90–6.80 (2H, m), 3.81 (3H, s), 3.05–2.84 (4H, m). HRESI-MS m/z 253.1589 $[M+Na]^+$ (calcd formula weight for $C_{15}H_{15}FO$, 230.2774).

2.7. Expression of $GABA_A$ receptors

Stage V–VI oocytes from *Xenopus laevis* were prepared, and cRNA injected as previously described.[23] Female *Xenopus laevis* (NASCO, Fort Atkinson, WI) were anesthetized by exposing them for 15 min to a 0.2% MS-222 (methanesulfonate salt of 3-aminobenzoic acid ethyl, Sigma) solution before surgically removing parts of the ovaries. Follicle membranes from isolated oocytes were enzymatically digested with 2 mg/mL collagenase from *Clostridium histolyticum* (Type 1A, Sigma). Synthesis of capped runoff poly(A+) cRNA transcripts was obtained from linearized cDNA templates (pCMV vector). Directly after enzymatic isolation, the oocytes were injected with 50 nL of DEPC-treated water (Sigma) containing different cRNAs at a concentration of approximately 300–3000 pg/nL per subunit. The amount of injected cRNA mixture was determined by means of a NanoDrop ND-1000 (Kisker Biotech). To ensure expression of the gamma subunit in $\alpha_1\beta_2\gamma_{2S}$ receptors, rat cRNAs were mixed in a 1:1:10 ratio. Oocytes were then stored at 18 °C in ND96 solution containing 1% of penicillin–streptomycin solution (Sigma–Aldrich). Voltage clamp measurements were performed between days 1 and 5 after cRNA injection.

2.8. Positive control

Diazepam (7-chloro-1,3-dihydro-1-methyl-5-phenyl-2*H*-1,4-benzodiazepin-2-one, Sigma, purity not less than 98%) was used as positive control. At 1 μM diazepam enhanced I_{GABA} up to 231.3 ± 22.6% (n = 3). See also Figure S1, Supporting information.

2.9. Two-microelectrode voltage clamp studies

Electrophysiological experiments were performed by the two-microelectrode voltage clamp method making use of a TURBO TEC 03X amplifier (npi electronic GmbH) at a holding potential of −70 mV and pCLAMP 10 data acquisition software (Molecular Devices). Currents were low-pass-filtered at 1 kHz and sampled at 3 kHz. The bath solution contained 90 mM NaCl, 1 mM KCl, 1 mM $MgCl_2$, 1 mM $CaCl_2$, and 5 mM HEPES (pH 7.4). Electrode filling solution contained 2 M KCl. Oocytes with maximal current amplitudes >3 μA were discarded to exclude voltage clamp errors.

2.10. Fast solution exchange during I_{GABA} recordings

Test solutions (100 μL) were applied to the oocytes at a speed of 300 μL/s by means of the ScreeningTool (npi electronic, Tamm,

Germany) automated fast perfusion system.[5] In order to determine GABA EC_{3-10} (typically between 3 and 10 μM for receptors of subunit composition $\alpha_1\beta_2\gamma_{2s}$), a dose–response experiment with GABA concentrations ranging from 0.1 μM to 1 mM was performed. Stock solution of the DCM extract (10 mg/mL in DMSO) was diluted to a concentration of 100 μg/mL with bath solution containing GABA EC_{3-10} according to a validated protocol.[23] As previously described, microfractions collected from the semi-preparative HPLC separations were dissolved in 30 μL of DMSO and subsequently mixed with 2.97 mL of bath solution containing GABA EC_{3-10}.[23] A stock solution of each pure compound tested (100 mM in DMSO) was diluted to concentrations of 0.1, 1.0, 3.0, 10, 30, 100, 300, and 500 μM with bath solution for measuring direct activation, or with bath solution containing GABA EC_{3-10} for measuring modulation of $GABA_A$ receptors. The final DMSO concentration in all the samples including the GABA control samples was adjusted to 1% to avoid solvent effect at the $GABA_A$ receptor.

2.11. Data analysis

Enhancement of the I_{GABA} was defined as $I_{(GABA+Comp)}/I_{GABA} - 1$, where $I_{(GABA+Comp)}$ is the current response in the presence of a given compound, and I_{GABA} is the control GABA-induced chloride current. Data were analyzed using the ORIGIN 7.0 SR0 software (OriginLab Corporation) and are given as mean ± SE of at least two oocytes and ⩾2 oocyte batches.

3. Results and discussion

3.1. Isolation and structure elucidation of active compounds

Screening for $GABA_A$ modulating activity was performed with *Xenopus laevis* oocytes transiently expressing $GABA_A$ receptors of the subtype $\alpha_1\beta_2\gamma_{2s}$. In an automated fast-perfusion system used for two-microelectrode voltage clamp measurements,[5] a dichloromethane extract (100 μg/mL) of *P. chinensis* roots enhanced the GABA-induced chloride ion current (I_{GABA}) by 132.8 ± 36.7%. To track the activity in the extract, we used HPLC-based activity profiling with a validated protocol.[23] The chromatogram (210–700 nm) of a semipreparative HPLC separation (10 mg of extract) and the corresponding activity profile of the time-based fractionation (24 microfractions of 90 s each) are shown in Figure 1B and A, respectively. The major peak of activity was found in fraction 9, which potentiated I_{GABA} by 119.1 ± 19.1%. Fraction 8 showed marginal activity (enhancement of I_{GABA} by 26.5 ± 4.7%). All the remaining fractions showed minimal activity and were not considered further.

Isolation of the active compounds was achieved by flash chromatography and subsequent purification by semi-preparative HPLC. Compounds were tracked with the aid of TLC and HPLC–ESIMS. The three structurally related stilbenoids coelonin (**1**), batatasin III (**2**), and pholidotol D (**3**) (Fig. 2) were identified by ESI-TOF-MS, 1D and 2D microprobe NMR, and comparison with published data.[14,29–31] The *Z* configuration in compound **3** was corroborated by proton NMR, using the chemical shifts and coupling constant of the two olefinic protons at δ_H 6.95 (2H, d, J = 6.0 Hz, H-β and α), which discards the presence of the *trans*-stereoisomer thunalbene. Detailed spectroscopic data of compounds **1**–**3** are available as Supporting information.

Stilbenoids are the major secondary metabolites in the genus *Pholidota*,[10] and the identification of compounds **1**–**3** in the active fractions of *P. chinensis* DCM extract was not surprising. The three compounds have been previously isolated from the species,[10,12,14] but they have not been reported as $GABA_A$ receptor modulators.

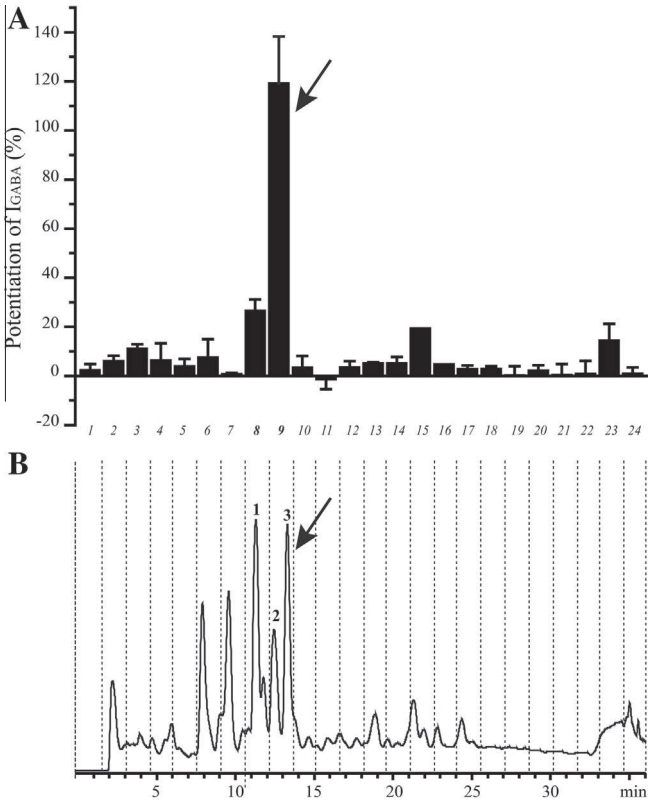

Figure 1. HPLC-based activity profiling of a DCM extract of stems and roots of *P. chinensis*, for $GABA_A$ receptor modulatory activity. (B) HPLC chromatogram (210–700 nm) of a semipreparative separation of 10 mg of extract. The numbers above peaks designate compounds **1**–**3**. The 24 time-based fractions of 90 s each are indicated with dashed lines. (A) Potentiation of the I_{GABA} by each microfraction (error bars correspond to SE).

3.2. Modulation of $GABA_A$ receptors

For a preliminary activity profile at $GABA_A$Rs of the subtype $\alpha_1\beta_2\gamma_{2s}$, **1**–**3** were tested at a concentration of 100 μM in the *Xenopus* oocyte assay. Batatasin III (**2**) was the most efficient among the three compounds. It potentiated I_{GABA} by 628.3 ± 87.1%, while compounds **1** and **3** exhibited weaker enhancements (139.5 ± 14.4% and 192.0 ± 64.1%, respectively) (Fig. 3A). Further concentration–response experiments on $\alpha_1\beta_2\gamma_{2s}$ receptors were performed with compounds **1**–**3**, at concentrations ranging from 1 to 300 μM (500 μM for compound **3**). As shown in Figure 3B, all stilbenoids enhanced I_{GABA} at a GABA EC_{3-10} in a concentration-dependent manner. The bibenzyl batatasin III (**2**) displayed strong $GABA_A$ receptor modulatory activity, with an efficiency (maximal stimulation of I_{GABA}) of 1512.9 ± 176.5% and a potency (higher concentration for half-maximal stimulation of I_{GABA}, or EC_{50}) of 52.5 ± 17.0 μM. The structurally related stilbene pholitodol D (**3**) showed much lower activity, with an efficiency of 786.8 ± 72.1% and potency of 175.5 ± 25.5 μM. The dihydrophenanthrene coelonin (**1**) showed activity similar to compound **2**, but no saturation of the receptors was reached at the highest concentration tested (300 μM). None of the compounds induced direct activation of the receptors when applied prior to GABA, at concentrations lower than 100 μM. This was indicative of an allosteric modulation of the receptor with the subunit composition $\alpha_1\beta_2\gamma_{2s}$, rather than direct agonistic activity (Fig. 3C).

Compared to other natural products tested in the same in vitro model and $GABA_A$ receptor subtype,[24,27,28,33] batatasin III (**2**) exhibited much higher efficiency. The efficiency of **2** in $GABA_A$Rs of the

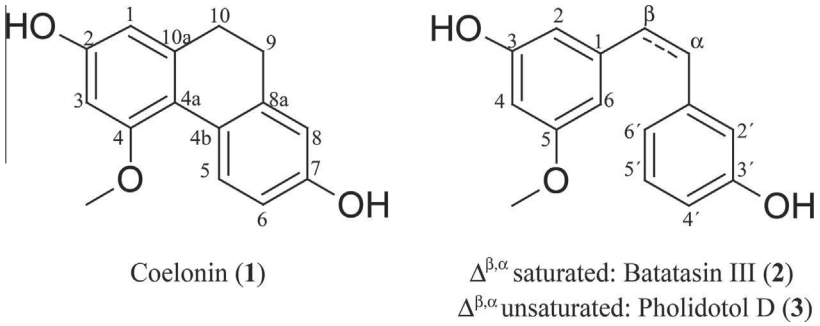

Figure 2. Chemical structures of compounds **1**–**3**.

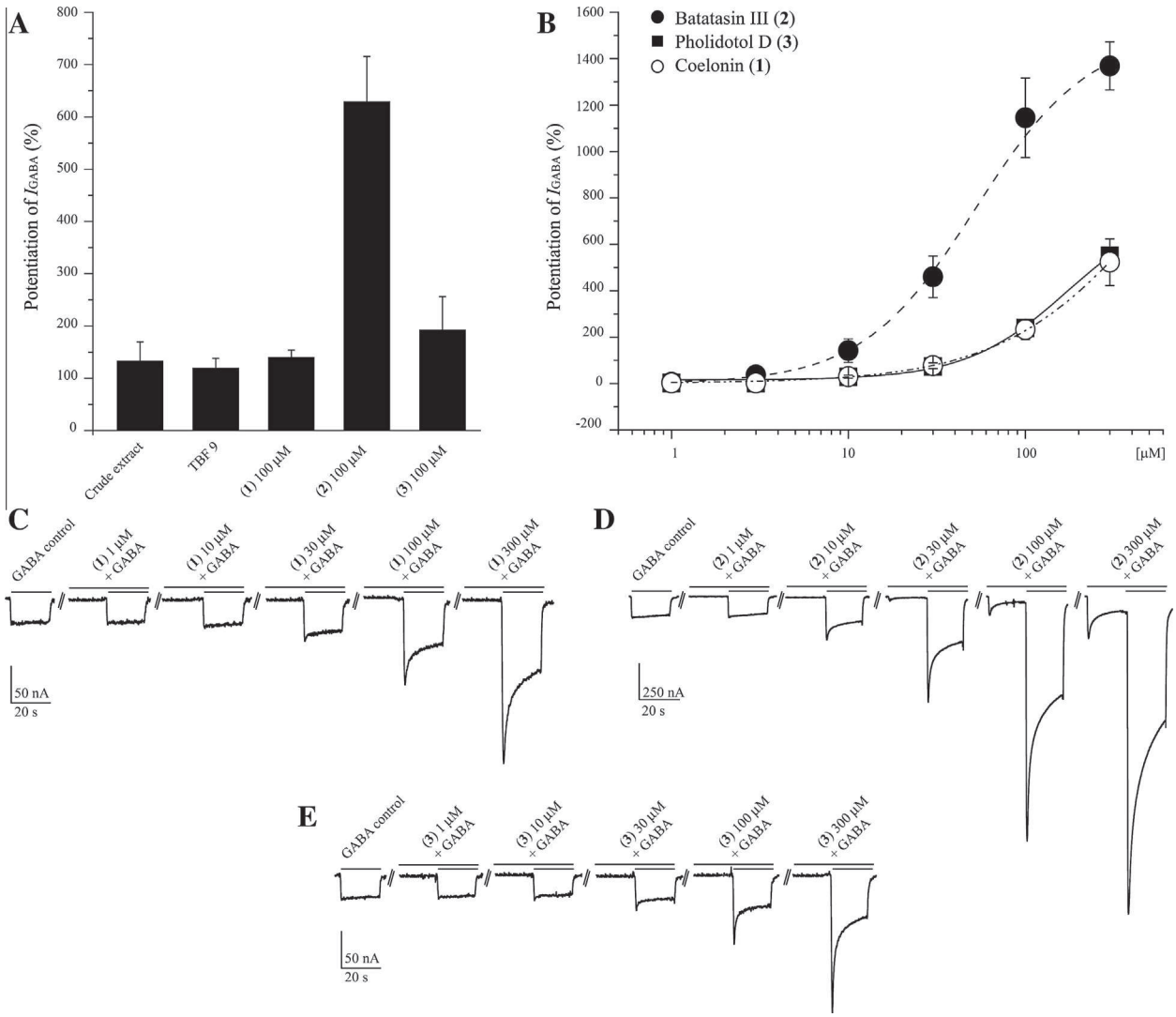

Figure 3. (A) Potentiation of I_{GABA} by the DCM extract of *P. chinensis* stems and roots (100 μg/mL), by microfraction 9, and compounds **1**–**3** (100 μM). (B) Concentration–response curve for compounds **1**–**3** on $GABA_A$ receptors of the subunit composition $\alpha_1\beta_2\gamma_{2S}$. (C–E) Typical traces for modulation of I_{GABA} by compounds **1**–**3**, respectively. The flat segments in the currents indicate the absence of direct activation of the receptors. All experiments in A–E were carried out using a GABA EC_{3-10}.

subtype $\alpha_1\beta_2\gamma_{2s}$ was also significantly higher than that of classical BDZs, with a potentiation of I_{GABA} at least fourfold that of triazolam, clotiazepam, and midazolam.[34] However, its EC_{50} value was significantly higher than that of BDZs and indicated a much lower binding affinity.

Despite the small number of compounds, preliminary structure–activity considerations could be derived. Conformational flexibility as in batatasin III (**2**) appeared to be critical for the modulatory activity of stilbenoids, since introduction of a double bond $\Delta^{\beta,\alpha}$ in pholidotol D (**3**) drastically decreased potency and efficiency. The importance of flexibility was confirmed by the weak activity of coelonin (**1**) in which the dihydrophenanthrene ring conferred additional rigidity to the structure. Although stilbenoids such as resveratrol have been described as neuroprotective

agents,[17,35–38] none of them has been reported as $GABA_A$ receptor ligand so far. Batatasin III (**2**) is thus the first representative of a new scaffold for $GABA_A$ receptor modulators. It is noteworthy that compounds with biosynthetically related scaffolds such as flavonoids,[25,39] coumarins,[24] and lignans[40] have been previously shown to possess $GABA_A$ receptor modulatory properties.

3.3. $GABA_A$ receptor subtype selectivity

Batatasin III (**2**) was tested for potential α subunit specificity, by replacing the α_1 subunit in the receptor subtype $\alpha_1\beta_2\gamma_{2s}$ with α_2, α_3, α_4, and α_5. Likewise, β subunit specificity was evaluated by replacing β_2 with β_1 and β_3. Concentration-dependent I_{GABA} modulation of compound **2** was evaluated on receptor subtypes $\alpha_2\beta_2\gamma_{2s}$, $\alpha_3\beta_2\gamma_{2s}$, $\alpha_4\beta_2\gamma_{2s}$, $\alpha_5\beta_2\gamma_{2s}$, $\alpha_1\beta_1\gamma_{2s}$, and $\alpha_1\beta_3\gamma_{2s}$ (Table 1).

As shown in Figure 4 and summarized in Table 1, compound **2** did not exhibit subtype specificity, as reflected by comparable EC_{50} values with all receptor subtypes studied ($p > 0.05$). The order of potency of batatasin III (**2**) in receptor composed by different α subunits was $\alpha_4\beta_2\gamma_{2s} > \alpha_5\beta_2\gamma_{2s} > \alpha_1\beta_2\gamma_{2s} > \alpha_3\beta_2\gamma_{2s} > \alpha_2\beta_2\gamma_{2s}$. The lower potency on $\alpha_2\beta_2\gamma_{2s}$ receptors compared to $\alpha_4\beta_2\gamma_{2s}$ was statistically significant, while there were no significant differences in efficiency among the other α-containing receptor subtypes. On $GABA_A$ receptors comprising different β subunits, almost no differences in potency and efficiency were observed. Thus, batatasin III (**2**) was a positive allosteric modulator of $GABA_A$Rs, devoid of significant subtype specificity.

Table 1
Potencies and efficiencies of batatasin III (**2**) for $GABA_A$ receptors of different subunit compositions

Subtype	EC_{50} (μM)	Max. potentiation of I_{GABA} (EC_{3-10}) (I_{max}) (%)	Hill coeff. (n_H)	n[a]
$\alpha_1\beta_2\gamma_{2s}$	52.5 ± 17.0	1512.9 ± 176.5	1.4 ± 0.3	5
$\alpha_2\beta_2\gamma_{2s}$	80.8 ± 22.1	1026.5 ± 139.2	1.2 ± 0.1	6
$\alpha_3\beta_2\gamma_{2s}$	67.3 ± 18.6	1694.2 ± 229.0	1.2 ± 0.1	5
$\alpha_4\beta_2\gamma_{2s}$	26.2 ± 3.6	1588.2 ± 97.5	1.5 ± 0.1	6
$\alpha_5\beta_2\gamma_{2s}$	46.7 ± 9.0	1375.7 ± 76.5	1.3 ± 0.1	5
$\alpha_1\beta_1\gamma_{2s}$	66.7 ± 21.0	1251.3 ± 157.0	1.8 ± 0.4	5
$\alpha_1\beta_3\gamma_{2s}$	67.2 ± 10.5	1252.9 ± 79.9	1.4 ± 0.1	5

[a] Number of experiments.

3.4. $GABA_A$R modulatory activity of dihydrostilbenes

Flexibility appeared to be a critical factor for the $GABA_A$R modulatory activity of stilbenoids. To confirm the influence of the double bond $\Delta^{\beta,\alpha}$, 13 commercially available stilbenoids and their corresponding dihydro derivatives (compounds **4**–**25**; Fig. 5) were tested in the *Xenopus* oocyte assay. Compounds were initially tested at a concentration of 100 μM on $GABA_A$Rs of the subtype $\alpha_1\beta_2\gamma_{2s}$. As expected, dihydrostilbenes showed higher activity than the corresponding stilbenes (Table 2, Fig. 6A). These differences in the activity of stilbenes and their dihydro derivatives were statistically significant in almost every case, with the exception of the pairs **4** and **5**/**6**, **9**/**10**, **13**/**14**, and **23**/**24** ($p > 0.05$).

Among the stilbenes, tetramethoxy-piceatannol (**11**), resveratrol (**13**), pterostilbene (**19**), and resveratrol triacetate (**21**), displayed the highest activity, potentiating I_{GABA} between 100% and 200%. Their corresponding dihydro derivatives showed the highest activity among dihydrostilbenes, but only compounds **12** and **20** showed efficiencies comparable to that of batatasin III (**2**) (544.5 ± 104.4% and 660.6 ± 100.2% respectively). A comparison of the activity of the dihydrostilbenes at 100 μM revealed that the bibenzyl scaffold alone (**6**) does not possess any $GABA_A$R modulatory activity. In general, substituents at C-3 and C-5 (**12**, **14**, **16**, **18**, **20**, and **22**) resulted in an enhancement of the activity. Increasing the lipophilicity by replacing the hydroxy groups at C-3 and C-5 with bulkier oxygenated functions (**12**, **20**, and **22**) enhanced the

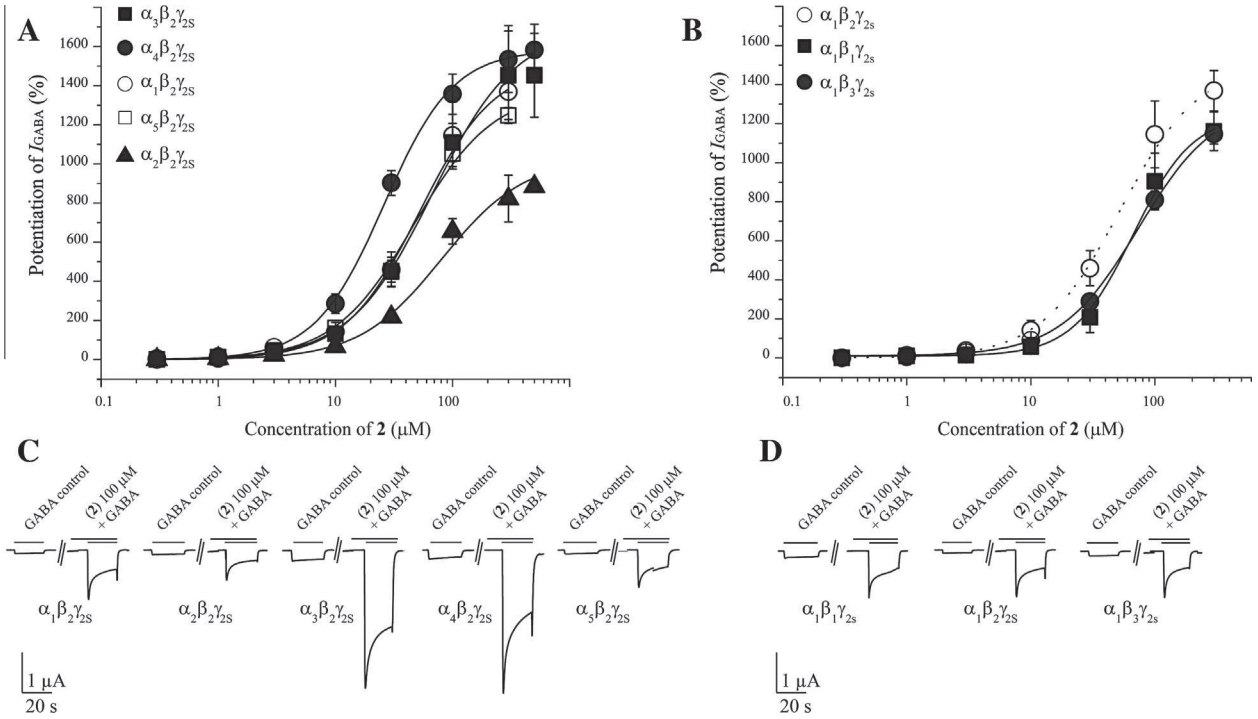

Figure 4. (A) α-Subunit dependency of batatasin III (**2**), depicted as concentration–response curves, with $GABA_A$ receptors of the subunit compositions $\alpha_1\beta_2\gamma_{2s}$, $\alpha_2\beta_2\gamma_{2s}$, $\alpha_3\beta_2\gamma_{2s}$, $\alpha_4\beta_2\gamma_{2s}$, and $\alpha_5\beta_2\gamma_{2s}$. (B) β-Subunit dependency of batatasin III (**2**), depicted as concentration–response curves with $GABA_A$ receptors of the subunit compositions $\alpha_1\beta_1\gamma_{2s}$, $\alpha_1\beta_2\gamma_{2s}$, and $\alpha_1\beta_3\gamma_{2s}$. (C and D) Typical traces for modulation of I_{GABA} by compound **2**, in receptors with different α and β subunit composition, respectively. All experiments were performed using a GABA EC_{3-10}.

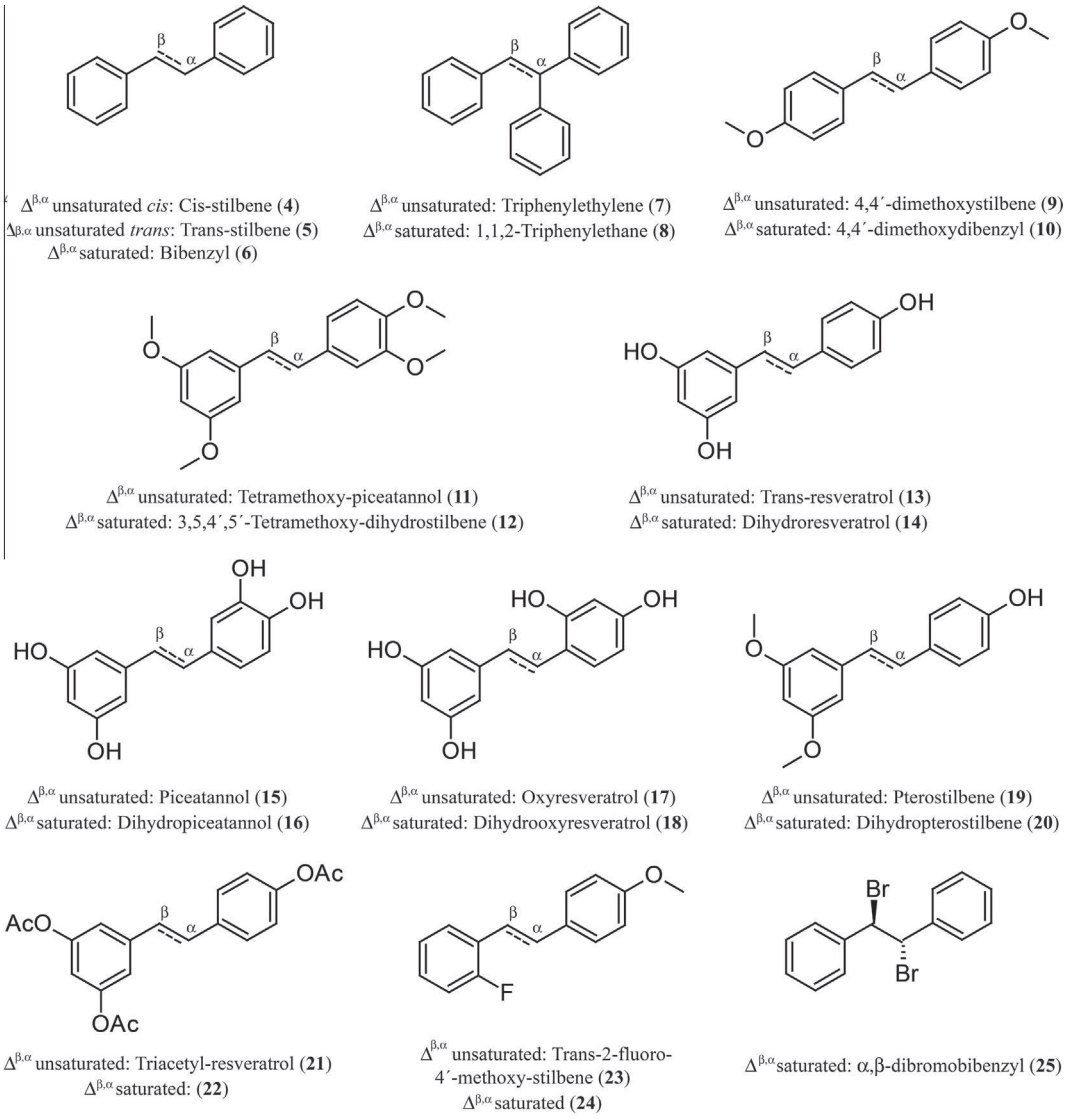

Figure 5. Chemical structures of compounds **4**–**25**.

Table 2
Potentiation of I_{GABA} in $\alpha_1\beta_2\gamma_{2s}$ receptors by compounds **4**–**25**, at a test concentration of 100 μM

Stilbenes			Dihydrostilbenes		
Compound	Max. potentiation of I_{GABA}	n[a]	Compound	Max. potentiation of I_{GABA}	n[a]
4	12.6 ± 9.2	3	**6**	8.3 ± 22.9	3
5	−11.3 ± 12.3	3			
7	−7.3 ± 0.1	3	**8**	51.6 ± 1.1	3
9	−24.8 ± 4.8	3	**10**	−20.9 ± 3.7	3
11	101.3 ± 0.9	3	**12**	544.5 ± 140.4	3
13	121.9 ± 21.8	3	**14**	162.2 ± 17.5	3
15	−35.4 ± 9.8	3	**16**	86.3 ± 9.9	3
17	−19.7 ± 3.9	3	**18**	44.1 ± 19.7	3
19	212.4 ± 10.9	3	**20**	660.6 ± 100.2	3
21	122.8 ± 18.6	3	**22**	227.7 ± 1.3	2
23	−22.9 ± 7.5	3	**24**	−16.8 ± 7.9	3
Diazepam[b] (1 μM)	231.3 ± 22.6	3	**25**	−12.9 ± 0.4	3

[a] Number of experiments.
[b] Positive control.

activity of dihydrostilbenes. The role of substituents in ring B was less clear within this compounds series. In the case of compounds **12** and **20**, different substitution patterns in ring B did not influence the activity. In contrast, when comparing compounds **14**, **16**, and **18**, addition of a hydroxy group in C-4′ or C-6′ led to a significant decrease of activity. Introduction of a halogen atom as in **25** induced slight negative receptor modulation, and substitution at C-4 (compound **10**) decreased activity. Since we had only one pair of *cis* and *trans* isomers (**4** and **5**, both inactive at 100 μM), the role of geometric isomerism could not be assessed in more detail.

The dihydro derivatives of tetramethoxy-piceatannol and pterostilbene (compounds **12** and **20**, respectively) were submitted to further concentration–response experiments on $\alpha_1\beta_2\gamma_{2s}$ receptors. Both compounds enhanced I_{GABA} at a GABA EC_{3-10} in a concentration-dependent manner (Fig. 6B). Compounds **12** and **20** had lower efficiency than the natural dihydrostilbene **2** (Table 3), with maximal stimulations of I_{GABA} of 870.7 ± 106.8% and 694.2 ± 86.0%, respectively. In terms of potency, **20** was comparable to **2** (EC_{50} 54.5 ± 13.4 μM), whereas **12** was twice as potent (EC_{50} 20.2 ±

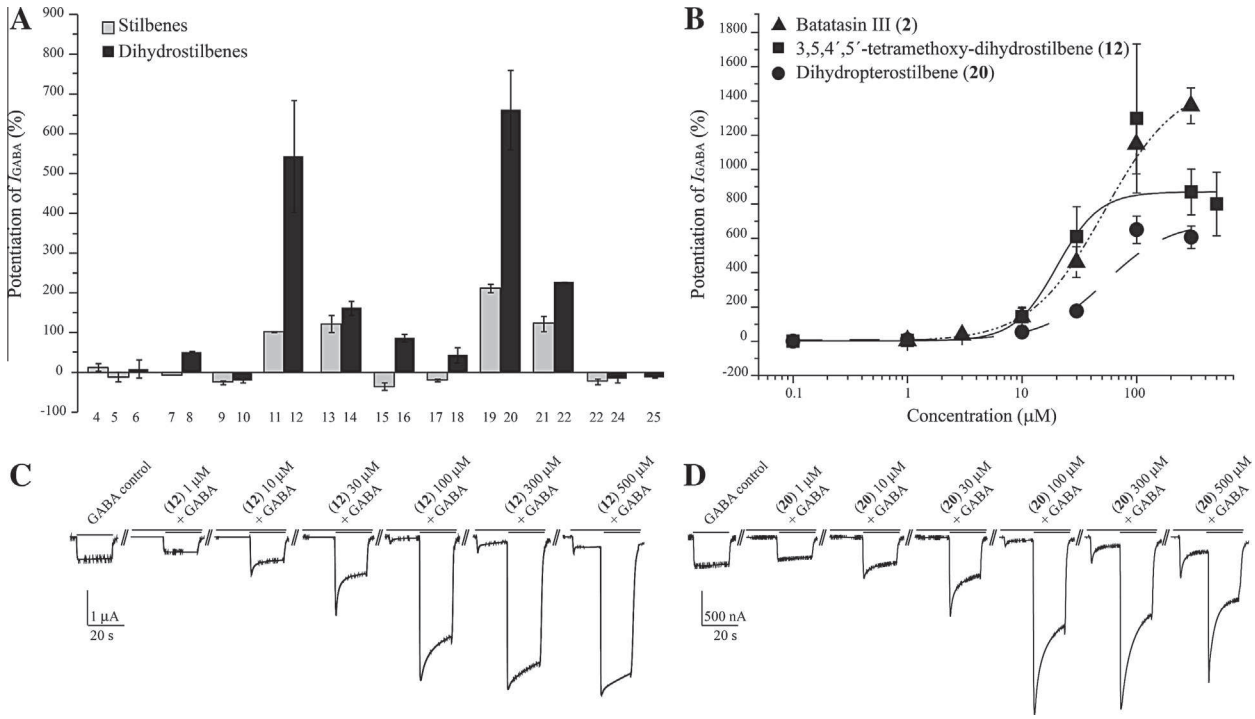

Figure 6. (A) Potentiation of I_{GABA} by compounds **4**–**25** (100 μM). (B) Potentiation of I_{GABA} by compounds **2**, **12** and **20**. Concentration–response curves are shown for $GABA_A$ receptors of the subunit composition $\alpha_1\beta_2\gamma_{2S}$. (C and D) Typical traces for modulation of I_{GABA} by compounds **12** and **20**, respectively. The inward currents induced in the absence of GABA (C and D) indicate direct activation of the receptors. All experiments shown in A–D were performed using a GABA EC_{3-10}.

Table 3
Potencies and efficiencies of compounds **2**, **3**, **12** and **20** for $\alpha_1\beta_2\gamma_{2s}$ $GABA_A$ receptors

Compound	EC_{50} (μM)	Max. potentiation of I_{GABA} (EC_{3-10}) (I_{max}) (%)	Hill coeff. (n_H)	n[a]
2	52.5 ± 17.0	1512.9 ± 176.5	1.2 ± 0.1	5
3	175.5 ± 25.5	786.8 ± 72.1	1.5 ± 0.2	5
12	20.2 ± 6.4	870.7 ± 106.8	2.3 ± 1.0	4
20	54.5 ± 13.4	694.2 ± 86.0	1.6 ± 0.2	4

[a] Number of experiments.

6.4 μM). This suggests that increased lipophilicity of ring B may have a positive effect on the potency of dihydrostilbenes. However, further studies with a larger series of compounds are needed for confirmation. None of the compounds induced direct activation of the receptors when applied prior to GABA, at concentrations lower than 100 μM (Fig. 6C).

Stilbenoids have attracted significant attention in recent years due to their wide range of useful properties, including applications in optics, biochemistry, and chemotherapy.[13,41] The stilbenoid scaffold can be considered as a priviledged structure.[42,43] However, there have been no reports on $GABA_A$ receptor modulatory activity of stilbenoids up to now, despite a significant number of publications on biological activities of natural stilbenoids, and in particular, on resveratrol. Dihydrostilbenes such as **2** may thus be an interesting starting point for the synthesis of new $GABA_A$ receptor modulators.

4. Conclusions

With the aid of an HPLC-based profiling approach, we identified batatasin III (**2**) as the major compound responsible for $GABA_AR$ modulatory activity of the dichloromethane extract of *P. chinensis*. This dihydrostilbene showed allosteric modulation in $\alpha_1\beta_2\gamma_{2s}$ $GABA_A$ receptors with a higher efficiency than any other natural products tested up to now, but its EC_{50} value was significantly higher than that of BDZs. Dihydrostilbenes represent a new scaffold for $GABA_A$ receptor modulators.

The conformational flexibility of dihydrostilbenoids appeared critical for $GABA_AR$ modulatory properties. For a further exploration of this scaffold, conformationally restricted derivatives should be synthesized in order to explore in more detail the optimal orientation of the aromatic rings and substituents.

Acknowledgements

Financial support was provided by the Swiss National Science Foundation through project 205320_126888 (M.H.). D.C.R. thanks the Swiss Federal Commission for Scholarships for Foreign Students (FCS) and the Department of Education of Canton Basel (Erziehungsdepartement des Kantons Basel-Stadt) for fellowships granted in 2011 and 2012, respectively.

Supplementary data

Supplementary data associated with this article can be found, in the online version, at http://dx.doi.org/10.1016/j.bmc.2014.01.008.

References and notes

1. Olsen, R. W.; Sieghart, W. *Pharmacol. Rev.* **2008**, *60*, 243.
2. Rudolph, U.; Knoflach, F. *Nat. Rev. Drug Disc.* **2011**, *10*, 685.
3. D'Hulst, C.; Atack, J. R.; Kooy, R. F. *Drug Discovery Today* **2009**, *14*, 866.
4. Tan, K. R.; Rudolph, U.; Lüscher, C. *Trends Neurosci.* **2011**, *34*, 188.
5. Baburin, I.; Beyl, S.; Hering, S. *Pflug. Arch. Eur. J. Physiol.* **2006**, *453*, 117.
6. Pérez Gutiérrez, R. M. *J. Med. Plants Res.* **2010**, *4*, 592.
7. Williams, R.; Martin, S.; Hu, J.-F.; Garo, E.; Rice, S.; Norman, V.; Lawrence, J.; Hough, G.; Goering, M.; O'Neil-Johnson, M.; Eldridge, G.; Starks, C. *Planta Med.* **2011**, *78*, 160.
8. Bulpitt, C. J.; Li, Y.; Bulpitt, P. F.; Wang, J. *J. R. Soc. Med.* **2007**, *100*, 558.
9. Wang, J.; Matsuzaki, K.; Kitanaka, S. *Chem. Pharm. Bull. (Tokyo)* **2006**, *54*, 1216.
10. Bandi, A. K. R.; Lee, D.-U. *Chem. Biodiversity* **2011**, *8*, 1400.
11. Wu, B.; Qu, H.; Cheng, Y. *Chem. Biodiversity* **1803**, *2008*, 5.

12. Yao, S.; Tang, C.-P.; Li, X.-Q.; Ye, Y. *Helv. Chim. Acta* **2008**, *91*, 2122.
13. Rivière, C.; Pawlus, A. D.; Mérillon, J.-M. *Nat. Prod. Rep.* **2012**, *29*, 1317.
14. Majumder, P. L.; Roychowdhury, M.; Chakraborty, S. *Phytochemistry* **1998**, *49*, 2375.
15. Kovacs, A.; Vasas, A.; Hohmann, J. *Phytochemistry* **2008**, *69*, 1084.
16. Shen, T.; Wang, X.-N.; Lou, H.-X. *Nat. Prod. Rep.* **2009**, *26*, 916.
17. Greger, H. *J. Nat. Prod.* **2012**, *75*, 2261.
18. Potterat, O.; Hamburger, M. *Curr. Org. Chem.* **2006**, *10*, 899.
19. Danz, H.; Stoyanova, S.; Wippich, P.; Brattstrom, A.; Hamburger, M. *Planta Med.* **2001**, *67*, 411.
20. Dittmann, K.; Gerhauser, C.; Klimo, K.; Hamburger, M. *Planta Med.* **2004**, *70*, 909.
21. Adams, M.; Christen, M.; Plitzko, I.; Zimmermann, S.; Brun, R.; Kaiser, M.; Hamburger, M. *J. Nat. Prod.* **2010**, *73*, 897.
22. Adams, M.; Zimmermann, S.; Kaiser, M.; Brun, R.; Hamburger, M. *Nat. Prod. Commun.* **2009**, *4*, 1377.
23. Kim, H. J.; Baburin, I.; Khom, S.; Hering, S.; Hamburger, M. *Planta Med.* **2008**, *74*, 521.
24. Li, Y.; Plitzko, I.; Zaugg, J.; Hering, S.; Hamburger, M. *J. Nat. Prod.* **2010**, *73*, 768.
25. Yang, X.; Baburin, I.; Plitzko, I.; Hering, S.; Hamburger, M. *Mol. Diversity* **2011**, *15*, 361.
26. Zaugg, J.; Khom, S.; Eigenmann, D.; Baburin, I.; Hamburger, M.; Hering, S. *J. Nat. Prod.* **2011**, *74*, 1764.
27. Zaugg, J.; Eickmeier, E.; Rueda, D. C.; Hering, S.; Hamburger, M. *Fitoterapia* **2011**, *82*, 434.
28. Zaugg, J.; Baburin, I.; Strommer, B.; Kim, H. J.; Hering, S.; Hamburger, M. *J. Nat. Prod.* **2010**, *73*, 185.
29. Wang, J.; Wang, L.; Kitanaka, S. *J. Nat. Med.* **2007**, *61*, 381.
30. Majumder, P.; Laha, S.; Datta, N. *Phytochemistry* **1982**, *21*, 478.
31. Hashimoto, T.; Hasegawa, K.; Yamaguchi, H.; Saito, M.; Ishimoto, S. *Phytochemistry* **1974**, *13*, 2849.
32. Oh, K. B.; Kim, S. H.; Lee, J.; Cho, W. J.; Lee, T.; Kim, S. *J. Med. Chem.* **2004**, *47*, 2418.
33. Zaugg, J.; Eickmeier, E.; Ebrahimi, S. N.; Baburin, I.; Hering, S.; Hamburger, M. *J. Nat. Prod.* **2011**, *74*, 1437.
34. Khom, S.; Baburin, I.; Timin, E. N.; Hohaus, A.; Sieghart, W.; Hering, S. *Mol. Pharmacol.* **2006**, *69*, 640.
35. Richard, T.; Pawlus, A. D.; Iglésias, M.-L.; Pedrot, E.; Waffo-Teguo, P.; Mérillon, J.-M.; Monti, J.-P. *Ann. N.Y. Acad. Sci.* **2011**, *1215*, 103.
36. Vingtdeux, V.; Dreses-Werringloer, U.; Zhao, H.; Davies, P.; Marambaud, P. *BMC Neurosci.* **2008**, *9*, S6.
37. Sun, A. Y.; Wang, Q.; Simonyi, A.; Sun, G. Y. *Mol. Neurobiol.* **2010**, *41*, 375.
38. Zhang, F.; Liu, J.; Shi, J. S. *Eur. J. Pharmacol.* **2010**, *636*, 1.
39. Hanrahan, J. R.; Chebib, M.; Johnston, G. A. *Br. J. Pharmacol.* **2011**, *163*, 234.
40. Zaugg, J.; Ebrahimi, S. N.; Smiesko, M.; Baburin, I.; Hering, S.; Hamburger, M. *Phytochemistry* **2011**, *72*, 2385.
41. Gray, E. E.; Rabenold, L. E.; Goess, B. C. *Tetrahedron Lett.* **2011**, *52*, 6177.
42. Welsch, M. E.; Snyder, S. A.; Stockwell, B. R. *Curr. Opin. Chem. Biol.* **2010**, *14*, 1.
43. Breinbauer, R.; Vetter, I. R.; Waldmann, H. *Angew. Chem., Int. Ed.* **2002**, *41*, 2878.

4.2.2 Identification of Dehydroabietic Acid from *Boswellia thurifera* Resin as a Positive $GABA_A$ Receptor Modulator

Fitoterapia **2014**, *99*, 28-34

Diana C. Rueda[a], Melanie Raith[a], Maria De Mieri[a], Angela Schöffmann[b], Steffen Hering[b], Matthias Hamburger[a]

[a] Division of Pharmaceutical Biology, University of Basel, Klingelbergstrasse 50, CH-4056 Basel, Switzerland

[b] Institute of Pharmacology and Toxicology, University of Vienna, Althanstrasse 14, A-1090 Vienna, Austria

Contribution Statement: *I contributed to the investigation of the modulatory effects of dehydroabietic acid through $\alpha_1\beta_2\gamma_{2S}$ $GABA_A$ receptors.*

For Supporting Information see Appendix 7.3.

Fitoterapia 99 (2014) 28–34

Contents lists available at ScienceDirect

Fitoterapia

journal homepage: www.elsevier.com/locate/fitote

Identification of dehydroabietc acid from *Boswellia thurifera* resin as a positive $GABA_A$ receptor modulator

Diana C. Rueda [a], Melanie Raith [a], Maria De Mieri [a], Angela Schöffmann [b], Steffen Hering [b], Matthias Hamburger [a,*]

[a] Division of Pharmaceutical Biology, University of Basel, Klingelbergstrasse 50, CH-4056 Basel, Switzerland
[b] Institute of Pharmacology and Toxicology, University of Vienna, Althanstrasse 14, A-1090 Vienna, Austria

ARTICLE INFO

Article history:
Received 14 July 2014
Accepted in revised form 27 August 2014
Accepted 1 September 2014
Available online 6 September 2014

Keywords:
Boswellia thurifera
Olibanum
HPLC-based activity profiling
$GABA_A$ receptor modulators
Abietane diterpenes
Dehydroabietic acid

ABSTRACT

In a two-microelectrode voltage clamp assay with *Xenopus laevis* oocytes, a petroleum ether extract (100 μg/mL) of the resin of *Boswellia thurifera* (Burseraceae) potentiated GABA-induced chloride currents (I_{GABA}) through receptors of the subtype $\alpha_1\beta_2\gamma_{2s}$ by 319.8% ± 79.8%. With the aid of HPLC-based activity profiling, three known terpenoids, dehydroabietic acid (**1**), incensole (**2**), and AKBA (**3**), were identified in the active fractions of the extract. Structure elucidation was achieved by means of HR-MS and microprobe 1D/2D NMR spectroscopy. Compound **1** induced significant receptor modulation in the oocyte assay, with a maximal potentiation of I_{GABA} of 397.5% ± 34.0%, and EC_{50} of 8.7 μM ± 1.3 μM. This is the first report of dehydroabietic acid as a positive $GABA_A$ receptor modulator.

1. Introduction

A number of plants belonging to the Burseraceae family are the source of strongly aromatic resins of considerable commercial value. The resin obtained by incision of *Boswellia* spp. (Burseraceae), also called *frankincense* or *olibanum*, has been used as incense in religious and cultural ceremonies since the beginning of written history and, in ancient times, was ranked along with gold and ivory as a precious trading good [1,2].

The genus *Boswellia* Roxb. ex Colebr. is mostly distributed in the Arabian Peninsula, India, and Northeast Africa [1,2]. *B. thurifera* Roxb. ex Flem. was first described from Asia in 1810 [3,4], and its resin has been studied for its antimicrobial properties [5–7] and its effect on the reproductive system [8]. Olibanum is known in Chinese and other traditional medicines for its anti-inflammatory, antiseptic, wound-healing, and sedative properties [1,9,10]. It is a complex mixture composed of polysaccharides, monoterpenes, sesquiterpenes, diterpenes like incensole, isoincensole, and their oxide or acetate derivatives, and triterpenoids such as boswellic acids [1,11,12]. Boswellic acids are considered as marker compounds of the resin, and they have been found responsible for the anti-inflammatory properties. Incensole acetate and its derivatives have been reported as inhibitors of NF-κB and potent activators of TRPV3 channels in the brain, which confers them antidepressant and anxiolytic properties [1,13]. Monographs on olibanum can be found in the Chinese Pharmacopoeia [14] and ESCOP monographs [15], where it is referred to as the dried resin from the bark of *B. carterii* Birdw. and *B. bhawdajiana* Birdw., or from stems and branches of *Boswellia serrata* Roxb. ex Colebr., respectively. Indications include the treatment of painful or inflammatory conditions. *B. carterii*, *B. frereana*, and *B. serrata* are the three main olibanum-producing species [6,16].

Abbreviations: AKBA, 3α-acetoxy-11-keto-β-boswellic acid; BBB, Blood–brain barrier; BDZs, benzodiazepines; CNS, central nervous system; DHA, Dehydroabietic acid; GABA, gamma-aminobutyric acid; $GABA_ARs$, gamma-aminobutyric acid type A receptors; I_{GABA}, GABA-induced chloride current.

* Corresponding author. Tel.: +41 61 2671425; fax: +41 61 2671474.
E-mail address: matthias.hamburger@unibas.ch (M. Hamburger).

http://dx.doi.org/10.1016/j.fitote.2014.09.002
0367-326X/

$GABA_A$ receptors ($GABA_ARs$) are ligand-gated chloride channels physiologically activated by GABA, the major inhibitory neurotransmitter in the brain. They are heteropentameric assemblies with a central chloride-selective channel. Up to now, 19 subunits (α_{1-6}, β_{1-3}, γ_{1-3}, δ, ε, θ, π, ρ_{1-3}) have been identified in $GABA_ARs$. GABA-induced chloride influx generates a negative potential in the postsynaptic neurons, thereby inhibiting further action potentials. Impaired GABAergic function results in CNS disorders such as epilepsy, insomnia, anxiety, and mood disorders [17,18]. A number of clinically important drugs like benzodiazepines (BDZs), barbiturates, neuroactive steroids, anesthetics, and certain other CNS depressants bind $GABA_ARs$.

In a search for natural products acting as $GABA_A$ receptor modulators, we tested a petroleum ether extract of the resin of *Boswellia thurifera* Roxb. ex Fleming in an automated two-microelectrode voltage clamp assay with *Xenopus* oocytes [19]. At a concentration of 100 μM, the extract enhanced I_{GABA} by 319.8% ± 79.8%, in receptors of the subtype $\alpha_1\beta_2\gamma_{2S}$. GABAergic activity of the active extract was traced using an HPLC-based activity profiling approach [20], which has been previously validated and used for the discovery of $GABA_A$ receptor ligands from plant sources [21–27]. Pure compounds isolated from the active time window of the extract were tested in the oocyte functional assay to assess their $GABA_A$ receptor modulatory activity.

2. Experimental

2.1. General procedures

1D and 2D NMR spectra were recorded on a Bruker Avance III spectrometer operating at 500.13 MHz. ^{1}H NMR, COSY, HSQC, HMBC, and NOESY spectra were measured at 18 °C in a 1 mm TXI probe with a *z*-gradient, using standard Bruker pulse sequences. Spectra were analyzed by Bruker TopSpin 3.0 software. ESI-TOF-MS spectra were recorded in positive mode, *m/z* range 100–800, on a Bruker microTOF ESIMS system. Nitrogen was used as a nebulizing gas at a pressure of 2.0 bar, and as drying gas at a flow rate of 9.0 L/min (dry gas temperature, 240 °C). Capillary voltage was set at 45,000 V; hexapole at 230.0 Vpp. Instrument calibration was done with a reference solution of sodium formate 0.1% in 2-propanol/water (1:1) containing 5 mM NaOH.

HPLC-PDA-ESIMS spectra were obtained in positive ion mode on a Bruker Daltonics Esquire 3000 Plus ion trap MS system, connected via T-splitter (1:10) to an Agilent HP 1100 system consisting of a degasser, a binary mixing pump, autosampler, column oven, and a diode array detector (G1315B). Data acquisition and processing was performed on Bruker Daltonics Hystar 3.0 software. Semipreparative HPLC separations were performed with an Agilent HP 1100 series system consisting of a quaternary pump, autosampler, column oven, and diode array detector (G1315B). Preparative HPLC separations were performed on a Shimadzu LC-8A preparative HPLC system with an SPD-M10A VP diode array detector. Flash chromatography was performed with prepacked Sepacore® silica flash cartridges (40–63 μm, 40 × 150 mm) on a Sepacore® system consisting of two C-605 pumps, a C-620 control unit, and a C-660 fraction collector (all Buchi, Flawil, Switzerland). The separation was monitored by TLC. Waters SunFire™ C18 (3.5 μm, 3.0 × 150 mm i.d.), SunFire™ Prep C18 (5 μm, 10 × 150 mm i.d.), and SunFire™ Prep C18 OBD (5 μM, 30 × 150 mm i.d.) columns were used for analytical, semipreparative, and preparative separations, respectively. HPLC-grade MeOH (Scharlau Chemie) and water, both containing 0.1% of formic acid, were used for HPLC separations. NMR spectra were recorded in methanol-d_4 and DMSO-d_6 (Armar Chemicals). For extraction and flash chromatography, technical grade solvents purified by distillation were used.

2.2. Plant material

Resin of *B. thurifera* Roxb. ex Fleming was purchased by Dan Yang in 2008 from Juhuayuan Herbal Market, Kunming, Yunnan province, China. The identity of the material was confirmed at Yunnan Baiyao group Co. Ltd., Kunming, China. A voucher specimen (433) is deposited at the Division of Pharmaceutical Biology, University of Basel.

2.3. Extraction

The petroleum ether extract for screening and HPLC-based activity profiling was prepared with an ASE 200 extraction system with solvent module (Dionex, Sunnyvale, CA). In total, 3 extraction cycles (5 min each) were performed, at an extraction pressure of 120 bar and a temperature of 70 °C. Extracts were combined, and the solvent was evaporated at reduced pressure. Extraction of 40 g of olibanum yielded 4.6 g of extract. The extract was stored at 2 °C–8 °C until use.

2.4. Microfractionation for activity profiling

Time-based microfractionation of the extract for $GABA_A$ receptor activity profiling was performed as previously described [28], with minor modifications: separation was done on a semipreparative HPLC column with MeOH (solvent A) and water (solvent B), using a gradient from 70% A to 100% A in 30 min, and held for 15 min. The flow rate was 4 mL/min, and 10 mg of extract (in 100 μL of DMSO) were injected. A total of 24 time-based microfractions of 90 s each were collected and evaporated in parallel. The dry films were redissolved in 1 mL of methanol, and aliquots of 0.5 mL were dispensed in two vials, dried under N_2 gas, and submitted to bioassay.

2.5. Isolation

An aliquot of the petroleum ether extract (1 g) was dissolved in *n*-hexane and submitted to purification by flash chromatography. Separation was performed on a Sepacore® silica gel cartridge eluted with an *n*-hexane (solvent A) and EtOAc (solvent B) gradient: 0% B to 30% B in 60 min, followed by 30% B to 50% B in 30 min, and 50% B to 100% B in 30 min. The flow rate was set at 15 mL/min. Fractions of 15 mL were collected and later combined to 13 fractions (A–M) on the basis of TLC analysis (detection at 254 nm, 366 nm, and at daylight after staining with anisaldehyde-sulfuric acid reagent). Fractions A–M were submitted to analytical HPLC-PDA-ESIMS with MeOH (solvent C) and water (solvent D), using an optimized gradient from 85% C to 100% C in 30 min, and held for 15 min. The flow rate was 0.4 mL/min, and 5 μg of each fraction (in 5 μL

of DMSO) were injected. Fractions F, G, and J were found to contain the compounds of interest and were submitted to purification by semipreparative HPLC using solvents C and D as eluents. Samples were separated under isocratic conditions (87% C, 20 min). The flow rate was 4 mL/min. Stock solutions in DMSO (100 mg/mL) were prepared and repeatedly injected in portions of 20–50 μL. Compound **1** (1 mg) was isolated from 10 mg of fraction G (63 mg). Compound **2** (0.6 mg) was isolated from 10 mg of fraction F (259 mg). Compound **3** (0.5 mg) was obtained from 5 mg of fraction J (72 mg). Structure elucidation was achieved by analysis of ESI-TOF-MS and 1D/2D NMR data, and by comparison with published values [29–31]. The purity was >95% (purity check by ^{1}H NMR).

*2.5.1. Dehydroabietic acid (**1**)*

^{1}H NMR (DMSO-d_6, 500.13 MHz) δ_H (ppm): 7.14 (1H, d, J = 8.2 Hz, H-11), 6.96 (1H, br d, J = 8.2 Hz, H-12), 6.84 (1H, br s, H-14), 2.81–2.77 (3H, m, CH_2-7, H-15), 2.28 (1H, br d, J = 12.8 Hz, H-1a), 2.03 (1H, br d, J = 12.4 Hz, H-5), 1.74–1.70 (3H, m, H-6a, H-2a, H-3a), 1.65 (1H, m, H-2b), 1.56 (1H, br d, J = 9.9Hz, H-3b), 1.44 (1H, br dd, J = 12.0 and 7.0 Hz, H-6b), 1.30 (1H, m, H-1b), 1.17 (6H, d, J = 6.9 Hz, CH_3-16, CH_3-17), 1.16 (3H, m, CH_3-19), 1.13 (3H, s, CH_3-20); ^{13}C NMR (DMSO-d_6, derived from multiplicity-edited HSQC and HMBC spectra) δ_C (ppm): 180.1 (C, C-18), 147.3 (C, C-9), 145.5 (C, C-13), 134.4 (C, C-8), 126.9 (CH, C-14), 124.2 (CH, C-11), 124.0 (CH, C-12), 47.1 (C, C-4), 45.2 (CH, C-5), 38.3 (CH_2, C-1), 37.7 (C, C-10), 36.8 (CH_2, C-3), 33.2 (CH, C-15), 29.9 (CH_2, C-7), 25.1 (CH_3, C-20), 24.3 (CH_3, C-16/C-17), 21.4 (CH_2, C-6), 18.6 (CH_2, C-2), 17.0 (CH_3, C-19). HR-ESIMS m/z 301.2161 $[M + H]^+$ (calculated for $C_{20}H_{29}O_2$, 301.2162).

*2.5.2. Incensole (**2**)*

^{1}H NMR (DMSO-d_6, 500.13 MHz) δ_H (ppm): 5.05 (1H, t, J = 7.0 Hz, H-3), 5.00 (1H, t, J = 6.8 Hz, H-7), 3.10 (1H, d, J = 9.9 Hz, H-11), 2.12–1.96 (9H, m, CH_2-6, H-2a, H-13a, CH_2-5, H-2b, CH_2-9), 1.83 (1H, sept, J = 6.7 Hz, H-15), 1.76 (1H, m, H-14a), 1.64 (1H, dd, J = 13.0 and 3.0 Hz, H-10a), 1.60–1.50 (5H, m, H-13b, CH_3-19, H-14b), 1.47 (3H, s, CH_3-18), 1.25 (1H, m, H-10b), 0.98 (3H, s, CH_3-20), 0.87 and 0.86 (6H, each d, J = 6.8 Hz, CH_3-16, CH_3-17); ^{13}C NMR (DMSO-d_6, derived from multiplicity-edited HSQC and HMBC spectra) δ_C (ppm): 134.0 (C, C-8), 133.5 (C, C-4), 124.7 (CH, C-7), 122.2 (CH, C-3), 87.8 (C, C-1), 85.0 (C, C-12), 73.7 (CH, C-11), 38.6 (CH_2, C-5), 36.3 (CH_2, C-13), 35.1 (CH, C-15), 33.8 (CH_2, C-9), 32.2 (CH_2, C-2), 30.7 (CH_2, C-14), 30.1 (CH_2, C-10), 24.7 (CH_2, C-6), 21.4 (CH_3, C-20), 18.4 (3CH_3, C-16, C-17, C-19), 16.3 (CH_3, C-18). HR-ESIMS m/z 307.2663 $[M + H]^+$ (calculated for $C_{20}H_{35}O_2$, 307.2632).

*2.5.3. 3α-Acetoxy-11-keto-β-boswellic acid (AKBA) (**3**)*

^{1}H NMR (methanol-d_4, 500.13 MHz) δ_H (ppm): 5.52 (1H, s, H-12), 5.27 (1H, t, J = 2.7 Hz, H-3), 2.49 (1H, br s, H-9), 2.46 (1H, m, H-1a), 2.27 (1H, tt, J = 14.8 and 3.4 Hz, H-2a), 2.17 (1H, td, J = 13.7 and 5.4 Hz, H-16a), 2.07 (3H, s, CH_3-2′), 2.00–1.90 (2H, m, H-6a, H-15a), 1.78 (1H, m, H-6b), 1.72 (1H, m, H-7a), 1.60–1.32 (12H, m, H-18, H-2b, H-22a, H-19, H-7b, H-21a, H-5, H-22b, CH_3-27, H-21b), 1.32–1.23 (2H, m, H-15b, H-1b), 1.20 (3H, s, CH_3-26), 1.18 (3H, s, H-23), 1.17 (3H, s, CH_3-25), 1.05 (1H, m, H-16b), 0.97 (4H, br s, H-20, CH_3-30), 0.86 (3H, s, CH_3-28), 0.83 (3H, d, J = 6.4 Hz, CH_3-29); ^{13}C NMR (DMSO-d_6, derived from multiplicity-edited HSQC and HMBC spectra) δ_C (ppm): 200.6 (C, C-11), 179.0 (C, C-24), 171.0 (C, C-1′), 166.2 (C, C-13), 129.9 (CH, C-12), 73.3 (CH, C-3), 60.2 (CH, C-9), 59.8 (CH, C-18), 50.3 (CH, C-5), 46.3 (C, C-4), 44.8 (C, C-8), 43.8 (C, C-14), 40.4 (CH_2, C-22), 39.2 (CH, C-19), 39.1 (CH, C-20), 37.3 (C, C-10), 34.7 (CH_2, C-1), 33.6 (C, C-17), 32.2 (CH_2, C-7), 30.6 (CH_2, C-21), 28.0 (CH_3, C-28), 27.1 (CH_2, C-16), 26.8 (CH_2, C-15), 23.2 (CH_2, C-2), 23.1 (CH_3, C-23), 19.9 (CH_3, C-30), 19.8 (CH_3, C-2′), 19.5 (CH_3, C-27), 18.4 (CH_2, C-6), 17.7 (CH_3, C-26), 16.4 (CH_3, C-29),12.6 (CH_3, C-25). HR-ESIMS m/z 535.3412 $[M + Na]^+$ (calculated for $C_{32}H_{48}NaO_5$, 535.3394).

Further purification of compounds **1**–**3** for activity assessment was achieved by submitting fractions F, G, and J to preparative HPLC separation, using solvents C and D as eluents. Samples were run under isocratic conditions (87% C, 20 min). The flow rate was 20 mL/min. Stock solutions in DMSO (150 mg/mL) were prepared and repeatedly injected in portions of 200–400 μL. Compounds **1** (3.13 mg), **2** (10 mg), and **3** (4 mg) were obtained from 35 mg of fraction G, 200 mg of fraction F, and 50 mg of fraction J, respectively.

2.6. Expression of $GABA_A$ receptors

Stage V–VI oocytes from *Xenopus laevis* were prepared, and cRNA was injected as previously described [28,32]. Female *X. laevis* (NASCO, Fort Atkinson, WI) were anesthetized by exposing them for 15 min to a 0.2% MS-222 (methane sulfonate salt of 3-aminobenzoic acid ethyl ester, Sigma) solution before surgically removing parts of the ovaries. All animal care and experimental procedures were approved by the Austrian Animal Experimentation Ethics Board, in compliance with the European convention for the protection of vertebrate animals used for experimental and other scientific purposes (ETS no. 123). Every effort was made to minimize the number of animals used. Follicle membranes from isolated oocytes were enzymatically digested with 2 mg/mL collagenase from *Clostridium histolyticum* (Type 1A, Sigma). Synthesis of capped runoff poly(A+) cRNA transcripts was obtained from linearized cDNA templates (pCMV vector). Directly after enzymatic isolation, the oocytes were injected with 50 nL of DEPC-treated water (Sigma) containing different cRNAs at a concentration of approximately 300–3000 pg/nL per subunit. The amount of injected cRNA mixture was determined by means of a NanoDrop ND-1000 (Kisker Biotech). To ensure the expression of gamma subunit in $\alpha_1\beta_2\gamma_{2S}$ receptors, rat cRNAs were mixed in a 1:1:10 ratio. Oocytes were then stored at 18 °C in ND96 solution containing 1% of penicillin-streptomycin solution (Sigma-Aldrich). Voltage clamp measurements were performed between days 1 and 5 after cRNA injection.

2.7. Positive control

Diazepam (7-chloro-1,3-dihydro-1-methyl-5-phenyl-2H-1,4-benzodiazepin-2-one; Sigma, purity not less than 98%) was used as positive control. At 1 μM diazepam induced a maximal potentiation of I_{GABA} of 231.3 ± 22.6% (n = 3). See also S1, supporting information.

2.8. Two-microelectrode voltage clamp studies

Electrophysiological experiments were performed with the two-microelectrode voltage clamp method making use of a TURBO TEC 03X amplifier (npi electronic GmbH) at a holding potential of −70 mV and pCLAMP 10 data acquisition software (Molecular Devices) [19]. Currents were low-pass-filtered at 1 kHz and sampled at 3 kHz. The bath solution contained 90 mM NaCl, 1 mM KCl, 1 mM $MgCl_2$, 1 mM $CaCl_2$, and 5 mM HEPES (pH 7.4). Electrode filling solution contained 2 M KCl. Oocytes with maximal current amplitudes >3 μA were discarded to exclude voltage clamp errors.

2.9. Fast solution exchange during I_{GABA} recordings

Test solutions (100 μL) were applied to the oocytes at a speed of 300 μL/s by means of the ScreeningTool automated fast perfusion system [19]. In order to determine GABA EC_{5-10} (typically between 3 and 10 μM for receptors of subunit composition $\alpha_1\beta_2\gamma_{2s}$), a dose–response experiment with GABA concentrations ranging from 0.1 μM to 1 mM was performed. A stock solution of the petroleum ether extract (10 mg/mL in DMSO) was diluted to a concentration of 100 μg/mL with bath solution containing GABA EC_{5-10} according to a validated protocol [28]. As previously described, microfractions collected from the semipreparative HPLC separations were dissolved in 30 μL of DMSO and subsequently mixed with 2.97 mL of bath solution containing GABA EC_{5-10} [28]. Stock solutions of compounds **1**–**3** (100 mM in DMSO) were diluted to a concentration of 100 μM with bath solution containing GABA EC_{5-10} for measuring modulation of $GABA_A$Rs. For concentration–response experiments, the stock solution of DHA (**1**) was diluted to concentrations of 0.1, 1.0, 3.0, 10, 30, 100, and 300 μM with bath solution for measuring direct activation, or with bath solution containing GABA EC_{5-10} for measuring receptor modulation. The final DMSO concentration in all the samples, including the GABA control samples, was adjusted to 1% to avoid solvent effect at the receptors.

2.10. Data analysis

Enhancement of the I_{GABA} was defined as $I_{(GABA\ +\ Comp)}/I_{GABA} - 1$, where $I_{(GABA\ +\ Comp)}$ is the current response in the presence of a given compound, and I_{GABA} is the control GABA-

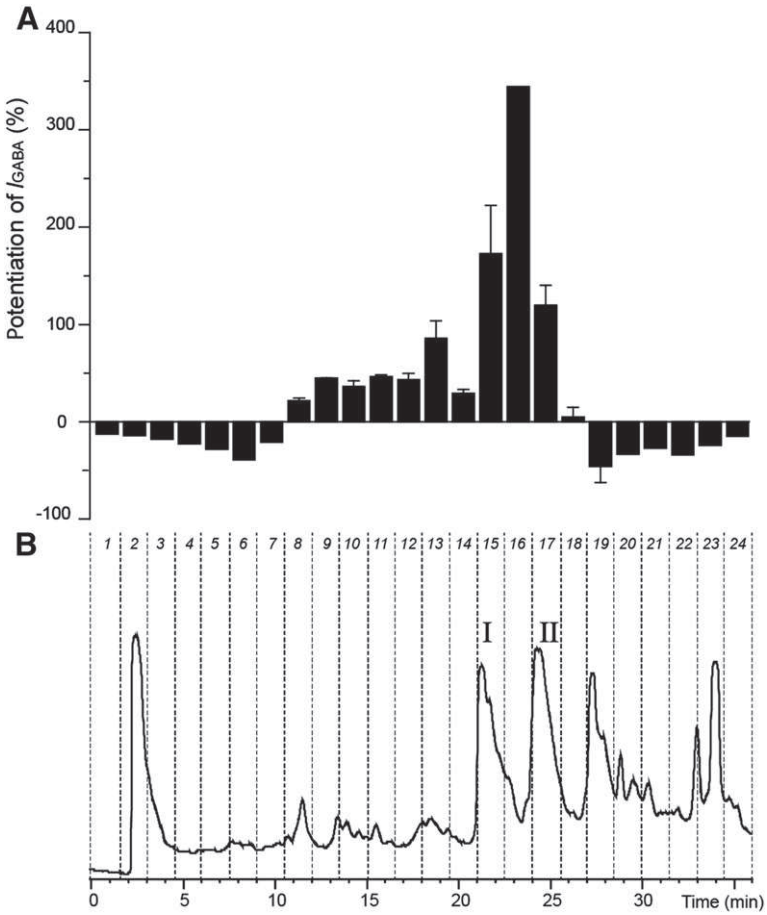

Fig. 1. HPLC-based activity profiling of the petroleum ether extract for $GABA_A$ receptor modulatory activity. A. Potentiation of the I_{GABA} by each microfraction (error bars correspond to S.E.). B. HPLC chromatogram (210–700 nm) of a semipreparative separation of 10 mg of extract. The 24 time-based fractions of 90 s each are indicated with dashed lines. Peaks contained in the active time window of the extract are indicated as I and II. After optimization of separation conditions, peak I was resolved into compounds **1** and **2**. Compound **3** was the main constituent of peak II.

induced chloride current. Data were analyzed using the ORIGIN 7.0 SR0 software (OriginLab Corporation) and are given as mean ± S.E. of at least two oocytes and ≥2 oocyte batches.

3. Results and discussion

At a test concentration of 100 μg/mL, the petroleum ether extract of *B. thurifera* resin enhanced I_{GABA} by 319.8% ± 79.8% through $GABA_A$Rs with $\alpha_1\beta_2\gamma_{2s}$ subunit composition. Active compounds were tracked with the aid of a validated protocol for HPLC-based activity profiling [28]. The chromatogram (210–700 nm) of a semipreparative HPLC separation (10 mg of extract) and the corresponding activity profile (24 microfractions of 90 s each) are shown in Fig. 1. Fractions 15, 16, and 17 potentiated I_{GABA} by 172.8% ± 49.5%, 344.3% ± 78.5%, and 119.7% ± 20.7%, respectively. Optimization of separation conditions enabled resolution of peaks in the active time window (indicated with roman numbers in Fig. 1). Therefore, peak I was resolved into compounds **1** and **2**, and compound **3** was the main constituent of peak II.

To obtain the active compounds in sufficient amounts for structure elucidation and pharmacological testing, a targeted preparative isolation was carried out, combining flash chromatography on silica gel with subsequent purification by semipreparative and preparative HPLC. Two diterpenes, dehydroabietic acid (**1**) and incensole (**2**), and the triterpene AKBA (**3**) (Fig. 2) were identified with the aid of ESI-TOF-MS, 1D and 2D microprobe NMR, and by comparison with published data [29–31]. Spectroscopic data of **1**–**3** are available as supporting information. Compounds **2** and **3** have been previously reported from olibanum, although not specifically from the resin of *B. thurifera*.

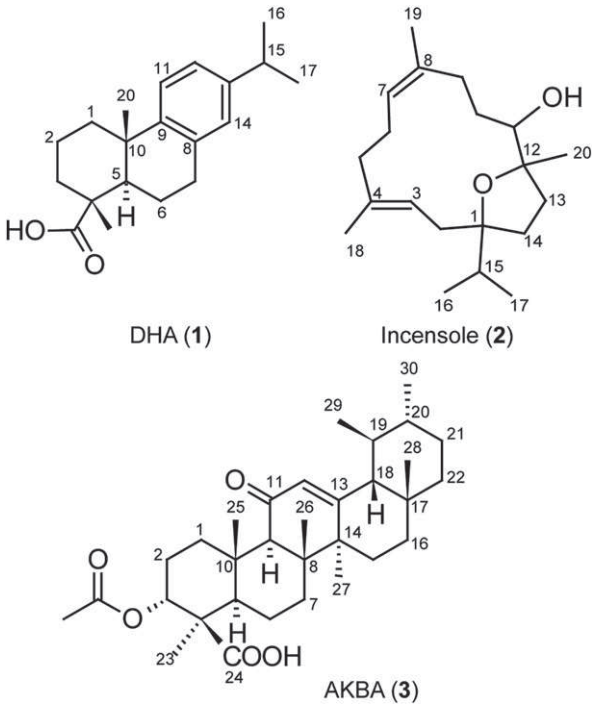

Fig. 2. Chemical structures of compounds **1**–**3**.

Compounds **1**–**3** were tested at a concentration of 100 μM in the oocyte assay, for a preliminary assessment of their activity in $\alpha_1\beta_2\gamma_{2s}$ $GABA_A$Rs (Table 1). Only DHA (**1**) modulated the receptors (potentiation of I_{GABA} of 682.3% ± 44.7%), while incensole and AKBA were inactive (enhancements of −13.9% ± 3.2% and −19.8% ± 4.5%, respectively) (Fig. 3A). Thus, further concentration–response experiments were performed only with DHA at concentrations ranging from 0.1 to 300 μM. In $GABA_A$Rs of $\alpha_1\beta_2\gamma_{2s}$ subunit composition DHA enhanced I_{GABA} in a concentration-dependent manner (Fig. 3B). At a GABA EC_{5-10}, maximal potentiation of I_{GABA} (397.5% ± 34.0%) was observed at ~100 μM, with an EC_{50} of 8.7 μM ± 1.3 μM. Direct activation of the receptor was observed at DHA concentrations higher than 30 μM, which suggests that the mechanism of action involves allosteric receptor modulation and possibly partial agonistic activity (Fig. 3C).

Due to their toxicity to fish, DHA and other abietane monocarboxylic acids (resin acids) were studied for their potential effect on the CNS. DHA was shown to induce release of GABA from nerve terminals in trout brain synaptosomes, while 12,14-dichlorodehydroabietic acid inhibited I_{GABA} in patch-clamped rat cortical neurons. However, modulatory effects on the GABAergic system have been suggested to be secondary to the elevation in cytoplasmic Ca^{2+} induced by these compounds [33,34]. This work constitutes the first report on $GABA_A$ receptor modulatory properties of the abietane diterpene DHA. Pimarane type diterpenoids, closely related to the abietanes, have been previously identified in our research group as a structural scaffold for $GABA_A$ receptor modulators [35]. However, the potency of DHA on receptors of the subtype $\alpha_1\beta_2\gamma_{2s}$ was higher than that of isopimaric acid (EC_{50} 141.6 μM ± 96.5 μM) and sandaracopimaric acid (EC_{50} 33.3 μM ± 8.7 μM), suggesting that an aromatic ring C is favorable for increasing the potency of this scaffold. However, more compounds need to be tested for establishing structure–activity relationships for these diterpenoids. DHA also showed higher potency than the labdane diterpenoids zerumin A (EC_{50} 24.9 μM ± 8.8 μM) and coronarin D (EC_{50} 35.7 μM ± 8.8 μM) [21]. However, the potency of DHA is significantly lower than that of classic BDZs like triazolam, clotiazepam, and midazolam, which modulate $GABA_A$Rs at nanomolar concentrations [32].

The physicochemical properties of dehydroabietic acid are favorable for oral bioavailability and BBB permeation [36,37]. In fish, the compound has been found to be readily absorbed and distributed to most organs, including the brain [34]. Although the toxicity observed in fish is a potential liability for DHA [33,38], *in vitro* and *in vivo* pharmacological and pharmacokinetic studies with the compound should be

Table 1
Potentiation of I_{GABA} in $\alpha_1\beta_2\gamma_{2s}$ receptors by compounds **1**–**3**, at a test concentration of 100 μM.

Compound	Maximal potentiation of I_{GABA} (%)[a]
1	682.3 ± 44.7
2	−13.9 ± 3.2
3	−19.8 ± 4.5
Diazepam (1 μM)[b]	231.3 ± 22.6

[a] Modulation measured in 4 oocytes from 3 different batches.
[b] Positive control.

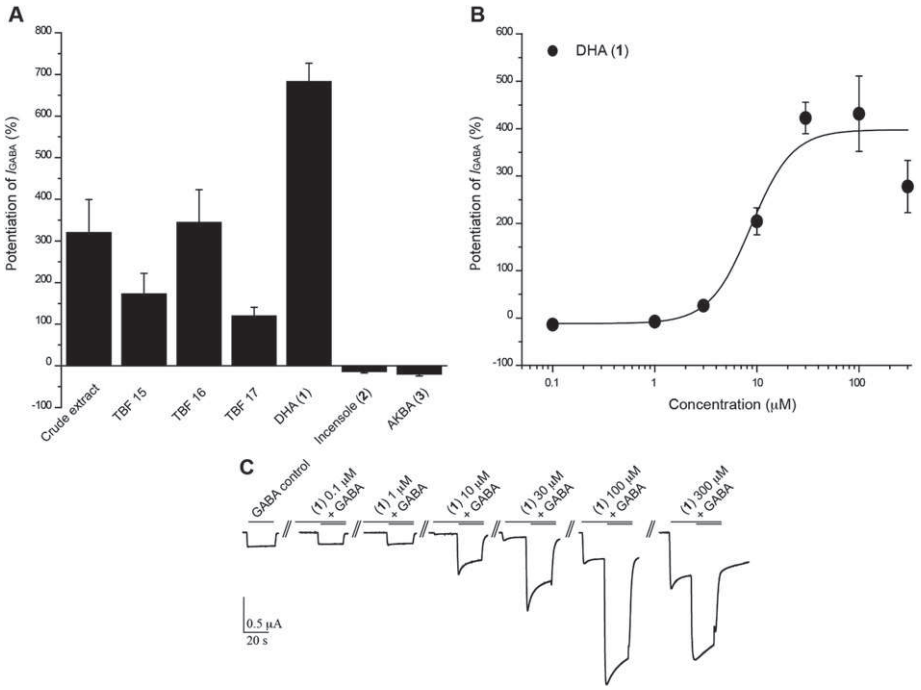

Fig. 3. A. Potentiation of I_{GABA} by the petroleum ether extract (100 μg/mL), by time-based fractions 15–17, and by compounds **1**–**3** (100 μM). B. Concentration–response curve for compound **1** on $GABA_A$Rs of the subunit composition $\alpha_1\beta_2\gamma_{2S}$. C. Typical traces for modulation of I_{GABA} by compound **1**. Pronounced receptor activation in the absence of GABA was observed at DHA concentrations of >30 μM. All experiments were carried out using a GABA EC_{5-10}.

performed to explore the potential of this scaffold as a starting point for medicinal chemistry.

4. Conclusions

HPLC-based activity profiling of olibanum from *B. thurifera* led to the identification of dehydroabietic acid as a positive allosteric modulator of $GABA_A$Rs of the subtype $\alpha_1\beta_2\gamma_{2s}$ that additionally displays properties of a partial agonist. The EC_{50} of DHA was lower than for other diterpenes (e.g. sandaracopimaric acid), indicating higher affinity to the receptor, even though it is far from the affinity of BDZs. Further assessment of subunit selectivity and activity *in vivo* are needed.

The terpenoids AKBA and incensole have also been isolated from the active time window of the extract, but were lacking $GABA_A$ receptor modulatory properties. Anxiolytic effects in behavioral models have been reported for incensole acetate, but were attributed to activation of TRPV3 channels in the brain [1]. At this point, the potential CNS modulating effects of frankincense are still a matter of speculation.

Acknowledgements

Financial support was provided by the Swiss National Science Foundation through project 205320_126888 (MH). D.C. Rueda thanks the Department of Education of Canton Basel (Erziehungsdepartement des Kantons Basel-Stadt) for a fellowship granted in 2012. This work was supported by the Austrian Science Fund (FWF doctoral program "Molecular Drug Targets" W1232 to S.H).

Appendix A. Supplementary data

Supplementary data to this article can be found online at http://dx.doi.org/10.1016/j.fitote.2014.09.002.

References

[1] Moussaieff A, Mechoulam R. *Boswellia* resin: from religious ceremonies to medical uses; a review of in vitro, in vivo and clinical trials. J Pharm Pharmacol 2009;61:1281–93.
[2] Mothana RAA, Hasson SS, Schultze W, Mowitz A, Lindequist U. Phytochemical composition and in vitro antimicrobial and antioxidant activities of essential oils of three endemic Soqotraen *Boswellia* species. Food Chem 2011;126:1149–54.
[3] Tropicos.org. Missouri Botanical Garden. http://www.tropicos.org; 2014. [Search: *Boswellia thurifera*].
[4] The International Plant Names Index. http://www.ipni.org/ipni/plantnamesearchpage.do; 2014. [Search: *Boswellia thurifera*.].
[5] Lee J-H, Lee J-S. Chemical composition and antifungal activity of plant essential oils against *Malassezia furfur*. Korean J Microbiol Biotechnol 2010;38:315–21.
[6] Van Vuuren SF, Kamatou GPP, Viljoen AM. Volatile composition and antimicrobial activity of twenty commercial frankincense essential oil samples. Chem Divers Biol Funct Plant Volatiles 2010;76:686–91.
[7] Pires R, Montanari L, Martins C, Zaia J, Almeida A, Matsumoto M, et al. Anticandidal efficacy of cinnamon oil against planktonic and biofilm cultures of *Candida parapsilosis* and *Candida orthopsilosis*. Mycopathologia 2011;172:453–64.
[8] Nusier M, Bataineh H, Bataineh Z, Daradka H. Effect of frankincense (*Boswellia thurifera*) on reproductive system in adult male rat. J Health Sci 2007;53:365–70.
[9] Fu-Shuang L, Dong-Lan Y, Rang-Ru L, Kang-Ping X, Gui-Shan T. Chemical constituents of *Boswellia carterii* (Frankincense). Chin J Nat Med 2010;8:25–7.
[10] Yoshikawa M, Morikawa T, Oominami H, Matsuda H. Absolute stereostructures of olibanumols A, B, C, H, I, and J from olibanum, gum-resin of *Boswellia carterii*, and inhibitors of nitric oxide production in

lipopolysaccharide-activated mouse peritoneal macrophages. Chem Pharm Bull (Tokyo) 2009;57:957–64.
[11] Al-Harrasi A, Al-Saidi S. Phytochemical analysis of the essential oil from botanically certified oleogum resin of *Boswellia sacra* (Omani Luban). Molecules 2008;13:2181–9.
[12] Hamm S, Bleton J, Connan J, Tchapla A. A chemical investigation by headspace SPME and GC-MS of volatile and semi-volatile terpenes in various olibanum samples. Phytochemistry 2005;66:1499–514.
[13] Banno N, Akihisa T, Yasukawa K, Tokuda H, Tabata K, Nakamura Y, et al. Anti-inflammatory activities of the triterpene acids from the resin of *Boswellia carteri*. J Ethnopharmacol 2006;107:249–53.
[14] Chinese Pharmacopoeia Commission. Pharmacopoeia of the People's Republic of China, vol. I, vol. 1. Beijing: China Medical Science Press; 2010.
[15] European Scientific Cooperative on Phytotherapy. Olibanum indicum. ESCOP Monogr. Second Ed. Suppl. 2009. ESCOP & Thieme; 2009. p. 184–97.
[16] Tucker A. Frankincense and myrrh. Econ Bot 1986;40:425–33.
[17] Olsen RW, Sieghart W. International Union of Pharmacology. LXX. Subtypes of γ-aminobutyric acid A receptors: classification on the basis of subunit composition, pharmacology, and function. Update. Pharmacol Rev 2008;60:243–60.
[18] Rudolph U, Knoflach F. Beyond classical benzodiazepines: novel therapeutic potential of $GABA_A$ receptor subtypes. Nat Rev Drug Discov 2011; 10:685–97.
[19] Baburin I, Beyl S, Hering S. Automated fast perfusion of *Xenopus* oocytes for drug screening. Pflugers Arch 2006;453:117–23.
[20] Potterat O, Hamburger M. Concepts and technologies for tracking bioactive compounds in natural product extracts: generation of libraries, and hyphenation of analytical processes with bioassays. Nat Prod Rep 2013;30:546.
[21] Schramm A, Ebrahimi SN, Raith M, Zaugg J, Rueda DC, Hering S, et al. Phytochemical profiling of *Curcuma kwangsiensis* rhizome extract, and identification of labdane diterpenoids as positive $GABA_A$ receptor modulators. Phytochemistry 2013;96:318–29.
[22] Zaugg J, Eickmeier E, Ebrahimi SN, Baburin I, Hering S, Hamburger M. Positive $GABA_A$ receptor modulators from *Acorus calamus* and structural analysis of (+)-dioxosarcoguaiacol by 1D and 2D NMR and molecular modeling. J Nat Prod 2011;74:1437–43.
[23] Zaugg J, Eickmeier E, Rueda DC, Hering S, Hamburger M. HPLC-based activity profiling of *Angelica pubescens* roots for new positive $GABA_A$ receptor modulators in *Xenopus* oocytes. Fitoterapia 2011;82:434–40.
[24] Zaugg J, Ebrahimi SN, Smiesko M, Baburin I, Hering S, Hamburger M. Identification of GABAA receptor modulators in *Kadsura longipedunculata* and assignment of absolute configurations by quantum-chemical ECD calculations. Phytochemistry 2011;72:2385–95.
[25] Zaugg J, Baburin I, Strommer B, Kim H-J, Hering S, Hamburger M. HPLC-based activity profiling: discovery of piperine as a positive $GABA_A$ receptor modulator targeting a benzodiazepine-independent binding site. J Nat Prod 2010;73:185–91.
[26] Li Y, Plitzko I, Zaugg J, Hering S, Hamburger M. HPLC-based activity profiling for $GABA_A$ receptor modulators: a new dihydroisocoumarin from *Haloxylon scoparium*. J Nat Prod 2010;73:768–70.
[27] Yang X, Baburin I, Plitzko I, Hering S, Hamburger M. HPLC-based activity profiling for $GABA_A$ receptor modulators from the traditional Chinese herbal drug Kushen (*Sophora flavescens* root). Mol Divers 2011;15: 361–72.
[28] Kim H, Baburin I, Khom S, Hering S, Hamburger M. HPLC-based activity profiling approach for the discovery of $GABA_A$ receptor ligands using an automated two microelectrode voltage clamp assay on *Xenopus* oocytes. Planta Med 2008;74:521–6.
[29] González MA, Pérez-Guaita D, Correa-Royero J, Zapata B, Agudelo L, Mesa-Arango A, et al. Synthesis and biological evaluation of dehydroabietic acid derivatives. Eur J Med Chem 2010;45:811–6.
[30] Corsano S, Nicoletti R. The structure of incensole. Tetrahedron 1967;23: 1977–84.
[31] Belsner K, Büchele B, Werz U, Syrovets T, Simmet T. Structural analysis of pentacyclic triterpenes from the gum resin of *Boswellia serrata* by NMR spectroscopy. Magn Reson Chem 2003;41:115–22.
[32] Khom S, Baburin I, Timin EN, Hohaus A, Sieghart W, Hering S. Pharmacological properties of $GABA_A$ receptors containing γ1 subunits. Mol Pharmacol 2006;69:640–9.
[33] Lees G, Coyne L, Zheng J, Nicholson RA. Mechanisms for resin acid effects on membrane currents and $GABA_A$ receptors in mammalian CNS. Environ Toxicol Pharmacol 2004;15:61–9.
[34] Zheng J, Nicholson RA. Influence of two naturally occurring abietane monocarboxylic acids (resin acids) and a chlorinated derivative on release of the inhibitory neurotransmitter| γ-aminobutyric acid from trout brain synaptosomes. Bull Environ Contam Toxicol 1996;56:114–20.
[35] Zaugg J, Khom S, Eigenmann D, Baburin I, Hamburger M, Hering S. Identification and characterization of GABAA receptor modulatory diterpenes from *Biota orientalis* that decrease locomotor activity in mice. J Nat Prod 2011;74:1764–72.
[36] Pajouhesh H, Lenz GR. Medicinal chemical properties of successful central nervous system drugs. NeuroRx 2005;2:541–53.
[37] Lipinski CA. Lead- and drug-like compounds: the rule-of-five revolution. Drug Discov Today Technol 2004;1:337–41.
[38] San Feliciano A, Gordaliza M, Salinero M, del Corral J. Abietane acids: sources, biological activities, and therapeutic uses. Planta Med 2007;59: 485–90.

4.2.3 Nitrogenated Honokiol Derivatives Allosterically Modulate $GABA_A$ Receptors and Act as Strong Partial Agonists

Accepted and resubmitted after revision to the Journal of Medicinal Bioorganic Chemistry (04-Aug-2015).

Marketa Bernaskova[†a], Angela Schöffmann[‡], Wolfgang Schühly[†b,§], Antje Hüfner[†a], Igor Baburin[‡], and Steffen Hering[‡]

[†]Institute of Pharmaceutical Sciences, [a]Pharmaceutical Chemistry, University of Graz, Schubertstrasse 1, and [b]Department of Pharmacognosy, University of Graz, Universitätsplatz 4, 8010 Graz, Austria
[§]Institute of Zoology, University of Graz, Universitätsplatz 2, 8010 Graz, Austria
[‡]Department of Pharmacology and Toxicology, University of Vienna, Althanstrasse 14, 1090 Vienna, Austria

Contribution Statement: *Investigation of modulatory activity of honokiol derivatives through $GABA_A$ receptors, writing of the manuscript (in vitro pharmacological results and discussion part) and preparation of figures and tables were my contributions to this work.*

For Supporting Information see Appendix 7.4.

Nitrogenated honokiol derivatives allosterically modulate $GABA_A$ receptors and act as strong partial agonists

Marketa Bernaskova,[†a] Angela Schoeffmann,[‡] Wolfgang Schuehly,[†b,§,*] Antje Huefner,[†a] Igor Baburin,[‡] Steffen Hering[‡]

[†]Institute of Pharmaceutical Sciences, [a]Pharmaceutical Chemistry, University of Graz, Schubertstrasse 1, and [b]Department of Pharmacognosy, University of Graz, Universitätsplatz 4, 8010 Graz, Austria

[§]Institute of Zoology, University of Graz, Universitätsplatz 2, 8010 Graz, Austria

[‡]Department of Pharmacology and Toxicology, University of Vienna, Althanstrasse 14, 1090 Vienna, Austria

[*]Author to whom correspondence should be addressed.

Phone: +43-316-380 8754

Fax: +43-316-380 9875

E-mail: wolfgang.schuehly@uni-graz.at

Abstract

In traditional Asian medicinal systems, preparations of the root and stem bark of *Magnolia* species are widely used to treat anxiety and other nervous disturbances. The biphenyl-type neolignan honokiol together with its isomer magnolol are the main constituents of *Magnolia* bark extracts. We have previously identified a nitrogen-containing honokiol derivative (3-acetylamino-4'-*O*-methylhonokiol, **AMH**) as a high efficient modulator of $GABA_A$ receptors. Here we further elucidate the structure-activity relation of a series of nitrogenated biphenyl-neolignan derivatives by analysing allosteric modulation and agonistic effects on $\alpha_1\beta_2\gamma_{2S}$ $GABA_A$ receptors. The strongest I_{GABA} enhancement was induced by compound **5** (3-acetamido-4'-ethoxy-3',5-dipropylbiphenyl-2-ol, E_{max}: 123.4 ± 9.4% of $I_{GABA\text{-}max}$) and **6** (5'-amino-2-ethoxy-3',5-dipropylbiphenyl-4'-ol, E_{max}: 117.7 ± 13.5% of $I_{GABA\text{-}max}$). Compound **5** displayed, however, a significantly higher potency (EC_{50} = 1.8 ± 1.1 µM) than compounds **6** (EC_{50} = 20.4 ± 4.3 µM).

Honokiol, **AMH** and four of the derivatives induced significant inward currents in the absence of GABA. Strong partial agonists were honokiol (inducing 78 ± 6% of $I_{GABA\text{-}max}$), **AMH** (63 ± 6%), 5'-amino-2-*O*-methylhonokiol (**1**) (59 ± 1%) and 2-methoxy-5'-nitro-3',5-dipropylbiphenyl-4'-ol (**3**) (52 ± 1%). 3-*N*-Acetylamino-4′-ethoxy-3′,5-dipropyl-biphenyl-4′-ol (**5**) and 3-amino-4′-ethoxy-3′,5-dipropyl-biphenyl-4′-ol (**7**) were less efficacious but even more potent (**5**: EC_{50}= 6.9 ± 1.0 µM; **7**: EC_{50}= 33.2 ± 5.1 µM) than the full agonist GABA.

Key words:

honokiol derivatives, $GABA_A$ receptor, nitrogenation, *Magnolia*

1. Introduction

γ-Aminobutyric acid (GABA) is the most important inhibitory neurotransmitter in the mammalian central nervous system (CNS). The action of GABA is primarily exerted through ligand-gated ion channels, the $GABA_A$ receptors. The $GABA_A$ receptor is a co-assembly of five subunits, which together form a central pore in the cell membrane for selective chloride ion transport (Macdonald & Olsen, 1994). $GABA_A$ receptors exist in different subtypes, which are characterizied by the type of subunit and the respective assemblage and they depend on the tissue in which they occur. The different $GABA_A$ subtypes exert different physiological effects (Rudolph et al., 2001; Sieghart & Sperk, 2002) and react differently to $GABA_A$ receptor modulatory compounds making the search for subtype-selective chemical entities interesting (Sieghart & Ernst, 2005). The $GABA_A$ receptor plays a crucial role in several disorders of the CNS such as depression, anxiety, epilepsy. Among many other classes of $GABA_A$ receptor modulators, two classes that are clearly identifiable upon their mode of action are benzodiazepines that exert their action upon the presence of a γ_2 subunit within the presence of either α_1, α_2, α_3 or α_5 subunits (Wafford et al., 1993) and barbiturates, etomidat, propofol, valerenic acid which do not require the presence of a γ subunit (Hevers et al., 1998, Sieghard, 2014, Khom et al. 2010).

The study of Asian medicinal preparations with anxiolytic and CNS relaxing effects such as Saiboku-to from Japan led to the identification of the biphenyl neolignans honokiol and magnolol as the major active constituents of the Asian *Magnolia* bark preparations that contain e.g. *M. officinalis* Rehd. et Wils. (Maruyama et al., 1998). Besides the great multitude of pharmacological activities that are ascribed to especially honokiol (**H**) (Mayurama & Kuribara, 2000), the CNS activity of honokiol and magnolol could be linked to their interaction with $GABA_A$ receptors (Ai et al., 2001).

The modulatory effect of honokiol on chloride currents through a set of $GABA_A$ receptor subtypes expressed in *Xenopus* oocytes was previously investigated in our group using a series of 31 analogs of honokiol. It led to the discovery of the very potent 3-acetylamino-4'-*O*-methylhonokiol (**AMH**) that enhanced I_{GABA} trough $\alpha_1\beta_2$ receptors by more than 2600 % (Taferner et al., 2011). In that communication, it was also shown that for **H**, the potentiation was about equal for $\alpha_1\beta_2\gamma_{2S}$ and $\alpha_1\beta_2$ receptor subtypes, i.e., the potentiation did not require the presence of a γ_{2S} subunit, which hints to a binding site of **H** different from the benzodiazepine binding site. Accordingly, Baur et al. (2014) could demonstrate through an indepth study on subunit-specificity of 4'-*O*-methylhonokiol (**MH**) that the current

potentiation by **MH** was also not depending on the presence of a γ_{2S} subunit. The binding of benzodiazepine requires the presence of a γ_2 receptor subunit, however, benzodiazepine effects are usually accompanied by undesired side effects (Wieland et al., 1992) rendering a drug candidate interacting with a novel (non benzodiazepine) binding site especially interesting. Recent data of Alexeev et al. (2012) who analysed the effects of several point mutations on **H** action suggest that its binding site may be separate from the binding site of neurosteroids, anesthetics, ethanol and picrotoxin.

The structural similarity of **AMH** to **H** and **MH** prompted us to further explore this lead as a candidate with potentially lacking of benzodiazepine side-effects through the study of structure activity-relationships of nitrogenated honokiol derivatives by analysing allosteric modulation of $\alpha_1\beta_2\gamma_{2S}$ $GABA_A$ receptors with particular focus on partial agonistic effects.

2. Results and discussion

2.1. Syntheses

Seven honokiol derivatives with nitrogen-containing moieties (**1 – 7; Scheme 1, Table 1**) were synthesized and the enhancement of GABA-induced chloride currents (I_{GABA}) was studied. Aside, a potential induction of chloride currents through $GABA_A$ receptors composed of $\alpha_1\beta_2\gamma_{2S}$ subunits was analysed subsequently.

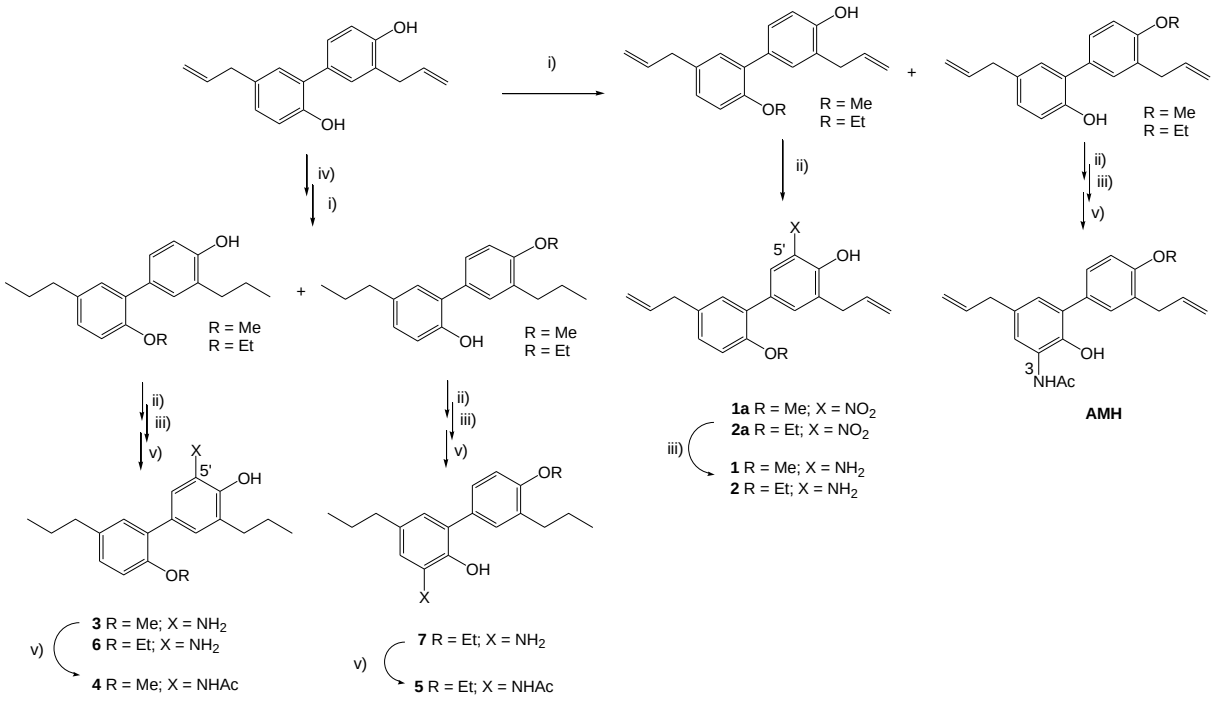

i) MW irradiation 1. KOH, 2. Me_2SO_4 or Et_2SO_4; ii) HNO_3 (65%), EtOAc; iii) $SnCl_2$ x $2H_2O$, EtOH; iv) H_2, [Pd/C]; v) Ac_2O, H_2O

Scheme 1. Synthesis of a series of nitrogenated honokiol analogs.

The syntheses aimed at combining pharmacophore features that turned out to be most promising from previous $GABA_A$ receptor modulatory studies (Taferner et al., 2011), i.e., nitrogenation of the aromatic ring using either an amino function or an acetylated amino function as well as the substitution of the free hydroxy groups with either methyl or ethyl moieties. The hydrogenation of the initial 2-propenyl chain into a propyl chain was in most cases undertaken to enhance overall chemical stability.

The 2-*O*-alkylated honokiols 2-*O*-methylhonokiol and 2-*O*-ethylhonokiol resp. were nitrated in ortho position to the free hydroxy group according to Johnson et al., (2001) resulting in 2-*O*-methyl-5'-nitrohonokiol (**1a**) and 2-*O*-ethyl-5'-nitrohonokiol (**2a**), resp., which were reduced to the corresponding amines (**1**) and (**2**) according to literature (Widdowson et al., 2004). It is worth to note that the carbons of the B-ring of the amines **1** and **2** give very broad signals in the ^{13}C-NMR-spectra. Therefore their resonances are often only visible in the HMBC spectra. C-5 of **2** is not even definitely found in HMBC.

The synthesis of the five hydrogenated honokiol derivatives **3 – 7** is described in Bernaskova et al. (2014), the general route to alkylated honokiols is described in Schuehly et al. (2011).

2.2. Pharmacological evaluation

2.2.1. Concentration-dependent enhancement of I_{GABA} by honokiol derivatives

I_{GABA} ($EC_{3\text{-}7}$) modulation by derivatives **1–7** was determined (**Figure 1**, **Table 2**).

Table 1 Structures of compounds based on nitrogenated honokiol for the evaluation of $GABA_A$ receptor modulatory activity including the previously identified highly efficient 3-acetylamino-4'-*O*-methylhonokiol (**AMH**, i.e. cpd. **31** in Taferner et al. (2014)) and honokiol (**H**).

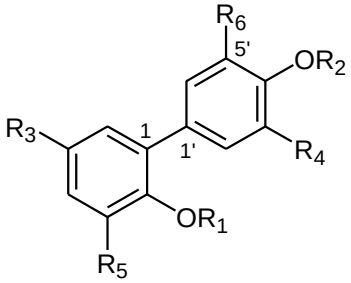

Cpd.	R_1	R_2	R_3	R_4	R_5	R_6
H	-H	-H	-2-propenyl	-2-propenyl	-H	-H
AMH	-H	$-CH_3$	-2-propenyl	-2-propenyl	$-NHCOCH_3$	-H
1	$-CH_3$	-H	-2-propenyl	-2-propenyl	-H	$-NH_2$
2	$-C_2H_5$	-H	-2-propenyl	-2-propenyl	-H	$-NH_2$

3	$-CH_3$	-H	-2-propyl	-2-propyl	-H	$-NH_2$
4	$-CH_3$	-H	-2-propyl	-2-propyl	-H	$-NHCOCH_3$
5	-H	$-C_2H_5$	-2-propyl	-2-propyl	$-NHCOCH_3$	-H
6	$-C_2H_5$	-H	-2-propyl	-2-propyl	-H	$-NH_2$
7	-H	$-C_2H_5$	-2-propyl	-2-propyl	$-NH_2$	-H

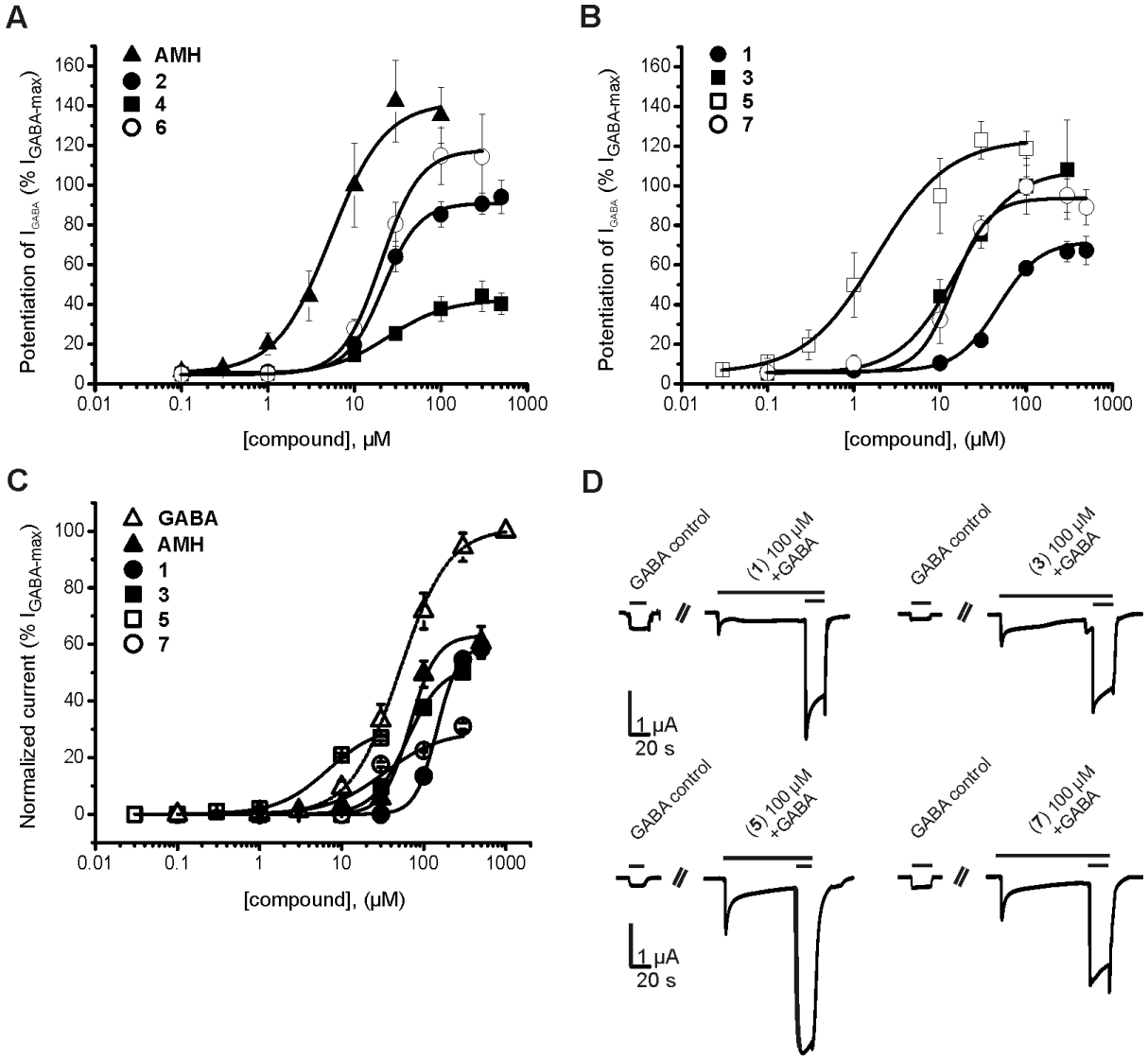

Figure 1 Concentration-effect curves for I_{GABA} potentiation ($\alpha_1\beta_2\gamma_{2S}$) by (**A**) AMH (▲),**2** (●), **4** (■) and **6** (○) and (**B**) **1** (●), **3** (■), **5** (□) and **7** (○). (**C**) Partial agonistic effect induced by **AMH** (▲), **1** (●), **3** (■), **5** (□) and **7** (○) on $\alpha_1\beta_2\gamma_{2S}$ $GABA_A$ receptors compared to I_{GABA} induced by the full agonist GABA (△, from Baburin et al., 2008). Each data point represents the mean±SE from at least three oocytes and two different frogs. (**D**) Typical inward currents illustrating direct activation of $\alpha_1\beta_2\gamma_{2S}$ $GABA_A$ receptors (single horizontal bar) and I_{GABA} modulation (double horizontal bar) by 100 µM of compounds **1**, **3**, **5** and **7**.

2.2.2. Honokiol derivatives as partial agonist on $GABA_A$ receptors

Honokiol and its nitrogenated derivatives **AMH**, **1**, **3**, **5** and **7** induced chloride currents through $GABA_A$ receptors in the absence of GABA (see **Figure 1D** for representative currents evoked by 100 µM of the indicated compound). **Figure 1C** illustrates the partial agonistic effects. Inward currents are expressed as fractions of $I_{GABA\text{-}max}$ induced by 1 mM GABA.

H, **AMH** and **1** were identified as the strongest partial agonists on $\alpha_1\beta_2\gamma_{2S}$ $GABA_A$ receptors with maximal inward currents ranging between 59 ± 1% (**1**, n=3) and 78 ± 6% (**H**, n=4) of $E_{max\text{-}dir}$, followed by the slightly less efficient compound **3** (52 ± 1%, n=3). The weakest partial agonists were compounds **5** and **7**, however still inducing approximately 30% of $E_{max\text{-}dir}$ (**Table 3**, **Figure 1C**). Compounds **2**, **4** and **6** did not induce chloride currents in the absence of GABA (**Table 3**).

Table 2 Efficiency and potency of I_{GABA} modulation ($\alpha_1\beta_2\gamma_{2S}$) by **AMH** and derivatives **1- 7**. E_{max} indicates maximum enhancement of chloride current through $\alpha_1\beta_2\gamma_{2S}$ $GABA_A$ receptors induced by the indicated compound in % of the maximal I_{GABA} induced by 1 mM GABA. Hill-coefficient (n_H) and number of experiments are given.

Compound	E_{max} (%)	EC_{50} (µM)	n_H	n
AMH	141.6 ± 14.1	5.3 ± 1.9	1.4 ± 0.3	5
1	72.0 ± 4.8	47.6 ± 6.8	1.8 ± 0.2	6
2	91.0 ± 4.2	21.5 ± 3.3	2.1 ± 0.4	4
3	108.0 ± 8.0	15.8 ± 4.4	1.3 ± 0.1	4
4	42.5 ± 4.9	24.6 ± 7.4	1.3 ± 0.3	4
5	123.4 ± 9.4	1.8 ± 1.1	1.0 ± 0.3	7
6	117.7 ± 13.5	20.4 ± 4.3	1.9 ± 0.3	5
7	93.7 ± 5.8	14.4 ± 3.2	2.2 ± 0.8	4

Table 3 Direct activation of $\alpha_1\beta_2\gamma_{2S}$ $GABA_A$ receptors by honokiol derivatives. $E_{max\text{-}dir}$ indicates maximum chloride current through $\alpha_1\beta_2\gamma_{2S}$ $GABA_A$ receptors induced by a saturating concentration of the indicated compound in % of the maximal I_{GABA} induced by 1 mM GABA (see **Fig. 1c2**). EC_{50} value and n_H of the GABA concentration-response curves for comparison were taken from Baburin et

al. (2008). Asterisks indicate statistically significant differences to $I_{Honokiol}$ as follows: * = $p<0.05$, ** = $p<0.01$.

Compound	$E_{max\text{-}dir}$ (%)	EC_{50} (µM)	n_H	n
GABA	100	51.0 ± 3.0*	1.4 ± 0.1	27
H	78 ± 6	76.2 ± 10.3	2.6 ± 0.4	4
AMH	63 ± 6	68.1 ± 9.7	2.7 ± 0.4	3
1	59 ± 1	144.3 ± 5.7**	3.3 ± 0.3	3
2	No agonist activity			
3	52 ± 1	62.2 ± 2.4	2.1 ± 0.1	3
4	No agonist activity			
5	32 ± 2	6.9 ± 1.0**	1.4 ± 0.1	3
6	No agonist activity			
7	29 ± 2	33.2 ± 5.1**	1.3 ± 0.2	3

3. Conclusion

In a previous study on I_{GABA} modulation by honokiol and derivatives, it has been found that derivatives comprising nitrogen-containing moieties potentiate I_{GABA} more efficiently and also display higher potencies compared to the parent molecule honokiol (Taferner et al., 2011). Based on these findings, 7 nitrogen-containing honokiol derivatives have been synthesized combining molecular features that were recognized to be important functional groups and subsequently studied for I_{GABA} enhancement and direct activation of $GABA_A$ receptors composed of $\alpha_1\beta_2\gamma_{2S}$ subunits. Altogether two compounds of the tested series and two precursors are new chemical entities.

Besides their modulatory activity, **H**, **AMH** and four of the newly synthesized derivatives activated $GABA_A$ receptors in the absence of GABA (**Fig. 1C, D, Table 3**). Partial agonism was most pronounced for **H**, **AMH** and **1** followed by **3**. Compounds **5** and **7** are only weak partial agonists but apparently more potent on $\alpha_1\beta_2\gamma_{2S}$ receptors than the full agonist GABA. Partial agonist activity was previously reported for **H** and magnolol (at concentrations > 10 µM) by Alexeev et al. (2012), though in a different cell system. Our data confirm and extend this finding to nitrogenated derivatives such as **AMH**, **1**, **3**, **5** and **7** (**Table 3**). Remarkably, small structural changes completely diminish partial agonism while preserving positive

allosteric modulation of $GABA_A$ receptors (**2**, **4**, **6** in **Tables 2** and **3**). First studies with **H** on mutated $GABA_A$ receptors (including $\alpha1_{(Q240W)}$, essential for the action of neurosteroids; $\beta3_{(M286W)}$, preventing the action of general anesthetics; $\beta3_{(T256F)}$ or $\alpha1_{(T260F)}$ essential for the interaction with picrotoxine) did not affect allosteric modulation of $GABA_A$ receptors by either **H** or magnolol suggesting that these molecules interact with an yet unidentfied binding site (Alexeev et al., 2012). We show here that the agonistic activity of **H** and the studied nitrogenated derivatives does not correlate with allosteric modulation. Future studies will show if agonistic and modulatory effects of these compounds are mediated via separate binding sites.

4. Experimental

4.1. General

Infrared spectra were recorded on a Bruker Alpha Platinum ATR spectrometer. ^{1}H and ^{13}C NMR spectra were recorded on a Varian 400 MHz spectrometer (400 and 100 MHz) using chloroform-d as solvent and were referenced using TMS as internal standard.

EI-MS were recorded on an Agilent Technologies HP 7890A instrument fitted with detector HP 5975C VL MSD (70 eV, ion source 250 °C, quadrupole temperature 150 °C). Column: Agilent HP-5MS 30 m, ID 0.25 mm, film 5% phenyl95%methypolysiloxane 9.25 µm. Oven temperature was kept at 45 °C for 2 min and programmed to 300 °C at a rate of 3 °C/min, then kept constant at 300 °C for 20 min.

ESI-MS were recorded in ESI positive and negative mode on a Thermo Finnigan LCQ Deca XP Plus mass spectrometer with autosampler. Column: Zorbax SB-C18 (3.5 µm; 150 x 2.1 mm; Agilent Technologies) with guard column at a flowrate: 300 µL/min.

The purity of synthesized compounds was verified using HPLC on an Agilent 1260 series equipped with diode array detector and by NMR spectroscopy. For analytical HPLC-DAD, an SB-C18 Zorbax column (3.5 µm; 150 x 2.1 mm; Agilent Technologies) equipped with guard column at a flow rate of 300 µL/min was used. The gradient elution program was as follows: CH_3CN in water (0→25 min/10→90%, 25→30 min/90→100%, 30→38 min/100%).

For TLC analysis, precoated Si60 F_{254} plates (Merck, Darmstadt) were used. Detection was done by UV/254 nm and spraying with molybdato-phosphoric acid and subsequent heating.

Compound mixtures were separated by PTLC (Merck; PLC silica gel 60 F_{254}, 1 mm), using cyclohexane/ethyl acetate mixtures. Honokiol was purchased from APIChem Technology Co., Hangzhou, China (purity >98%).

4.2. Synthesis

4.2.1. Synthesis of 2-*O*-methyl-5'-nitro-honokiol (1a)

Nitric acid (65%, 3.6 mmol, 0.25 mL) was added under intense stirring within ca. 5 sec to a solution of 2-*O*-methyl-honokiol (101 mg, 0.360 mmol; synthesis see Schuehly et al., 2011) in ethyl acetate (10 mL) at room temperature. The reaction mixture was stirred for 10 min and neutralized with NaOH (2 N). The organic phase was separated and the water phase was extracted with ethyl acetate (3 x 15 mL). The combined organic layers were washed with brine (15 mL), dried over Na_2SO_4 and concentrated under reduced pressure yielding 115 mg (98 %) of methyl-5'-nitro-honokiol (**1a**) as orange oil.

1a: IR (ATR, ν_{max}, cm^{-1}): 3209, 3079, 2909, 2835, 1638, 1621, 1536, 1498, 1464, 1431, 1323, 1239, 1179, 1129, 1027, 912, 810, 768, 676, 606; ^{1}H NMR ($CDCl_3$) δ10.97 (s, 1H, O*H*), 8.15 (d, J = 1.8 Hz, 1H, H-6'), 7.65 (d, J = 1.8 Hz, 1H, H-2'), 7.16 (dd, J = 8.4, 2.2 Hz, 1H, H-4), 7.10 (d, J = 2.2 Hz, 1H, H-6), 6.92 (d, J = 8.4 Hz, 1H, H-3), 6.01 (ddt, J ~2'"), 5.97 (ddt, J ~17, 10.2, 6.6 Hz, 1H, H-2"), 5.13 (m, 2H, H-3'"), 5.09 (m, 2H, H-3"), 3.80 (s, 3H, OC*H*$_3$), 3.53 (d, J = 6.6 Hz, 2H, H-1'"), 3.38 (d, J = 6.6 Hz, 2H, H-1"); ^{13}C NMR ($CDCl_3$) 1710.3, 6.8 Hz, 1H, H, δ154.8 (C-2), 152.3 (C-4'), 139.1 (C-2'), 137.5 (C-2"), 135.3 (C-2'"), 133.3 (C-5'), 132.6 (C-5), 130.6 (C-3'), 130.5 (C-6), 130.2 (C-1'), 129.2 (C-4), 127.8 (C-1), 123.4 (C-6'), 116.7 (C-3'"), 115.8 (C-3"), 111.4 (C-3), 55.7 (O*C*H3), 39.3 (C-1"), 33.8 (C-1'"); MS (ESI^-) m/z (%): 324.22 ($[M-H]^-$, 100).

4.2.2. Synthesis of 5'-amino-2-*O*-methylhonokiol (1)

$SnCl_2$ x $2H_2O$ (70 mg, 0.310 mmol) was added to a solution of 2-*O*-methyl-5'-nitro-honokiol (**1a**) (98 mg, 0.301 mmol) in MeOH (10 mL) and was stirred for 72 h at room temperature, an additional amount of $SnCl_2$ x $2H_2O$ (100 mg, 0.443 mmol) was added and stirring was continued for 24 h. The foamy precipitate resulting from the addition of $NaHCO_3$ (1 N, 20 mL) was filtered off with Celite® and rinsed with EtOH (30 mL). After evaporation of the alcohols the resulting mixture was extracted with dichloromethane (3 x 10 mL). The combined extracts were dried over Na_2SO_4, concentrated under reduced pressure and purified by PTLC (silica, cyclohexane / ethyl acetate 5:3) to yield **1** (25 mg, 39%) as a brown oil. **1:** IR spectra (ATR, ν_{max}, cm^{-1}): 3373, 3313, 3074, 3000, 2974, 2903, 2832, 1637, 1606, 1488, 1240, 1141, 907, 809; ^{1}H NMR ($CDCl_3$) δ7.12 (s, 1H, H-6), 7.10 (d, J = 8.8 Hz, 1H, H-4), 6.90 (d, J ~ 8 Hz, 1H, H-3), 6.89 (s, 1H, H-6'), 6.75 (s, 1H, H-2'), 6.00 (ddt, J = 16.9, 10.2, 6.4 Hz, 1H, H-2'"), 6.04 (ddt, J = 16.9, 10.9, 6.6 Hz, 1H, H-2"), 5.28 (d, J = 17.6 Hz, 1H, H-3'"),

5.21 (d, J = 9.9 Hz, 1H, H-3'''), 5.11 (dq, J = 16.9, 1.2 Hz, 1H, H-3''), 5.07 (d, J ~ 8 Hz, 1H, H-3''), 3.79 (s, 3H, OCH_3), 3.45 (d, J = 6.0 Hz, 2H, H-1'''), 3.37 (d, J = 6.5 Hz, 2H, H-1''); ^{13}C NMR ($CDCl_3$) δ 154.8 (C-2), 142.3 (C-4), 137.8 (C-2''), 136.7 (C-2'''), 134.4 (C-5'), 132.1 (C-5), 131.3 (C-1'), 131.0 (C-6), 130.5 (C-1), 127.8 (C-4), 124.7 (C-3'),122.1 (C-2'), 117.0 (C-6'), 116.7 (C-3'''), 115.5 (C-3''), 111.2 (C-3), 55.7 (O*C*H_3), 39.4 (C-1''), 36.0 (C-1'''); MS (ESI) *m/z* (%): 296.17 $[M+H]^+$ (100).

4.2.3. Synthesis of 2-*O*-ethyl-5'-nitro-honokiol (2a)

Nitric acid (65%, 0.182 mL, 2.62 mmol) was added under intense stirring within ca. 5 sec to a solution of 2-*O*-ethyl-honokiol (77 mg, 0.262 mmol; synthesis see Schuehly et al., 2011) in ethyl acetate (10 mL) at room temperature. The reaction mixture was stirred for 60 sec and carefully neutralized with NaOH (2 N). The organic phase was separated, and the aqueous phase was extracted with ethyl acetate (3 x 15 mL). The combined organic phases were washed with brine (3 x 15 mL), dried over Na_2SO_4, and concentrated under reduced pressure. Because of incomplete reaction the residue was solved again in ethyl acetate (10 mL) nitration and workup were repeated but with a reaction time of 10 min resulting in 88 mg of 2-*O*-ethyl-5'-nitro-honokiol (**2a**) as an orange oil, yield 98%.

IR (ATR, ν_{max}, cm^{-1}): 3204, 3079, 2978, 1638, 1621, 1536, 1499, 1466, 1323, 1238, 1129, 1042, 912, 674, 551; ^{1}H NMR ($CDCl_3$) δ 10.97 (s, 1H, O*H*), 8.20 (d, J = 2.2 Hz, 1H, H-6'), 7.73 (d, J = 1.5 Hz, 1H, H-2'), 7.13 (d, J ~7, 1H, H-4), 7.12 (s, 1H, H-6), 6.90 (d, J = 8.8 Hz, 1H, H-3), 6.02 (ddt, J ~ 17, 10.3, 6.7 Hz, 1H, H-2'''), 5.98 (ddt, J ~ 17, 9.9, 6.6 Hz, 1H, H-2''), 5.15 (m, 2H, H-3'''), 5.09 (m, 2H, H-3''), 4.03 (q, J = 6.9 Hz, 2H, OCH_2CH$_3$), 3.53 (d, J = 6.6 Hz, 2H, H-1'''), 3.38 (d, J = 6.6 Hz, 2H, H-1''), 1.35 (t, J = 6.9 Hz, 3H, OCH$_2$CH_3); ^{13}C NMR ($CDCl_3$) δ 154.1 (C-2), 152.2 (C-4'), 139.3 (C-2'), 137.5 (C-2''), 135.3 (C-2'''), 133.3 (C-5'), 132.5 (C-5), 130.4, 2 x 130.3 (C-6, C-1', C-3'), 129.2 (C-4), 127.7 (C-1), 123.3 (C-6'), 116.8 (C-3'''), 115.8 (C-3''), 112.5 (C-3), 64.1 (O*C*H$_2$CH$_3$), 39.3 (C-1''), 33.7 (C-1'''), 14.8 (OCH$_2$*C*H$_3$); MS (ESI) m/z (%): 340.24 ($[M+H]^+$, 100).

4.2.4. Synthesis of 5'-amino-2-*O*-ethylhonokiol (2)

$SnCl_2$ x 2H2O (426 mg, 1.89 mmol) was added to a solution of 2-*O*-ethyl-5'-nitro-honokiol (**2a**) (71 mg, 0.21 mmol) in EtOH (10 mL). After stirring for 72 h at room temperature $NaHCO_3$ (1 N, 30 mL) was added. The foamy precipitate was filtered off with Celite and rinsed with EtOH (5 x 10 mL). The solutions were concentrated under reduced pressure and the resulting aqueous solution was extracted with dichloromethane (3 x 10 mL). The organic

layer was concentrated to final volume 15 mL, washed with brine, dried over Na_2SO_4, concentrated under reduced pressure and purified by PTLC (silica, cyclohexane / ethyl acetate 5:3) to yield **2** (22 mg, 34%) as a brown oil yield **2**: IR (ATR, ν_{max}, cm^{-1}): 3374, 3313, 3075, 2976, 2922, 1638, 1607, 1489, 1437, 1472; 1410, 1392, 1236, 1142, 993, 909, 805, 732; ^1H NMR ($CDCl_3$) δ 7.13 (s, 1H, H-6), 7.06 (d, J = 8.3 Hz, 1H, H-4), 6.91 (s, 1H, H-6'), 6.88 (d, J = 8.3 Hz, 1H, H-3), 6.82 (s, 1H, H-2'), 6.06 (ddt, J = 16.9, 10.2, 5.9 Hz, 1H, H-2'"), 5.99 (ddt, J = 16.8, 9.9, 6.6 Hz, 1H, H-2"), 5.26 (d, J = 17.2 Hz, 1H, H-3'"), 5.20 (d, J = 10.1 Hz, 1H, H-3'"), 5.09 (d, J = 17.0 Hz, 1H, H-3"), 5.08 (d, J = 10.4 Hz, 1H, H-3"), 4.00 (q, J = 6.8 Hz, 2H, OC*H*$_2$), 3.44 (d, J = 5.9 Hz, 2H, H-1'"), 3.36 (d, J = 6.6 Hz, 2H, H-1"), 1.34 (t, J = 6.8 Hz, 3H, OCH_3C*H*$_3$); ^{13}C NMR ($CDCl_3$) δ 154.2 (C-2), 142.3 (C-4), 137.8 (C-2"), 136.7 (C-2'"), 132.3 (C-5), 131.4 (C-1'), 130.9 (C-6), 130.8 (C-1), 127.8 (C-4), 125.2 (C-3'), 122.1 (C-2'), 117.0 (C-6'), 116.4 (C-3'"), 115.4 (C-3"), 111.3 (C-3), 55.6 (O*C*H_3), 39.3 (C-1"), 35.6 (C-1'"); MS (ESI) m/z (%): 310.14 $[M+H]^+$ (100).

4.3. Pharmacological experiments

4.3.1. Expression of $GABA_A$ receptors in *Xenopus laevis* oocytes and two-microelectrode voltage-clamp experiments

Preparation of stage V–VI oocytes from *Xenopus laevis* and synthesis of capped runoff poly(A) cRNA transcripts from linearized cDNA templates (pCMV vector) was performed as previously described (Khom et al., 2006). Female *Xenopus laevis* frogs (NASCO, USA) were anesthetized by 15 min incubation in a 0.2% MS-222 (methane sulfonate salt of 3-aminobenzoic acid ethyl ester; Sigma Aldrich, Vienna, Austria) solution before removal of parts of the ovaries. Follicle membranes from isolated oocytes were enzymatically digested with 2 mg/mL collagenase (Type 1A, Sigma-Aldrich, Vienna, Austria).

Selected oocytes were injected with 10–50 nL of DEPC-treated water (diethyl pyrocarbonate, Sigma, Vienna, Austria) containing the different $GABA_A$ cRNAs at a concentration of approximately 300–3000 pg/nL/subunit. To ensure expression of the γ_{2S} subunit in the case of $\alpha_1\beta_2\gamma_{2S}$ receptors, cRNAs were mixed in a ratio of 1:1:10. The amount of cRNAs was determined by means of a NanoDrop ND-1000 (Kisker-Biotech, Steinfurt, Germany).

Oocytes were stored at +18°C in modified ND96 solution (90 mM NaCl, 1mM $CaCl_2$, 1 mM KCl, 1 mM $MgCl_2$ x $6H_2O$, and 5 mM HEPES (4-(2-hydroxyethyl)-1-piperazineethane-sulfonic acid); pH 7.4, all from Sigma-Aldrich, Vienna, Austria).

Chloride currents through $GABA_A$ receptors (I_{GABA}) were measured at room temperature (+21±1°C) by means of the two-microelectrode voltage clamp technique making use of a TURBO TEC-05X amplifier (npi electronic, Tamm, Germany). I_{GABA} were elicited at a holding potential of –70 mV. Data acquisition was carried out by means of an Axon Digidata 1322A interface using pCLAMP v.10 (Molecular Devices, Sunnyvale, CA, USA). The modified ND96 solution was used as bath solution. Microelectrodes were filled with 2 M KCl and had resistances between 1 and 3 MΩ.

4.3.2. Perfusion System

GABA and the studied derivatives were applied by means of the ScreeningTool (npi electronic, Tamm, Germany) perfusion system as described previously (Baburin et al., 2006, Khom et al. 2006). To elicit I_{GABA}, the chamber was perfused with 120 µL of GABA- or compound-containing solutions, respectively, at a volume rate of 300 µL/s (Khom et al., 2013). Care was taken to account for possible slow recovery from increasing levels of desensitization in the presence of high drug concentrations. The duration of washout periods was therefore extended from 1.5 min (<10 µM compounds) to 30 min (≥10 µM compounds), respectively. Oocytes with maximal current amplitudes >3 µA were discarded to exclude voltage clamp errors.

4.3.3. Data Analysis

Stimulation of chloride currents by modulators of the $GABA_A$ receptor was measured at a GABA concentration eliciting between 3% and 7% of the maximal current amplitude ($EC_{3–7}$). The GABA $EC_{3–7}$ was determined for each oocyte individually. Enhancement of the chloride current was defined as $I_{(GABA+compound)}/I_{GABA\text{-}max}*100\%$, where $I_{(GABA+compound)}$ is the current response in the presence of a given compound and $I_{GABA\text{-}max}$ is the current response induced by 1 mM GABA. Concentration–response curves were generated and the data were fitted by nonlinear regression analysis using Origin Software (OriginLab Corporation, USA). Data were fitted to the equation $1/(1 + (EC_{50}/[compound])^{nH})$, where n_H is the Hill coefficient. Each data point represents the mean±SE from at least 3 oocytes and ≥ 2 oocyte batches. Statistical significance was calculated using paired Student *t*-test with a confidence interval of <0.05.

Acknowledgements

Parts of this work were supported by the Austrian Science Fund (FWF) under project P21241. The authors wish to express their gratitude to R. Bauer (Graz) for allowing access to analytical HPLC equipment as well as to the ESI-MS facility.

Supplementary data

Supplementary data associated with this article can be found in the online version.

References

Ahn, K. W.; Sethi, G.; Shishodia, S.; Sung, B.; Arbiser, J. L.; Aggarwal, B. B. *Mol. Cancer Res.* **2006**, *4*, 621.

Ai, J., Wang, X.; Nielsen, M. *Pharmacology* **2001**, *63*, 34.

Alexeev M.; Grosenbaugh, D. K.; Mott, D. D.; Fisher, J. L. *Neuropharmacology* **2012**, *62*, 2507.

Baur, R.; Schuehly, W.; Sige, E. *Biochim Biophys Acta* **2014**, *1840*,, 3017.

Bernaskova, M.; Kretschmer, N., Schuehly, W.; Huefner, A., Weis, R., Bauer, R. *Molecules* **2014**, *19*, 1223.

Baburin, I.; Beyl, S.; Hering, S. *Pflugers Arch. – Eur. J. Physiol*. **2006**, 453, 117.

Hevers, W.; Luddens, H. *Mol. Neurobiol*. **1998**, *18*, 35.

Johnson, T. W.; Corey, E. J. *J. Am. Chem. Soc*. **2001**, *123*, 4475.

Khom, S.; Baburin, I.; Timin, E. N.; Hohaus, A.; Sieghart, W.; Hering, S. *Mol. Pharm.* **2006**, *69*, 640.

Khom, S.; Strommer, B.; Ramharter, J.; Schwarz, T.; Schwarzer, C.; Erker, T.; Ecker, G. F.; Mulzer, J.; Hering, S. *Br J Pharmacol*. **2010**, *161*, 65.

Khom, S.; Strommer, B.; Schöffmann, A.; Hintersteiner, J.; Baburin, I.; Erker, T.; Schwarz, T.; Schwarzer, C.; Zaugg, J.; Hamburger, M.; Hering, S. *Biochem. Pharm.* **2013**, 85, 1827.

Macdonald, R. L.; Olsen, R.W. $GABA_A$ receptor channels. *Annu. Rev. Neurosci*. **1994**, *17*, 569.

Maruyama, Y.; Kuribara, H. *CNS Drug Rev.* **2000**, *6*, 35.

Rudolph, U.; Crestani, F.; Mohler, H. *Trends Pharmacol. Sci*. **2001**, *22*, 188.

Schuehly, W.; Viveros Paredes, J. M.; Kleyer, J.; Huefner, A.; Raduner, S.; Altmann, K.-H.; Gertsch, J. *Chem. Biol*. **2011**, *18*, 1053.

Sieghart, W.; Sperk, G. *Curr. Top. Med. Chem*. **2002**, *2*, 795.

Sieghart, W.; Ernst, M. *Curr. Med. Chem.* **2005**, *5*, 217.

Sieghart W. *Adv. Pharmacol*. **2015**, 72, 53.

Taferner, B.; Schuehly, W.; Huefner, A.; Baburin, I.; Wiesner K.; Ecker, G. F.; Hering S. *J. Med. Chem.* **2011**, *54*, 5349.

Wafford, K. A.; Bain, C. J.; Whiting, P. J.; Kemp, J. A. *Mol. Pharmacol*. **1993**, *44*, 437.

Widdowson, K. L.; Elliott, J. D.; Veber, D. F.; Nie, H.; Rutledge, M. C.; McCleland, B. W.; Xiang, J-N.; Jurewicz, A. J.; Hertzberg, R. P.; Foley, J. J.; Griswold, D. E.; Martin, G. L.; Lee, J. M.; White, J. R.; Sarau, H. M. *J. Med. Chem*. **2004**, *47*, 1319.

Wieland, H. A.; Luddens, H.; Seeburg, P. H. *J. Biol. Chem*. **1992**, *267*, 1426.

5 Summary and Conclusions

In the course of this thesis, novel $GABA_A$ receptor modulators from plant origin belonging to different classes of secondary metabolites – alkaloids, stilbenoids, abietan diterpenes and (neo)lignans – have been identified (**Figure 20**) and need to be pursued further: **piperine derivatives 24** and **6**; the dihydrostilbenoid **batatasin III** derived from the orchid species *Pholidota chinensis*; **dehydroabietic acid** derived from *Olibanum*; and **nitrogenated honokiol derivatives**.

In 2010, piperine (**Figure 14**) was identified as allosteric modulator of $GABA_A$ receptor modulator[253]. Black pepper (*Piper nigrum*, *Piperaceae*) or its pungent alkaloid piperine, respectively, is an integral part of various traditional folk medicines, such as TCM and African folk medicines, and was demonstrated to hold a plethora of physiological effects. The spectrum of these effects ranges from protection against oxidative damage, cytoprotective, anti-tumor, anti-inflammatory and anti-diarrhoral effects, to the rather unfavourable inhibition of phase-I and –II hepatic metabolism via interference with the cytochrome P450 system[254].

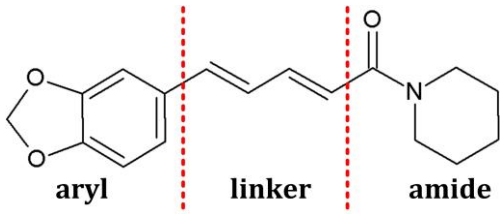

Figure 14 *Strucutral key features of the piperine molecule.*

Aiming at the development of more efficacious, more potent and subunit selective compounds, the piperine molecule was subjected to a spectrum of

structural modifications (T. Schwarz[1], L. Wimmer[2]). It could be shown that the substitution of the amide function with linear (**23**, **25**) or arborised (**24**) carbon chains (**Figure 15**) *(i)* significantly enhanced efficacy and potency of the molecules; *(ii)* diminished interaction with TRPV1 channels; *(ii)* led to a more pronounced receptor subunit specificity compared to piperine *(iv)* and induced γ_2 subunit dependence. Interference with piperine's second structural moiety, the linker, however, did not influence efficacy and potency as expected: installing partially saturated linkers or increasing the structural flexibility by extending linker length decreased the derivatives' modulatory capacity. The investigation of a comprehensive library of amide- and linker-modified piperine derivatives led to the identification of both, favourable and unfavourable substituents or structural changes, in terms of $GABA_A$ receptor modulatory activity (**Chapter 4.1.1.** and **Chapter 4.1.2**)[250,251].

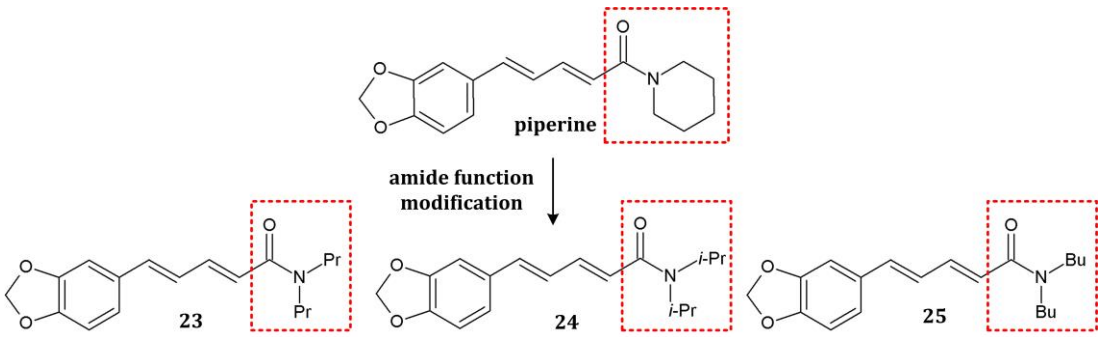

Figure 15 *Piperine analogues modulating GABAA receptor with the highest efficacy show a tertiary amide nitrogen, substituted with flexible alkyl chains with a total of 6–8 carbon atoms.*

Piperine, and therefore potentially also its analogues, is a known agonist of TRPV1; a characteristic which – for reasons such as piperine's potential to induce pain or deteriorations in thermoregulation[195] – states a problem in the course of drug development. An in-depth study of the effect of **24** on TRPV1 channels (**Chapter 4.1.4.**) showed that this derivative inhibited capsaicin-induced cationic currents through TRPV1 (maximum 95% reduction of current

[1] Division of Drug Design and Medicinal Chemistry, Department of Pharmaceutical Chemistry, University of Vienna, Althanstrasse 14, A-1090 Vienna, Austria; current affiliation: Institute of Medical Genetics Medical University of Vienna, Waehringerstrasse 10, 1090 Vienna, Austria

[2] Institute of Applied Synthetic Chemistry, Vienna University of Technology, Getreidemarkt 9, A-1060 Vienna, Austria

amplitude at a concentration of 300 µM). **24** may thus constitute a first promising scaffold for the further development of piperine analogues that efficaciously modulate I_{GABA} while antagonising capsaicin-induced effects on TRPV1 channels.

In vivo studies on compounds **23**, **24** and **25** conducted in mice within our department (J. Hintersteiner, S. Khom; **Chapter 4.1.1.** and **Chapter 4.1.2**)[250,251] showed anxiolytic-like effects with little sedation, and anticonvulsant activity for **24**. Sedative effects observed for **23**, **24** and **25** may reflect sedation resulting from the more pronounced enhancement of I_{GABA}, and may also include the analogues' altered α subunit preferences as distinguished from piperine. In contrast to piperine, TRPV1 channels most likely are not involved in the derivatives' sedative effects. The anticonvulsant effects observed for **24** may be related to enhancement of I_{GABA} modulation, and – since the derivative inhibits TRPV1 channels[255] – most likely involve further receptors. **24** constitutes a promising candidate for further development toward positive $GABA_A$ receptor modulators, additionally inhibiting capsaicin induced cationic currents through TRPV1 channels. The comparably easily synthesizable derivative may serve as model compound for a profound analysis of the underlying mechanism of TRPV1 inhibition and its structure-activity relationship (SAR), as well as such inhibition's effects *in vivo*.

The breakdown of the third structural feature, the *1,3*-benzodioxol (aryl) moiety, in combination with non-natural dibutylamide function led to compounds with a high efficacy (e.g. compound **6**) and selectivity for either the $GABA_A$ or the TRPV1 receptors[252] (**Figure 16; Chapter 4.1.3.1**). A preliminary study on β subunit selective I_{GABA} modulation on six aryl-modified compounds (**4**, **6**, **6a**, **15**, **16** and **17**) revealed that modifications introduced to the parent compound supported a preference for $\beta_{2/3}$ containing receptors (**Chapter 4.1.3.2**). Further investigation of the hypothesis if these *in vitro* observed effects can be confirmed *in vivo* is deemed necessary. None of the aryl-modified derivatives activated TRPV1 channels proposing that substitution of the structure's piperidine ring increased the selectivity for $GABA_A$ receptors over

TRPV1 channels. These results suggest either a strong positive influence of the breakdown of the aryl moiety, the installation of electronegative substituents and facilitated receptor binding due to reduced bulkiness of the molecule, or alleviated fitting in the binding pocket due to higher flexibility of the modified rest.

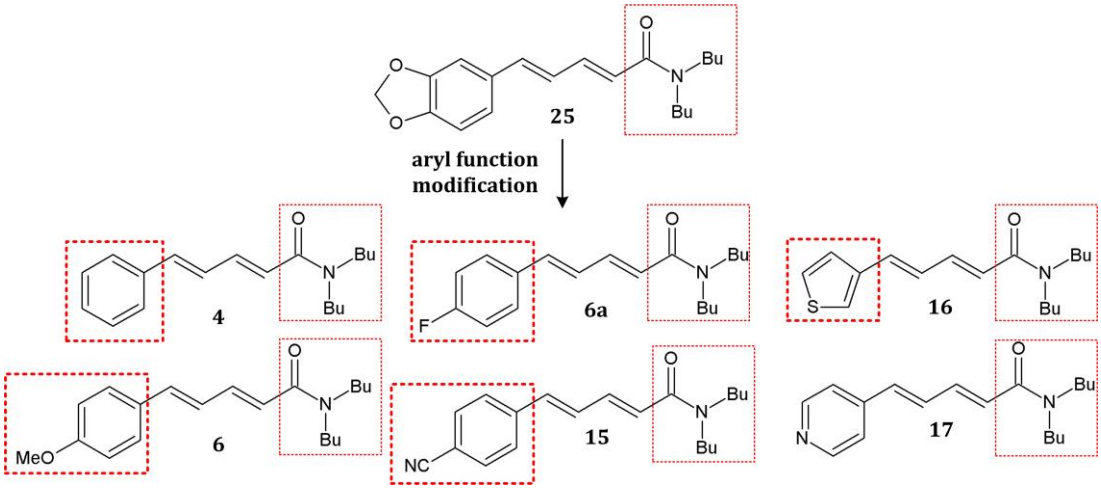

Figure 16 *Combining the non-natural dibutylamide function (**25**) with aryl-modifications led to compounds (**4**, **6**, **6a**, **15**, **16**, **17**) that highly efficaciously modulated I_{GABA} in a $\beta_{2/3}$ subtype selective manner, but did not activate TRPV1 channels.*

In search for novel $GABA_A$ receptor ligands derived from plant sources, extracts of *Pholidota chinensis* and of the resin of *Boswellia thurifera* were investigated in close collaboration with the University of Basel (D. Rueda[3]; **Chapter 4.2.1.**)[256].

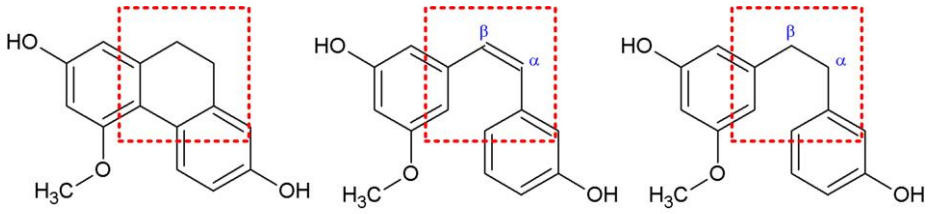

Figure 17 *Influence of conformational flexibility on the modulatory capacity of stilbenoids: dihydrophenanthrene ring (**1**), saturated bibenzyl (**2**), and double bond in $\Delta^{\beta,\alpha}$ (**3**).*

[3] Division of Pharmaceutical Biology, University of Basel, Klingelbergstrasse 50, CH-4056 Basel, Switzerland

In the active fractions of a dichloromethane extract of stems and roots of *Pholidota chinensis* (*shi xian tao*, *Orchidaceae*), a plant being used in TCM[7] and for treatment of various health conditions[257,258], batatasin III (**2**), together with the structurally related stilbenoids coelonin (**1**) and pholidotol D (**3**) (**Figure 17**), could be identified. While the saturated bibenzyl **2** displayed efficacious and potent I_{GABA} modulation, introduction of a double bond in $\Delta^{\beta,\alpha}$ (**3**) or introduction of a dihydrophenanthrene ring (**1**) – thereby conferring additional rigidity to this structure – drastically decreased potency and efficacy.
Studies on potential subunit specificity characterised **2** as positive allosteric modulator of $\alpha_1\beta_2\gamma_{2S}$ $GABA_A$ receptors, devoid of significant subtype specificity or the potential for direct activation of the receptors. Dihydrostilbenes such as **2** could be identified as new, currently unknown $GABA_A$ receptor modulators and may be an interesting starting point for the development of new $GABA_A$ receptor modulators.

In a petroleum-ether extract of the resin of *Boswellia thurifera*, the abietan terpenoid dehydroabietic acid (**1, Figure 18**Fehler! Verweisquelle konnte nicht gefunden werden.) could be identified as $GABA_A$ receptor modulator (**Chapter 4.2.2.**)[259]. *Boswellia*, better known as frankincence or *Olibanum*, contains a complex mixture of polysaccharides, monoterpenes, sesquiterpenes, diterpenes (incensole, isoincensole, oxide and acetate derivatives), and triterpenoids (e.g. boswellic acid)[260,261] and is an integral part of various religious and cultural ceremonies, and TCM.

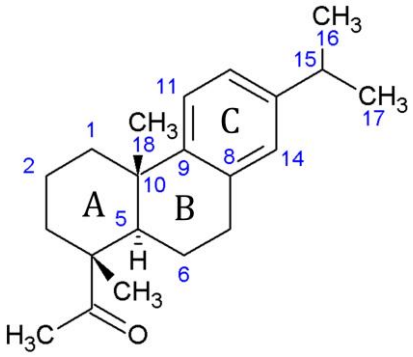

Figure 18 Chemical structure of dehydroabietic acid.

Dehydroabietc acid displayed direct activation of the receptor at concentrations >30 μM, suggesting a mechanism of action involving allosteric receptor modulation and possibly partial agonistic activity. It showed higher potency on $\alpha_1\beta_2\gamma_{2S}$ $GABA_A$ receptors when compared to the closely related group of pimarane diterpenes (e.g. sandaracopimaric acid)[262], and suggested an aromatic ring C being favourable for this scaffold's increase in potency. Keeping in mind that toxicity in fish has been observed for **1**[263,264], the potential of this scaffold as a starting point for medicinal chemistry should be elucidated in future studies.

Based on previous study[265], seven novel nitrogen-containing honokiol derivatives (**1** – **7**) were synthesised (M. Bernaskova[4]), out of which six derivatives displayed a more pronounced and potent I_{GABA} enhancement compared to honokiol (**Figure 19**). Nitrogenation of the aromatic ring and substitution of the molecule's free hydroxyl groups were identified as pharmacophore features favourable for potent and efficacious $GABA_A$ receptor modulation (**Chapter 4.2.3.**).

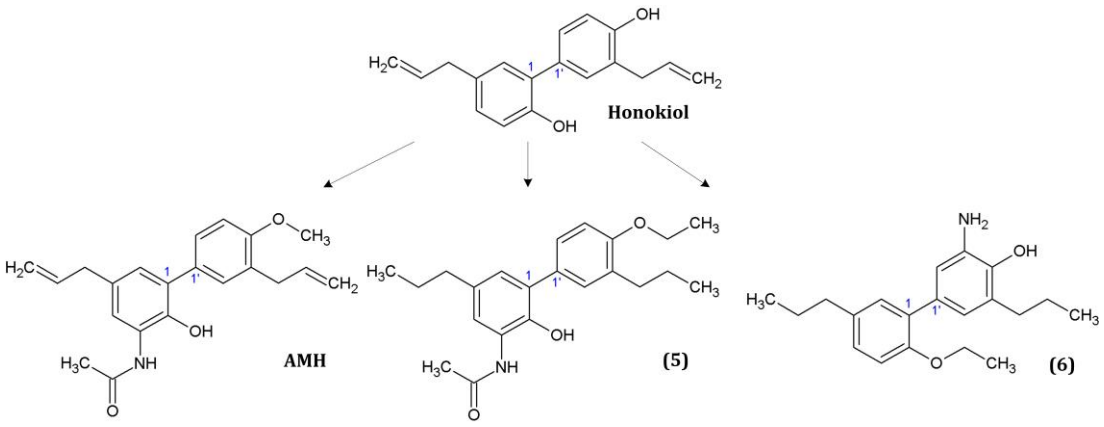

Figure 19 *The nitrogenated structural motif showed favourable influence on efficacy and potency toward $\alpha_1\beta_2\gamma_{2S}$ $GABA_A$ receptors, with most efficacious I_{GABA} enhancement by **AMH**[265], **5** and **6**.*

Four derivatives (**1**, **3**, **5**, and **7**) activated I_{GABA} receptors in the absence of GABA. These data confirm and extend a finding by Alexeev *et al.*[266]: though in

[4] Institute of Pharmaceutical Sciences, Pharmaceutical Chemistry, University of Graz, Schubertstrasse 1, 8010 Graz, Austria

another system, partial agonist activity has been previously reported for honokiol and magnolol[266]. Remarkably, small structural changes completely diminish partial agonism while preserving positive allosteric modulation of $GABA_A$ receptors (**2**, **4**, and **6**). These data suggest that the partial agonistic activity of honokiol and the studied nitrogenated derivatives does not correlate with allosteric modulation. Further research is warranted to study whether the agonistic and modulatory effects of these compounds are mediated via separate binding sites.

Table 2 *Physico-chemical properties, efficacy and potency ($\alpha_1\beta_2\gamma_{2S}$ $GABA_A$ receptors) for* ***piperine derivatives 24 and 6***, ***DHA***, ***batatasin III*** *(Bat. III) and* ***honokiol derivative 5****. Physico-chemical properties calculated with* molinspiration *(molinspiration.com).*

Comp.	H acceptors	H donors	MW (g/mol)	cLogP	Nº of rotable bonds	Polar surface area	Efficacy* (%)	Potency* (μM)
	Lipinski's Rule of Five criteria						* $\alpha_1\beta_2\gamma_{2S}$ $GABA_A$ r.	
24	4	0	301.4	3.8	5	38.8	359±4	21.5±1.7
6	3	0	315.5	5.5	10	29.5	1363±57	7.5±1.0
DHA	1	0	298.5	6.0	2	17.1	682±45	8.7±1.3
Bat. III	3	2	244.3	2.9	4	49.7	1513±177	52.5±17.0
5	4	2	355.5	5.6	8	58.6	1975±218	2.1±1.2

The structural modifications introduced to the natural compounds piperine and honokiol led to the successful development of more efficacious, more potent and more selective $GABA_A$ receptor ligands. The systematic study of a comprehensive set of modifications of piperine, interfering with all three structural key features of this compound – amide function, linker and aromatic core – allowed first insights into the derivatives' SAR in terms of $GABA_A$ receptor modulation. Also, derivatisation led to inhibition of TRPV1 channels in one case and thus prevention of the heat and pain inducing effects of the natural parent compound piperine[195], which renders such molecule very interesting as scaffold for novel $GABA_A$ receptor modulator. The introduced structural modifications to honokiol, i.e. nitrogenation of the aromatic ring, and substitution of the free hydroxy groups, could successfully be shown to enhance $GABA_A$ receptor modulation compared to the parent compound, while some

derivatives even displayed partial agonist effects. These interesting properties form a sound basis for an in-depth exploration of honokiol derivatives' SAR and the identification of their $GABA_A$ receptor binding site. Lastly, new $GABA_A$ receptor modulators from plant sources could be successfully identified from the two studied extracts of *Pholidota chinensis* and *Boswellia thurifera*. Such findings clearly reinforce the great potential of plants being used in traditional folk medicines such as TCM as source for the discovery of novel scaffolds for ($GABA_A$ receptor) drug development.

In fulfilment of the general requirements for a hit substance, defined as *(i)* relevant efficacy and potency at the target and drug-likeliness as defined by *Lipinski's Rule of Five*[267] (**Table 2**; fully met by piperine derivative **24** and natural product **batatasin III**); *(ii)* novelty of the scaffold; *(iii)* potential for blood-brain-barrier penetration[268]; and *(iv)* the possibility of resupply either from the original (plant) source or by means of synthetic chemistry – these compounds, subject to continued research, constitute potential scaffolds for the development of novel $GABA_A$ receptor modulators for the treatment of anxiety disorders, epilepsy and other disease states.

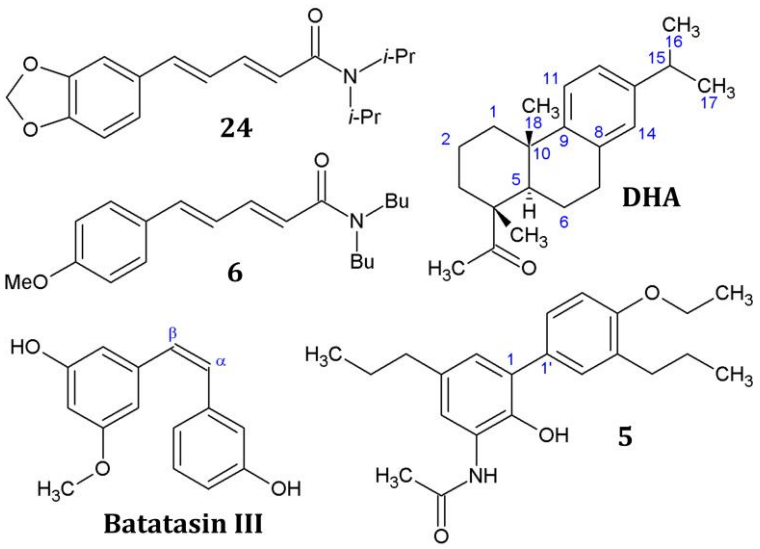

Figure 20 *Five prominent structures were identified:* ***Piperine derivatives 24*** *and* ***6,*** *dehydroabietic acid* ***(DHA), batatasin III, honokiol derivative 5****.*

6 References

Copyright Statement

I strived for identifying all copyright owners and for obtaining their permission, if applicable, for reuse of their content in this thesis. In case any copyright infringement should become acquainted despite my efforts, please notify immediately.

(1) Jones-Davis, D. M.; Macdonald, R. L. Gaba(a) Receptor Function and Pharmacology in Epilepsy and Status Epilepticus. *Curr Opin Pharmacol* **2003**, *3*, 12-18.

(2) Clapham, D. E.; Runnels, L. W.; Strubing, C. The Trp Ion Channel Family. *Nature reviews. Neuroscience* **2001**, *2*, 387-396.

(3) Simon, J.; Wakimoto, H.; Fujita, N.; Lalande, M.; Barnard, E. A. Analysis of the Set of Gaba(a) Receptor Genes in the Human Genome. *The Journal of biological chemistry* **2004**, *279*, 41422-41435.

(4) Johnston, G. A. Gabaa Receptor Pharmacology. *Pharmacology & therapeutics* **1996**, *69*, 173-198.

(5) Bateson, A. N. The Benzodiazepine Site of the Gabaa Receptor: An Old Target with New Potential? *Sleep Med* **2004**, *5 Suppl 1*, S9-15.

(6) Mohler, H. Gaba(a) Receptor Diversity and Pharmacology. *Cell and tissue research* **2006**, *326*, 505-516.

(7) Pérez Gutiérrez, R. M. Orchids: A Review of Uses in Traditional Medicine, Its Phytochemistry and Pharmacology. *J Med Plants Res* **2010**, *4*, 592-638.

(8) Lukas, R. J.; Bencherif, M. Recent Developments in Nicotinic Acetylcholine Receptor Biology. In: Arias, Hr., Editor. Biological and Biophysical Aspects of Ligand-Gated Ion Channel Receptor Superfamilies. . *Research Signpost; Kerala, India:* **2006**, 2-33.

(9) Breitinger, H. G.; Becker, C. M. The Inhibitory Glycine Receptor-Simple Views of a Complicated Channel. *Chembiochem* **2002**, *3*, 1042-1052.

(10) Corringer, P. J.; Le Novere, N.; Changeux, J. P. Nicotinic Receptors at the Amino Acid Level. *Annu Rev Pharmacol Toxicol* **2000**, *40*, 431-458.

(11) Davies, P. A.; Pistis, M.; Hanna, M. C.; Peters, J. A.; Lambert, J. J.; Hales, T. G.; Kirkness, E. F. The 5-Ht3b Subunit Is a Major Determinant of Serotonin-Receptor Function. *Nature* **1999**, *397*, 359-363.

(12) Thompson, A. J.; Lummis, S. C. 5-Ht3 Receptors. *Curr Pharm Des* **2006**, *12*, 3615-3630.

(13) Davies, P. A.; Wang, W.; Hales, T. G.; Kirkness, E. F. A Novel Class of Ligand-Gated Ion Channel Is Activated by Zn2+. *The Journal of biological chemistry* **2003**, *278*, 712-717.

(14) Chen, P. E.; Wyllie, D. J. Pharmacological Insights Obtained from Structure-Function Studies of Ionotropic Glutamate Receptors. *British journal of pharmacology* **2006**, *147*, 839-853.

(15) Khakh, B. S.; Burnstock, G.; Kennedy, C.; King, B. F.; North, R. A.; Seguela, P.; Voigt, M.; Humphrey, P. P. International Union of Pharmacology. Xxiv. Current Status

of the Nomenclature and Properties of P2x Receptors and Their Subunits. *Pharmacological reviews* **2001**, *53*, 107-118.

(16) Khakh, B. S.; North, R. A. P2x Receptors as Cell-Surface Atp Sensors in Health and Disease. *Nature* **2006**, *442*, 527-532.

(17) Sine, S. M.; Engel, A. G. Recent Advances in Cys-Loop Receptor Structure and Function. *Nature* **2006**, *440*, 448-455.

(18) Bali, M.; Akabas, M. H. Defining the Propofol Binding Site Location on the Gabaa Receptor. *Molecular pharmacology* **2004**, *65*, 68-76.

(19) Hosie, A. M.; Wilkins, M. E.; da Silva, H. M.; Smart, T. G. Endogenous Neurosteroids Regulate Gabaa Receptors through Two Discrete Transmembrane Sites. *Nature* **2006**, *444*, 486-489.

(20) Olsen, R.; Sawyer, G. Gabaa Receptor. *Encyclopedia of Biological Chemistry. Vol. 2. Elsevier; New York:* **2004**, 162-166.

(21) Sigel, E.; Buhr, A. The Benzodiazepine Binding Site of Gabaa Receptors. *Trends in pharmacological sciences* **1997**, *18*, 425-429.

(22) Martin, D. L.; Olsen, R. W. Gaba in the Nervous System. The View at Fifty Years. *Lippincott Williams and Wilkins Publishers, Philadelphia, PA, USA* **2000**, 65-80.

(23) Ben-Ari, Y. Excitatory Actions of Gaba During Development: The Nature of the Nurture. *Nature reviews. Neuroscience* **2002**, *3*, 728-739.

(24) Kaila, K.; Lamsa, K.; Smirnov, S.; Taira, T.; Voipio, J. Long-Lasting Gaba-Mediated Depolarization Evoked by High-Frequency Stimulation in Pyramidal Neurons of Rat Hippocampal Slice Is Attributable to a Network-Driven, Bicarbonate-Dependent K+ Transient. *The Journal of neuroscience : the official journal of the Society for Neuroscience* **1997**, *17*, 7662-7672.

(25) Borboni, P.; Porzio, O.; Fusco, A.; Sesti, G.; Lauro, R.; Marlier, L. N. Molecular and Cellular Characterization of the Gabaa Receptor in the Rat Pancreas. *Molecular and cellular endocrinology* **1994**, *103*, 157-163.

(26) Olsen, R. W.; DeLorey, T. M. Gaba Synthesis, Uptake and Release. *In: Siegel GJ, Agranoff BW, Albers RW, et al., editors. Basic Neurochemistry: Molecular, Cellular and Medical Aspects. 6th edition. Philadelphia: Lippincott-Raven; Available from: http://www.ncbi.nlm.nih.gov/books/NBK27979/* **1999**.

(27) Macdonald, R. L.; Olsen, R. W. Gabaa Receptor Channels. *Annual Review of Neuroscience* **1994**, *17*, 569-602.

(28) Sieghart, W. Structure and Pharmacology of Gamma-Aminobutyric Acida Receptor Subtypes. *Pharmacological reviews* **1995**, *47*, 181-234.

(29) Farrant, M.; Nusser, Z. Variations on an Inhibitory Theme: Phasic and Tonic Activation of Gaba(a) Receptors. *Nature reviews. Neuroscience* **2005**, *6*, 215-229.

(30) Mody, I.; Pearce, R. A. Diversity of Inhibitory Neurotransmission through Gaba(a) Receptors. *Trends Neurosci* **2004**, *27*, 569-575.

(31) Olsen, R. W.; Sieghart, W. International Union of Pharmacology. Lxx. Subtypes of Gamma-Aminobutyric Acid(a) Receptors: Classification on the Basis of Subunit Composition, Pharmacology, and Function. Update. *Pharmacological reviews* **2008**, *60*, 243-260.

(32) Bowery, N. G.; Bettler, B.; Froestl, W.; Gallagher, J. P.; Marshall, F.; Raiteri, M.; Bonner, T. I.; Enna, S. J. International Union of Pharmacology. Xxxiii. Mammalian Gamma-Aminobutyric Acid(B) Receptors: Structure and Function. *Pharmacological reviews* **2002**, *54*, 247-264.

(33) Bettler, B.; Kaupmann, K.; Mosbacher, J.; Gassmann, M. Molecular Structure and Physiological Functions of Gaba(B) Receptors. *Physiological reviews* **2004**, *84*, 835-867.

(34) Sigel, E.; Baur, R.; Kellenberger, S.; Malherbe, P. Point Mutations Affecting Antagonist Affinity and Agonist Dependent Gating of Gabaa Receptor Channels. *EMBO J* **1992**, *11*, 2017-2023.

(35) Amin, J.; Weiss, D. S. Gabaa Receptor Needs Two Homologous Domains of the Beta-Subunit for Activation by Gaba but Not by Pentobarbital. *Nature* **1993**, *366*, 565-569.

(36) Smith, G. B.; Olsen, R. W. Identification of a [3h]Muscimol Photoaffinity Substrate in the Bovine Gamma-Aminobutyric Acida Receptor Alpha Subunit. *The Journal of biological chemistry* **1994**, *269*, 20380-20387.

(37) Westh-Hansen, S. E.; Rasmussen, P. B.; Hastrup, S.; Nabekura, J.; Noguchi, K.; Akaike, N.; Witt, M. R.; Nielsen, M. Decreased Agonist Sensitivity of Human Gaba(a) Receptors by an Amino Acid Variant, Isoleucine to Valine, in the Alpha1 Subunit. *European journal of pharmacology* **1997**, *329*, 253-257.

(38) Ernst, M.; Brauchart, D.; Boresch, S.; Sieghart, W. Comparative Modeling of Gaba(a) Receptors: Limits, Insights, Future Developments. *Neuroscience* **2003**, *119*, 933-943.

(39) Boileau, A. J.; Czajkowski, C. Identification of Transduction Elements for Benzodiazepine Modulation of the Gaba(a) Receptor: Three Residues Are Required for Allosteric Coupling. *The Journal of neuroscience : the official journal of the Society for Neuroscience* **1999**, *19*, 10213-10220.

(40) Smith, G. B.; Olsen, R. W. Functional Domains of Gabaa Receptors. *Trends in pharmacological sciences* **1995**, *16*, 162-168.

(41) Westh-Hansen, S. E.; Witt, M. R.; Dekermendjian, K.; Liljefors, T.; Rasmussen, P. B.; Nielsen, M. Arginine Residue 120 of the Human Gabaa Receptor Alpha 1, Subunit Is Essential for Gaba Binding and Chloride Ion Current Gating. *Neuroreport* **1999**, *10*, 2417-2421.

(42) Wagner, D. A.; Czajkowski, C. Structure and Dynamics of the Gaba Binding Pocket: A Narrowing Cleft That Constricts During Activation. *The Journal of neuroscience : the official journal of the Society for Neuroscience* **2001**, *21*, 67-74.

(43) Bergmann, R.; Kongsbak, K.; Sorensen, P. L.; Sander, T.; Balle, T. A Unified Model of the Gaba(a) Receptor Comprising Agonist and Benzodiazepine Binding Sites. *PloS one* **2013**, *8*, e52323.

(44) Whiting, P.; McKernan, R. M.; Iversen, L. L. Another Mechanism for Creating Diversity in Gamma-Aminobutyrate Type a Receptors: Rna Splicing Directs Expression of Two Forms of Gamma 2 Phosphorylation Site. *Proceedings of the National Academy of Sciences of the United States of America* **1990**, *87*, 9966-9970.

(45) Barnard, E. A.; Skolnick, P.; Olsen, R. W.; Mohler, H.; Sieghart, W.; Biggio, G.; Braestrup, C.; Bateson, A. N.; Langer, S. Z. International Union of Pharmacology. Xv. Subtypes of Gamma-Aminobutyric Acida Receptors: Classification on the Basis of Subunit Structure and Receptor Function. *Pharmacological reviews* **1998**, *50*, 291-313.

(46) Woodward, R. M.; Polenzani, L.; Miledi, R. Effects of Steroids on Gamma-Aminobutyric Acid Receptors Expressed in Xenopus Oocytes by Poly(a)+ Rna from Mammalian Brain and Retina. *Molecular pharmacology* **1992**, *41*, 89-103.

(47) Johnston, G. A. Medicinal Chemistry and Molecular Pharmacology of Gaba(C) Receptors. *Curr Top Med Chem* **2002**, *2*, 903-913.

(48) Fritschy, J. M.; Benke, D.; Mertens, S.; Oertel, W. H.; Bachi, T.; Mohler, H. Five Subtypes of Type a Gamma-Aminobutyric Acid Receptors Identified in Neurons by Double and Triple Immunofluorescence Staining with Subunit-Specific Antibodies. *Proceedings of the National Academy of Sciences of the United States of America* **1992**, *89*, 6726-6730.

(49) Wisden, W.; Laurie, D. J.; Monyer, H.; Seeburg, P. H. The Distribution of 13 Gabaa Receptor Subunit Mrnas in the Rat Brain. I. Telencephalon, Diencephalon, Mesencephalon. *The Journal of neuroscience : the official journal of the Society for Neuroscience* **1992**, *12*, 1040-1062.

(50) Persohn, E.; Malherbe, P.; Richards, J. G. Comparative Molecular Neuroanatomy of Cloned Gabaa Receptor Subunits in the Rat Cns. *J Comp Neurol* **1992**, *326*, 193-216.

(51) Pirker, S.; Schwarzer, C.; Wieselthaler, A.; Sieghart, W.; Sperk, G. Gaba(a) Receptors: Immunocytochemical Distribution of 13 Subunits in the Adult Rat Brain. *Neuroscience* **2000**, *101*, 815-850.

(52) Bohlhalter, S.; Weinmann, O.; Mohler, H.; Fritschy, J. M. Laminar Compartmentalization of Gabaa-Receptor Subtypes in the Spinal Cord: An Immunohistochemical Study. *The Journal of neuroscience : the official journal of the Society for Neuroscience* **1996**, *16*, 283-297.

(53) Nusser, Z.; Roberts, J. D.; Baude, A.; Richards, J. G.; Sieghart, W.; Somogyi, P. Immunocytochemical Localization of the Alpha 1 and Beta 2/3 Subunits of the Gabaa Receptor in Relation to Specific Gabaergic Synapses in the Dentate Gyrus. *Eur J Neurosci* **1995**, *7*, 630-646.

(54) Somogyi, P.; Fritschy, J. M.; Benke, D.; Roberts, J. D.; Sieghart, W. The Gamma 2 Subunit of the Gabaa Receptor Is Concentrated in Synaptic Junctions Containing the Alpha 1 and Beta 2/3 Subunits in Hippocampus, Cerebellum and Globus Pallidus. *Neuropharmacology* **1996**, *35*, 1425-1444.

(55) Sieghart, W.; Sperk, G. Subunit Composition, Distribution and Function of Gaba(a) Receptor Subtypes. *Curr Top Med Chem* **2002**, *2*, 795-816.

(56) Sur, C.; Wafford, K. A.; Reynolds, D. S.; Hadingham, K. L.; Bromidge, F.; Macaulay, A.; Collinson, N.; O'Meara, G.; Howell, O.; Newman, R.; Myers, J.; Atack, J. R.; Dawson, G. R.; McKernan, R. M.; Whiting, P. J.; Rosahl, T. W. Loss of the Major Gaba(a) Receptor Subtype in the Brain Is Not Lethal in Mice. *The Journal of neuroscience : the official journal of the Society for Neuroscience* **2001**, *21*, 3409-3418.

(57) Barrera, N. P.; Betts, J.; You, H.; Henderson, R. M.; Martin, I. L.; Dunn, S. M.; Edwardson, J. M. Atomic Force Microscopy Reveals the Stoichiometry and Subunit Arrangement of the Alpha4beta3delta Gaba(a) Receptor. *Molecular pharmacology* **2008**, *73*, 960-967.

(58) Nusser, Z.; Sieghart, W.; Somogyi, P. Segregation of Different Gabaa Receptors to Synaptic and Extrasynaptic Membranes of Cerebellar Granule Cells. *The Journal of neuroscience : the official journal of the Society for Neuroscience* **1998**, *18*, 1693-1703.

(59) Peng, Z.; Hauer, B.; Mihalek, R. M.; Homanics, G. E.; Sieghart, W.; Olsen, R. W.; Houser, C. R. Gaba(a) Receptor Changes in Delta Subunit-Deficient Mice: Altered Expression of Alpha4 and Gamma2 Subunits in the Forebrain. *J Comp Neurol* **2002**, *446*, 179-197.

(60) Wei, W.; Zhang, N.; Peng, Z.; Houser, C. R.; Mody, I. Perisynaptic Localization of Delta Subunit-Containing Gaba(a) Receptors and Their Activation by Gaba Spillover in the Mouse Dentate Gyrus. *The Journal of neuroscience : the official journal of the Society for Neuroscience* **2003**, *23*, 10650-10661.

(61) Korpi, E. R.; Grunder, G.; Luddens, H. Drug Interactions at Gaba(a) Receptors. *Prog Neurobiol* **2002**, *67*, 113-159.

(62) Pritchett, D. B.; Sontheimer, H.; Shivers, B. D.; Ymer, S.; Kettenmann, H.; Schofield, P. R.; Seeburg, P. H. Importance of a Novel Gabaa Receptor Subunit for Benzodiazepine Pharmacology. *Nature* **1989**, *338*, 582-585.

(63) Sieghart, W. Multiplicity of Gabaa--Benzodiazepine Receptors. *Trends in pharmacological sciences* **1989**, *10*, 407-411.

(64) Olsen, R. W.; Gordey, M. Gabaa Receptor Chloride Ion Channels. In: Endo, M.; Kurachi, Y.; Mishina, M., Editors. Handbook of Experimental Pharmacology, Vol 147, Pharmacology of Ionic Channel Function: Activators and Inhibitors. Springer Verlag; Heidelberg: . **2000**, 499-517.

(65) Hadingham, K. L.; Wingrove, P. B.; Wafford, K. A.; Bain, C.; Kemp, J. A.; Palmer, K. J.; Wilson, A. W.; Wilcox, A. S.; Sikela, J. M.; Ragan, C. I.; et al. Role of the Beta Subunit in Determining the Pharmacology of Human Gamma-Aminobutyric Acid Type a Receptors. *Molecular pharmacology* **1993**, *44*, 1211-1218.

(66) Hevers, W.; Luddens, H. The Diversity of Gabaa Receptors. Pharmacological and Electrophysiological Properties of Gabaa Channel Subtypes. *Molecular neurobiology* **1998**, *18*, 35-86.

(67) Atack, J. R.; Wafford, K. A.; Tye, S. J.; Cook, S. M.; Sohal, B.; Pike, A.; Sur, C.; Melillo, D.; Bristow, L.; Bromidge, F.; Ragan, I.; Kerby, J.; Street, L.; Carling, R.; Castro, J. L.; Whiting, P.; Dawson, G. R.; McKernan, R. M. Tpa023 [7-(1,1-Dimethylethyl)-6-(2-Ethyl-2h-1,2,4-Triazol-3-Ylmethoxy)-3-(2-Fluorophenyl)-1,2,4-Triazolo[4,3-B]Pyridazine], an Agonist Selective for Alpha2- and Alpha3-Containing Gabaa Receptors, Is a Nonsedating Anxiolytic in Rodents and Primates. *The Journal of pharmacology and experimental therapeutics* **2006**, *316*, 410-422.

(68) Atack, J. R. The Benzodiazepine Binding Site of Gaba(a) Receptors as a Target for the Development of Novel Anxiolytics. *Expert opinion on investigational drugs* **2005**, *14*, 601-618.

(69) Morris, H. V.; Dawson, G. R.; Reynolds, D. S.; Atack, J. R.; Stephens, D. N. Both Alpha2 and Alpha3 Gabaa Receptor Subtypes Mediate the Anxiolytic Properties of Benzodiazepine Site Ligands in the Conditioned Emotional Response Paradigm. *Eur J Neurosci* **2006**, *23*, 2495-2504.

(70) Rudolph, U.; Mohler, H. Analysis of Gabaa Receptor Function and Dissection of the Pharmacology of Benzodiazepines and General Anesthetics through Mouse Genetics. *Annu Rev Pharmacol Toxicol* **2004**, *44*, 475-498.

(71) Whiting, P. J. Gaba-a Receptors: A Viable Target for Novel Anxiolytics? *Curr Opin Pharmacol* **2006**, *6*, 24-29.

(72) Rudolph, U.; Crestani, F.; Benke, D.; Brunig, I.; Benson, J. A.; Fritschy, J. M.; Martin, J. R.; Bluethmann, H.; Mohler, H. Benzodiazepine Actions Mediated by Specific Gamma-Aminobutyric Acid(a) Receptor Subtypes. *Nature* **1999**, *401*, 796-800.

(73) McKernan, R. M.; Rosahl, T. W.; Reynolds, D. S.; Sur, C.; Wafford, K. A.; Atack, J. R.; Farrar, S.; Myers, J.; Cook, G.; Ferris, P.; Garrett, L.; Bristow, L.; Marshall, G.; Macaulay, A.; Brown, N.; Howell, O.; Moore, K. W.; Carling, R. W.; Street, L. J.; Castro, J. L.; Ragan, C. I.; Dawson, G. R.; Whiting, P. J. Sedative but Not Anxiolytic Properties of Benzodiazepines Are Mediated by the Gaba(a) Receptor Alpha1 Subtype. *Nature neuroscience* **2000**, *3*, 587-592.

(74) Low, K.; Crestani, F.; Keist, R.; Benke, D.; Brunig, I.; Benson, J. A.; Fritschy, J. M.; Rulicke, T.; Bluethmann, H.; Mohler, H.; Rudolph, U. Molecular and Neuronal Substrate for the Selective Attenuation of Anxiety. *Science* **2000**, *290*, 131-134.

(75) Dias, R.; Sheppard, W. F.; Fradley, R. L.; Garrett, E. M.; Stanley, J. L.; Tye, S. J.; Goodacre, S.; Lincoln, R. J.; Cook, S. M.; Conley, R.; Hallett, D.; Humphries, A. C.; Thompson, S. A.; Wafford, K. A.; Street, L. J.; Castro, J. L.; Whiting, P. J.; Rosahl, T. W.; Atack, J. R.; McKernan, R. M.; Dawson, G. R.; Reynolds, D. S. Evidence for a Significant Role of Alpha 3-Containing Gabaa Receptors in Mediating the Anxiolytic Effects of Benzodiazepines. *The Journal of neuroscience : the official journal of the Society for Neuroscience* **2005**, *25*, 10682-10688.

(76) Yee, B. K.; Keist, R.; von Boehmer, L.; Studer, R.; Benke, D.; Hagenbuch, N.; Dong, Y.; Malenka, R. C.; Fritschy, J. M.; Bluethmann, H.; Feldon, J.; Mohler, H.; Rudolph, U. A Schizophrenia-Related Sensorimotor Deficit Links Alpha 3-Containing Gabaa Receptors to a Dopamine Hyperfunction. *Proceedings of the National Academy of Sciences of the United States of America* **2005**, *102*, 17154-17159.

(77) Mohler, H. Molecular Regulation of Cognitive Functions and Developmental Plasticity: Impact of Gabaa Receptors. *J Neurochem* **2007**, *102*, 1-12.

(78) Fradley, R. L.; Guscott, M. R.; Bull, S.; Hallett, D. J.; Goodacre, S. C.; Wafford, K. A.; Garrett, E. M.; Newman, R. J.; O'Meara, G. F.; Whiting, P. J.; Rosahl, T. W.; Dawson, G. R.; Reynolds, D. S.; Atack, J. R. Differential Contribution of Gaba(a) Receptor Subtypes to the Anticonvulsant Efficacy of Benzodiazepine Site Ligands. *J Psychopharmacol* **2007**, *21*, 384-391.

(79) Collinson, N.; Cothliff, R.; Rosahl, T. W.; Sur, C.; Kuenzi, F.; Howell, O.; Seabrook, G. R.; Atack, J. R.; McKernan, R. M.; Dawson, G. R. Role of the A5 Subunit of the Gabaa Receptor in Learning and Memory. . *Eur J Neurosci* **2000**, 12(Suppl 11):171.

(80) Dawson, G. R.; Maubach, K. A.; Collinson, N.; Cobain, M.; Everitt, B. J.; MacLeod, A. M.; Choudhury, H. I.; McDonald, L. M.; Pillai, G.; Rycroft, W.; Smith, A. J.; Sternfeld, F.; Tattersall, F. D.; Wafford, K. A.; Reynolds, D. S.; Seabrook, G. R.; Atack, J. R. An Inverse Agonist Selective for Alpha5 Subunit-Containing Gabaa Receptors Enhances Cognition. *The Journal of pharmacology and experimental therapeutics* **2006**, *316*, 1335-1345.

(81) Crestani, F.; Keist, R.; Fritschy, J. M.; Benke, D.; Vogt, K.; Prut, L.; Bluthmann, H.; Mohler, H.; Rudolph, U. Trace Fear Conditioning Involves Hippocampal Alpha5 Gaba(a) Receptors. *Proceedings of the National Academy of Sciences of the United States of America* **2002**, *99*, 8980-8985.

(82) Thompson, S. A.; Whiting, P. J.; Wafford, K. A. Barbiturate Interactions at the Human Gabaa Receptor: Dependence on Receptor Subunit Combination. *British journal of pharmacology* **1996**, *117*, 521-527.

(83) Smith, A. J.; Oxley, B.; Malpas, S.; Pillai, G. V.; Simpson, P. B. Compounds Exhibiting Selective Efficacy for Different Beta Subunits of Human Recombinant Gamma-Aminobutyric Acid a Receptors. *The Journal of pharmacology and experimental therapeutics* **2004**, *311*, 601-609.

(84) Cestari, I. N.; Uchida, I.; Li, L.; Burt, D.; Yang, J. The Agonistic Action of Pentobarbital on Gabaa Beta-Subunit Homomeric Receptors. *Neuroreport* **1996**, *7*, 943-947.

(85) Rudolph, U.; Antkowiak, B. Molecular and Neuronal Substrates for General Anaesthetics. *Nature reviews. Neuroscience* **2004**, *5*, 709-720.

(86) Wingrove, P. B.; Wafford, K. A.; Bain, C.; Whiting, P. J. The Modulatory Action of Loreclezole at the Gamma-Aminobutyric Acid Type a Receptor Is Determined by a Single Amino Acid in the Beta 2 and Beta 3 Subunit. *Proceedings of the National Academy of Sciences of the United States of America* **1994**, *91*, 4569-4573.

(87) Hill-Venning, C.; Belelli, D.; Peters, J. A.; Lambert, J. J. Subunit-Dependent Interaction of the General Anaesthetic Etomidate with the Gamma-Aminobutyric Acid Type a Receptor. *British journal of pharmacology* **1997**, *120*, 749-756.

(88) Reynolds, D. S.; Rosahl, T. W.; Cirone, J.; O'Meara, G. F.; Haythornthwaite, A.; Newman, R. J.; Myers, J.; Sur, C.; Howell, O.; Rutter, A. R.; Atack, J.; Macaulay, A. J.; Hadingham, K. L.; Hutson, P. H.; Belelli, D.; Lambert, J. J.; Dawson, G. R.; McKernan, R.; Whiting, P. J.; Wafford, K. A. Sedation and Anesthesia Mediated by Distinct Gaba(a) Receptor Isoforms. *The Journal of neuroscience : the official journal of the Society for Neuroscience* **2003**, *23*, 8608-8617.

(89) Jurd, R.; Arras, M.; Lambert, S.; Drexler, B.; Siegwart, R.; Crestani, F.; Zaugg, M.; Vogt, K. E.; Ledermann, B.; Antkowiak, B.; Rudolph, U. General Anesthetic Actions in Vivo Strongly Attenuated by a Point Mutation in the Gaba(a) Receptor Beta3 Subunit. *FASEB journal : official publication of the Federation of American Societies for Experimental Biology* **2003**, *17*, 250-252.

(90) Mihic, S. J.; Ye, Q.; Wick, M. J.; Koltchine, V. V.; Krasowski, M. D.; Finn, S. E.; Mascia, M. P.; Valenzuela, C. F.; Hanson, K. K.; Greenblatt, E. P.; Harris, R. A.; Harrison, N. L. Sites of Alcohol and Volatile Anaesthetic Action on Gaba(a) and Glycine Receptors. *Nature* **1997**, *389*, 385-389.

(91) Ernst, M.; Bruckner, S.; Boresch, S.; Sieghart, W. Comparative Models of Gabaa Receptor Extracellular and Transmembrane Domains: Important Insights in Pharmacology and Function. *Molecular pharmacology* **2005**, *68*, 1291-1300.

(92) Khom, S.; Baburin, I.; Timin, E. N.; Hohaus, A.; Sieghart, W.; Hering, S. Pharmacological Properties of Gabaa Receptors Containing Gamma1 Subunits. *Molecular pharmacology* **2006**, *69*, 640-649.

(93) Baur, R.; Simmen, U.; Senn, M.; Sequin, U.; Sigel, E. Novel Plant Substances Acting as Beta Subunit Isoform-Selective Positive Allosteric Modulators of Gabaa Receptors. *Molecular pharmacology* **2005**, *68*, 787-792.

(94) Wallner, M.; Hanchar, H. J.; Olsen, R. W. Ethanol Enhances Alpha 4 Beta 3 Delta and Alpha 6 Beta 3 Delta Gamma-Aminobutyric Acid Type a Receptors at Low Concentrations Known to Affect Humans. *Proceedings of the National Academy of Sciences of the United States of America* **2003**, *100*, 15218-15223.

(95) Kalueff, A.; Nutt, D. J. Role of Gaba in Memory and Anxiety. *Depress Anxiety* **1996**, *4*, 100-110.

(96) Crestani, F.; Lorez, M.; Baer, K.; Essrich, C.; Benke, D.; Laurent, J. P.; Belzung, C.; Fritschy, J. M.; Luscher, B.; Mohler, H. Decreased Gabaa-Receptor Clustering Results in Enhanced Anxiety and a Bias for Threat Cues. *Nature neuroscience* **1999**, *2*, 833-839.

(97) Mohler, H. Pathophysiological Aspects of Diversity in Neuronal Inhibition: A New Benzodiazepine Pharmacology. *Dialogues Clin Neurosci* **2002**, *4*, 261-269.

(98) Nutt, D. J.; Malizia, A. L. New Insights into the Role of the Gaba(a)-Benzodiazepine Receptor in Psychiatric Disorder. *Br J Psychiatry* **2001**, *179*, 390-396.

(99) Olsen, R. W.; DeLorey, T. M.; Gordey, M.; Kang, M. H. Gaba Receptor Function and Epilepsy. *Adv Neurol* **1999**, *79*, 499-510.

(100) Engel, J. Epilepsy: A Comprehensive Textbook. Philadelphia: Lippincott-Raven;. **1998**.

(101) Macdonald, R. L. Antiepileptic Drug Actions. *Epilepsia* **1989**, *30 Suppl 1*, S19-28; discussion S64-18.

(102) Macdonald, R. L.; Greenfield, L. J., Jr. Mechanisms of Action of New Antiepileptic Drugs. *Curr Opin Neurol* **1997**, *10*, 121-128.

(103) Holland, K. D.; McKeon, A. C.; Canney, D. J.; Covey, D. F.; Ferrendelli, J. A. Relative Anticonvulsant Effects of Gabamimetic and Gaba Modulatory Agents. *Epilepsia* **1992**, *33*, 981-986.

(104) Baulac, S.; Huberfeld, G.; Gourfinkel-An, I.; Mitropoulou, G.; Beranger, A.; Prud'homme, J. F.; Baulac, M.; Brice, A.; Bruzzone, R.; LeGuern, E. First Genetic Evidence of Gaba(a) Receptor Dysfunction in Epilepsy: A Mutation in the Gamma2-Subunit Gene. *Nat Genet* **2001**, *28*, 46-48.

(105) Wallace, R. H.; Marini, C.; Petrou, S.; Harkin, L. A.; Bowser, D. N.; Panchal, R. G.; Williams, D. A.; Sutherland, G. R.; Mulley, J. C.; Scheffer, I. E.; Berkovic, S. F. Mutant Gaba(a) Receptor Gamma2-Subunit in Childhood Absence Epilepsy and Febrile Seizures. *Nat Genet* **2001**, *28*, 49-52.

(106) Harkin, L. A.; Bowser, D. N.; Dibbens, L. M.; Singh, R.; Phillips, F.; Wallace, R. H.; Richards, M. C.; Williams, D. A.; Mulley, J. C.; Berkovic, S. F.; Scheffer, I. E.; Petrou, S. Truncation of the Gaba(a)-Receptor Gamma2 Subunit in a Family with Generalized Epilepsy with Febrile Seizures Plus. *Am J Hum Genet* **2002**, *70*, 530-536.

(107) Cossette, P.; Liu, L.; Brisebois, K.; Dong, H.; Lortie, A.; Vanasse, M.; Saint-Hilaire, J. M.; Carmant, L.; Verner, A.; Lu, W. Y.; Wang, Y. T.; Rouleau, G. A. Mutation of Gabra1 in an Autosomal Dominant Form of Juvenile Myoclonic Epilepsy. *Nat Genet* **2002**, *31*, 184-189.

(108) DeLorey, T. M.; Handforth, A.; Anagnostaras, S. G.; Homanics, G. E.; Minassian, B. A.; Asatourian, A.; Fanselow, M. S.; Delgado-Escueta, A.; Ellison, G. D.; Olsen, R. W. Mice Lacking the Beta3 Subunit of the Gabaa Receptor Have the Epilepsy Phenotype and Many of the Behavioral Characteristics of Angelman Syndrome. *The Journal of neuroscience : the official journal of the Society for Neuroscience* **1998**, *18*, 8505-8514.

(109) http://www.who.int/classifications/icd/en/ 2015.

(110) Weinberger, D. R.; Harrison, P. Schizophrenia. 3rd Edition. Blackwell Publishing Ltd., Uk. Isbn 978-1-4051-7697-2; P. 1919. **2011**.

(111) Roberts, E. Prospects for Research on Schizophrenia. An Hypotheses Suggesting That There Is a Defect in the Gaba System in Schizophrenia. *Neurosci Res Program Bull* **1972**, *10*, 468-482.

(112) Lewis, D. A.; Volk, D. W.; Hashimoto, T. Selective Alterations in Prefrontal Cortical Gaba Neurotransmission in Schizophrenia: A Novel Target for the Treatment of Working Memory Dysfunction. *Psychopharmacology (Berl)* **2004**, *174*, 143-150.

(113) Guidotti, A.; Auta, J.; Davis, J. M.; Dong, E.; Grayson, D. R.; Veldic, M.; Zhang, X.; Costa, E. Gabaergic Dysfunction in Schizophrenia: New Treatment Strategies on the Horizon. *Psychopharmacology (Berl)* **2005**, *180*, 191-205.

(114) Hashimoto, T.; Bazmi, H. H.; Mirnics, K.; Wu, Q.; Sampson, A. R.; Lewis, D. A. Conserved Regional Patterns of Gaba-Related Transcript Expression in the Neocortex of Subjects with Schizophrenia. *The American journal of psychiatry* **2008**, *165*, 479-489.

(115) Impagnatiello, F.; Guidotti, A. R.; Pesold, C.; Dwivedi, Y.; Caruncho, H.; Pisu, M. G.; Uzunov, D. P.; Smalheiser, N. R.; Davis, J. M.; Pandey, G. N.; Pappas, G. D.; Tueting, P.; Sharma, R. P.; Costa, E. A Decrease of Reelin Expression as a Putative Vulnerability Factor in Schizophrenia. *Proceedings of the National Academy of Sciences of the United States of America* **1998**, *95*, 15718-15723.

(116) Ishikawa, M.; Mizukami, K.; Iwakiri, M.; Hidaka, S.; Asada, T. Immunohistochemical and Immunoblot Study of Gaba(a) Alpha1 and Beta2/3 Subunits in the Prefrontal Cortex of Subjects with Schizophrenia and Bipolar Disorder. *Neurosci Res* **2004**, *50*, 77-84.

(117) Ongur, D.; Prescot, A. P.; McCarthy, J.; Cohen, B. M.; Renshaw, P. F. Elevated Gamma-Aminobutyric Acid Levels in Chronic Schizophrenia. *Biol Psychiatry* **2010**, *68*, 667-670.

(118) Wilson, S.; Nutt, D. Treatment of Insomnia. *Psychiatry* **2007**, *6*, 301-304.

(119) Morin, C. M.; Benca, R. Chronic Insomnia. *Lancet* **2012**, *379*, 1129-1141.

(120) Rama, A. N.; Cho, S. C.; Kushida, C. A. Normal Human Sleep. In: Sleep. A Comprehensive Textbook. New Jersey: John Wiley & Sons, Inc.; P. 3-4; Isbn-13 978-0-471-68371-1. **2006**.

(121) Ehlen, J. C.; Paul, K. N. Regulation of Light's Action in the Mammalian Circadian Clock: Role of the Extrasynaptic Gabaa Receptor. *American journal of physiology. Regulatory, integrative and comparative physiology* **2009**, *296*, R1606-1612.

(122) Brown, N.; Kerby, J.; Bonnert, T. P.; Whiting, P. J.; Wafford, K. A. Pharmacological Characterization of a Novel Cell Line Expressing Human Alpha(4)Beta(3)Delta Gaba(a) Receptors. *British journal of pharmacology* **2002**, *136*, 965-974.

(123) Decavel, C.; Van den Pol, A. N. Gaba: A Dominant Neurotransmitter in the Hypothalamus. *J Comp Neurol* **1990**, *302*, 1019-1037.

(124) Makara, G. B.; Rappay, G.; Stark, E. Autoradiographic Localization of 3h-Gamma-Aminobutyric Acid in the Medial Hypothalamus. *Exp Brain Res* **1975**, *22*, 449-455.

(125) Moore, R. Y.; Speh, J. C. Gaba Is the Principal Neurotransmitter of the Circadian System. *Neuroscience letters* **1993**, *150*, 112-116.

(126) Gao, B.; Fritschy, J. M.; Moore, R. Y. Gabaa-Receptor Subunit Composition in the Circadian Timing System. *Brain research* **1995**, *700*, 142-156.

(127) Naum, O. G.; Fernanda Rubio, M.; Golombek, D. A. Rhythmic Variation in Gamma-Aminobutyric Acid(a)-Receptor Subunit Composition in the Circadian System and Median Eminence of Syrian Hamsters. *Neuroscience letters* **2001**, *310*, 178-182.

(128) O'Hara, B. F.; Andretic, R.; Heller, H. C.; Carter, D. B.; Kilduff, T. S. Gabaa, Gabac, and Nmda Receptor Subunit Expression in the Suprachiasmatic Nucleus and Other Brain Regions. *Brain Res Mol Brain Res* **1995**, *28*, 239-250.

(129) Huhman, K. L.; Hennessey, A. C.; Albers, H. E. Rhythms of Glutamic Acid Decarboxylase Mrna in the Suprachiasmatic Nucleus. *J Biol Rhythms* **1996**, *11*, 311-316.

(130) Huhman, K. L.; Jasnow, A. M.; Sisitsky, A. K.; Albers, H. E. Glutamic Acid Decarboxylase Mrna in the Suprachiasmatic Nucleus of Rats Housed in Constant Darkness. *Brain research* **1999**, *851*, 266-269.

(131) van den Pol, A. N.; Gorcs, T. Synaptic Relationships between Neurons Containing Vasopressin, Gastrin-Releasing Peptide, Vasoactive Intestinal Polypeptide, and Glutamate Decarboxylase Immunoreactivity in the Suprachiasmatic Nucleus: Dual Ultrastructural Immunocytochemistry with Gold-Substituted Silver Peroxidase. *J Comp Neurol* **1986**, *252*, 507-521.

(132) Benke, D.; Barberis, A.; Kopp, S.; Altmann, K. H.; Schubiger, M.; Vogt, K. E.; Rudolph, U.; Mohler, H. Gaba a Receptors as in Vivo Substrate for the Anxiolytic Action of Valerenic Acid, a Major Constituent of Valerian Root Extracts. *Neuropharmacology* **2009**, *56*, 174-181.

(133) Wafford, K. A.; Ebert, B. Emerging Anti-Insomnia Drugs: Tackling Sleeplessness and the Quality of Wake Time. *Nature reviews. Drug discovery* **2008**, *7*, 530-540.

(134) Winsky-Sommerer, R. Role of Gabaa Receptors in the Physiology and Pharmacology of Sleep. *Eur J Neurosci* **2009**, *29*, 1779-1794.

(135) Wiegand, M. H. Antidepressants for the Treatment of Insomnia : A Suitable Approach? *Drugs* **2008**, *68*, 2411-2417.

(136) Shorter, E. "Benzodiazepines". A Historical Dictionary of Psychiatry. Oxford University Press. Pp. 41–2. Isbn 0-19-517668-5. **2005**.

(137) MacDonald, R. L.; Twyman, R. E. Kinetic Properties and Regulation of Gabaa Receptor Channels. *Ion Channels* **1992**, *3*, 315-343.

(138) Study, R. E.; Barker, J. L. Diazepam and (--)-Pentobarbital: Fluctuation Analysis Reveals Different Mechanisms for Potentiation of Gamma-Aminobutyric Acid Responses in Cultured Central Neurons. *Proceedings of the National Academy of Sciences of the United States of America* **1981**, *78*, 7180-7184.

(139) Inomata, N.; Tokutomi, N.; Oyama, Y.; Akaike, N. Intracellular Picrotoxin Blocks Pentobarbital-Gated Cl- Conductance. *Neurosci Res* **1988**, *6*, 72-75.

(140) Bormann, J. Electrophysiology of Gabaa and Gabab Receptor Subtypes. *Trends Neurosci* **1988**, *11*, 112-116.

(141) Kokate, T. G.; Svensson, B. E.; Rogawski, M. A. Anticonvulsant Activity of Neurosteroids: Correlation with Gamma-Aminobutyric Acid-Evoked Chloride Current Potentiation. *The Journal of pharmacology and experimental therapeutics* **1994**, *270*, 1223-1229.

(142) Majewska, M. D. Neurosteroids: Endogenous Bimodal Modulators of the Gabaa Receptor. Mechanism of Action and Physiological Significance. *Prog Neurobiol* **1992**, *38*, 379-395.

(143) Callachan, H.; Cottrell, G. A.; Hather, N. Y.; Lambert, J. J.; Nooney, J. M.; Peters, J. A. Modulation of the Gabaa Receptor by Progesterone Metabolites. *Proceedings of the Royal Society of London. Series B, Containing papers of a Biological character. Royal Society* **1987**, *231*, 359-369.

(144) Peters, J. A.; Kirkness, E. F.; Callachan, H.; Lambert, J. J.; Turner, A. J. Modulation of the Gabaa Receptor by Depressant Barbiturates and Pregnane Steroids. *British journal of pharmacology* **1988**, *94*, 1257-1269.

(145) Celentano, J. J.; Gyenes, M.; Gibbs, T. T.; Farb, D. H. Negative Modulation of the Gamma-Aminobutyric Acid Response by Extracellular Zinc. *Molecular pharmacology* **1991**, *40*, 766-773.

(146) Smart, T. G.; Xie, X.; Krishek, B. J. Modulation of Inhibitory and Excitatory Amino Acid Receptor Ion Channels by Zinc. *Prog Neurobiol* **1994**, *42*, 393-441.

(147) Xie, X. M.; Smart, T. G. A Physiological Role for Endogenous Zinc in Rat Hippocampal Synaptic Neurotransmission. *Nature* **1991**, *349*, 521-524.

(148) Smart, T. G. A Novel Modulatory Binding Site for Zinc on the Gabaa Receptor Complex in Cultured Rat Neurones. *The Journal of physiology* **1992**, *447*, 587-625.

(149) Smart, T. G.; Constanti, A. Differential Effect of Zinc on the Vertebrate Gabaa-Receptor Complex. *British journal of pharmacology* **1990**, *99*, 643-654.

(150) Lambert, S.; Arras, M.; Vogt, K. E.; Rudolph, U. Isoflurane-Induced Surgical Tolerance Mediated Only in Part by Beta3-Containing Gaba(a) Receptors. *European journal of pharmacology* **2005**, *516*, 23-27.

(151) Liao, M.; Sonner, J. M.; Jurd, R.; Rudolph, U.; Borghese, C. M.; Harris, R. A.; Laster, M. J.; Eger, E. I., 2nd. Beta3-Containing Gamma-Aminobutyric Acida Receptors Are Not Major Targets for the Amnesic and Immobilizing Actions of Isoflurane. *Anesthesia and analgesia* **2005**, *101*, 412-418, table of contents.

(152) Zeller, A.; Arras, M.; Lazaris, A.; Jurd, R.; Rudolph, U. Distinct Molecular Targets for the Central Respiratory and Cardiac Actions of the General Anesthetics Etomidate and Propofol. *FASEB journal : official publication of the Federation of American Societies for Experimental Biology* **2005**, *19*, 1677-1679.

(153) Cirone, J.; Rosahl, T. W.; Reynolds, D. S.; Newman, R. J.; O'Meara, G. F.; Hutson, P. H.; Wafford, K. A. Gamma-Aminobutyric Acid Type a Receptor Beta 2 Subunit Mediates the Hypothermic Effect of Etomidate in Mice. *Anesthesiology* **2004**, *100*, 1438-1445.

(154) Kissin, I.; Gelman, S. Components of Anaesthesia. *British journal of anaesthesia* **1988**, *61*, 237-238.

(155) Belelli, D.; Pistis, M.; Peters, J. A.; Lambert, J. J. General Anaesthetic Action at Transmitter-Gated Inhibitory Amino Acid Receptors. *Trends in pharmacological sciences* **1999**, *20*, 496-502.

(156) Eger, E. I., 2nd; Koblin, D. D.; Harris, R. A.; Kendig, J. J.; Pohorille, A.; Halsey, M. J.; Trudell, J. R. Hypothesis: Inhaled Anesthetics Produce Immobility and Amnesia by Different Mechanisms at Different Sites. *Anesthesia and analgesia* **1997**, *84*, 915-918.

(157) Franks, N. P.; Lieb, W. R. Neuron Membranes: Anaesthetics on the Mind. *Nature* **1987**, *328*, 113-114.

(158) Franks, N. P.; Lieb, W. R. Molecular and Cellular Mechanisms of General Anaesthesia. *Nature* **1994**, *367*, 607-614.

(159) Harris, R. A.; Mihic, S. J.; Dildy-Mayfield, J. E.; Machu, T. K. Actions of Anesthetics on Ligand-Gated Ion Channels: Role of Receptor Subunit Composition. *FASEB journal : official publication of the Federation of American Societies for Experimental Biology* **1995**, *9*, 1454-1462.

(160) Koblin, D. D.; Chortkoff, B. S.; Laster, M. J.; Eger, E. I., 2nd; Halsey, M. J.; Ionescu, P. Polyhalogenated and Perfluorinated Compounds That Disobey the Meyer-Overton Hypothesis. *Anesthesia and analgesia* **1994**, *79*, 1043-1048.

(161) Krazowski, M.; Harrison, N. L. *Cell. Mol. Life Sci.* **1999**, *55*, 1278-1303.

(162) Lambert, J. J.; al., E. In Gases in Medicine: Anaesthesia. 8th Boc Priestly Conference, Pp. 121–137, Royal Society of Chemistry Special Publication 220. **1998**.

(163) Tanelian, D. L.; Kosek, P.; Mody, I.; MacIver, M. B. The Role of the Gabaa Receptor/Chloride Channel Complex in Anesthesia. *Anesthesiology* **1993**, *78*, 757-776.

(164) Belelli, D.; Lambert, J. J.; Peters, J. A.; Wafford, K.; Whiting, P. J. The Interaction of the General Anesthetic Etomidate with the Gamma-Aminobutyric Acid Type a Receptor Is Influenced by a Single Amino Acid. *Proceedings of the National Academy of Sciences of the United States of America* **1997**, *94*, 11031-11036.

(165) Macdonald, R. L. Ethanol, Gamma-Aminobutyrate Type a Receptors, and Protein Kinase C Phosphorylation. *Proceedings of the National Academy of Sciences of the United States of America* **1995**, *92*, 3633-3635.

(166) Pandey, S. C. Neuronal Signaling Systems and Ethanol Dependence. *Molecular neurobiology* **1998**, *17*, 1-15.

(167) Davies, M. The Role of Gabaa Receptors in Mediating the Effects of Alcohol in the Central Nervous System. *J Psychiatry Neurosci* **2003**, *28*, 263-274.

(168) Grilly, D. Drugs and Human Behavior. 4th Ed. Toronto: Allyn and Bacon. **2002**.

(169) Sundstrom-Poromaa, I.; Smith, D. H.; Gong, Q. H.; Sabado, T. N.; Li, X.; Light, A.; Wiedmann, M.; Williams, K.; Smith, S. S. Hormonally Regulated Alpha(4)Beta(2)Delta Gaba(a) Receptors Are a Target for Alcohol. *Nature neuroscience* **2002**, *5*, 721-722.

(170) Cosens, D. J.; Manning, A. Abnormal Electroretinogram from a Drosophila Mutant. *Nature* **1969**, *224*, 285-287.

(171) Montell, C.; Rubin, G. M. Molecular Characterization of the Drosophila Trp Locus: A Putative Integral Membrane Protein Required for Phototransduction. *Neuron* **1989**, *2*, 1313-1323.

(172) Wes, P. D.; Chevesich, J.; Jeromin, A.; Rosenberg, C.; Stetten, G.; Montell, C. Trpc1, a Human Homolog of a Drosophila Store-Operated Channel. *Proceedings of the National Academy of Sciences of the United States of America* **1995**, *92*, 9652-9656.

(173) Zhu, X.; Chu, P. B.; Peyton, M.; Birnbaumer, L. Molecular Cloning of a Widely Expressed Human Homologue for the Drosophila Trp Gene. *FEBS letters* **1995**, *373*, 193-198.

(174) Clapham, D. E. Trp Channels as Cellular Sensors. *Nature* **2003**, *426*, 517-524.

(175) Wu, L. J.; Sweet, T. B.; Clapham, D. E. International Union of Basic and Clinical Pharmacology. Lxxvi. Current Progress in the Mammalian Trp Ion Channel Family. *Pharmacological reviews* **2010**, *62*, 381-404.

(176) Nelson, P. L.; Beck, A.; Cheng, H. Transient Receptor Proteins Illuminated: Current Views on Trps and Disease. *Veterinary journal* **2011**, *187*, 153-164.

(177) Nilius, B.; Owsianik, G. The Transient Receptor Potential Family of Ion Channels. *Genome biology* **2011**, *12*, 218.

(178) Wheeler, G. L.; Brownlee, C. Ca2+ Signalling in Plants and Green Algae--Changing Channels. *Trends in plant science* **2008**, *13*, 506-514.

(179) Chang, Y.; Schlenstedt, G.; Flockerzi, V.; Beck, A. Properties of the Intracellular Transient Receptor Potential (Trp) Channel in Yeast, Yvc1. *FEBS letters* **2010**, *584*, 2028-2032.

(180) Kalia, J.; Swartz, K. J. Exploring Structure-Function Relationships between Trp and Kv Channels. *Scientific reports* **2013**, *3*, 1523.

(181) Cheng, W.; Sun, C.; Zheng, J. Heteromerization of Trp Channel Subunits: Extending Functional Diversity. *Protein & cell* **2010**, *1*, 802-810.

(182) Planells-Cases, R.; Ferrer-Montiel, A. In *Trp Ion Channel Function in Sensory Transduction and Cellular Signaling Cascades*; Liedtke, W. B., Heller, S., Eds. Boca Raton (FL), 2007.

(183) Szallasi, A.; Cortright, D. N.; Blum, C. A.; Eid, S. R. The Vanilloid Receptor Trpv1: 10 Years from Channel Cloning to Antagonist Proof-of-Concept. *Nature reviews. Drug discovery* **2007**, *6*, 357-372.

(184) Putney, J. W., Jr.; McKay, R. R. Capacitative Calcium Entry Channels. *BioEssays : news and reviews in molecular, cellular and developmental biology* **1999**, *21*, 38-46.

(185) Patapoutian, A.; Tate, S.; Woolf, C. J. Transient Receptor Potential Channels: Targeting Pain at the Source. *Nature reviews. Drug discovery* **2009**, *8*, 55-68.

(186) Szallasi, A.; Blumberg, P. M. Vanilloid (Capsaicin) Receptors and Mechanisms. *Pharmacological reviews* **1999**, *51*, 159-212.

(187) Singh, B. B.; Pabelick, C. M.; Prakash, Y. S. 2012, p 61-88.

(188) Kaneko, Y.; Szallasi, A. Transient Receptor Potential (Trp) Channels: A Clinical Perspective. *British journal of pharmacology* **2013**.

(189) Brederson, J. D.; Kym, P. R.; Szallasi, A. Targeting Trp Channels for Pain Relief. *European journal of pharmacology* **2013**, *716*, 61-76.

(190) Moran, M. M.; McAlexander, M. A.; Biro, T.; Szallasi, A. Transient Receptor Potential Channels as Therapeutic Targets. *Nature reviews. Drug discovery* **2011**, *10*, 601-620.

(191) Tominaga, M. 2007, p 271-286.

(192) Nilius, B.; Appendino, G. Spices: The Savory and Beneficial Science of Pungency. *Reviews of physiology, biochemistry and pharmacology* **2013**, *164*, 1-76.

(193) Pedersen, S. F.; Nilius, B. Transient Receptor Potential Channels in Mechanosensing and Cell Volume Regulation. *Methods in enzymology* **2007**, *428*, 183-207.

(194) Guilak, F.; Leddy, H. A.; Liedtke, W. Transient Receptor Potential Vanilloid 4: The Sixth Sense of the Musculoskeletal System? *Annals of the New York Academy of Sciences* **2010**, *1192*, 404-409.

(195) Minke, B. The History of the Drosophila Trp Channel: The Birth of a New Channel Superfamily. *Journal of neurogenetics* **2010**, *24*, 216-233.

(196) Suri, A.; Szallasi, A. The Emerging Role of Trpv1 in Diabetes and Obesity. *Trends in pharmacological sciences* **2008**, *29*, 29-36.

(197) Zhu, Z.; Luo, Z.; Ma, S.; Liu, D. Trp Channels and Their Implications in Metabolic Diseases. *Pflugers Archiv : European journal of physiology* **2011**, *461*, 211-223.

(198) Binder, A.; May, D.; Baron, R.; Maier, C.; Tolle, T. R.; Treede, R. D.; Berthele, A.; Faltraco, F.; Flor, H.; Gierthmuhlen, J.; Haenisch, S.; Huge, V.; Magerl, W.; Maihofner, C.; Richter, H.; Rolke, R.; Scherens, A.; Uceyler, N.; Ufer, M.; Wasner, G.; Zhu, J.; Cascorbi, I. Transient Receptor Potential Channel Polymorphisms Are Associated with the Somatosensory Function in Neuropathic Pain Patients. *PloS one* **2011**, *6*, e17387.

(199) Smit, L. A.; Kogevinas, M.; Anto, J. M.; Bouzigon, E.; Gonzalez, J. R.; Le Moual, N.; Kromhout, H.; Carsin, A. E.; Pin, I.; Jarvis, D.; Vermeulen, R.; Janson, C.; Heinrich, J.; Gut, I.; Lathrop, M.; Valverde, M. A.; Demenais, F.; Kauffmann, F. Transient Receptor Potential Genes, Smoking, Occupational Exposures and Cough in Adults. *Respiratory research* **2012**, *13*, 26.

(200) Hartmann, J.; Dragicevic, E.; Adelsberger, H.; Henning, H. A.; Sumser, M.; Abramowitz, J.; Blum, R.; Dietrich, A.; Freichel, M.; Flockerzi, V.; Birnbaumer, L.; Konnerth, A. Trpc3 Channels Are Required for Synaptic Transmission and Motor Coordination. *Neuron* **2008**, *59*, 392-398.

(201) Kuwahara, K.; Wang, Y.; McAnally, J.; Richardson, J. A.; Bassel-Duby, R.; Hill, J. A.; Olson, E. N. Trpc6 Fulfills a Calcineurin Signaling Circuit During Pathologic Cardiac Remodeling. *The Journal of clinical investigation* **2006**, *116*, 3114-3126.

(202) Kiselyov, K.; Patterson, R. L. The Integrative Function of Trpc Channels. *Frontiers in bioscience* **2009**, *14*, 45-58.

(203) Zygmunt, P. M.; Petersson, J.; Andersson, D. A.; Chuang, H.; Sorgard, M.; Di Marzo, V.; Julius, D.; Hogestatt, E. D. Vanilloid Receptors on Sensory Nerves Mediate the Vasodilator Action of Anandamide. *Nature* **1999**, *400*, 452-457.

(204) Ambrosino, P.; Soldovieri, M. V.; Russo, C.; Taglialatela, M. Activation and Desensitization of Trpv1 Channels in Sensory Neurons by the Pparalpha Agonist Palmitoylethanolamide. *British journal of pharmacology* **2013**, *168*, 1430-1444.

(205) Watanabe, H.; Vriens, J.; Prenen, J.; Droogmans, G.; Voets, T.; Nilius, B. Anandamide and Arachidonic Acid Use Epoxyeicosatrienoic Acids to Activate Trpv4 Channels. *Nature* **2003**, *424*, 434-438.

(206) Grimm, C.; Kraft, R.; Schultz, G.; Harteneck, C. Activation of the Melastatin-Related Cation Channel Trpm3 by D-Erythro-Sphingosine [Corrected]. *Molecular pharmacology* **2005**, *67*, 798-805.

(207) Vriens, J.; Nilius, B.; Vennekens, R. Herbal Compounds and Toxins Modulating Trp Channels. *Current neuropharmacology* **2008**, *6*, 79-96.

(208) Caterina, M. J.; Schumacher, M. A.; Tominaga, M.; Rosen, T. A.; Levine, J. D.; Julius, D. The Capsaicin Receptor: A Heat-Activated Ion Channel in the Pain Pathway. *Nature* **1997**, *389*, 816-824.

(209) Szallasi, A.; Szabo, T.; Biro, T.; Modarres, S.; Blumberg, P. M.; Krause, J. E.; Cortright, D. N.; Appendino, G. Resiniferatoxin-Type Phorboid Vanilloids Display Capsaicin-Like Selectivity at Native Vanilloid Receptors on Rat Drg Neurons and at the Cloned Vanilloid Receptor Vr1. *British journal of pharmacology* **1999**, *128*, 428-434.

(210) McNamara, F. N.; Randall, A.; Gunthorpe, M. J. Effects of Piperine, the Pungent Component of Black Pepper, at the Human Vanilloid Receptor (Trpv1). *British journal of pharmacology* **2005**, *144*, 781-790.

(211) Xu, H.; Blair, N. T.; Clapham, D. E. Camphor Activates and Strongly Desensitizes the Transient Receptor Potential Vanilloid Subtype 1 Channel in a Vanilloid-Independent Mechanism. *The Journal of neuroscience : the official journal of the Society for Neuroscience* **2005**, *25*, 8924-8937.

(212) McKemy, D. D.; Neuhausser, W. M.; Julius, D. Identification of a Cold Receptor Reveals a General Role for Trp Channels in Thermosensation. *Nature* **2002**, *416*, 52-58.

(213) Peier, A. M.; Moqrich, A.; Hergarden, A. C.; Reeve, A. J.; Andersson, D. A.; Story, G. M.; Earley, T. J.; Dragoni, I.; McIntyre, P.; Bevan, S.; Patapoutian, A. A Trp Channel That Senses Cold Stimuli and Menthol. *Cell* **2002**, *108*, 705-715.

(214) Smith, P. L.; Maloney, K. N.; Pothen, R. G.; Clardy, J.; Clapham, D. E. Bisandrographolide from Andrographis Paniculata Activates Trpv4 Channels. *The Journal of biological chemistry* **2006**, *281*, 29897-29904.

(215) Chung, M. K.; Lee, H.; Mizuno, A.; Suzuki, M.; Caterina, M. J. 2-Aminoethoxydiphenyl Borate Activates and Sensitizes the Heat-Gated Ion Channel Trpv3. *The Journal of neuroscience : the official journal of the Society for Neuroscience* **2004**, *24*, 5177-5182.

(216) Hu, H. Z.; Gu, Q.; Wang, C.; Colton, C. K.; Tang, J.; Kinoshita-Kawada, M.; Lee, L. Y.; Wood, J. D.; Zhu, M. X. 2-Aminoethoxydiphenyl Borate Is a Common Activator of Trpv1, Trpv2, and Trpv3. *The Journal of biological chemistry* **2004**, *279*, 35741-35748.

(217) Story, G. M.; Peier, A. M.; Reeve, A. J.; Eid, S. R.; Mosbacher, J.; Hricik, T. R.; Earley, T. J.; Hergarden, A. C.; Andersson, D. A.; Hwang, S. W.; McIntyre, P.; Jegla, T.; Bevan, S.; Patapoutian, A. Anktm1, a Trp-Like Channel Expressed in Nociceptive Neurons, Is Activated by Cold Temperatures. *Cell* **2003**, *112*, 819-829.

(218) Iida, T.; Moriyama, T.; Kobata, K.; Morita, A.; Murayama, N.; Hashizume, S.; Fushiki, T.; Yazawa, S.; Watanabe, T.; Tominaga, M. Trpv1 Activation and Induction of Nociceptive Response by a Non-Pungent Capsaicin-Like Compound, Capsiate. *Neuropharmacology* **2003**, *44*, 958-967.

(219) Watanabe, H.; Davis, J. B.; Smart, D.; Jerman, J. C.; Smith, G. D.; Hayes, P.; Vriens, J.; Cairns, W.; Wissenbach, U.; Prenen, J.; Flockerzi, V.; Droogmans, G.; Benham, C. D.; Nilius, B. Activation of Trpv4 Channels (Hvrl-2/Mtrp12) by Phorbol Derivatives. *The Journal of biological chemistry* **2002**, *277*, 13569-13577.

(220) Gomtsyan, A.; Faltynek, C.; Gomtsyan, A., Faltynek, C., Eds.; John Wiley & Sons: Hoboken, NJ, 2010.

(221) Jordt, S. E.; Julius, D. Molecular Basis for Species-Specific Sensitivity to "Hot" Chili Peppers. *Cell* **2002**, *108*, 421-430.

(222) Cao, E.; Liao, M.; Cheng, Y.; Julius, D. Trpv1 Structures in Distinct Conformations Reveal Activation Mechanisms. *Nature* **2013**, *504*, 113-118.

(223) Gavva, N. R.; Klionsky, L.; Qu, Y.; Shi, L.; Tamir, R.; Edenson, S.; Zhang, T. J.; Viswanadhan, V. N.; Toth, A.; Pearce, L. V.; Vanderah, T. W.; Porreca, F.; Blumberg, P. M.; Lile, J.; Sun, Y.; Wild, K.; Louis, J. C.; Treanor, J. J. Molecular Determinants of Vanilloid Sensitivity in Trpv1. *The Journal of biological chemistry* **2004**, *279*, 20283-20295.

(224) Pingle, S. C.; Matta, J. A.; Ahern, G. P. Capsaicin Receptor: Trpv1 a Promiscuous Trp Channel. *Handbook of experimental pharmacology* **2007**, 155-171.

(225) Caterina, M. J.; Leffler, A.; Malmberg, A. B.; Martin, W. J.; Trafton, J.; Petersen-Zeitz, K. R.; Koltzenburg, M.; Basbaum, A. I.; Julius, D. Impaired Nociception and Pain Sensation in Mice Lacking the Capsaicin Receptor. *Science* **2000**, *288*, 306-313.

(226) Davis, J. B.; Gray, J.; Gunthorpe, M. J.; Hatcher, J. P.; Davey, P. T.; Overend, P.; Harries, M. H.; Latcham, J.; Clapham, C.; Atkinson, K.; Hughes, S. A.; Rance, K.; Grau, E.; Harper, A. J.; Pugh, P. L.; Rogers, D. C.; Bingham, S.; Randall, A.; Sheardown, S. A. Vanilloid Receptor-1 Is Essential for Inflammatory Thermal Hyperalgesia. *Nature* **2000**, *405*, 183-187.

(227) Chuang, H. H.; Prescott, E. D.; Kong, H.; Shields, S.; Jordt, S. E.; Basbaum, A. I.; Chao, M. V.; Julius, D. Bradykinin and Nerve Growth Factor Release the Capsaicin Receptor from Ptdins(4,5)P2-Mediated Inhibition. *Nature* **2001**, *411*, 957-962.

(228) Wang, X.; Miyares, R. L.; Ahern, G. P. Oleoylethanolamide Excites Vagal Sensory Neurones, Induces Visceral Pain and Reduces Short-Term Food Intake in Mice Via Capsaicin Receptor Trpv1. *The Journal of physiology* **2005**, *564*, 541-547.

(229) Ahern, G. P. Activation of Trpv1 by the Satiety Factor Oleoylethanolamide. *The Journal of biological chemistry* **2003**, *278*, 30429-30434.

(230) Szabo, A.; Helyes, Z.; Sandor, K.; Bite, A.; Pinter, E.; Nemeth, J.; Banvolgyi, A.; Bolcskei, K.; Elekes, K.; Szolcsanyi, J. Role of Transient Receptor Potential Vanilloid 1 Receptors in Adjuvant-Induced Chronic Arthritis: In Vivo Study Using Gene-Deficient Mice. *The Journal of pharmacology and experimental therapeutics* **2005**, *314*, 111-119.

(231) Joshi, S. K.; Honore, P. In *Vanilloid Receptor Trpv1 in Drug Discovery. Targeting Pain and Other Pathological Disorders.*; Gomtsyan, A., Faltynek, C., Eds.; John Wiley & Sons: Hoboken, NJ, 2010, p 175-190.

(232) Jimenez-Andrade, J. M.; Mantyh, P. In *Vanilloid Receptor Trpv1 in Drug Discovery. Targeting Pain and Other Pathological Disorders.*; Gomtsyan, A., Faltynek, C., Eds.; John Wiley & Sons: Hoboken, NJ., 2010, p 191-205.

(233) Knotkova, H.; Pappagallo, M.; Szallasi, A. Capsaicin (Trpv1 Agonist) Therapy for Pain Relief: Farewell or Revival? *The Clinical journal of pain* **2008**, *24*, 142-154.

(234) Szallasi, A.; Sheta, M. Targeting Trpv1 for Pain Relief: Limits, Losers and Laurels. *Expert opinion on investigational drugs* **2012**, *21*, 1351-1369.

(235) Brown, D. C.; Iadarola, M. J.; Perkowski, S. Z.; Erin, H.; Shofer, F.; Laszlo, K. J.; Olah, Z.; Mannes, A. J. Physiologic and Antinociceptive Effects of Intrathecal Resiniferatoxin in a Canine Bone Cancer Model. *Anesthesiology* **2005**, *103*, 1052-1059.

(236) Iadarola, M. J.; Gonnella, G. L. Resiniferatoxin for Pain Treatment: An Interventional Approach to Personalized Pain Medicine. *The Open Pain Journal* **2013**, *6 (Suppl 1: M10)* 95-107.

(237) Gurdon, J. B.; Lane, C. D.; Woodland, H. R.; Marbaix, G. Use of Frog Eggs and Oocytes for the Study of Messenger Rna and Its Translation in Living Cells. *Nature* **1971**, *233*, 177-182.

(238) Sumikawa, K.; Houghton, M.; Emtage, J. S.; Richards, B. M.; Barnard, E. A. Active Multi-Subunit Ach Receptor Assembled by Translation of Heterologous Mrna in Xenopus Oocytes. *Nature* **1981**, *292*, 862-864.

(239) Rungger, D. Xenopus Helveticus, an Endangered Species? *The International journal of developmental biology* **2002**, *46*, 49-63.

(240) Marsal, J.; Tigyi, G.; Miledi, R. Incorporation of Acetylcholine Receptors and Cl- Channels in Xenopus Oocytes Injected with Torpedo Electroplaque Membranes.

Proceedings of the National Academy of Sciences of the United States of America **1995**, *92*, 5224-5228.

(241) Sigel, E.; Minier, F. The Xenopus Oocyte: System for the Study of Functional Expression and Modulation of Proteins. *Molecular nutrition & food research* **2005**, *49*, 228-234.

(242) Sigel, E. Use of Xenopus Oocytes for the Functional Expression of Plasma Membrane Proteins. *The Journal of membrane biology* **1990**, *117*, 201-221.

(243) Wagner, C. A.; Friedrich, B.; Setiawan, I.; Lang, F.; Broer, S. The Use of Xenopus Laevis Oocytes for the Functional Characterization of Heterologously Expressed Membrane Proteins. *Cellular physiology and biochemistry : international journal of experimental cellular physiology, biochemistry, and pharmacology* **2000**, *10*, 1-12.

(244) Gundersen, C. B.; Miledi, R.; Parker, I. Serotonin Receptors Induced by Exogenous Messenger Rna in Xenopus Oocytes. *Proceedings of the Royal Society of London. Series B, Containing papers of a Biological character. Royal Society* **1983**, *219*, 103-109.

(245) Miledi, R.; Parker, I.; Sumikawa, K. Recording of Single Gamma-Aminobutyrate- and Acetylcholine-Activated Receptor Channels Translated by Exogenous Mrna in Xenopus Oocytes. *Proceedings of the Royal Society of London. Series B, Containing papers of a Biological character. Royal Society* **1983**, *218*, 481-484.

(246) Baumgartner, W.; Islas, L.; Sigworth, F. J. Two-Microelectrode Voltage Clamp of Xenopus Oocytes: Voltage Errors and Compensation for Local Current Flow. *Biophysical journal* **1999**, *77*, 1980-1991.

(247) Stühmer, W.; Parekh, A. B. In *Single-Channel Recording.* ; Sakmann, B., Neher, E., Eds.; Plenum Press: New York, 1995, p 341-356.

(248) Baburin, I.; Beyl, S.; Hering, S. Automated Fast Perfusion of Xenopus Oocytes for Drug Screening. *Pflugers Archiv : European journal of physiology* **2006**, *453*, 117-123.

(249) Dascal, N. Voltage Clamp Recordings from Xenopus Oocytes. *Current protocols in neuroscience / editorial board, Jacqueline N. Crawley ... [et al.]* **2001**, *Chapter 6*, Unit 6 12.

(250) Schoffmann, A.; Wimmer, L.; Goldmann, D.; Khom, S.; Hintersteiner, J.; Baburin, I.; Schwarz, T.; Hintersteininger, M.; Pakfeifer, P.; Oufir, M.; Hamburger, M.; Erker, T.; Ecker, G. F.; Mihovilovic, M. D.; Hering, S. Efficient Modulation of Gamma-Aminobutyric Acid Type a Receptors by Piperine Derivatives. *Journal of medicinal chemistry* **2014**, *57*, 5602-5619.

(251) Khom, S.; Strommer, B.; Schoffmann, A.; Hintersteiner, J.; Baburin, I.; Erker, T.; Schwarz, T.; Schwarzer, C.; Zaugg, J.; Hamburger, M.; Hering, S. Gabaa Receptor Modulation by Piperine and a Non-Trpv1 Activating Derivative. *Biochemical pharmacology* **2013**, *85*, 1827-1836.

(252) Wimmer, L.; Schonbauer, D.; Pakfeifer, P.; Schoffmann, A.; Khom, S.; Hering, S.; Mihovilovic, M. D. Developing Piperine Towards Trpv1 and Gabaa Receptor Ligands--Synthesis of Piperine Analogs Via Heck-Coupling of Conjugated Dienes. *Organic & biomolecular chemistry* **2015**, *13*, 990-994.

(253) Zaugg, J.; Baburin, I.; Strommer, B.; Kim, H. J.; Hering, S.; Hamburger, M. Hplc-Based Activity Profiling: Discovery of Piperine as a Positive Gaba(a) Receptor Modulator Targeting a Benzodiazepine-Independent Binding Site. *Journal of natural products* **2010**, *73*, 185-191.

(254) Srinivasan, K. Black Pepper and Its Pungent Principle-Piperine: A Review of Diverse Physiological Effects. *Critical Reviews in Food Science and Nutrition* **2007**, *47*, 735-748.

(255) Chen, C.-Y.; Li, W.; Qu, K.-P.; Chen, C.-R. Piperine Exerts Anti-Seizure Effects Via the Trpv1 Receptor in Mice. *European journal of pharmacology* **2013**, *714*, 288-294.

(256) Rueda, D. C.; Schoffmann, A.; De Mieri, M.; Raith, M.; Jahne, E. A.; Hering, S.; Hamburger, M. Identification of Dihydrostilbenes in Pholidota Chinensis as a New Scaffold for Gabaa Receptor Modulators. *Bioorganic & medicinal chemistry* **2014**, *22*, 1276-1284.

(257) Wang, J.; Matsuzaki, K.; Kitanaka, S. Stilbene Derivatives from Pholidota Chinensis and Their Anti-Inflammatory Activity. *Chemical & pharmaceutical bulletin* **2006**, *54*, 1216-1218.

(258) Li, S. X.; Li, B.; Ali, Z.; Abe, N.; Khan, I. A.; Wang, M.; Wu, C. R. Constituents of Pholidota Cantonensis Rolfe. *Planta medica* **2013**, *79*, P31.

(259) Rueda, D. C.; Raith, M.; De Mieri, M.; Schoffmann, A.; Hering, S.; Hamburger, M. Identification of Dehydroabietc Acid from Boswellia Thurifera Resin as a Positive Gabaa Receptor Modulator. *Fitoterapia* **2014**, *99*, 28-34.

(260) Al-Harrasi, A.; Al-Saidi, S. Phytochemical Analysis of the Essential Oil from Botanically Certified Oleogum Resin of Boswellia Sacra (Omani Luban). *Molecules* **2008**, *13*, 2181-2189.

(261) Hamm, S.; Bleton, J.; Connan, J.; Tchapla, A. A Chemical Investigation by Headspace Spme and Gc-Ms of Volatile and Semi-Volatile Terpenes in Various Olibanum Samples. *Phytochemistry* **2005**, *66*, 1499-1514.

(262) Zaugg, J.; Khom, S.; Eigenmann, D.; Baburin, I.; Hamburger, M.; Hering, S. Identification and Characterization of Gaba(a) Receptor Modulatory Diterpenes from Biota Orientalis That Decrease Locomotor Activity in Mice. *Journal of natural products* **2011**, *74*, 1764-1772.

(263) Lees, G.; Coyne, L.; Zheng, J.; Nicholson, R. A. Mechanisms for Resin Acid Effects on Membrane Currents and Gaba(a) Receptors in Mammalian Cns. *Environmental toxicology and pharmacology* **2004**, *15*, 61-69.

(264) San Feliciano, A.; Gordaliza, M.; Salinero, M. A.; Miguel del Corral, J. M. Abietane Acids: Sources, Biological Activities, and Therapeutic Uses. *Planta medica* **1993**, *59*, 485-490.

(265) Taferner, B.; Schuehly, W.; Huefner, A.; Baburin, I.; Wiesner, K.; Ecker, G. F.; Hering, S. Modulation of Gabaa-Receptors by Honokiol and Derivatives: Subtype Selectivity and Structure-Activity Relationship. *Journal of medicinal chemistry* **2011**, *54*, 5349-5361.

(266) Alexeev, M.; Grosenbaugh, D. K.; Mott, D. D.; Fisher, J. L. The Natural Products Magnolol and Honokiol Are Positive Allosteric Modulators of Both Synaptic and Extra-Synaptic Gaba(a) Receptors. *Neuropharmacology* **2012**, *62*, 2507-2514.

(267) Lipinski, C. A. Lead- and Drug-Like Compounds: The Rule-of-Five Revolution. *Drug discovery today. Technologies* **2004**, *1*, 337-341.

(268) Pajouhesh, H.; Lenz, G. R. Medicinal Chemical Properties of Successful Central Nervous System Drugs. *NeuroRx : the journal of the American Society for Experimental NeuroTherapeutics* **2005**, *2*, 541-553.

7 Appendix

7.1 Supporting Information: Efficient Modulation of $GABA_A$ receptors by Piperine Derivatives

Supporting Information

Efficient Modulation of γ-Aminobutyric Acid Type A ($GABA_A$) Receptors by Piperine Derivatives

Angela Schöffmann, Laurin Wimmer, Daria Goldmann, Sophia Khom, Juliane Hintersteiner, Igor Baburin, Thomas Schwarz, Michael Hintersteininger, Peter Pakfeifer, Mouhssin Oufir, Matthias Hamburger, Thomas Erker, Gerhard F. Ecker, Marko D. Mihovilovic, Steffen Hering

Content of Supplementary Information

1 Synthetic procedures and characterization data for piperine analogues

1.1 General Methods

Method A: Hydrolysis of Methyl Esters

Methylester (0.8mmol, 1equiv.) was suspended in THF/water 1:1 (7.5ml/mmol ester). Lithium hydoxide (1.3equiv.) was added and the reaction mixture was stirred at rt until reaction control by TLC showed complete consumption of the starting material. The solution was adjusted to pH = 1 by addition of 0.5N HCl followed by extraction with ethyl acetate. The combined organic extracts were washed with water and brine, dried over sodium sulfate and evaporated. If necessary, the crude product was recrystallized from water/ethanol to afford the pure product.

Method B: Suzuki Cross-Coupling Reactions

Amounts are given for 1mmol of starting material. The corresponding boronic acid (1mmol, 1equiv.), aryl bromide (1equiv.), $Pd(PPh_3)_4$ (2mol%) and sodium carbonate (7equiv.) were placed in a microwave vial. Then a mixture of DME/EtOH 5:1 (7.7ml) and water (2.2ml) were added and the resulting suspension was degassed by passing through argon for 5 minutes. The vial was closed and heated to 140°C for 1 hour in the microwave. The reaction was monitored by TLC.

Work-up procedure for carboxylic acid products:

The reaction mixture was diluted with water (30ml) and extracted with DCM (16ml). Then the aqueous phase was acidified to pH = 1 by addition of 1.4ml of HCl conc. and extracted 4x11ml of ethylacetate. The organic extracts were washed with brine and dried with sodium sulfate. Evaporation of the solvent afforded the crude product. The pure products were obtained by recrystallization from water/EtOH mixtures.

Work-up procedure for amide products:

The reaction mixture was extracted with DCM, the solvent evaporated and the crude product directly subjected to column chromatography using LP/EtOAc mixtures as eluent.

Method C: Synthesis of amides from carboxylic acids via acid chlorides

To a suspension of carboxylic acid (0.2mmol, 1equiv.) in dry dichloromethane (3ml) under argon at 0°C was added oxalyl chloride (1.2equiv.) via microliter syringe. Then two drops of DMF were added immediately resulting in the evolution of gas. The reaction mixture was allowed to warm to rt. Stirring continued until the evolution of gas ceased (10-30min) and a clear solution was obtained.

The reaction mixture was again cooled to 0°C and the corresponding amine (0.5ml) in DCM (1.5ml) was added. Then the solution was allowed to reach rt and stirring continued overnight.

Washing of the reaction mixture with each 7ml of 2N HCl, sat. $NaHCO_3$, water and brine followed by drying of the organic phase with sodium sulfate and evaporation of the solvent afforded the crude product. The pure product was obtained after column chromatography (10g

SiO_2, LP/EtOAc mixtures 10:1 to 2:1) and removal of all volatiles in vacuum (<0.1mbar). In some cases vacuum together with elevated temperatures up to 80°C had to be applied in order to remove trace impurities from the product.

Method D: This is a modification of Method C: Here the intermediate acid chloride solution was evaporated to dryness at 50°C and reduced pressure. The resulting solid was redissolved in anhydrous DCM (3ml) under argon and used as described in Method C.

Removal of the excess oxalyl chloride eliminates the formation of oxalylic diamide, an impurity which can be difficult to remove in some cases.

Method E: Synthesis of amides from carboxylic acids using EDCI·HCl/HOBt

To a suspension of the carboxylic acid (0.17mmol, 1equiv.) and HOBt (2 equiv.) in dry dichloromethane (2ml) under argon at rt was added EDCI·HCl (2equiv.). After 2 hours the suspension was transformed into an opaque solution and TLC indicated full consumption of the starting material. The corresponding amine (0.5ml) was added at rt and stirring continued overnight.

After full conversion was detected by TLC the reaction mixture was diluted with EtOAc (30ml) and washed with each 20ml of 0.5N HCl, sat. $NaHCO_3$, brine, dried with sodium sulfate and evaporated. The crude product was purified by column chromatography using LP/EtOAc mixtures as eluent.

Method F: Piperic acid chloride (1mmol, 218mg) was dissolved in 2.5ml of dry THF. The corresponding amine (3.5mmol) was added and the reaction mixture was stirred overnight at rt. After evaporation of the solvent the residue was suspended in water, filtered and washed. Pure products were obtained after recrystallization.

Method G: Piperic acid chloride (1mmol, 218mg) was dissolved in 2.5ml of dry THF. The corresponding amine (3.5mmol) was added and the reaction mixture was stirred overnight at rt. After evaporation of the solvent the residue was taken up in EtOAc (40ml) and washed three times with water. The organic layer was separated, dried with sodium sulfate, filtered and evaporated.

Method H: Piperic acid chloride (1mmol, 218mg) was dissolved in 2.5ml of dry THF. The corresponding amine (3.5mmol) was added and the reaction mixture was stirred overnight at rt. After evaporation of the solvent the residue was taken up in EtOAc (40ml) and washed two times with each $NaHCO_3$ 5% and 2N HCl. The organic layer was separated, dried with sodium sulfate, filtered and evaporated.

1.2 Compound synthesis and characterization data

***(2E,4E)*-5-(1,3-Benzodioxol-5-yl)-*N*-(4-(methylthio)phenyl)-2,4-pentadienamide (1)**

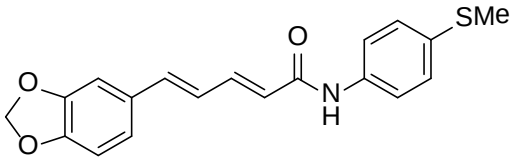

Method: F

The pure product was obtained by recrystallization from ethanol.

Yield: 77% (780mg, 2.31mmol)

Appearance: beige crystals

M.p.: 200-201°C

^{1}H NMR (DMSO, 200MHz): δ= 2.44 (s, 3H), 6.05 (s, 2H), 6.27 (d, *J* = 14.8 Hz, 1H), 7.10 6.87 (m, 4H), 7.40-7.18 (m, 4H), 7.65 (d, *J* = 8.6 Hz, 2H), 10.12 (s, 1H)

^{13}C (DMSO, 50MHz): δ= 15.5 (q), 101.3 (t, O-CH_2-O), 105.7(d), 108.5(d), 119.8(d), 123.0(d), 124.2(d), 125.1(d), 127.1(d), 130.8(s), 131.7(s), 136.9(s), 138.9(d), 141.0(d), 147.9(s, C-O), 148.0(s, C-O), 163.8 (s, CO-NH)

CHN-Analysis: found: C 65.97%, H 4.54%, N 4.07% (calculated (·0.4H_2O): C 65.84%, H 5.18%, N 4.04%).

***(2E,4E)*-5-(1,3-Benzodioxol-5-yl)-*N*-(3,4,5-trimethoxyphenyl)-2,4-pentadienamide (2)**

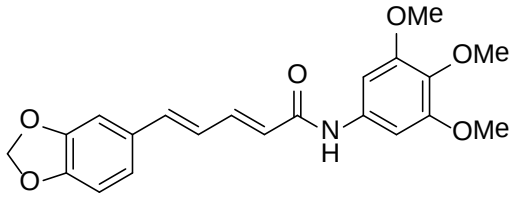

Method: H

The pure product was obtained by recrystallization from ethanol.

Yield: 35% (267mg, 0.69mmol)

Appearance: yellow crystals

M.p.: 153-156°C

^{1}H NMR (DMSO-d_6, 200MHz): δ= 3.62 (s, 3H, 4'-CH_3), 3.75 (s, 6H, 3'-CH_3, 5'-CH_3), 6.06 (s, 2H, O-CH_2-O), 6.62 (d, *J* = 14.7 Hz, 1H, H2), 6.88-7.06 (m, 4H), 7.09 (s, 2H), 7.20-7.37 (m, 2H), 10.6 (s, 1H, CO-NH).

^{13}C (DMSO-d_6, 50MHz): δ= 55.7(q), 60.1(q), 96.8(d), 101.3(t, O-CH_2-O), 105.7 (d), 108.5 (d), 123.0(d), 124.4 (d), 125.1(d), 130.8(s), 133.4(s), 135.6(s), 138.9(d), 140.9(d), 147.9(s, C-O), 148.0 (s, C-O, 152.7(s), 163.7 (s, CO-NH).

CHN-Analysis: found: C 65.25%, H 5.26%, N 3.47% (calculated (·0.2H_2O): C 65.17%, H 5.57%, N 3.62%).

(2E,4E)*-5-(1,3-Benzodioxol-5-yl)-*N*-(2,4,6-trifluorophenyl)-2,4-pentadienamide *(3)

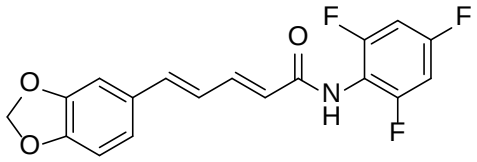

Method: F

The pure product was obtained by recrystallization from ethanol.

Yield: 75% (778mg, 2.24mmol)

Appearance: pale yellow crystals

M.p.: 234-235°C

^{1}H NMR (DMSO-*d6*, 200MHz): δ= 6.05 (s, 2H, O-CH_2-O), 6.30 (d, *J* = 14.9 Hz, 1H, H2), 7.07-6.87 (m, 4H), 7.40-7.21 (m, 4H), 9.80 (s, 1H, CONH).

^{13}C (DMSO-*d6*, 50MHz): δ= 100.4-101.4 (m, CH-F coupling, C3', C5'), 101.4 (t, O-CH_2-O), 105.8(d), 108.5(d), 111.2-112.0 (m, C_q-F coupling), 122.3 (d), 123.1(d), 124.9(d), 130.7(s), 139.6(d), 142.0(d), 148.0(s, O-CH_2-O), 155.2-160.7 (m, C_q-F coupling), 157.1-162.6 (m, C_q-F coupling), 164.3 (s, CO-NH)

CHN-Analysis: found: C 62.00%, H 3.21%, N 3.97% (calculated: C 62.25%, H 3.48%, N 4.03%).

***(2E,4E)*-5-(1,3-Benzodioxol-5-yl)-*N*-(2-(dimethylamino)ethyl)-2,4-pentadienamide (4)**

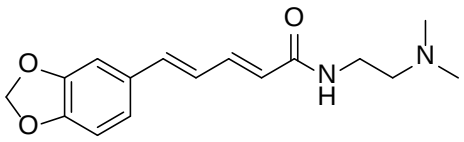

Method: H

The pure product was obtained by recrystallization from toluene.

Yield: 62% (450mg, 1.87mmol)

Appearance: pale orange crystals

M.p.: 131°C

^{1}H NMR (DMSO-d_6, 200MHz): δ= 2.14 (s, 6H, CH_3), 2.30 (t, *J* = 6.6 Hz, 2H), 3.29-3.16 (m, 2H), 6.04 (s, 2H, O-CH_2-O), 6.10 (d, *J* = 14.8 Hz, 1H, H2), 7.03-6.83 (m, 4H), 7.14 (ddd, *J* = 14.8, 8.4, 1.8 Hz, 1H), 7.25 (s, 1H), 7.98 (t, *J* = 5.5 Hz, 1H, CO-NH).

^{13}C (DMSO-d_6, 50MHz): δ= 36.8 (t, $NHCH_2$), 45.2 (q, CH_3), 58.4 (t, CH_2-N), 101.3 (t, O-CH_2-O), 105.6(d), 108.4(d), 122.6(d), 124.6(d), 125.3(d), 130.9(s), 137.8(d), 139.2(d), 147.7(s, C-O), 147.9(s, C-O), 165.1 (s, CONH).

CHN-Analysis: found: C 66.52%, H 6.83%, N 9.66% (calculated: C 66.65%, H 6.99%, N 9.72%).

***(2E,4E)*-5-(1,3-Benzodioxol-5-yl)-*N*-(2-(3,4-dimethoxyphenyl)ethyl)-2,4-pentadienamide (5)**

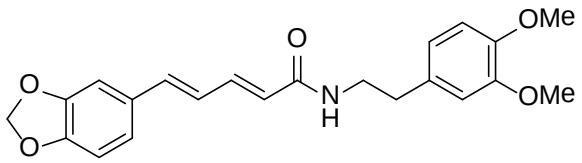

Method: G

Yield: 58% (661mg, 1.73mmol)

Appearance: amorphous colorless solid

M.p.: 185-188°C

CHN-Analysis: found: C 68.79%, H 5.77%, N 3.57% (calculated (·0.15 H_2O): C 68.79%, H 6.11%, N 3.65%).

Spectral data is in agreement with literature.[1]

***(2E,4E)*-5-(1,3-Benzodioxol-5-yl)-*N*-(pyridin-3-yl)-2,4-pentadienamide (6)**

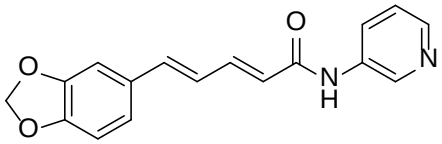

Method: G

The pure product was obtained by recrystallization from ethyl acetate.

Yield: 39% (347mg, 1.04mmol)

Appearance: amorphous grey solid

M.p.: 209-210°C

^{1}H NMR (DMSO-d_6, 200MHz): δ= 6.05 (s, 2H, O-CH_2-O), 6.30 (d, J = 14.8 Hz, 1H, H2), 6.85-7.17 (m, 4H), 7.26-7.53 (m, 3H), 8.14 (dd, J = 8.2, 1.3 Hz, 1H), 8.26 (d, J = 4.5 Hz, 1H), 8.81 (d, J = 2.1 Hz, 1H), 10.34 (s, 1H, CONH).

^{13}C (DMSO-d_6, 50MHz): δ= 101.3 (O-CH_2-O), 105.8(d), 108.5(d), 123.1(d), 123.6(d), 123.7(d), 125.0(d), 126.0(d), 130.7(s), 136.1(s), 139.5(d), 140.8(d), 141.7(d), 144.1(d), 148.0 (s, C-O), 164.4 (s, CONH).

CHN-Analysis: found: C 68.71%, H 4.54%, N 9.35% (calculated (·0.2 H_2O): C 68.54%, H 4.87%, N 9.40%).

***(2E,4E)*-5-(1,3-Benzodioxol-5-yl)-*N*-(5-chloropyridin-2-yl)-2,4-pentadienamide (7)**

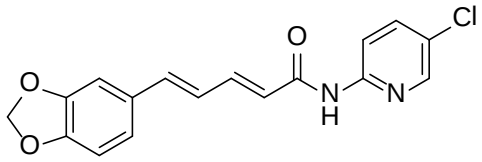

Method: G

The pure product was obtained by recrystallization from ethanol.

Yield: 29% (282mg, 0.86mmol)

Appearance: yellow crystals

M.p.: 216-218°C

^{1}H NMR (DMSO-d_6, 200MHz): δ= 6.05 (s, 2H, O-CH_2-O), 6.45 (d, *J* = 14.9 Hz, 1H, H2), 6.87-7.08 (m, 4H), 7.23 (dd, J_1 = 5.5, J_2 = 1.8 Hz, 1H), 7.30-7.33 (m, 1H), 7.33-7.48 (m, 1H), 8.21-8.41 (m, 2H), 10.95 (s, 1H, CONH).

^{13}C (DMSO-d_6, 50MHz): δ= 101.3 (t, O-CH_2-O), 105.8(d), 108.5(d), 113.1(d), 119.3(d), 123.2(d), 123.3(d), 124.8(d), 130.6(s), 140.1(d), 142.6(d), 143.9(s), 148.0(s), 148.1(s), 149.5(d), 153.5(s), 164.8(s, CO-NH).

CHN-Analysis: found: C 60.80%, H 3.83%, N 8.10% (calculated (·0.4H_2O): C 60.78%, H 4.14%, N 8.34%).

***(2E,4E)*-5-(1,3-Benzodioxol-5-yl)-*N*-(3-phenylpropyl)-2,4-pentadienamide (8)**

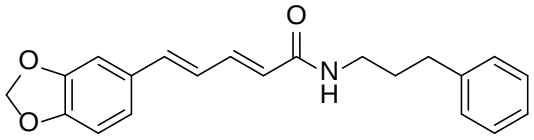

Method: F

The pure product was obtained by recrystallization from ethanol.

Yield: 69% (693mg, 2.07mmol)

Appearance: orange crystals

M.p.: 161-162°C

^{1}H NMR ($CDCl_3$, 200MHz): δ= 1.98 (bm, 2H, CH_2), 2.71 (t, *J* = 7 Hz, 2H, CH_2-Ph), 3.45 (t, *J* = 7 Hz, 2H, NH-CH_2), 5.90 (d, *J* = 14 Hz, 1H), 6.01 (s, 1H, O-CH_2-O), 6.54-7.06 (m, 5H), 7.12-7.48 (m, 6H).

^{13}C ($CDCl_3$, 50MHz): δ= 30.6 (t, CH_2), 33.4(t,CH_2), 40.9(t, CH_2-NH), 101.7(t, O-CH_2-O), 106.2(d), 108.9(d), 119.0(d), 123.8(s), 123.8(d), 126.6(d), 128.6(d), 128.9(d), 130.3(s), 142.8(d), 145.2(d), 148.6(s), 169.6(s, CO-NH).

CHN-Analysis: found: C 74.62%, H 6.10%, N 4.10% (calculated (·0.15H_2O): C 74.60%, H 6.35%, N 4.14%).

***(2E,4E)*-5-(1,3-Benzodioxol-5-yl)-*N*-(2-hydroxyphenyl)-2,4-pentadienamide (9)**

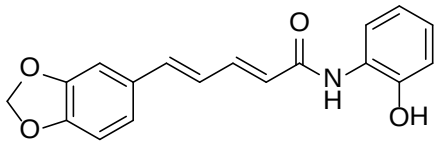

Method: F

The pure product was obtained by recrystallization from ethanol.

Yield: 45% (414mg, 1.34mmol)

Appearance: black crystals

M.p.: 192-193°C

^{1}H NMR (DMSO-d_6, 200MHz): δ= 6.05 (s, 2H, O-CH_2-O), 6.52 (d, *J* = 14.8 Hz, 1H), 6.73-7.10 (m, 7H), 7.24-7.43 (m, 2H), 7.76 (d, *J* = 7.6 Hz, 1H), 9.58 (s, 1H, OH), 9.94 (s, 1H, CO-NH).

^{13}C (DMSO-d_6, 50MHz): δ= 101.3 (t, O-CH_2-O), 105.7 (d), 108.5(d), 116.2(d), 119.1(d), 122.3 (d), 122.9(d), 124.0(d), 124.9(d), 125.0(d), 126.5(s), 130.7(s), 139.1(d), 141.3(d), 147.9(s), 148.0(s), 164.5(s, CO-NH).

CHN-Analysis: found: C 69.56%, H 4.64%, N 4.59% (calculated: C 69.89%, H 4.89%, N 4.53%).

***(2E,4E)*-5-(1,3-Benzodioxol-5-yl)-*N*-(2-hydroxy-4-nitrophenyl)-2,4-pentadienamide (10)**

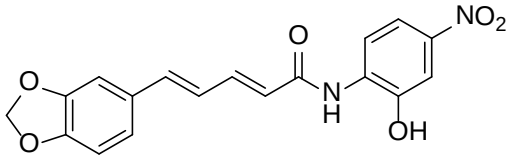

Method: F

The pure product was obtained by recrystallization from 1,4-dioxane.

Yield: 16% (171mg, 0.48mmol)

Appearance: yellow solid

M.p.: 284-286°C

^{1}H NMR (DMSO-d_6, 200MHz): δ= 6.01 (s, 2H, O-CH_2-O), 6.61 (d, *J* = 14.8 Hz, 1H), 6.79-7.12 (m, 5H), 7.19-7.55 (m, 2H), 7.87 (dd, *J* = 8.9, 2.6 Hz, 1H), 9.07 (s, 1H, CO-NH).

^{13}C (DMSO-d_6, 50MHz): δ= 101.6 (t, O-CH_2-O), 106.0(d), 108.7(d), 114.9(d), 116.8(d), 120.7(d), 123.2(d), 124.1(d), 125.2(d), 127.2(s), 131.0(s), 139.7(s), 139.7(d), 142.1(d), 148.3(s, C-O), 153.8(s, C-NO_2), 165.0(s, CO-NH).

CHN-Analysis: found: C 60.15%, H 4.34%, N 6.92% (calculated (· 0.45 dioxane): C 60.36%, H 4.50%, N 7.11%).

***(2E,4E)*-5-(1,3-Benzodioxol-5-yl)-*N*-butyl-2,4-pentadienamide (11)**

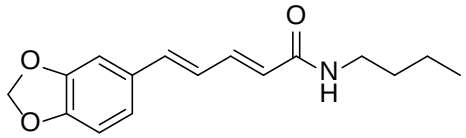

Method: F

The pure product was obtained by recrystallization from ethanol.

Yield: 45% (366mg, 1.34 mmol)

Appearance: beige crystals

M.p.: 141-143°C

CHN-Analysis: found: C 69.24%, H 6.64%, N 4.68% (calculated (·0.25 H_2O): C 69.17%, H 7.07%, N 5.04%).

Spectral data is in agreement with literature.[2]

***(2E,4E)*-5-(1,3-Benzodioxol-5-yl)-*N*-(3,3-diphenylpropyl)-2,4-pentadienamide (12)**

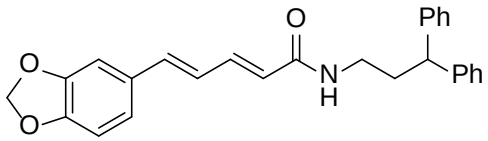

Method: G

The pure product was obtained after flash column chromatography (SiO_2, eluent: LP/EtOAc 20%)

Yield: 55% (682mg, 1.66mmol)

Appearance: colorless crystals

M.p.: 125-127°C

^{1}H NMR (DMSO-d_6, 200MHz): δ= 2.13-2.28 (m, 2H, CH_2), 2.93-3.13 (m, 2H, N-CH_2), 3.91-4.07 (m, 1H, $CHPh_2$), 6.00 (s, 2H, O-CH_2-O), 6.08 (d, *J* = 14.8 Hz, 1H, H2), 6.75-7.02 (m, 4H), 7.07-7.34 (m, 12H).

^{13}C (DMSO-d_6, 50MHz): δ= 34.8 (t, CH_2), 37.7(t, NH-CH_2), 48.4 (d, $CHPh_2$), 101.5 (t, O-CH_2-O), 105.9(d), 108.7(d), 122.9(d), 124.7(d), 125.5(d), 126.4(d), 127.9(d), 128.7(d), 131.2(s), 138.1(d), 139.6(d), 145.0(s), 148.1(s, C-O), 148.3(s, C-O), 165.5(s, CO-NH).

CHN-Analysis: found: C 78.68%, H 5.93%, N 3.40% (calculated (·0.1 H_2O): C 78.46%, H 6.15%, N 3.39%).

***(2E,4E)*-5-(1,3-Benzodioxol-5-yl)-*N*-cyclopentyl-2,4-pentadienamide (13)**

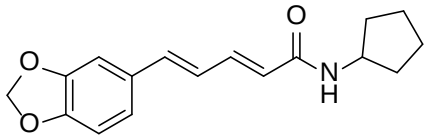

Method: F

The pure product was obtained by recrystallization from ethanol.

Yield: 55% (474mg, 1.66mmol)

Appearance: pale pink crystals

M.p.: 189-190°C

^{1}H NMR ($CDCl_3$, 200MHz): δ= 1.33-1.53 (m, 2H), 1.54-1.80 (m, 4H), 1.90-2.15 (m, 2H), 4.21-4.42 (m, 1H), 5.73 (d, *J* = 7.2 Hz, 1H), 5.85-6.04 (m, 3H, O-CH_2-O, H2), 6.56-6.82 (m, 3H), 6.87 (d, *J* = 8.1 Hz, 1H), 6.95 (s, 1H), 7.35 (dd, *J* = 14.8, 9.6 Hz, 1H).

^{13}C ($CDCl_3$, 50MHz): δ= 23.9(t, CH_2, H3', H4'), 33.4(t, CH_2, H2', H5'), 51.4(d, N-CH), 101.5(t, O-CH_2-O), 105.8(d), 108.6(d), 122.8(d), 123.6(d), 124.9(d), 131.0(s), 138.8(d), 140.9(d), 148.3(s, C-O), 165.9(s, CO-NH).

CHN-Analysis: found: C 71.75%, H 6.50%, N 4.84% (calculated: C 71.56%, H 6.71%, N 4.91%).

***(2E,4E)*-5-(1,3-Benzodioxol-5-yl)-*N*-benzyl-2,4-pentadienamide (14)**

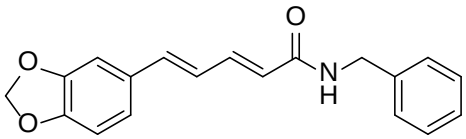

Method: F

The pure product was obtained by recrystallization from toluene.

Yield: 78% (722mg, 2.35mmol)

Appearance: colorless crystals

M.p.: 180-182°C

CHN-Analysis: found: C 74.19%, H 5.28%, N 4.50% (calculated: C 74.25%, H 5.58%, N 4.56%).

Spectral data is in agreement with literature.[3]

(2E,4E)-5-(1,3-Benzodioxol-5-yl)-*N*-decyl-2,4-pentadienamide (15)

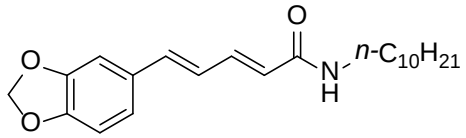

Method: G

The pure product was obtained by recrystallization from ethyl acetate.

Yield: 85% (912mg, 2.55mmol)

Appearance: colorless crystals

M.p.: 102-105°C

CHN-Analysis: found: C 71.50%, H 10.14%, N 5.49% (calculated (·0.75 H_2O): C 71.22%, H 8.83%, N 3.78%).

Spectral data is in agreement with literature.[4]

(2E,4E)-5-(1,3-Benzodioxol-5-yl)-*N*-adamantyl-2,4-pentadienamide (16)

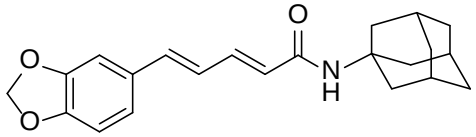

A flame-dried round bottom flask was charged with adamantylamine hydrochloride (3.5equiv., 10.5mmol, 1.97g) which was dissolved in dry THF (5ml). The solution was treated with triethylamine (3.5equiv., 10.5mmol, 1.06g) at rt. To this solution piperic acid chloride (1 equiv., 3mmol, 710mg) was added and stirred overnight. The solvent was evaporated and the residue taken up in water. The precipitate was collected and recrystallized from toluene.

Yield: 50% (523mg, 1.49mmol)

Appearance: beige crystals

M.p.: 156-158°C

CHN-Analysis: found: C 74.81%, 6.99H %, N 3.91% (calculated (·0.15 H_2O): C 74.61%, H 7.20%, N 3.96%).

Spectral data is in agreement with literature.[4]

***(2E)*-3-(1,3-Benzodioxol-5-yl)-1-(1-piperidinyl)-2-propen-1-one (17)**

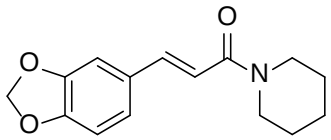

Prepared analogously to method G from 3,4-(methylenedioxy)cinnamoyl chloride (632mg, 3mmol). The pure product was obtained by recrystallization from LP.

Yield: 25% (191mg, 0.74mmol)

Appearance: colorless crystals

M.p.: 86°C[5]

CHN-Analysis: found: C 69.48%, H 6.35%, N 5.32% (calculated: C 69.48%, H 6.61%, N 5.40%).

Spectral data is in agreement with literature.[5]

***(2E)*-3-(1,3-Benzodioxol-5-yl)-*N*,*N*-diisopropyl-2-propenamide (18)**

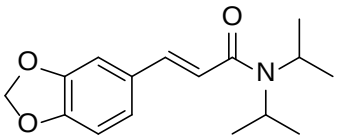

Prepared analogously to method G from 3,4-(methylenedioxy)cinnamoyl chloride (632mg, 3mmol). The pure product was obtained by recrystallization from ethanol.

Yield: 66% (544mg, 1.98mmol)

Appearance: colorless crystals

M.p.: 138-139°C

CHN-Analysis: found: C 69.75%, H 7.45%, N 5.02% (calculated: C 69.79%, H 7.69%, N 5.09%).

Spectral data is in agreement with literature.[6]

***(2E,4E)*-5-(1,3-Benzodioxol-5-yl)-*N*,*N*-dimethyl-2,4-pentadienamide (20)**

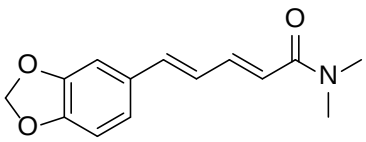

Method: F

The pure product was obtained by recrystallization from toluene.

Yield: 48% (354mg, 1.44mmol)

Appearance: beige crystals

M.p.: 148-150°C

^{1}H NMR ($CDCl_3$, 200MHz): δ= 3.04(s, 3H, CH_3), 3.11 (s, 3H, CH_3), 5.98(s, 2H, O-CH_2-O), 6.42 (d, J = 14.7Hz, 1H, H2), 6.71-6.83 (m, 3H), 6.86-6.95 (m, 1H), 6.98 (s, 1H), 7.33-7.53 (m, 1H)

^{13}C ($CDCl_3$, 50MHz): δ= 36.0(q, CH_3), 37.5 (q, CH_3), 101.5 (t, O-CH_2-O), 105.8 (d), 108.7(d), 122.8 (d), 125.4 (d), 131.1(s), 138.8 (d), 142.7 (d), 148.4 (s, C-O), 167.0 (s, CO-NH)

CHN-Analysis: found: C 68.15%, H 5.88%, N 5.23% (calculated (·0.1 H_2O:) C 68.06%, H 6.20%, N 5.67%.

***(2E,4E)*-5-(1,3-Benzodioxol-5-yl)-*N*,*N*-diethyl-2,4-pentadienamide (21)**

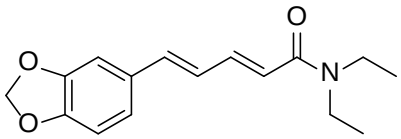

Method: G

The pure product was obtained by recrystallization from ethanol.

Yield: 27% (0.82mmol, 224mg)

Appearance: orange crystals

M.p.: 87-88°C

^{1}H NMR ($CDCl_3$, 200MHz): δ= 1.08-1.33 (m, 6H, CH_3), 3.34-3-54 (m, 4H, CH_2), 5.98 (s, 2H, O-CH_2-O), 6.36 (d, J = 14.6Hz, 1H, H2), 6.72-6.82 (m, 3H), 6.85-6.95 (m, 1H), 6.99 (s, 1H, H4'), 7.38-7.53 (m, 1H)

^{13}C ($CDCl_3$, 50MHz): δ= 13.4 (q), 15.2 (q), 41.1 (t, N-CH_2), 42.4 (t, N-CH_2), 101.5 (t, O-CH_2-O), 105.9 (d), 108.7 (d), 120.4 (d), 122.7 (d), 125.5 (d), 131.2 (s), 138.6 (d), 142.7 (d), 148.4 (s, 2C, C-O), 166.0 (q, CO-N)

CHN-Analysis: found: C 69.60%, H 6.65%, N 4.53% (calculated (·0.14 H_2O): C 69.67%, H 7.04%, N 5.08%).

***(2E,4E)*-5-(1,3-Benzodioxol-5-yl)-*N*,*N*-diisopropyl-2,4-pentadienamide (22)**

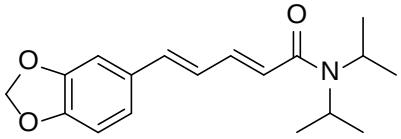

Method: G

The pure product was obtained after column chromatography (SiO_2, eluent: toluene/EtOAc 20%).

Yield: 53% (1.58mmol, 476mg)

Appearance: yellow solid

M.p.: 80-82°C

^{1}H NMR ($CDCl_3$, 200MHz): δ= 1.33 (s, 12H, CH_3), 3.64-4.23 (m, 2H, N-CH), 5.97 (s, 2H, O-CH_2-O), 6.38(d, J= 14.6Hz, 1H, H2), 6.70-6.83 (m, 3H), 6.85-6.93(m, 1H), 6.98 (d, J = 1.6Hz, 1H), 7.36 (ddd, J^1 = 14.6Hz, J^2 = 6.0Hz, J^3 = 4.3Hz, 1H)

^{13}C ($CDCl_3$, 50MHz): δ= 20.9 (q, CH_3, 2C), 21.8 (q, CH_3, 2C), 46.0 (d, N-CH), 48.2 (d, N-CH), 101.4(t, O-CH_2-O), 105.8 (d), 108.6(d), 122.6(d), 123.2(d), 125.7(d), 131.3(s), 138.0(d), 141.5(d), 148.2(s, C-O), 148.3(s, C-O), 166.4(s, CO-N)

CHN-Analysis: found: C 71.85%, H 7.48%, N 4.57% (calculated: C 71.73%, H 7.69%, N 4.65%).

***(2E,4E)*-5-(1,3-Benzodioxol-5-yl)-*N*,*N*-dipropyl-2,4-pentadienamide (23)**

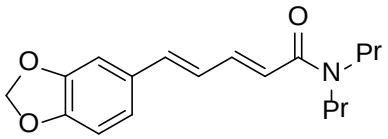

Method: G

Yield: 61% (1.83mmol, 554mg)

Appearance: yellow crystals

M.p.: 59-62°C

^{1}H NMR ($CDCl_3$, 200MHz): δ= 0.84-1.03 (m, 6H, CH_3), 1.48-1.74 (m, 4H, CH_2), 3.22-3.44 (m, 4H, CH_2), 5.97 (s, 2H, O-CH_2-O), 6.36 (d, J = 14.6Hz, 1H, H2), 6.71-6.82 (m, 3H), 6.86-6.95 (m, 1H), 6.99 (d, J = 1.4Hz, 1H, H4'), 7.37-7.54 (m, 1H)

^{13}C ($CDCl_3$, 50MHz): δ= 11.5 (q, CH_3), 11.6 (q, CH_3), 21.3 (t, CH_2), 23.2 (t, CH_2), 48.7 (t, CH_2), 50.0 (t, CH_2), 101.4 (t, O-CH_2-O), 105.8 (d), 108.6 (d), 120.5 (d), 122.7 (d), 125.5 (d), 131.2 (s), 138.5 (d), 142.6 (d), 148.3 (s, C-O), 148.4 (s, C-O), 166.4 (s, CO-N)

CHN-Analysis: found: C 72.04%, H 7.58%, N 4.60% (calculated: C 71.73%, H 7.69%, N 4.65%).

***(2E,4E)*-5-(1,3-Benzodioxol-5-yl)-*N*,*N*-dihexyl-2,4-pentadienamide (26)**

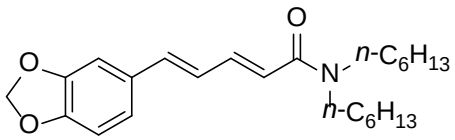

Method: G

The pure product was obtained after column chromatography (SiO_2, eluent: toluene/EtOAc 20%).

Yield: 76% (2.27mmol, 877mg)

Appearance: orange solid

M.p.: 49-50°C

^{1}H NMR ($CDCl_3$, 200MHz): δ= 0.82-0.99 (m, 6H, CH_3), 1.22-1.40 (m, 12H, CH_2), 1.46-1.71 (m, 4H, CH_2), 3.23-3.47(m, 4H, N-CH_2), 5.97(s, O-CH_2-O), 6.35 (d, J=14.6Hz, 1H, H2), 6.70-6.85 (m, 3H), 6.90 (dd, J^1 = 8.0Hz, J^2 = 1.5Hz, 1H), 7.00 (d, J= 1.4Hz, 1H), 7.35-7.53 (m, 1H)

^{13}C NMR ($CDCl_3$, 50MHz): δ= 14.2 (q, CH_3, 2C), 22.8 (t, CH_2, 2C), 26.8 (t, CH_2), 27.0 (t, CH_2), 28.1 (t, CH_2), 30.0 (t, CH_2), 31.7(t, CH_2), 31.9(t, CH_2), 47.1(t, N-CH_2), 48.4 (t, N-CH_2), 101.5 (t, O-CH_2-O), 105.9 (d), 108.7 (d), 120.5(d), 122.7(d), 125.6(d), 131.2(s), 138.5 (d), 142.6(d), 148.3(s, C-O), 148.4(s, C-O), 166.3(s, CO-N)

CHN-Analysis: found: C 74.71%, H 8.95%, N 3.57% (calculated: C 74.77%, H 9.15%, N 3.63%).

***(2E,4E)*-5-(1,3-Benzodioxol-5-yl)-*N*,*N*-dicyclohexyl-2,4-pentadienamide (27)**

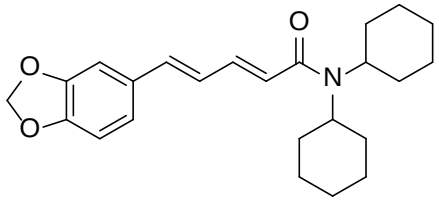

Method: G

The pure product was obtained after recrystallization from toluene.

Yield: 10% (0.29mmol, 112mg)

Appearance: colorless crystals

M.p.: 133-134°C

^{1}H NMR ($CDCl_3$, 200MHz): δ= 1.04 - 1.97 (m, 20H, CH_2), 3.20-3.79 (m, 2H, CH), 5.79 (s, O-CH_2-O), 6.39 (d, J=14.6Hz, 1H, H2), 6.66-6.82 (m, 3H), 6.90 (dd, J^1 = 8.1Hz, J^2 = 1.6Hz, 1H), 7.00 (d, J= 1.5Hz, 1H), 7.34 (ddd, J^1=14.7Hz, J^2=7.4Hz, J^3=2.9Hz, 1H)

^{13}C NMR ($CDCl_3$, 50MHz): δ= 25.0 (t, CH_2, 2C), 25.6 (t, CH_2, 2C), 26.4 (t, CH_2), 26.6 (t, CH_2), 30.5 (t, CH_2, 2C), 32.1 (t, CH_2, 2C), 53.8 (t, N-CH_2, 2C), 101.4 (t, O-CH_2-O), 105.8

(d), 108.7 (d), 122.6(d), 123.4(d), 125.8(d), 131.3(s), 137.9 (d), 141.5(d), 148.2(s), 148.4(s), 166.6(s, CO-N)

CHN-Analysis: found: C 73.77%, H 7.78%, N 3.65% (calculated (·0.45H_2O) : C 73.99%, H 8.25%, N 3.60%).

***(2E,4E)*-1-(Azepan-1-yl)-5-(1,3-benzodioxol-5-yl)-2,4-pentadien-1-one (28)**

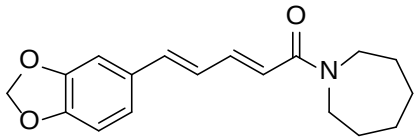

Method: F

The pure product was obtained after recrystallization from ethanol.

Yield: 26% (0.52, 155mg)

Appearance: light brown crystals

M.p.: 120-121°C

^{1}H NMR ($CDCl_3$, 200MHz): δ= 1.38 - 1.55 (m, 4H, CH_2), 1.57-1.73 (m, 4H, CH_2), 3.42-3.61 (m, 4H, CH_2), 6.04 (s, O-CH_2-O), 6.59 (d, J=14.4Hz, 1H, H2), 6.81-7.09 (m, 4H), 7.15-7.34 (m, 2H)

^{13}C NMR ($CDCl_3$, 50MHz): δ= 26.0 (t, CH_2), 26.4 (t, CH_2), 27.3 (t, CH_2), 29.0 (t, CH_2), 45.7 (t, N-CH_2), 47.1 (t, N-CH_2), 101.3 (t, O-CH_2-O), 105.5 (d), 108.5 (d), 121.0(d), 122.6(d), 125.7(d), 130.9(s), 137.8 (d), 141.7(d), 147.8(s, C-O), 147.9(s, C-O), 165.2(s, CO-N)

CHN-Analysis: found: C 72.12%, H 6.52%, N 4.42% (calculated (·0.08H_2O) : C 71.87%, H 7.09%, N 4.66%).

***(2E,4E)*-5-(1,3-Benzodioxol-5-yl)-1-(4-morpholinyl)-2,4-pentadien-1-one (29)**

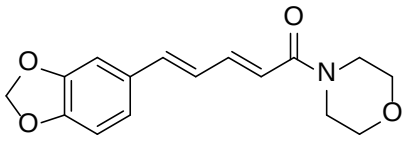

Method: F

The pure product was obtained after recrystallization from ethanol.

Yield: 56% (0.38mmol, 110mg)

Appearance: yellow crystals

M.p.: 176-179°C

^{1}H NMR ($CDCl_3$, 200MHz): δ= 3.50-3.85 (m, 8H, CH_2), 5.98 (s, O-CH_2-O), 6.37 (d, J=14.6Hz, 1H, H2), 6.63-6.83 (m, 3H), 6.90 (dd, J=8.1Hz, J=1.5Hz, 1H), 6.98 (d, J=1.4Hz, 1H), 7.46 (ddd, J^1= 14.7Hz, J^2= 9.0Hz, J^3=1.1Hz, 1H)

^{13}C NMR ($CDCl_3$, 50MHz): δ= 67.1 (t, CH_2, 4C), 101.5 (t, O-CH_2-O), 105.9 (d), 108.7 (d), 118.9(d), 122.9(d), 125.2(d), 131.0 (s), 139.3 (d), 143.7(d), 148.4(s), 148.5(s), 165.9(s, CO-N)

CHN-Analysis: found: C 66.45%, H 5.73%, N 4.80% (calculated (0.1H_2O) : C 66.47%, H 6.00%, N 4.84%).

***(2E,4E)*-5-(1,3-Benzodioxol-5-yl)-1-(4-thiomorpholinyl)-2,4-pentadien-1-one (30)**

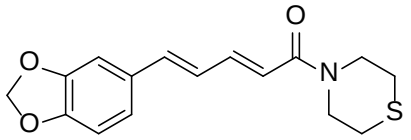

Method: H

The pure product was obtained after recrystallization from ethanol.

Yield: 50% (1.00mmol, 304mg)

Appearance: light brown crystals

M.p.: 125-127°C

^{1}H NMR ($CDCl_3$, 200MHz): δ= 2.54-2.72(m, 4H, S-CH_2), 3.69-3.95 (m, 4H, N-CH_2), 6.05 (s, O-CH_2-O), 6.66 (d, J=14.5Hz, 1H, H2), 6.87-7.04 (m, 4H), 7.13-7.34 (m, 2H)

^{13}C NMR ($CDCl_3$, 50MHz): δ= 25.8 (t, S-CH_2), 26.6 (t, S-CH_2), 44.3 (t, N-CH_2), 45.1(t, N-CH_2), 101.3 (t, O-CH_2-O), 105.5 (d), 108.5 (d), 120.3(d), 122.6(d), 125.5(d), 130.8 (s), 138.1 (d), 142.4(d), 147.8 (s, C-O), 148.0 (s, C-O), 164.6 (s, CO-N)

CHN-Analysis: found: C 61.11%, H 5.21%, N 4.10% (calculated (·0.6H_2O) : C 61.16%, H 5.84%, N 4.46%).

***(2E,4E)*-5-(1,3-Benzodioxol-5-yl)-1-(4-methyl-1-piperazinyl)-2,4-pentadien-1-one (31)**

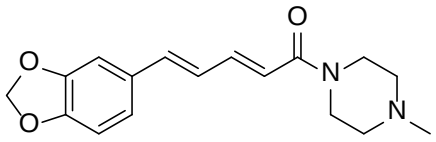

Method: F

The pure product was obtained after recrystallization from EtOAc.

Yield: 19% (0.57mmol, 172mg)

Appearance: brown crystals

M.p.: 140-141°C

^{1}H NMR ($CDCl_3$, 200MHz): δ= 2.31 (s, 3H, CH_3), 2.37-2.48 (m, 4H, CH_2NMe), 3.54-3.80 (m, 4H, CO-N-CH_2), 5.98(s, 2H, O-CH_2-O), 6.40 (d, J=14.6Hz, 1H, H2), 6.70-6.85(m, 3H), 6.86-6.95(m, 1H), 6.98 (d, J=1.4Hz, 1H), 7.43(ddd, J^1=14.6Hz, J^2=8.2Hz, J^3=2.1Hz, 1H)

^{13}C NMR ($CDCl_3$, 50MHz): δ= 42.2 (t, CH_2), 45.8 (t, CH_2), 46.2 (q, CH_3), 54.9 (t, CH_2), 55.5 (t, CH_2), 101.5 (t, O-CH_2-O), 105.9 (d), 108.7 (d), 119.5 (d), 122.8(d), 125.3(d), 131.1 (s), 138.9 (d), 143.2(d), 148.4(s, 2C), 165.7(s, CO-N)

CHN-Analysis: found: C 68.02%, H 6.44%, N 9.28% (calculated: C 67.98%, H 6.71%, N 9.33%).

***(2E,4E)*-5-(1,3-Benzodioxol-5-yl)-1-(4-ethylpiperazin-1-yl)-2,4-pentadien-1-one (32)**

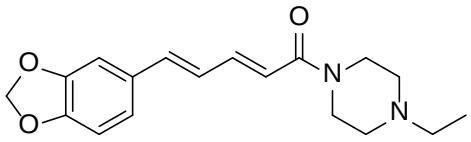

Method: F

The pure product was obtained after recrystallization from ethanol.

Yield: 23% (0.16mmol, 50mg)

Appearance: yellow crystals

M.p.: 145-146°C

^{1}H NMR ($CDCl_3$, 200MHz): δ= 1.00 (t, J=7.2Hz, CH_2Me), 2.36-2.55(m, 6H), 3.55-3.83(m, 4H, CO-N-CH_2), 5.98(s, 2H, O-CH_2-O), 6.41 (d, J=15.0Hz, 1H, H2), 6.70-6.84(m, 3H), 6.90 (dd, J^1=8.1Hz, J^2=1.4Hz, 1H), 6.98 (s, 1H), 7.43(ddd, J^1=14.6Hz, J^2=8.0Hz, J^3=2.2Hz, 1H)

^{13}C NMR ($CDCl_3$, 50MHz): δ= 12.1 (q, CH_3), 42.2 (t, CH_2), 45.9 (t, CH_2), 52.4 (t, CH_2), 52.7 (t, CH_2), 53.3 (t, CH_2), 101.5 (t, O-CH_2-O), 105.9 (d), 108.7 (d), 119.6 (d), 122.8(d), 125.3(d), 131.1 (s), 138.9 (d), 143.2(d), 148.4(s, 2C, C-O), 165.7(s, CO-N)

CHN-Analysis: found: C 67.93%, H 6.76%, N 8.62% (calculated (·0.2H_2O): C 67.99%, H 7.10%, N 8.81%).

***rac-(2E,4E)*-5-(1,3-Benzodioxol-5-yl)-1-(2-methylpiperidin-1-yl)-2,4-pentadien-1-one (33)**

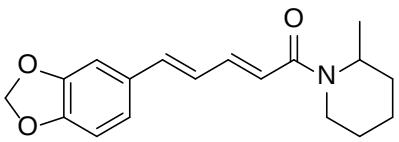

Method: H

The pure product was obtained after column chromatography (SiO_2, eluent: toluene/EtOAc 20%)

Yield: 29% (0.86mmol, 256mg)

Appearance: yellowish solid

M.p.: 96-97°C

^{1}H NMR ($CDCl_3$, 200MHz): δ= 1.23 (d, J=7.0Hz, 3H, CH_3), 1.35-1.83 (m, 6H, CH_2), 2.62-3.27 (m, 1H), 3.74-5.13 (m, 2H), 5.97 (s, 2H, O-CH_2-O), 6.43 (d, J=14.6, 1H, H2), 6.69-6.84 (m, 3H), 6.89 (dd, J^1=8.0Hz, J^2=1.6Hz, 1H), 6.98 (d, J=1.4Hz, 1H), 7.40 (ddd, J^1=14.6Hz, J^2=6.2Hz, J^3=4.0Hz, 1H)

^{13}C NMR ($CDCl_3$, 50MHz): δ= 19.3 (t, CH_2, 2C), 26.4 (t, CH_2), 30.8 (t, CH_2), 36.7 (d, CH), 101.7 (t, O-CH_2-O), 106.1 (d), 108.9 (d), 121.0 (d), 122.9(d), 125.9(d), 131.5 (s), 138.5 (d), 142.8 (d), 148.5 (s, C-O), 148.6(s, C-O), 166.1(s, CO-N). The CH_3-signal could not be identified due to low signal intensity.

CHN-Analysis: found: C 71.70%, H 6.71%, N 4.59% (calculated (·0.12H_2O): C 71.70%, H 7.10%, N 4.65%).

***rac-(2E,4E)*-5-(1,3-Benzodioxol-5-yl)-1-(3-methylpiperidin-1-yl)-2,4-pentadien-1-one (34)**

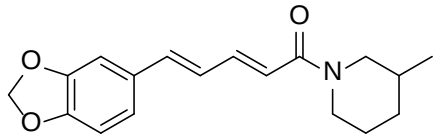

Method: H

The pure product was obtained after column chromatography (SiO_2, eluent: toluene/EtOAc 20%)

Yield: 32% (0.96mmol, 287mg)

Appearance: orange solid

M.p.: 104-106°C

^{1}H NMR ($CDCl_3$, 200MHz): δ= 0.93 (d, J=6.6Hz, 3H, CH_3), 1.06-1.29 (m, 1H), 1.33-1.94 (m, 4H), 2.24-2.44 (m, 1H), 2.64-2.84 (m, 1H), 2.90-3.12 (m, 1H), 3.77-4.01 (m, 1H), 4.37-4.62 (m, 1H), 5.97(s, 2H, O-CH_2-O), 6.44 (d, J=14.7, 1H, H2), 6.70-6.76 (m, 3H), 6.83 (d, J^1=8.1Hz, 1H), 6.98 (s, 1H), 7.40 (ddd, J^1=14.6Hz, J^2=6.3Hz, J^3=3.9Hz, 1H)

^{13}C NMR ($CDCl_3$, 50MHz): δ= 19.1 (q, CH_3), 25.0 (t, CH_2), 26.4 (t, CH_2), 31.3 (t, CH_2), 32.2 (t, CH_2), 33.4 (t, CH_2), 43.0 (d, CH), 46.6 (t, CH_2), 49.8 (t, CH_2), 53.6 (t, CH_2), 101.5 (t, O-CH_2-O), 105.9 (d), 108.7 (d), 120.3 (d), 122.7(d), 125.6(d), 131.2 (s), 138.4 (d), 142.7 (d), 148.3 (s, C-O), 148.4 (s, C-O), 165.6(s, CO-N)

CHN-Analysis: found: C 71.97%, H 6.83%, N 4.55% (calculated: C 72.22%, H 7.07%, N 4.68%)

(2E,4E)*-5-(1,3-Benzodioxol-5-yl)-1-(4-methylpiperidin-1-yl)-2,4-pentadien-1-one *(35)

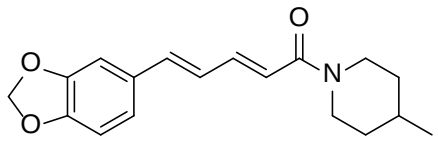

Method: H

The pure product was obtained after column chromatography (SiO_2, eluent: toluene/EtOAc 20%)

Yield: 27% (0.81mmol, 243mg)

Appearance: orange solid

M.p.: 80-83°C

^{1}H NMR ($CDCl_3$, 200MHz): δ= 0.96 (d, J=6.6Hz, 3H, CH_3), 1.02-1.32 (m, 2H), 1.53-1.83 (m, 3H), 2.54-2.79 (m, 1H), 2.91-3.19 (m, 1H), 3.91-4.13 (m, 1H), 4.55-4.77 (m, 1H), 5.98 (s, 2H, O-CH_2-O), 6.44 (d, J=14.6, 1H, H2), 6.69-6.82 (m, 3H), 6.89 (dd, J^1=8.0Hz, J^2=1.5Hz, 1H), 6.98 (d, J=1.4Hz, 1H), 7.40(ddd, J^1=14.7Hz, J^2=6.8Hz, J^3=3.4Hz, 1H)

^{13}C NMR ($CDCl_3$, 50MHz): δ= 21.9 (q, CH_3), 31.4 (d, CH), 34.0 (t, CH_2), 35.1 (t, CH_2), 42.8 (d, CH), 46.4 (t, CH_2), 101.5 (t, O-CH_2-O), 105.9 (d), 108.7 (d), 120.3 (d), 122.7(d), 125.5(d), 131.2 (s), 138.4 (d), 142.7 (d), 148.3 (s, C-O), 148.4 (s, C-O), 165.6(s, CO-N)

CHN-Analysis: found: C 72.04%, H 6.88%, N 4.55% (calculated: C 72.22%, H 7.07%, N 4.68%).

***rac-(2E,4E)*-5-(1,3-Benzodioxol-5-yl)-1-(3-hydroxypiperidin-1-yl)-2,4-pentadien-1-one (36)**

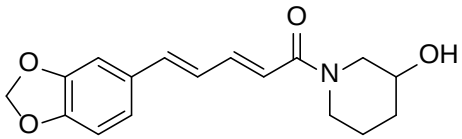

Method: H

The pure product was obtained after recrystallization from ethanol.

Yield: 45% (1.35mmol, 407mg)

Appearance: pink crystals

M.p.: 146-147°C

^{1}H NMR ($CDCl_3$, 200MHz): δ= 1.42-1.73 (m, 2H), 1.80-2.03 (m, 2H), 3.21-3.48 (m, 2H), 3.54-4.10 (m, 3H), 5.97 (s, 2H, O-CH_2-O), 6.44 (d, J=14.2, 1H, H2), 6.69-6.81 (m, 3H), 6.88 (dd, J^1=8.1Hz, J^2=1.3Hz, 1H), 6.96 (s, 1H), 7.41 (ddd, J^1=14.6Hz, J^2=8.0Hz, J^3=2.2Hz, 1H)

^{13}C NMR ($CDCl_3$, 50MHz): δ= 22.4 (t, CH_2), 23.8 (t, CH_2), 32.7 (t, CH_2), 33.4 (t, CH_2), 42.9 (d, CH), 46.7 (t, CH_2), 49.8 (t, CH_2), 53.1 (t, CH_2), 66.4 (d, CH), 67.0 (t, CH), 101.7 (t, O-CH_2-O), 106.1 (d), 108.9 (d), 119.9 (d), 123.1(d), 125.6(d), 131.3 (s), 139.3 (d), 143.7 (d), 148.6 (s, 2C, C-O), 166.8 (s, CO-N)

CHN-Analysis: found: C 67.38%, H 6.19%, N 4.46% (calculated: C 67.76%, H 6.36%, N 4.65%).

***(2E,4E)*-5-(1,3-Benzodioxol-5-yl)-1-(4-hydroxypiperidin-1-yl)-2,4-pentadien-1-one (37)**

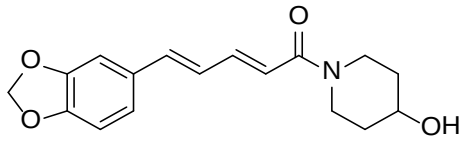

Method: F

The pure product was obtained after recrystallization from ethanol.

Yield: 44% (1.32mmol, 397mg)

Appearance: beige crystals

M.p.: 170°C

^{1}H NMR ($CDCl_3$, 200MHz): δ= 1.43-1.70 (m, 2H, CH_2), 1.78-2.02 (m, 3H, CH_2, CH), 3.20-3.43 (m, 2H, CH_2), 3.79-4.04 (m, 2H, CH_2), 4.04-4.29 (m, 1H, OH), 5.98 (s, 2H, O-CH_2-O), 6.44 (d, J=14.6, 1H, H2), 6.69-6.84 (m, 3H), 6.90 (dd, J^1=8.1Hz, J^2=1.4Hz, 1H), 6.98 (s, 1H), 7.41(ddd, J^1=14.6Hz, J^2=7.9Hz, J^3=2.3Hz, 1H)

^{13}C NMR ($CDCl_3$, 50MHz): δ= 34.2 (t, CH_2), 35.0 (t, CH_2), 39.7 (t, CH_2), 43.2 (t, CH_2), 67.4 (d, CH), 101.5 (t, O-CH_2-O), 105.9 (d), 108.7 (d), 119.7 (d), 122.8(d), 125.4(d), 131.1 (s), 138.9 (d), 143.2 (d), 148.4 (s, 2C. C-O), 165.8(s, CO-N)

CHN-Analysis: found: C 67.27%, H 6.16%, N 4.49% (calculated (·0.12H_2O): C 67.28%, H 6.39%, N 4.62%).

***(2E,4E)*-5-(1,3-Benzodioxol-5-yl)-1-(*cis*-2,6-dimethylpiperidin-1-yl)-2,4-pentadien-1-one (38)**

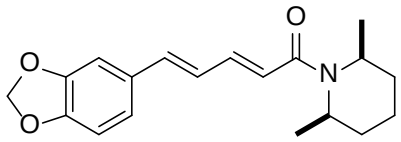

Method: G

The pure product was obtained after column chromatography (SiO_2, eluent: toluene/EtOAc 20%)

Yield: 30% (0.91mmol, 286mg)

Appearance: orange solid

M.p.: 90-93°C

^{1}H NMR ($CDCl_3$, 200MHz): δ= 1.26 (s, CH_3), 1.29 (s, CH_3), 1.44-1.84 (m, 6H, CH_2), 4.57 (s, CH), 5.97 (s, 2H, O-CH_2-O), 6.55 (d, J=14.6, 1H, H2), 6.80-6.93 (m, 3H), 6.95-7.03 (m, 1H), 7.08 (s, 1H), 7.46-7.62 (m, 1H)

^{13}C NMR ($CDCl_3$, 50MHz): δ= 14.4 (t, CH_2, 2C), 30.7 (t, CH_2), 101.7 (t, O-CH_2-O), 106.1 (d), 108.9 (d), 121.3 (d), 122.9(d), 126.0(d), 131.5 (s), 138.4 (d), 142.9 (d), 148.6 (s, 2C, C-O), 166.7 (s, CO-N); The CH- and CH_3-signals could not be identified due to low signal intensity.

CHN-Analysis: found: C 69.86%, H 6.84%, N 4.25% (calculated (·0.7H_2O): C 70.0%, H 7.54%, N 4.30%).

rac-(2E,4E)-5-(1,3-Benzodioxol-5-yl))-1-(3-(trifluoromethyl)piperidin-1-yl)-2,4-pentadien-1-one (39)

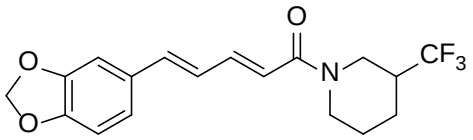

Method: F

The pure product was obtained after recrystallization from ethanol.

Yield: 51% (0.51mmol, 180mg)

Appearance: colorless crystals

M.p.: 140°C

^{1}H NMR ($CDCl_3$, 200MHz): δ= 1.35-1.67 (m, 2H, CH_2), 1.77-1.93 (m, 1H, CH), 2.02-2.41 (m, 2H, CH_2), 2.49-3.25 (m, 2H, CH_2), 3.87-5.09 (m, 2H, CH_2), 5.98 (s, 2H, O-CH_2-O), 6.40 (d, J=14.6, 1H, H2), 6.71-6.86 (m, 3H), 6.90 (dd, J^1=8.1Hz, J^2=1.5Hz, 1H), 6.99 (d, J=1.3Hz, 1H), 7.44(ddd, J^1=14.6Hz, J^2=8.2Hz, J^3=2.0Hz, 1H)

^{13}C NMR ($CDCl_3$, 50MHz): δ= 23.8 (t, CH_2), 101.5 (t, O-CH_2-O), 105.9 (d), 108.7 (d), 119.1 (d), 122.9(d), 123.7 (s, CF_3), 125.2(d), 129.3 (s, CF_3), 131.0 (s), 139.3 (d), 143.9 (d), 148.4 (s, 2C, C-O), 166.0(s, CO-N); The CH-CF_3 and some CH_2-signals could not be identified due to low signal intensity.

CHN-Analysis: found: C 61.12%, H 4.89%, N 3.93% (calculated: C 61.19%, H 5.13%, N 3.96%).

_(2E,4E)_-5-(1,3-Benzodioxol-5-yl)-1-(4-(2-(2-hydroxyethoxy)ethyl)piperazin-1-yl)-2,4-pentadien-1-one (40)

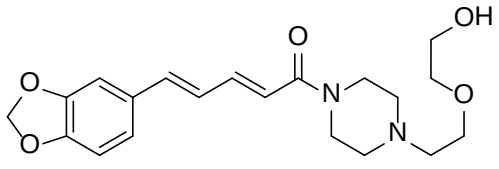

Method: G

The pure product was obtained after column chromatography (SiO_2, eluent: toluene/EtOAc 20%) and subsequent recrystallization from toluene.

Yield: 40% (1.20mmol, 448mg)

Appearance: orange crystals

M.p.: 75-78°C

^{1}H NMR ($CDCl_3$, 200MHz): δ= 1.97 (s,1H, OH) 2.49-2.68 (m, 6H, CH_2), 3.57-3.81 (m, 10H, CH_2), 5.98 (s, 2H, O-CH_2-O), 6.39 (d, J=14.6, 1H, H2), 6.71-6.82 (m, 3H), 6.90 (dd, J^1=8.0Hz, J^2=1.5Hz, 1H), 6.98 (d, J=1.3Hz, 1H), 7.42(ddd, J^1=14.7Hz, J^2=8.3Hz, J^3=1.8Hz, 1H)

^{13}C NMR ($CDCl_3$, 50MHz): δ= 42.0 (t, CH_2), 45.6 (t, CH_2), 53.2 (t, CH_2), 53.8 (t, CH_2), 58.0 (t, CH_3), 62.2(t, CH_2), 67.8 (t, CH_2), 72.6 (t, CH_2), 101.5 (t, O-CH_2-O), 105.9 (d), 108.7 (d), 119.3 (d), 122.9(d), 125.3(d), 131.1 (s), 139.1 (d), 143.4 (d), 148.4 (s, C-O), 165.7 (s, CO-N)

CHN-Analysis: found: C 61.41%, H 6.88%, N 6.91% (calculated (·0.9H_2O): C 61.49%, H 7.17%, N 7.17%).

***(2E,4E)*-5-(1,3-Benzodioxol-5-yl)-1-(4-(2-methoxyphenyl)piperazin-1-yl)-2,4-pentadien-1-one (41)**

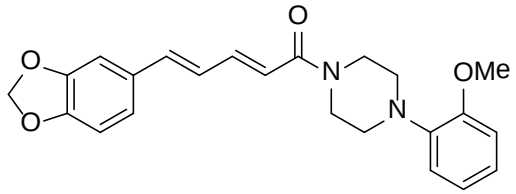

Method: H

The pure product was obtained after recrystallization from toluene.

Yield: 27% (0.80mmol, 312mg)

Appearance: beige crystals

M.p.: 199-202°C

^{1}H NMR ($CDCl_3$, 200MHz): δ= 2.98-3.20 (m, 4H, CH_2), 3.63-4.02 (m, 7H, CH_2, CH_3), 5.98 (s, 2H, O-CH_2-O), 6.46 (d, J=14.6, 1H, H2), 6.73-6.85 (m, 3H), 6.85-6.97 (m, 4H), 6.99 (s, J=1.4Hz, 1H), 7.01-7.10 (m, 1H), 7.46(ddd, J^1=14.6Hz, J^2=7.9Hz, J^3=2.3Hz, 1H)

^{13}C NMR ($CDCl_3$, 50MHz): δ= 42.4 (t, CH_2), 46.2 (t, CH_2), 50.8 (t, CH_2), 51.3 (t, CH_2), 55.6 (q, CH_3), 101.5 (t, O-CH_2-O), 105.9 (d), 108.7 (d), 111.5(d), 118.7 (d), 119.5 (d), 121.2(d), 122.8(d), 123.7(d), 125.4(d), 131.1 (s), 139.0 (d), 140.9(s), 143.3 (d), 148.4 (s), 152.4(s), 165.8(s, CO-N)

CHN-Analysis: found: C 69.95%, H 6.12%, N 6.94% (calculated: C 70.39%, H 6.61%, N 7.14%).

***(2E,4E)*-5-(1,3-Benzodioxol-5-yl)-1-(4-benzylpiperazin-1-yl)-2,4-pentadien-1-one (42)**

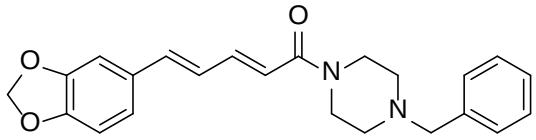

Method: G

The pure product was obtained after recrystallization from EtOAc.

Yield: 62% (1.85mmol, 695mg)

Appearance: yellow crystals

M.p.: 81-84°C

^{1}H NMR ($CDCl_3$, 200MHz): δ= 2.41-2.52 (m, 4H, CH_2), 3.53 (s, 2H, $ArCH_2$), 3.55-3.66 (m, 4H, CH_2), 3.65-3.80 (m, 4H, CH_2), 5.97 (s, 2H, O-CH_2-O), 6.39 (d, J=14.6, 1H, H2), 6.69-6.84 (m, 3H), 6.89 (dd, J^1=8.1Hz, J^2=1.5Hz, 1H), 6.98 (d, J=1.3Hz, 1H), 7.28-7.51 (m, 6H)

^{13}C NMR ($CDCl_3$, 50MHz): δ= 42.3 (t, CH_2), 45.9 (t, CH_2), 53.0 (t, CH_2), 53.4 (t, CH_2), 63.1 (t, CH_2), 101.5 (t, O-CH_2-O), 105.9 (d), 108.7 (d), 119.6 (d), 122.8(d), 125.4(d), 127.5(d), 128.5(d), 129.3(d), 131.1 (s), 137.8(s), 138.9 (d), 143.2 (d), 148.4 (s), 165.7(s, CO-N)

CHN-Analysis: found: C 71.36%, H 6.27%, N 7.44% (calculated (·0.6H_2O): C 71.33%, H 6.56%, N 7.23%).

***(2E,4E)*-5-(benzo[*d*][1,3]dioxol-5-yl)-*N*,*N*-bis(2,2,2-trifluoroethyl)penta-2,4-dienamide (43)**

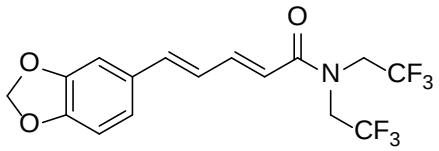

Method: H

The pure product was obtained after flash column chromatography (silica, eluent: toluene) with partial decomposition on the column.

Yield: 12% (0.42mmol, 160mg)

M.p.: 76-79°C

^{1}H NMR ($CDCl_3$, 200MHz): δ= 4.20 (bs, 4H, CH_2), 5.99 (s, 2H, O-CH_2-O), 6.25-6.50 (m, 1H), 6.65-7.11 (m, 5H), 7.50-7.66 (dd, J^1=8.1Hz, J^2=1.5Hz, 1H), 6.98 (d, J=1.3Hz, 1H), 7.28-7.51 (m, 6H)

^{13}C NMR ($CDCl_3$, 50MHz): δ= 44.3 (t, CH_2), 44.5 (t, CH_2), 101.4 (t, O-CH_2-O), 105.9 (d), 108.6 (d), 116.2 (d), 121.4(d), 123.2(d), 124.3, 127.0(d), 130.4(d), 141.2, 146.7, 148.3 (s, C-O), 148.7 (s, C-O), 167.2 (s, CO-N)

CHN-Analysis: found: C 51.19%, H 3.55%, N 3.31% (calculated (·0.1 toluene): C 51.37%, H 3.56%, N 3.59%).

(2E,4E)-5-(1,3-Benzodioxol-5-yl)-1-(piperidin-1-yl)-2,4-pentadien-1-thione (44)

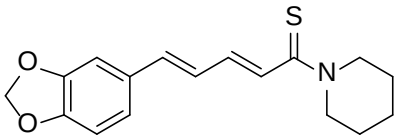

Piperine (1equiv., 2mmol, 571mg,) was stirred with Lawessons reagent (1.5equiv., 3mmol, 1.23g) in THF at rt. After 20 hours the solvent was evaporated and the residue recrystallized from DMF.

Yield: 85% (2.55mmol, 771mg)

Appearance: orange-red crystals

M.p.: 177-178°C

^{1}H NMR ($CDCl_3$, 200MHz): δ= 1.73 (m, 6H, CH_2), 3.70-3.91 (m, 2H, CH_2), 4.22-4.43 (m, 2H, CH_2), 5.98 (s, 2H, O-CH_2-O), 6.65 (d, J=14.4, 1H, H2), 6.71-6.81 (m, 3H), 6.89 (dd, J^1=8.1Hz, J^2=1.5Hz, 1H), 6.98 (d, J = 1.3Hz, 1H), 7.41(ddd, J^1=14.4Hz, J^2=8.7Hz, J^3=1.4Hz, 1H)

^{13}C NMR ($CDCl_3$, 50MHz): δ= 24.5 (t, CH_2), 25.7 (t, CH_2), 27.0 (t, CH_2), 51.6 (t, CH_2), 51.9 (t, CH_2), 101.5 (t, O-CH_2-O), 105.8 (d), 108.7 (d), 122.8(d), 125.8(d), 128.0 (d), 131.3(s), 138.6 (d), 144.3 (d), 148.4 (s, 2C, C-O), 194.0 (s, CS-N)

CHN-Analysis: found: C 65.96%, H 6.49%, N 4.51% (calculated (·0.5H_2O): C 65.78%, H 6.49%, N 4.51%).

1-((2*E*,4*E*)-5-(1,3-Benzodioxol-5-yl)-2,4-pentadien-1-yl)-piperidine (45)

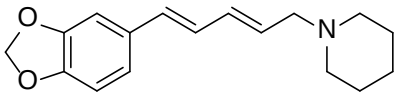

Piperine (2mmol, 571mg) was dissolved in dry THF (10ml) under argon atmosphere. A solution of 1M $LiAlH_4$ (1.5equiv, 3mmol, 3ml) was added dropwise. The reaction mixture was stirred for 3days. Excess $LiAlH_4$ was destroyed by addition of EtOAc. The solvent was evaporated and the residue was redissolved up in EtOAc. The organic phase was washed with water three times. Precipitates formed upon mixing with water were removed by filtration. The organic phase was separated, dried with sodium sulfate, filtered and evaporated. The pure product was obtained after column chromatography (SiO_2, eluent toluene/MeOH 6:4)

Yield: 34% (0.671mmol, 182mg)

Appearance: brown solid

M.p.: 124-128°C

^{1}H NMR ($CDCl_3$, 200MHz): δ= 1.36-1.49 (m, 2H, CH_2), 1.52-1.64 (m, 4H, CH_2), 2.32-2.47 (m, 4H, CH_2), 2.97-3.08 (m, 2H, CH_2), 5.74-5.90 (m, 1H, CH), 5.92 (s, 2H, O-CH_2-O), 6.17-6.45 (m, 2H), 6.53-6.76 (m, 2H), 6.80 (dd, J^1=8.1Hz, J^2=1.4Hz, 1H), 6.92 (d, J=1.2Hz, 1H).

^{13}C NMR ($CDCl_3$, 50MHz): δ= 24.4 (t, CH_2), 26.1 (t, CH_2, 2C), 54.6 (t, CH_2, 2C), 61.7 (t, CH_2), 101.1 (t, O-CH_2-O), 105.5 (d), 108.4 (d), 121.2 (d), 127.1(d), 130.8 (s), 131.4(d), 132.0 (s), 133.4 (d), 147.2 (s), 148.1 (s)

CHN-Analysis: found: C 73.03%, H 7.08%, N 4.71% (calculated (·0.5H_2O): C 72.83%, H 7.91%, N 5.00%).

4-(Benzo[*d*][1,3]dioxol-5-yl)benzoic acid (46a)

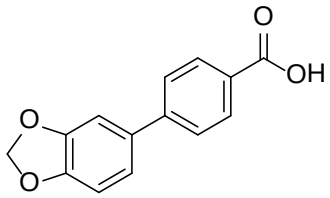

Method: B

Yield: 56% (1.01mmol, 245mg)

Appearance: beige solid

TLC: 0.38 ($CHCl_3$/MeOH 10%)

M.p.: 277-280°C

^{1}H NMR (DMSO-*d6*, 200MHz): δ= 6.08 (s, 2H, O-CH_2-O), 7.03 (d, J = 8.1Hz, 1H, H7'), 7.24 (dd, J^1 = 8.1Hz, J^2 = 1.7Hz, H6'), 7.33 (d, J = 1.7Hz, 1H, H4'), 7.74 (d, J = 8.3Hz, 2H, H3, H5), 7.97 (d, J = 8.3Hz, 2H, H2, H6), 12.92 (bs, 1H, COOH)

^{13}C NMR (DMSO-*d6*, 50MHz): δ= 101.3 (t, O-CH_2-O), 107.2 (d), 108.7(d), 120.8(d), 126.4 (d), 129.0(s), 129.8(d), 133.1(s), 143.9(s), 147.5(s), 148.1(s), 167.1(s, COOH)

HR-MS: $[M-H]^-$ m/z (predicted) = 241.0506, m/z (measured) = 241.0507, difference = 0.41 ppm

(4-(Benzo[*d*][1,3]dioxol-5-yl)phenyl)(piperidin-1-yl)methanone (46)

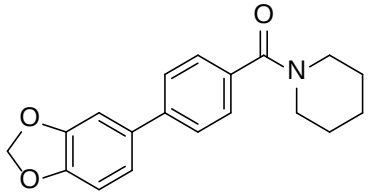

Method: E
Yield: 85% (54.0 mg, 0.175mmol)
Appearance: colorless solid
M.p.: 120-122°C

^{1}H NMR ($CDCl_3$, 200MHz): δ = 1.67 (bm, 6H), 3.41-3.70 (bm, 4H), 5.99 (s, 2H, O-CH_2-O), 6.85-6.89 (m, 1H), 7.02-7.07 (bm, 2H), 7.40-7.44 (m, 2H), 7.50-7.54 (m, 2H)
^{13}C NMR ($CDCl_3$, 50MHz): δ = 24.6 (t), 25.8 (t), 26.3(t), 43.2(t), 101.2(t), 107.6 (d), 108.6 (d), 120.7 (d), 126.8 (d), 127.4 (d), 134.7 (s), 134.9 (s), 142.0 (s), 147.4 (s), 148.2 (s), 170.1 (s, CO-N)

4-Bromo-*N,N*-dipropylbenzamide (47a)

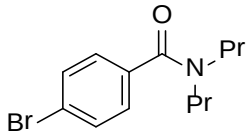

Method: C

Yield: 93% (2.79mmol, 794mg)

Appearance: brown oil

^{1}H NMR ($CDCl_3$, 200MHz): δ= 0.64-1.07 (m, 6H, CH_3), 1.39-1.80 (m, 4H, CH_2), 3.02-3.56 (m, 4H, N-CH_2), 7.23 (td, J^1 = 8.8Hz, J^2 = 2.0Hz, 2H, H3, H5), 7.53 (td, J^1 = 8.8Hz, J^2 = 2.0Hz, 2H, H2, H6)

^{13}C NMR ($CDCl_3$, 50MHz): δ= 11.0 (q, CH_3), 11.4 (q, CH_3), 20.7 (t), 21.9 (t), 46.4 (t), 50.7 (t), 123.2 (s), 128.2 (d), 131.6 (d), 136.2 (s), 170.7(s, CO-N)

HR-MS: $[M+H]^+$ m/z (predicted) = 284.0645, m/z (measured) = 284.0655, difference = 3.52 ppm

4-(Benzo[*d*][1,3]dioxol-5-yl)-*N,N*-dipropylbenzamide (47)

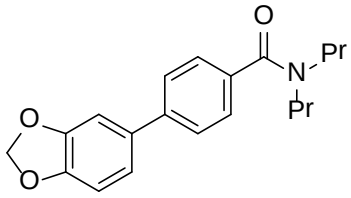

Method: B

Yield: 75% (0.22mmol, 73mg)

Appearance: colorless solid

TLC: 0.29 (LP/EtOAc 4:1)

M.p.: 52°C

^{1}H NMR ($CDCl_3$, 200MHz): δ= 0.67-1.08 (bm, 6H, CH_3), 1.45-1.82(bm, 4H, CH_2), 3.07-3.60 (bm, 4H, N-CH_2), 5.99 (s, 2H, O-CH_2-O), 6.86-6.90 (m, 1H, ArH), 7.04-7.08 (m, 2H, ArH), 7.39 (d, J = 8.2Hz, 2H, H2', H6'), 7.52 (d, J = 8.2Hz, 2H, H3', H5')

^{13}C NMR ($CDCl_3$, 50MHz): δ= 11.4 (q, 2C, CH_3), 20.7(t, CH_2), 21.9 (t, CH_2), 46.3 (t, N-CH_2), 50.8(t, N-CH_2), 101.2(t, O-CH_2-O), 107.5(d), 108.6(d), 120.7(d), 126.7(d), 127.0(d), 134.7(s), 135.8(s), 141.6(s), 147.4(s), 148.2(s), 171.6(s, CO-N)

HR-MS: $[M+H]^+$ m/z (predicted) = 326.1751, m/z (measured) = 326.1743, difference = -2.45ppm

4-Bromo-*N,N*-dibutylbenzamide (48a)

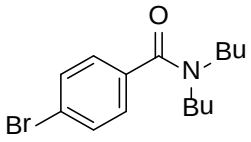

Method: C

Yield: 94% (2.81mmol, 876mg)

Appearance: brown oil

^{1}H NMR ($CDCl_3$, 200MHz): δ= 0.74-1.75 (m, 14H, CH_2, CH_3), 3.10-3.56 (m, 4H, N-CH_2), 7.23 (td, J^1 = 8.7Hz, J^2 = 2.1Hz, 2H, H3, H5), 7.53 (td, J^1 = 8.7Hz, J^2 = 2.1Hz, 2H, H2, H6)

^{13}C NMR ($CDCl_3$, 50MHz): δ= 13.7 (q, CH_3), 13.8 (q, CH_3), 19.7 (t), 20.2 (t), 29.6 (t), 30.8 (t), 44.6 (t), 48.8 (t), 123.2 (s), 128.2 (d), 131.5 (d), 136.2 (s), 170.5(s, CO-N)

HR-MS: $[M+H]^+$ m/z (predicted) = 312.0958, m/z (measured) = 312.0974, difference = 5.13 ppm

4-(Benzo[*d*][1,3]dioxol-5-yl)-*N,N*-dibutylbenzamide (48)

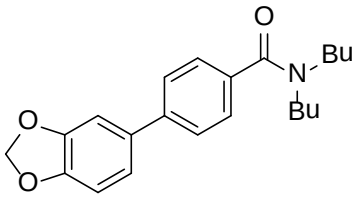

Method: B

Yield: 66% (0.20mmol, 70mg)

Appearance: colorless solid

TLC: 0.35 (LP/EtOAc 4:1)

M.p.: 68-70°C

^{1}H NMR ($CDCl_3$, 200MHz): δ= 0.72-1.78 (m, 14H,CH_2, CH_3), 3.42-3.49 (bm, 4H, N-CH_2), 5.98 (s, 2H, O-CH_2-O), 6.85-6.89 (m, 1H, ArH), 7.04-7.09 (m, 2H, ArH), 7.39 (d, J = 8.3Hz, 2H, H2', H6'), 7.52 (d, J = 8.3Hz, 2H, H3', H5')

^{13}C NMR ($CDCl_3$, 50MHz): δ= 13.8 (q, 2C, CH_3), 19.8(t, CH_2), 20.3 (t, CH_2), 29.6(t, CH_2), 30.9(t, CH_2), 44.5 (t, N-CH_2), 48.9(t, N-CH_2), 101.2(t, O-CH_2-O), 107.5(d), 108.6(d), 120.7(d), 126.7(d), 127.0(d), 134.7(s), 135.8(s), 141.6(s), 147.4(s), 148.2(s), 171.4(s, CO-N)

HR-MS: $[M+H]^+$ m/z (predicted) =354.2064, m/z (measured) = 354.2064, difference = 0.0ppm

4-(Benzo[*d*][1,3]dioxol-5-yl)-*N*,*N*-diisopropylbenzamide (49)

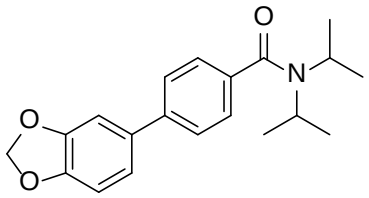

Method: C

Yield: 50% (0.12mmol, 39mg)

Appearance: colorless oil

TLC: 0.20 (LP/EtOAc 4:1)

^{1}H NMR ($CDCl_3$, 200MHz): δ= 0.88-1.91 (m, 12H, CH_3), 3.48-4.05 (bm, 2H, N-CHR_2), 6.01 (s, 2H, O-CH_2-O), 6.86-6.91 (m, 1H, ArH), 7.04-7.08 (m, 2H, ArH), 7.35 (d, J = 8.2Hz, 2H, H2', H6'), 7.52 (d, J = 8.2Hz, 2H, H3', H5')

^{13}C NMR ($CDCl_3$, 50MHz): δ= 13.8 (q, 2C, CH_3), 19.8(t, CH_2), 20.3 (t, CH_2), 29.6(t, CH_2), 30.9(t, CH_2), 44.5 (t, N-CH_2), 48.9(t, N-CH_2), 101.2(t, O-CH_2-O), 107.5(d), 108.6(d), 120.7(d), 126.7(d), 127.0(d), 134.7(s), 135.8(s), 141.6(s), 147.4(s), 148.2(s), 171.4(s, CO-N)

HR-MS: $[M+H]^+$ m/z (predicted) = 326.1751, m/z (measured) = 326.1747, difference = -1.23ppm

(3-Bromophenyl)(piperidin-1-yl)methanone (50a)

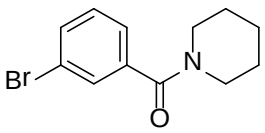

Method: C

Yield: 88% (2.63mmol, 705mg)

Appearance: brown oil

^{1}H NMR ($CDCl_3$, 200MHz): δ= 1.42-1.77 (m, 6H, CH_2), 3.22-3.82 (m, 4H, N-$CH_{2)}$, 7.26-7.34 (m, 2H, ArH), 7.50-7.55 (m, 2H, ArH)

^{13}C NMR ($CDCl_3$, 50MHz): δ= 24.5 (t, CH_2), 25.5 (t, CH_2), 26.5 (t, CH_2), 43.1 (t, N-CH_2), 48.7 (t, N-CH_2), 122.5 (s), 125.3 (d), 129.8 (d), 130.0 (d), 132.4 (d), 138.4(s), 168.5 (s, CO-N)

HR-MS: $[M+H]^+$ m/z (predicted) = 268.0332, m/z (measured) = 268.0334, difference = 0.75 ppm

(3-(Benzo[*d*][1,3]dioxol-5-yl)phenyl)(piperidin-1-yl)methanone (50)

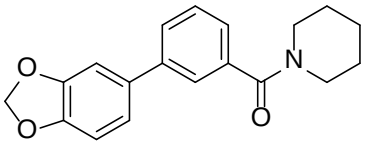

Method: B

Yield: 91% (0.27mmol,84mg)

Appearance: colorless oil

TLC: 0.15 (LP/EtOAc 4:1)

^{1}H NMR ($CDCl_3$, 200MHz): δ= 1.56-1.68 (m, 6H, CH_2), 3.38-3.73 (m, 4H, N-CH_2), 6.00 (s, 2H, O-CH_2-O), 6.86-6.90 (m, 1H, ArH), 7.03-7.08 (m, 2H, ArH), 7.26-7.33 (m, 1H, ArH), 7.43 (t, J = 7.4Hz, 1H, ArH), 7.52-7.55 (m, 2H, ArH)

^{13}C NMR ($CDCl_3$, 50MHz): δ= 24.6 (t, CH_2), 25.6 (t, CH_2), 26.5 (t, CH_2), 43.1 (t, CH_2), 48.8 (t, CH_2), 101.2 (t, O-CH_2-O), 107.6 (d), 108.6 (d), 120.7 (d), 125.2 (d, 2C), 127.7 (d), 128.8 (d), 134.7 (s), 137.0 (s), 141.1 (s), 147.4 (s), 148.2 (s), 171.2 (s, -CO-N)

HR-MS: $[M+H]^+$ m/z (predicted) = 310.1438, m/z (measured) = 310.1427, difference = -3.55ppm

3-Bromo-*N*,*N*-dipropylbenzamide (51a)

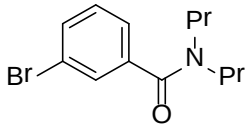

Method: C

Yield: 90% (2.69mmol, 765mg)

Appearance: colorless oil

^{1}H NMR ($CDCl_3$, 200MHz): δ= 0.67-1.07 (m, 6H, CH_3), 1.47-1.73 (m, 4H, CH_2), 3.10-3.48 (m, 4H, N-CH_2), 7.25-7.31 (m, 2H, ArH), 7.48-7.55 (m, 2H, ArH)

^{13}C NMR ($CDCl_3$, 50MHz): δ= 11.0 (q, CH_3), 11.4 (q, CH_3), 20.6 (t), 21.9 (t), 46.3 (t, N-CH_2), 50.6 (t, N-CH_2), 122.5 (s), 125.0 (d), 129.5 (d), 130.0 (d), 132.1 (d), 139.3 (s), 170.0 (s, CO-N)

HR-MS: $[M+H]^+$ m/z (predicted) = 284.0645, m/z (measured) = 284.0652, difference = 2.46 ppm

3-Bromo-*N,N*-dibutylbenzamide (52a)

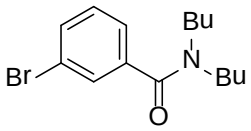

Method: C

Yield: 87% (2.62mmol, 817mg)

Appearance: brown oil

^{1}H NMR ($CDCl_3$, 200MHz): δ= 0.72-1.06 (m, 6H, CH_3), 1.07-1.74 (m, 8H, CH_2), 3.13-3.51 (m, 4H, N-CH_2), 7.25-7.31 (m, 2H, ArH), 7.48-7.55 (m, 2H, ArH)

^{13}C NMR ($CDCl_3$, 50MHz): δ= 13.6 (q, CH_3), 13.9 (q, CH_3), 19.7 (t, CH_2), 20.3 (t, CH_2),19.6 (t, CH_2), 30.8 (t, CH_2), 44.5 (t, N-CH_2), 48.7 (t, N-CH_2), 122.4 (s), 125.0 (d), 129.5 (d), 130.0 (d), 132.1 (d), 139.2(s), 169.8 (s, CO-N)

HR-MS: $[M+H]^+$ m/z (predicted) = 312.0958, m/z (measured) = 312.0970, difference = 3.84 ppm

3-(Benzo[*d*][1,3]dioxol-5-yl)-*N,N*-dibutylbenzamide (52)

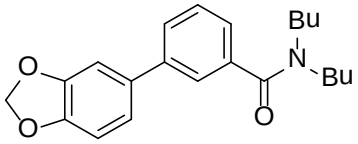

Method: B

Yield: 73% (0.22mmol, 77mg)

Appearance: colorless oil

TLC: 0.31 (LP/EtOAc 4:1)

^{1}H NMR ($CDCl_3$, 200MHz): δ= 0.78-1.66 (m, 14H, CH_2, CH_3), 3.22-3.50 (m, 4H, N-CH_2), 6.00 (s, 2H, O-CH_2-O), 6.86-6.90 (m, 1H, ArH), 7.03-7.08 (m, 2H, ArH), 7.25-7.30 (m, 1H, ArH), 7.41 (t, J = 7.4Hz, 1H, ArH), 7.49-7.54 (m, 2H, ArH)

^{13}C NMR ($CDCl_3$, 50MHz): δ= 13.6 (q, CH_3), 13.9 (q, CH_3), 19.7 (t, CH_2), 20.3 (t, CH_2), 29.7 (t, CH_2), 30.8 (t, CH_2), 44.5 (t, CH_2), 48.8 (t, CH_2), 101.2 (t, O-CH_2-O), 107.6 (d), 108.6 (d), 120.7 (d), 124.8 (d), 124.9 (d), 127.4 (d), 128.7 (d), 134.8 (s), 137.8 (s), 141.1 (s), 147.3 (s), 148.2 (s), 171.5 (s, -CO-N)

HR-MS: $[M+H]^+$ m/z (predicted) = 354.2064, m/z (measured) = 354.2062, difference = -0.56ppm

3-(Benzo[*d*][1,3]dioxol-5-yl)benzoic acid (53a)

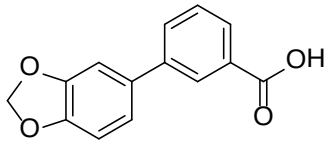

Method: B

Yield: 51% (0.92mmol, 222mg)

Appearance: colorless solid

TLC: 0.25 ($CHCl_3$/MeOH 10%)

M.p.: 228-232°C

^{1}H NMR (DMSO-*d6*, 200MHz): δ= 6.08 (s, 2H, O-CH_2-O), 7.02 (d, J = 8.1Hz, 1H, H7'), 7.18 (dd, J^1 = 8.1Hz, J^2 = 1.3Hz, 1H, H6'), 7.28 (s, 1H, ArH), 7.55 (t, J = 7.7Hz, 1H, H5), 7.83-7.91 (m, 2H, ArH), 8.11 (s, 1H, H2), 13.04 (bs, 1H, COOH)

^{13}C NMR (DMSO-*d6*, 50MHz): δ= 101.3 (t, O-CH_2-O), 107.1 (d), 108.7(d), 120.4(d), 127.0 (d), 127.7 (d), 129.1(s), 130.8(d), 131.3(s), 133.4(s), 140.2 (s), 147.1 (s), 148.0 (s), 167.2 (s, COOH)

3-(Benzo[*d*][1,3]dioxol-5-yl)-*N*,*N*-diisopropylbenzamide (53)

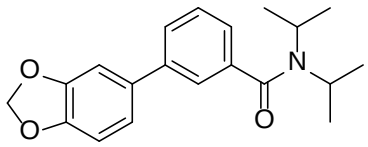

Method: C

Yield: 66% (0.16mmol,52mg)

Appearance: colorless solid

M.p.: 136-139°C

^{1}H NMR ($CDCl_3$, 200MHz): δ= 0.95-1.77 (m, 12H, CH_2), 3.35-4.13 (m, 2H, N-CH), 6.00 (s, 2H, O-CH_2-O), 6.85-6.90 (m, 1H, ArH), 7.04-7.07 (m, 2H, ArH), 7.38 (d, J = 7.6Hz, 1H, ArH), 7.44-7.52 (m, 2H, ArH),

^{13}C NMR ($CDCl_3$, 50MHz): δ= 20.7 (q, 4C, CH_3), 101.2 (t, O-CH_2-O), 107.6 (d), 108.6 (d), 120.7 (d), 124.0 (d), 124.1(d), 127.1 (d), 128.9 (d), 134.9 (s), 139.4 (s), 141.2 (s), 147.3 (s), 148.2 (s), 170.9 (s, -CO-N)

HR-MS: $[M+H]^+$ m/z (predicted) = 326.1751, m/z (measured) = 326.1751, difference = -2.15ppm

(2-Bromophenyl)(piperidin-1-yl)methanone (54a)

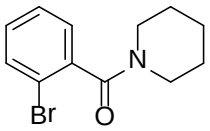

Method: C

Yield: 84% (2.51mmol, 673mg)

Appearance: brown oil

^{1}H NMR ($CDCl_3$, 200MHz): δ= 1.38-1.76 (m, 6H, CH_2), 3.10-3.28 (m, 2H, N-CH_2) 3.65-3.86 (m, 2H, N-CH_2), 7.18-7.39 (m, 3H, ArH), 7.55-7.59 (m, 1H, ArH)

^{13}C NMR ($CDCl_3$, 50MHz): δ= 24.5 (t, CH_2), 25.5 (t, CH_2), 26.3 (t, CH_2), 42.5 (t, N-CH_2), 47.8 (t, N-CH_2), 119.1 (s), 127.5 (d), 127.6(d), 130.0(d), 132.7 (d), 138.6 (s), 167.5(s, CO-N)

HR-MS: $[M+H]^+$ m/z (predicted) = 268.0332, m/z (measured) = 268.0337, difference = 1.87 ppm

(2-(Benzo[*d*][1,3]dioxol-5-yl)phenyl)(piperidin-1-yl)methanone (54)

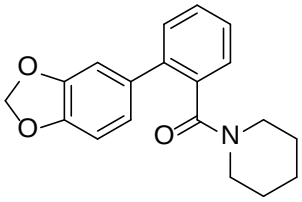

Method: B

Yield: 84% (0.25mmol, 78mg)

Appearance: colorless oil

TLC: 0.13 (LP/EtOAc 4:1)

^{1}H NMR ($CDCl_3$, 200MHz): δ= 0.72-0.94 (m, 1H, CH_2), 1.12-1.59 (m, 5H, CH_2), 2.71-2.83 (m, 1H, CH_2), 2.89-3.02 (m, 1H, CH_2), 3.47-3.64 (m, 2H, CH_2), 5.97-5.89 (m, 2H, O-CH_2-O), 6.83 (d, J = 8.4Hz, 1H, ArH), 6.94-6.99 (m, 2H, ArH), 7.32-7.42 (m, 4H, ArH)

^{13}C NMR ($CDCl_3$, 50MHz): δ= 24.2(t, CH_2), 25.2 (t,CH_2), 25.6 (t, CH_2), 42.3 (t, CH_2), 47.5 (t, CH_2), 101.1(t, O-CH_2-O), 108.3(d), 109.2(d), 122.5(d), 127.3(d), 127.4(d), 129.1(d), 129.2(d), 134.0(s), 135.7 (s), 138.0(s), 147.2(s), 147.7(s), 169.7 (s, CO-N)

HR-MS: $[M+H]^+$ m/z (predicted) = 310.1438, m/z (measured) =310.1430, difference = -2.58ppm

2-Bromo-*N*,*N*-dipropylbenzamide (55a)

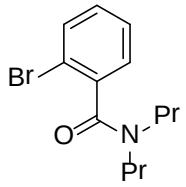

Method: C

Yield: 74% (2.22mmol, 632mg)

Appearance: brown oil

^{1}H NMR ($CDCl_3$, 200MHz): δ= 0.73 (t, J = 7.4Hz, 3H CH_3), 1.00 (t, J = 7.4Hz, 3H, CH_3), 1.38-1.83 (m, 4H, CH_2), 2.96-3.25 (m, 3H, N-CH_2), 3.70-3.84 (m, 1H, N-CH_2), 7.17-7.38 (m, 3H, ArH), 7.53-7.59 (m, 1H, ArH)

^{13}C NMR ($CDCl_3$, 50MHz): δ= 11.1 (q, CH_3), 11.6 (q, CH_3), 20.4 (t, CH_2), 21.6 (t, CH_2), 46.2 (t, N-CH_2), 50.0 (t, N-CH_2), 119.2 (s), 127.4 (d), 127.9(d), 129.9(d), 132.7 (d), 138.9 (s), 168.9(s, CO-N)

HR-MS: $[M+H]^+$ m/z (predicted) = 284.0645, m/z (measured) = 284.0652, difference = 2.46 ppm

2-(Benzo[*d*][1,3]dioxol-5-yl)-*N*,*N*-dipropylbenzamide (55)

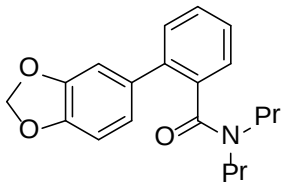

Method: B

Yield: 56% (0.17mmol, 55mg)

Appearance: colorless oil

TLC: 0.36 (LP/EtOAc 4:1)

^{1}H NMR ($CDCl_3$, 200MHz): δ= 0.61 (t, J = 7.4Hz, 3H, CH_3), 0.76 (t, J = 7.4Hz, 3H, CH_3), 1.15-1.44 (m, 4H, CH_2), 2.51-2.65(m, 1H, N-CH_2), 2.82-2.93 (m, 2H, N-CH_2), 3.65-3.79 (m, 1H, N-CH_2), 5.96 (s, 2H, O-CH_2-O), 6.81(d, J = 7.8Hz, 1H, ArH), 6.92-6.97 (m, 2H, ArH), 7.31-7.43 (m, 4H, ArH)

^{13}C NMR ($CDCl_3$, 50MHz): δ= 11.0(q, CH_3), 11.4(q,CH_3), 19.9(t, CH_2), 21.2(t, CH_2), 45.9(t, N-CH_2), 49.8(t, N-CH_2), 101.1(t, O-CH_2-O), 108.2(d), 109.4(d), 122.5(d), 127.2(d), 127.3(d), 128.8(d), 129.3(d), 134.0(s), 136.4(s), 138.0(s), 147.1(s), 147.6(s), 171.0(s, CO-N)

HR-MS: $[M+H]^+$ m/z (predicted) = 326.1751, m/z (measured) = 326.1752, difference = 0.31ppm

2-Bromo-*N*,*N*-dibutylbenzamide (56a)

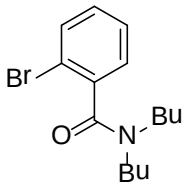

Method: C

Yield: 76% (2.28mmol, 712mg)

Appearance: brown oil

^{1}H NMR ($CDCl_3$, 200MHz): δ= 0.76 (t, J = 7.2Hz, 3H, CH_3), 0.98 (t, J = 7.2 Hz, 3H, CH_3), 1.06-1.21 (m, 2H, CH_2), 1.31-1.71 (m, 6H, CH_2), 3.02-3.11 (m, 2H, N-CH_2), 3.15-3.29 (m, 1H, N-CH_2), 3.71-3.86 (m, 1H, N-CH_2), 7.17-7.38 (m, 3H, ArH), 7.53-7.59 (m, 1H, ArH)

^{13}C NMR ($CDCl_3$, 50MHz): δ= 13.5 (q, CH_3), 13.9 (q, CH_3), 19.8 (t, CH_2), 20.4 (t, CH_2), 19.2 (t, CH_2), 30.5 (t, CH_2), 44.3 (t, N-CH_2), 48.1 (t, N-CH_2), 119.2 (s), 127.4 (d), 127.8(d), 129.9(d), 132.7 (d), 138.9 (s), 168.8(s, CO-N)

HR-MS: $[M+H]^+$ m/z (predicted) = 312.0958, m/z (measured) = 312.0974, difference = 5.13 ppm

2-(Benzo[*d*][1,3]dioxol-5-yl)-*N*,*N*-dibutylbenzamide (56)

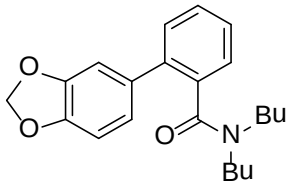

Method: B

Yield: 74% (0.22mmol, 78mg)

Appearance: colorless oil

TLC: 0.38 (LP/EtOAc 4:1)

^{1}H NMR ($CDCl_3$, 200MHz): δ= 0.68 (t, J = 7.0Hz, 3H, CH_3), 0.87 (t, J = 6.9Hz, 3H, CH_3), 0.94-1.44 (m, 8H, CH_2), 2.50-2.63(m, 1H, N-CH_2), 2.82-2.96 (m, 2H, N-CH_2), 3.68-3.82 (m, 1H, N-CH_2), 5.96 (s, 2H, O-CH_2-O), 6.81(d, J = 7.9Hz, 1H, ArH), 6.92-6.98 (m, 2H, ArH), 7.29-7.42 (m, 4H, ArH)

^{13}C NMR ($CDCl_3$, 50MHz): δ= 13.5(q, CH_3), 13.9(q,CH_3), 19.7(t, CH_2), 20.2(t, CH_2), 28.9(t, CH_2), 30.1(t, CH_2), 43.9(t, N-CH_2), 47.8(t, N-CH_2), 101.1(t, O-CH_2-O), 108.2(d), 109.4(d), 122.5(d), 127.2(d), 127.3(d), 128.8(d), 129.2(d), 134.0(s), 136.4(s), 138.0(s), 147.1(s), 147.5(s), 170.9(s, CO-N)

HR-MS: $[M+H]^+$ m/z (predicted) = 354.2064, m/z (measured) = 354.2067, difference = 0.85ppm

2-Bromo-*N,N*-diisopropylbenzamide (57a)

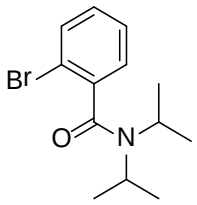

Method: C

Yield: 77% (3.89mmol, 1.10g)

Appearance: colorless solid

M.p.: 148-149°C

^{1}H NMR ($CDCl_3$, 200MHz): δ= 1.07 (d, J = 6.8Hz, 3H, CH_3), 1.24 (d, J = 6.8Hz, 3H, CH_3), 1.57 (d, J = 6.9Hz, 3H, CH_3), 1.58 (d, J = 6.9Hz, 3H, CH_3), 3.53 (sept, J = 6.8Hz, 1H, N-CH), 3.60 (sept, J = 6.9Hz, 1H, N-CH), 7.16-7.37 (m, 3H, ArH), 7.53-7.58 (m, 1H, ArH)

^{13}C NMR ($CDCl_3$, 50MHz): δ= 20.1 (q, CH_3), 20.6 (q, CH_3), 20.7 (q, CH_3), 20.8 (q, CH_3), 46.0 (d, N-CH), 51.1 (d, N-CH), 118.9 (s), 126.6(d), 127.5(d), 129.4(d), 132.8(d), 140.1(s), 168.2(s, CO-N)

HR-MS: $[M+H]^+$ m/z (predicted) = 284.0645, m/z (measured) = 284.0635, difference = -3.52ppm

2-(Benzo[*d*][1,3]dioxol-5-yl)-*N,N*-diisopropylbenzamide (57)

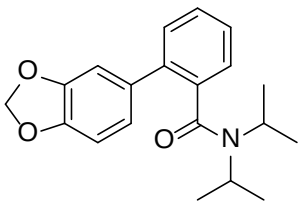

Method: B

Yield: 77% (0.27mmol, 88mg)

Appearance: colorless solid

TLC: 0.40 (LP/EtOAc 4:1)

M.p.: 141-144°C

^{1}H NMR ($CDCl_3$, 200MHz): δ= 0.61 (t, J = 7.4Hz, 3H, CH_3), 0.76 (t, J = 7.4Hz, 3H, CH_3), 1.15-1.44 (m, 4H, CH_2), 2.51-2.65(m, 1H, N-CH_2), 2.82-2.93 (m, 2H, N-CH_2), 3.65-3.79 (m, 1H, N-CH_2), 5.96 (s, 2H, O-CH_2-O), 6.81(d, J = 7.8Hz, 1H, ArH), 6.92-6.97 (m, 2H, ArH), 7.31-7.43 (m, 4H, ArH)

^{13}C NMR ($CDCl_3$, 50MHz): δ= 19.5 (q, CH_3), 19.7 (q,CH_3), 20.7 (q, CH_3), 20.8 (q, CH_3), 45.5(d, N-CH), 50.5 (d, N-CH), 101.1(t, O-CH_2-O), 108.2(d), 109.8(d), 122.9(d), 126.5(d), 127.3(d), 128.5(d), 129.1(d), 133.9(s), 137.2(s), 137.8(s), 147.1(s), 147.6(s), 170.3(s, CO-N)

HR-MS: $[M+H]^+$ m/z (predicted) =326.1751, m/z (measured) =326.1746, difference = -1.53ppm

5-(Benzo[*d*][1,3]dioxol-5-yl)thiophene-2-carboxylic acid (58a)

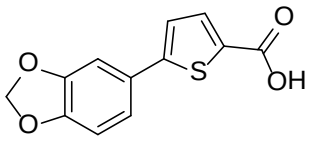

Method: B

Yield: 63% (1.15mmol, 282mg)

Appearance: beige solid

TLC: 0.25 ($CHCl_3$/MeOH 10%)

M.p.: 251-254°C

^{1}H NMR (DMSO-*d6*, 200MHz): δ= 6.09 (s, 2H O-CH_2-O), 6.99 (d, J = 8.1Hz, 1H, H7'), 7.23 (dd, J^1 = 8.1Hz, J^2 = 1.8Hz, 1H, H6'), 7.35 (d, J = 1.8Hz, 1H, H4'), 7.46 (d, J = 3.9Hz, 1H, H4), 7.67 (d, J = 3.9Hz, 1H, H3), 13.08 (bs, 1H, COOH)

^{13}C NMR (DMSO-*d6*, 50MHz): δ= 101.5 (t, O-CH_2-O), 106.2 (d), 108.8(d), 120.0(d), 123.8 (d), 127.0(s), 132.2(s), 134.2(d), 147.9 (s), 148.1 (s), 149.8(s), 162.8 (s, COOH)

HR-MS: $[M+H]^+$ m/z (predicted) = 247.0071, m/z (measured) = 247.0065, difference = -2.43 ppm

(5-(Benzo[*d*][1,3]dioxol-5-yl)thiophen-2-yl)(piperidin-1-yl)methanone (58)

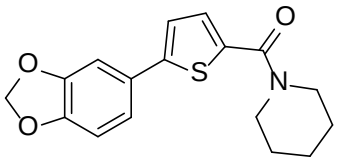

Method: C

Yield: 75% (0.15mmol, 48mg)

Appearance: beige solid

TLC: 0.14 (LP/EtOAc 4:1)

M.p.: 158-159°C

^{1}H NMR ($CDCl_3$, 200MHz): δ= 1.57-1.72 (m, 6H, CH_2), 3.66-3.71 (bm, 4H, N-CH_2), 5.98 (s, 2H, O-CH_2-O), 6.81 (d, J = 7.9Hz, 1H, ArH), 7.05-7.12(m, 3H, ArH), 7.19 (d, 3.8Hz, 1H, ArH)

^{13}C NMR ($CDCl_3$, 50MHz): δ= 24.6 (t, CH_2), 26.2 (t, CH_2), 101.4 (t, O-CH_2-O), 106.6(d), 108.7(d), 120.0(d), 121.9(d), 127.9(s), 129.5(d), 135.7(s), 147.2(s), 147.8(s), 148.2(s), 163.3 (s, CO-N)

HR-MS: $[M+H]^+$ m/z (predicted) = 316.1002, m/z (measured) = 316.0992, difference = -3.16ppm

5-(Benzo[*d*][1,3]dioxol-5-yl)-*N*,*N*-dipropylthiophene-2-carboxamide (59)

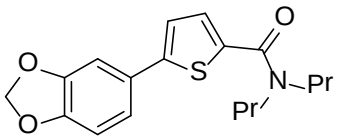

Method: C

Yield: 87% (0.17mmol, 58mg)

Appearance: colorless solid

TLC: 0.28 (LP/EtOAc 4:1)

M.p.: 158-159°C

^{1}H NMR ($CDCl_3$, 200MHz): δ= 0.93 (t, J = 7.4Hz, 6H, CH_3), 1.60-1.79 (m, 4H, CH_2), 3.42-3.50 (m, 4H, N-CH_2), 5.99 (s, 2H, O-CH_2-O), 6.82 (d, J = 7.9Hz, 1H, ArH), 7.07-7.13 (m, 3H, ArH), 7.23 (d, J = 3.8Hz, 1H, ArH)

^{13}C NMR ($CDCl_3$, 50MHz): δ= 11.2 (q, CH_3), 21.6 (t, CH_2), 101.4 (t, O-CH_2-O), 106.6(d), 108.7(d), 120.0(d), 122.0 (d), 127.9(s), 129.4 (s), 136.4(s), 147.2(s), 147.8(s), 148.2(s), 163.9 (s, CO-N)

HR-MS: $[M+H]^+$ m/z (predicted) = 332.1315, m/z (measured) = 332.1313, difference = -0.60ppm

5-(Benzo[*d*][1,3]dioxol-5-yl)-*N*,*N*-dibutylthiophene-2-carboxamide (60)

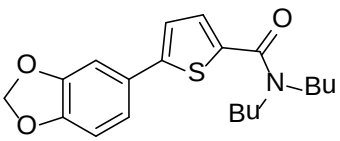

Method: C

Yield: 90% (0.11mmol, 39mg)

Appearance: colorless solid

TLC: 0.36 (LP/EtOAc 4:1)

M.p.: 78-79°C

^{1}H NMR ($CDCl_3$, 200MHz): δ= 0.95 (t, J = 7.1Hz, 6H, CH_3), 1.26-1.41 (m, 4H, CH_2), 1.60-1.70 (m, 4H, CH_2), 3.46-3.54 (m, 4H, N-CH_2), 5.99 (s, 2H, O-CH_2-O), 6.82 (d, J = 7.9Hz, 1H, ArH), 7.07-7.13 (m, 3H, ArH), 7.24 (d, J = 3.9Hz, 1H, ArH)

^{13}C NMR ($CDCl_3$, 50MHz): δ= 13.9 (q, 2C, CH_3), 20.1 (t, 2C, CH_2), 29.3 (t, CH_2), 30.5 (t, CH_2) 43.6 (t, N-CH_2), 47.8 (t, N-CH_2), 101.4 (t, O-CH_2-O), 106.6(d), 108.7(d), 120.0(d), 122.0 (d), 127.9(s), 129.3 (s), 136.5(s), 147.2(s), 147.8(s), 148.2(s), 163.8 (s, CO-N)

HR-MS: $[M+H]^+$ m/z (predicted) = 360.1628, m/z (measured) = 360.1621, difference = 1.94ppm

5-(Benzo[*d*][1,3]dioxol-5-yl)-*N*,*N*-diisopropylthiophene-2-carboxamide (61)

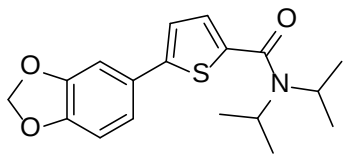

Method: C

Yield: 63% (0.15mmol, 49mg)

Appearance: beige solid

M.p.: 152-153°C

^{1}H NMR ($CDCl_3$, 200MHz): δ= 1.39 (d, J = 6.7Hz, 12H, CH_3), 4.02 (bm, 2H, N-CH), 5.99 (s, 2H, O-CH_2-O), 6.82 (d, J = 7.9Hz, 1H, ArH), 7.04-7.14(m, 4H, ArH)

^{13}C NMR ($CDCl_3$, 50MHz): δ= 20.9 (q, 4C, CH_3), 48.9 (d, 2C, N-CH), 101.3 (t, O-CH_2-O), 106.6(d), 108.7(d), 120.0(d), 121.8(d), 127.9(d), 128.0(s), 138.2(s), 146.3(s), 147.7(s), 148.2(s), 163.6 (s, CO-N)

HR-MS: $[M+H]^+$ m/z (predicted) = 332.1315, m/z (measured) =332.1309, difference = -1.81ppm

5-(Benzo[*d*][1,3]dioxol-5-yl)-1-naphthoic acid (62a)

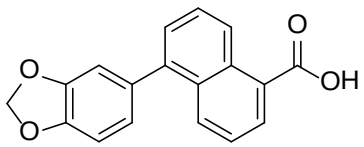

Compound **62a** was synthesized starting from 3,4-(methylenedioxy)phenyl boronic acid and 5-bromo-1-naphtoic acid according to general procedure B.

Yield: 59% (208mg, 0.71mmol)

M.p.: 246-249°C, sublimation above 210°C

Appearance: colorless solid

TLC: 0.42 (LP/EtOAc 4:1 + drops of AcOH)

^{1}H NMR (DMSO, 200 MHz): δ=6.12 (s, 2H, O-CH_2-O), 6.91 (dd, $^{3}J_{H7'}$=7.9Hz, $^{4}J_{H4'}$=1.6Hz, 1H, H6'), 7.03 (d, $^{4}J_{H6'}$=1.6Hz, 1H, H4'), 7.08 (d, $^{3}J_{H6'}$=7.9Hz, 1H, H7'), 7.48 (dd, J^{1}=7.0Hz, J^{2}=1.1Hz, 1H, ArH), 7.56 (dd, ^{3}J=8.5Hz, ^{3}J=7.2Hz, 1H, ArH), 7.67 (dd, ^{3}J=8.7Hz, ^{3}J=7.1Hz, 1H, ArH), 8.04 (d, ^{3}J=8.5Hz, 1H, ArH), 8.13 (dd, ^{3}J=7.2Hz, ^{4}J=1.1Hz, 1H, ArH), 8.84 (d, ^{3}J=8.6Hz, 1H, ArH), 13.22 (bs, 1H, COOH)

^{13}C NMR (DMSO, 50 MHz): 106.4 (t, O-CH2-O), 113.5 (d), 115.5 (d), 128.6 (d), 130.1 (d), 130.3 (d), 132.1 (d), 132.3 (d), 133.7 (s), 134.6 (d), 135.3 (d), 136.2 (s), 136.8 (s), 138.9 (s), 145.0 (s), 152.0 (s), 152.6 (s), 174.1 (s, COOH)

HR-MS: $[M-H]^{-}$ m/z (predicted) = 291.0663, m/z (measured) = 291.0656, difference = -2.40 ppm

5-(Benzo[*d*][1,3]dioxol-5-yl)-*N*,*N*-dipropyl-1-naphthamide (63)

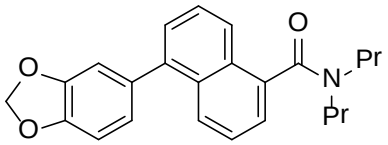

The title compound was prepared according to the modified general method E: instead of HOBt, two equivalents of N-hydroxysuccinimide were used.

Yield: 33% (0.056mmol, 21mg)

Appearance: colorless oil

TLC: 0.60 (LP/EtOAc 2:1)

^{1}H NMR ($CDCl_3$, 200MHz): δ= 0.66 (t, J = 7.4Hz, 3H, CH_3), 1.07 (t, J = 7.4Hz, 3H, CH_3), 1.40-1.59 (m, 2H, CH_2), 1.75-1.91 (m, 2H, CH_2), 3.00-3.09 (m, 2H, N-CH_2), 3.36-3.50 (m, 1H, N-CH_2), 3.72-3.82 (m, 1H, N-CH_2), 6.05 (s, 2H, O-CH_2-O), 6.93-6.96 (m, 3H, ArH), 7.36-7.55 (m, 4H, ArH), 7.79 (d, J = 8.3Hz, 1H, ArH), 7.93 (dd, J^{1} = 7.3Hz, J^{2} = 2.5Hz, 1H, ArH)

^{13}C NMR ($CDCl_3$, 50MHz): δ= 11.1 (q, CH_3), 11.6 (q, CH_3), 20.8 (t, CH_2), 21.9 (t, CH_2), 46.2 (t, N-CH_2), 50.4 (t, N-CH_2), 101.2 (t, O-CH_2-O), 108.2 (d), 110.6 (d), 123.4 (d), 123.5 (d), 124.3 (d), 125.1(d), 126.2(d), 126.8(d), 127.3(d), 129.9(s), 131.9(s), 134.4(s), 135.5(s), 140.2(s), 147.0(s), 147.5(s), 170.8 (s, CO-N)

HR-MS: $[M+H]^{+}$ m/z (predicted) = 376.1907, m/z (measured) =376.1912, difference = 1.33ppm

5-(Benzo[*d*][1,3]dioxol-5-yl)-*N*,*N*-dibutyl-1-naphthamide (64)

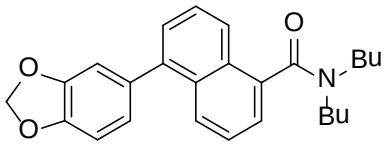

Method: E

Yield: 59% (0.10mmol, 38mg)

Appearance: colorless oil

TLC: 0.31 (LP/EtOAc 4:1)

^{1}H NMR ($CDCl_3$, 200MHz): δ= 0.68 (t, J = 7.2Hz, 3H, CH_3), 1.04 (t, J = 7.2Hz, 3H, CH_3), 1.40-1.55 (m, 4H, CH_2), 1.71-1.85 (m, 2H, CH_2), 3.02-3.09 (m, 2H, N-CH_2), 3.38-3.53 (m, 1H, N-CH_2), 3.75-3.90 (m, 1H, N-CH_2), 6.05 (s, 2H, O-CH_2-O), 6.93-6.95 (m, 3H, ArH), 7.36-7.56 (m, 4H, ArH), 7.79 (d, J = 8.3Hz, 1H, ArH), 7.93 (dd, J^1 = 7.3Hz, J^2 = 2.5Hz, 1H, ArH)

^{13}C NMR ($CDCl_3$, 50MHz): δ= 13.7 (q, CH_3), 14.1 (q, CH_3), 19.8(t, CH_2), 20.6 (t, CH_2), 29.8(t, CH_2), 30.9(t, CH_2), 44.5 (t, N-CH_2), 48.6(t, N-CH_2), 101.3 (t, O-CH_2-O), 108.4 (d), 110.7 (d), 123.5 (d), 123.6 (d), 124.5 (d), 125.2(d), 126.3(d), 126.9(d), 127.4(d), 130.0(s), 132.0(s), 134.5(s), 135.7(s), 140.3(s), 147.1(s), 147.6(s), 170.8 (s, CO-N)

HR-MS: $[M+H]^+$ m/z (predicted) = 404.2220, m/z (measured) = 404.2238, difference = 4.45ppm

(*E*)-3-(Naphtho[2,3-*d*][1,3]dioxol-5-yl)acrylic acid (65b)

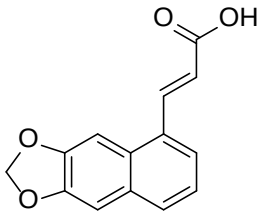

Method: A

Yield: 97% (0.74mmol, 180mg)

Appearance: colorless solid

M.p.: 267-271°C

^{1}H NMR (DMSO-*d6*, 200MHz): δ= 6.16 (s, 2H, O-CH_2-O), 6.51 (d, J = 15.7Hz, 1H, H2), 7.32-7.39 (m, 2H, H4', H7'), 7.51 (s, 1H, H9'), 7.74 (d, J = 7.3Hz, 1H), 7.81 (d, J = 8.1Hz, 1H), 8.23 (d, J = 15.7Hz, 1H, H3), 12.52 (bs, 1H, COOH)

^{13}C NMR (DMSO-*d6*, 50MHz): δ= 99.3 (d), 101.5 (t, O-CH_2-O), 104.2 (d), 121.3 (d), 123.5 (d), 124.0 (d), 128.1 (s), 129.3 (d), 130.1 (s), 130.6 (s), 140.7 (d), 147.3 (s), 148.4 (s), 167.4 (s, COOH)

(*E*)-3-(Naphtho[2,3-*d*][1,3]dioxol-5-yl)-1-(piperidin-1-yl)prop-2-en-1-one (65)

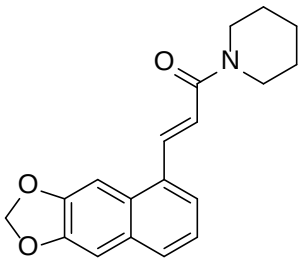

Method: C

Yield: 69% (0.11mmol,35mg)

Appearance: colorless solid

TLC: 0.06 (LP/EtOAc 4:1)

M.p.: 144-148°C

^{1}H NMR ($CDCl_3$, 200MHz): δ= 1.58-1.75 (m, 6H, CH_2), 3.55-3.79 (m, 4H, N-CH_2), 6.05 (s, 2H, O-CH_2-O), 6.92 (d, J = 15.1Hz, 1H, H2), 7.12 (s, 1H, ArH), 7.31 (t, J = 7.8H, H7'), 7.51 (s, 1H, ArH), 7.56 (d, J^1 = 7.1Hz, 1H, ArH), 7.66 (d, 1H, ArH), 8.31 (d, J = 15.1Hz, 1H, H3)

^{13}C NMR ($CDCl_3$, 50MHz): δ= 24.6 (t, CH_2), 100.4(s), 101.3 (t, O-CH_2-O), 104.3 (d), 120.4(d), 123.1 (d), 123.9(d), 128.6(d), 128.8(s), 130.9(s), 132.4(s), 139.9 (d), 147.6(s), 148.4(s), 165.3 (s, CO-N)

HR-MS: $[M+H]^+$ m/z (predicted) = 310.1438, m/z (measured) = 310.1441, difference = 0.97ppm

(*E*)-3-(Naphtho[2,3-*d*][1,3]dioxol-5-yl)-*N*,*N*-dipropylacrylamide (66)

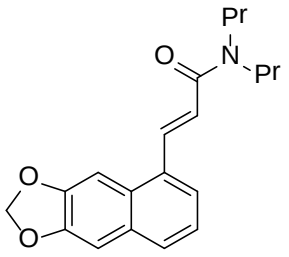

Method: C

Yield: 74% (0.13mmol,40mg)

Appearance: colorless solid

TLC: 0.17 (LP/EtOAc 4:1)

M.p.: 86-89°C

^{1}H NMR ($CDCl_3$, 200MHz): δ= 0.96 (t, J = 7.4Hz, 6H, CH_3), 1.58-1.79 (m, 4H, CH_2), 3.35-3.47 (m, 4H, N-CH_2), 6.05 (s, 2H, O-CH_2-O), 6.84 (d, J = 15.0Hz, 1H, H2), 7.12 (s, 1H,

ArH), 7.31 (t, J = 7.7H, H7'), 7.52-7.56 (m, 2H, ArH), 7.66 (d, J = 8.0Hz, 1H, ArH), 8.35 (d, J = 15.0Hz, 1H, H3)

^{13}C NMR ($CDCl_3$, 50MHz): δ= 11.3 (q, CH_3), 11.5 (q, CH_3), 21.2 (t, CH_2), 23.1 (t, CH_2), 48.7 (t, N-CH_2), 49.9 (t, N-CH_2),100.5(d), 101.3 (t, O-CH_2-O), 104.3 (d), 120.6(d), 123.1 (d), 123.9(d), 128.6(d), 128.8(s), 130.9(s), 132.5(s), 139.9 (d), 147.6(s), 148.4(s), 166.1 (s, CO-N)

HR-MS: $[M+H]^+$ m/z (predicted) = 326.1751, m/z (measured) = 326.1755, difference = 1.23ppm

(*E*)-3-(Naphtho[2,3-*d*][1,3]dioxol-5-yl)-*N*,*N*-dibutylacrylamide (67)

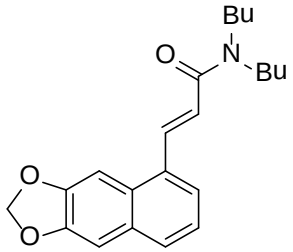

Method: C

Yield: 86% (0.14mmol, 50mg)

Appearance: colorless solid

TLC: 0.29 (LP/EtOAc 4:1)

M.p.: 46-49°C

^{1}H NMR ($CDCl_3$, 200MHz): δ= 0.88 (t, J = 7.2Hz, 6H, CH_3), 1.20-1.39 (m, 4H, CH_2), 1.46-1.63 (m, 4H, CH_2), 3.29-3.42 (m, 4H, N-CH_2), 5.96 (s, 2H, O-CH_2-O), 6.76 (d, J = 15.0Hz, 1H, H2), 7.03 (s, 1H, ArH), 7.23 (t, J = 7.7H, H7'), 7.44-7.47 (m, 2H, ArH), 7.58 (d, J = 8.0Hz, 1H, ArH), 8.28 (d, J = 15.0Hz, 1H, H3)

^{13}C NMR ($CDCl_3$, 50MHz): δ= 13.8 (q, CH_3), 13.9 (q, CH_3), 20.1 (t, CH_2), 20.4 (t, CH_2), 30.1 (t, CH_2), 32.0 (t, CH_2), 46.8 (t, N-CH_2), 48.0 (t, N-CH_2), 100.5(d), 101.3 (t, O-CH_2-O), 104.3 (d), 120.5(d), 123.1 (d), 123.9(d), 128.6(d), 128.8(s), 130.9(s), 132.5(s), 139.9 (d), 147.6(s), 148.4(s), 165.9 (s, CO-N)

HR-MS: $[M+H]^+$ m/z (predicted) = 354.2064, m/z (measured) = 354.2071, difference = 1.98ppm

(*E*)-3-(Naphtho[2,3-*d*][1,3]dioxol-6-yl)acrylic acid (68d)

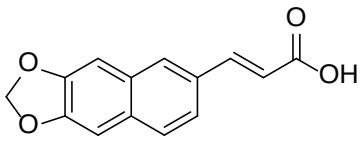

Method: A

Yield: 100% (0.84mmol, 204mg)

Appearance: colorless solid

M.p.: 265-270°C

^{1}H NMR (DMSO-*d6*, 200MHz): δ= 6.14 (s, 2H, O-CH_2-O), 6.55 (d, J = 16.0Hz, 1H, H2), 7.30-7.32 (m, 2H, H4', H9'), 7.61-7.76 (m, 3H), 7.97 (s 1H, ArH), 12.35 (bs, 1H, COOH)

^{13}C NMR (DMSO-*d6*, 50MHz): δ= 101.5 (t, O-CH_2-O), 103.7 (d), 104.1 (d), 118.4 (d), 122.7 (d), 127.5 (d), 128.5 (d), 130.0 (s), 130.2 (s), 131.3 (s), 144.2 (d), 147.9 (s), 148.5 (s), 167.7 (s, COOH)

(*E*)-3-(Naphtho[2,3-*d*][1,3]dioxol-6-yl)-1-(piperidin-1-yl)prop-2-en-1-one (68)

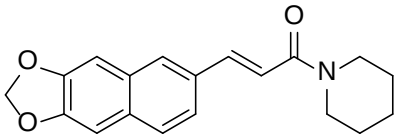

Method: C

Yield: 76% (0.13mmol, 39mg)

Appearance: colorless solid

TLC: 0.10 (LP/EtOAc 4:1)

M.p.: 204-206°C

^{1}H NMR ($CDCl_3$, 200MHz): δ= 1.47-1.68 (m, 6H, CH_2), 3.44-3.72(m, 4H, N-CH_2), 5.96 (s, 2H, O-CH_2-O), 6.88 (d, J = 15.4Hz, 1H, H2), 7.01 (s, 1H, ArH), 7.03 (1H, ArH), 7.44 (dd, J^1 = 8.5Hz, J^2 = 1.4Hz, 1H, H7'), 7.54 (d, J^1 = 8.5Hz, 1H, H8'), 7.65 (s, 1H, H5'), 7.67 (d, J = 15.4Hz, 1H, H3)

^{13}C NMR ($CDCl_3$, 50MHz): δ= 24.7 (t, CH_2), 25.6 (t, CH_2), 26.8 (t, CH_2), 43.4 (t, N-CH_2), 47.0 (t, N-CH_2), 101.2 (t, O-CH_2-O), 103.9 (d), 104.3 (d), 117.0(d), 122.5 (d), 127.4(d), 127.9(d), 130.4(s), 131.1(s), 131.6(s), 142.4 (d), 148.0(s), 148.4(s), 165.5(s, CO-N)

HR-MS: $[M+H]^+$ m/z (predicted) = 310.1438, m/z (measured) = 310.1437, difference = -0.32ppm

(*E*)-3-(Naphtho[2,3-*d*][1,3]dioxol-6-yl)-*N*,*N*-dipropylacrylamide (69)

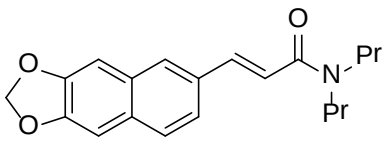

Method: C

Yield: 61% (0.10mmol, 33mg)

Appearance: colorless solid

TLC: 0.22 (LP/EtOAc 4:1)

M.p.: 85-87°C

^{1}H NMR ($CDCl_3$, 200MHz): δ= 0.90-1.01 (m, 6H, CH_3), 1.55-1.79 (m, 4H, CH_2), 3.35-3.45 (m, 4H, N-CH_2), 6.03 (s, 2H, O-CH_2-O), 6.88 (d, J = 15.3Hz, 1H, H2), 7.09 (s, 1H, ArH), 7.11 (1H, ArH), 7.50 (dd, J^1 = 8.5Hz, J^2 = 1.5Hz, 1H, H7'), 7.62 (d, J^1 = 8.5Hz, 1H, H8'), 7.72 (s, 1H, H5'), 7.80 (d, J = 15.3Hz, 1H, H3)

^{13}C NMR ($CDCl_3$, 50MHz): δ=11.4 (q,CH_3), 11.4 (q, CH_3), 21.2 (t, CH_2), 23.1 (t, CH_2), 48.6 (t, N-CH_2), 49.9 (t, N-CH_2), 101.2 (t, O-CH_2-O), 103.9 (d), 104.3 (d), 117.1(d), 122.4 (d), 127.4(d), 128.0(d), 130.5(s), 131.2(s), 131.6(s), 142.4 (d), 148.1(s), 148.4(s), 166.3 (s, CO-N)

HR-MS: $[M+H]^+$ m/z (predicted) = 326.1751, m/z (measured) = 326.1747, difference = -1.23ppm

(*E*)-3-(Naphtho[2,3-*d*][1,3]dioxol-6-yl)-*N*,*N*-dibutylacrylamide (70)

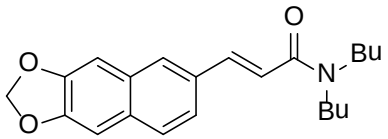

Method: C

Yield: 82% (0.14mmol,48mg)

Appearance: colorless solid

TLC: 0.31 (LP/EtOAc 4:1)

M.p.: 59-61°C

^{1}H NMR ($CDCl_3$, 200MHz): δ= 0.92-1.03 (m, 6H, CH_3), 1.26-1.46 (m, 4H, CH_2), 1.50-1.73 (m, 4H, CH_2), 3.39-3.49 (m, 4H, N-CH_2), 6.05 (s, 2H, O-CH_2-O), 6.89 (d, J = 15.3Hz, 1H, H2), 7.10 (s, 1H, ArH), 7.13 (1H, ArH), 7.51 (dd, J^1 = 8.5Hz, J^2 = 1.5Hz, 1H, H7'), 7.64 (d, J^1 = 8.5Hz, 1H, H8'), 7.73 (s, 1H, H5'), 7.80 (d, J = 15.3Hz, 1H, H3)

^{13}C NMR ($CDCl_3$, 50MHz): δ=13.8 (q, CH_3), 13.9 (q, CH_3), 20.1 (t, CH_2), 20.3 (t, CH_2), 30.1 (t, CH_2), 32.0 (t, CH_2), 46.7 (t, N-CH_2), 48.0 (t, N-CH_2), 101.2 (t, O-CH_2-O), 103.9 (d), 104.3 (d), 117.1(d), 122.4 (d), 127.4(d), 128.1(d), 130.5(s), 131.2(s), 131.6(s), 142.4 (d), 148.1(s), 148.4(s), 166.2 (s, CO-N)

HR-MS: $[M+H]^+$ m/z (predicted) = 354.2064, m/z (measured) = 354.2068, difference = 1.13ppm

Naphtho[2,3-*d*][1,3]dioxol-5-yl(piperidin-1-yl)methanone (71)

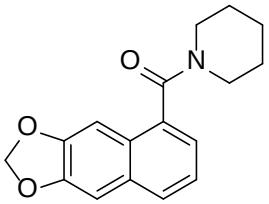

Method: E

Yield: 79% (0.092mmol, 26mg)

Appearance: colorless solid

TLC: 0.10 (LP/EtOAc 4:1)

M.p.: 116-120°C

^{1}H NMR ($CDCl_3$, 200MHz): δ= 1.35-1.47 (m, 2H, CH_2), 1.69-1.75 (m, 4H, CH_2), 3.12-3.18 (m, 2H, N-CH_2), 3.82-3.87 (m, 2H, N-CH_2), 6.04 (s, 2H, O-CH_2-O), 7.12-7.14 (m, 2H, H4, H9), 7.21-7.35 (m, 2H, ArH), 7.65 (d, J = 7.91Hz, ArH)

^{13}C NMR ($CDCl_3$, 50MHz): δ= 24.7 (t, CH_2), 25.9 (t, CH_2), 26.9 (t, CH_2), 42.8 (t, N-CH_2), 48.4 (t, N-CH_2), 101.3 (t, O-CH_2-O), 101.3 (d), 104.3(d), 122.1 (d), 123.9(d), 126.8(s), 127.9(d), 130.9(s), 134.1(s), 148.0(s), 148.5(s), 169.6 (s, CO-N)

HR-MS: $[M+H]^+$ m/z (predicted) =284.1281, m/z (measured) =284.1265, difference = -5.63ppm

_N,N_-Dipropylnaphtho[2,3-_d_][1,3]dioxole-5-carboxamide (72)

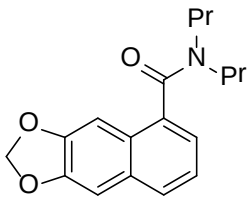

Method: C

Yield: 90% (0.17mmol, 50mg)

Appearance: colorless solid

M.p.: 60-62°C

^{1}H NMR ($CDCl_3$, 200MHz): δ= 0.57 (t, 3H, J = 7.4Hz, CH_3), 0.97 (t, 3H, J = 7.4Hz, CH_3), 1.29-1.48 (m, 2H, CH_2), 1.64-1.83 (m, 2H, CH_2), 2.89-2.99 (m, 2H, N-CH_2), 3.33-3.65 (m, 2H, N-CH_2), 5.96 (s, 2H, O-CH_2-O), 7.00 (s, 1H, ArH), 7.04 (s, 1H, ArH), 7.15 (dd, J^1 = 7.1Hz, J^2 = 1.4Hz, 1H, ArH), 7.21 (d, J = 7.8Hz, 1H, ArH), 7.57 (d, J = 7.8Hz, ArH)

^{13}C NMR ($CDCl_3$, 50MHz): δ= 11.1 (q, CH_3), 11.6 (q, CH_3), 20.8 (t, CH_2), 21.9 (t, CH_2), 46.2 (t, N-CH_2), 50.4 (t, N-CH_2), 101.2 (t, O-CH_2-O), 101.2 (d), 104.2(d), 122.1 (d), 123.7(d), 126.6(s), 127.7(d), 130.8(s), 134.3(s), 147.8(s), 148.4(s), 170.9 (s, CO-N)

HR-MS: $[M+H]^+$ m/z (predicted) = 300.1594, m/z (measured) = 300.1580, difference = -4.66ppm

_N,N_-Dibutylnaphtho[2,3-_d_][1,3]dioxole-5-carboxamide (73)

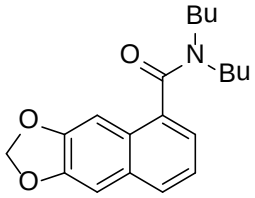

Method: C

Yield: 83% (0.15mmol, 50mg)

Appearance: colorless solid

TLC: 0.30 (LP/EtOAc 4:1)

M.p.: 77-79°C

^{1}H NMR ($CDCl_3$, 200MHz): δ= 0.59 (t, 3H, J = 7.2Hz, CH_3), 0.86-1.04 (m, 5H, CH_2, CH_3), 1.26-1.45 (m, 4H, CH_2), 1.63-1.72 (m, 2H, CH_2), 2.91-3.00 (m, 2H, N-CH_2), 3.29-3.43 (m, 1H, N-CH_2), 3.62-3.75 (m, 1H, N-CH_2), 5.96 (s, 2H, O-CH_2-O), 7.00 (s, 1H, ArH), 7.04 (s, 1H, ArH), 7.14 (dd, J^1 = 7.0Hz, J^2 = 1.3Hz, 1H, ArH), 7.21 (d, J = 7.8Hz, 1H, ArH), 7.57 (d, J = 7.8Hz, ArH)

^{13}C NMR ($CDCl_3$, 50MHz): δ= 13.5 (q, CH_3), 14.0 (q, CH_3), 19.7 (t, CH_2), 20.5 (t, CH_2), 29.7 (t, CH_2), 30.8 (t, CH_2), 44.4 (t, N-CH_2),48.5 (t, N-CH_2), 101.2 (t, O-CH_2-O), 101.2 (d), 104.2(d), 122.1 (d), 123.7(d), 126.6(s), 127.7(d), 130.8(s), 134.3(s), 147.8(s), 148.4(s), 170.8 (s, CO-N)

HR-MS: $[M+H]^+$ m/z (predicted) = 328.1907, m/z (measured) =328.1901, difference = -1.83ppm

_N,N_-Diisobutylnaphtho[2,3-_d_][1,3]dioxole-5-carboxamide (74)

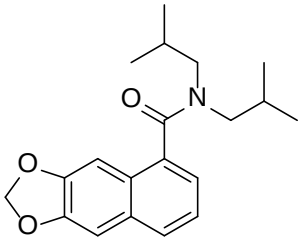

Method: D

Yield: 69% (0.16mmol, 52mg)

Appearance: colorless solid

TLC: 0.60 (LP/EtOAc 4:1)

M.p.: 124-126°C

^{1}H NMR ($CDCl_3$, 200MHz): δ= 0.64-0.74 (m, 6H, , CH_3), 1.07 (d, J = 6.6Hz, 6H, CH_3), 1.71-1.92 (m, 1H, CH), 2.12-2.32 (m, 1H, CH), 2.85-3.09 (m, 2H, N-CH_2), 3.49 (d, J = 7.5Hz, 2H, N-CH_2), 6.02 (s, 2H, O-CH_2-O), 7.11 (s, 1H, ArH), 7.17 (s, 1H, ArH), 7.22 (dd, J^1 = 7.1Hz, J^2 = 1.6Hz, 1H, ArH), 7.27-7.34 (m, 1H, ArH), 7.64 (dd, J^1 = 7.9Hz, J^2 = 0.9Hz, ArH)

^{13}C NMR ($CDCl_3$, 50MHz): δ= 19.7 (q, CH_3), 20.0 (q, CH_3), 20.5(q, CH_3), 20.6(q, CH_3), 26.3(d), 26.5(d), 51.2 (t, N-CH_2), 56.2 (t, N-CH_2), 101.2 (t, O-CH_2-O), 101.2 (d), 104.2(d), 122.0 (d), 123.5(d), 126.9(s), 127.8(d), 130.9(s), 134.3(s), 147.8(s), 148.4(s), 171.7 (s, CO-N)

HR-MS: $[M+H]^+$ m/z (predicted) = 328.1907, m/z (measured) = 328.1901, difference = -1.83ppm

Naphtho[2,3-*d*][1,3]dioxole-6-carboxylic acid (75c)

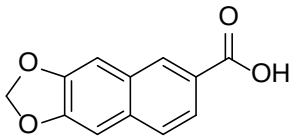

Method: A

Yield: 84% (1.46mmol, 315mg)

Appearance: colorless solid

M.p.: 316-317°C

^{1}H NMR (DMSO-*d6*, 200MHz): δ= 6.18 (s, 2H, O-CH_2-O), 7.39 (s, 1H, ArH), 7.51 (s, 1H, ArH), 7.81 (s, 2H, H7, H8), 8.42 (s, 1H, ArH), 12.88 (bs, 1H, COOH)

^{13}C NMR (DMSO-*d6*, 50MHz): δ= 101.6 (t, O-CH_2-O), 103.4 (d), 104.6 (d), 123.8 (d), 126.3 (s), 126.9 (d), 129.3 (d), 132.8 (s), 147.9 (s), 149.2 (s), 167.5 (s, COOH); one singulett is missing due to signal overlap.

HR-MS: $[M-H]^-$ m/z (predicted) = 215.0350, m/z (measured) = 215.0367, difference = 7.91ppm

Naphtho[2,3-*d*][1,3]dioxol-6-yl(piperidin-1-yl)methanone (75)

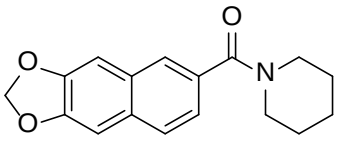

Method: C

Yield: 87% (0.20mmol, 57mg)

Appearance: colorless solid

M.p.: 137-138°C

^{1}H NMR ($CDCl_3$, 200MHz): δ= 1.40-1.69 (m, 6H, CH_2) 3.34-3.63 (m, 4H, N-CH_2), 5.97 (s, 2H, O-CH_2-O), 7.03-7.04 (m, 2H, H4, H9), 7.24 (dd, J^1 = 8.3Hz, J^2 = 1.6Hz, 1H, H7), 7.58 (d, J = 8.3Hz, 1H, H8), 7.63 (d, J = 1.6Hz, H5)

^{13}C NMR ($CDCl_3$, 50MHz): δ= 24.6 (t, CH_2), 26.3 (bt, CH_2), 101.2 (t, O-CH_2-O), 103.7 (d), 104.2(d), 122.8 (d), 125.7(d), 127.0(d), 129.9(s), 130.9(s), 132.3(s), 148.1(s), 148.4(s), 170.5 (s, CO-N)

HR-MS: $[M+H]^+$ m/z (predicted) = 284.1281, m/z (measured) = 284.1261, difference = -7.04ppm

_N,N_-Dipropylnaphtho[2,3-_d_][1,3]dioxole-6-carboxamide (76)

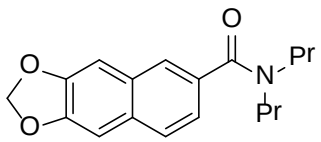

Method: C

Yield: 100% (0.23mmol, 69mg)

Appearance: colorless solid

M.p.: 60-62°C

^{1}H NMR ($CDCl_3$, 200MHz): δ= 0.44-1.09 (m, 6H, CH_3) 1.28-1.83 (m, 4H, CH_2), 2.83-3.67 (m, 4H, N-CH_2), 5.96 (s, 2H, O-CH_2-O), 7.03-7.04 (m, 2H, H4, H9), 7.24 (dd, J^1 = 8.3Hz, J^2 = 1.5Hz, 1H, H7), 7.56-7.60 (m, 2H, H5, H8)

^{13}C NMR ($CDCl_3$, 50MHz): δ= 11.2 (q, CH_3), 11.3 (q, CH_3), 20.7 (t, CH_2), 21.9 (t, CH_2), 46.3 (t, N-CH_2), 50.8 (t, N-CH_2), 101.2 (t, O-CH_2-O), 103.7 (d), 104.1(d), 122.6 (d), 125.2(d), 127.1(d), 129.9(s), 130.6(s), 133.2(s), 148.1(s), 148.3(s), 171.9 (s, CO-N)

HR-MS: $[M+H]^+$ m/z (predicted) = 300.1594, m/z (measured) = 300.1581, difference = -4.33ppm

_N,N_-Dibutylnaphtho[2,3-_d_][1,3]dioxole-6-carboxamide (77)

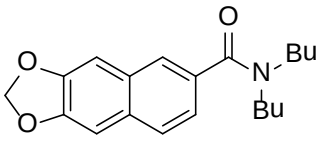

Method: C

Yield: 95% (0.22mmol, 72mg)

Appearance: colorless solid

M.p.: 46-51°C

^{1}H NMR ($CDCl_3$, 200MHz): δ= 0.47-1.71 (m, 14H, CH_3), 3.05-3.56 (m, 4H, N-CH_2), 5.96 (s, 2H, O-CH_2-O), 7.03 (m, 2H, H4, H9), 7.22 (dd, J^1 = 8.3Hz, J^2 = 1.4Hz, 1H, H7), 7.58 (d, J = 8.3Hz, 1H, H8), 7.58 (d, J = 1.4Hz, 1H, H5)

^{13}C NMR ($CDCl_3$, 50MHz): δ= 13.8 (q, 2C, CH_3), 19.8 (t, CH_2), 20.2 (t, CH_2), 29.7 (t, CH_2), 30.8(t, CH_2), 44.5 (t, N-CH_2), 48.9 (t, N-CH_2), 101.2 (t, O-CH_2-O), 103.7 (d), 104.1(d), 122.7 (d), 125.2(d), 127.0(d), 129.9(s), 130.6(s), 133.2(s), 148.1(s), 148.3(s), 171.8 (s, CO-N)

HR-MS: $[M+H]^+$ m/z (predicted) =328.1907, m/z (measured) =328.1905, difference = -0.61ppm

2 A shell script for evaluation the costs: costsensitive.sh

```
#!/bin/bash

cd $1
training=$2
EXPECTED_ARGS=2
E_BADARGS=65
if [ $# -ne $EXPECTED_ARGS ]
then echo "Usage: `basename $0` path training-set test-set" exit $E_BADARGS
fi
for method in NB IBk J48 RF SMO; do
mkdir ./$method;
folder=./$method;
echo "Now calculating CostSensitive + $method";
 summary="${method}_summary.txt"
echo "$method" > $summary
echo "method Cost_FN Cost_FP TN FN TP FP total_negative total_positive total spec sens
accuracy precision g-mean f-measure mcc " >> $summary
FP=0;
FN=1;
counter_FN=0;
while [ $counter_FN -le 200 ]; do
counter_FP=0;
FP=0;
while [ $counter_FP -le 200 ]; do
out="${method}_${FN}_${FP}"
case "$method" in
NB)  java -cp /home/daria/tools/weka/weka-3-7-9/weka.jar
weka.filters.unsupervised.attribute.Remove -R 1 \
 -W weka.classifiers.meta.CostSensitiveClassifier \
-cost-matrix "[0.0 $FN; $FP 0.0]" -W weka.classifiers.bayes.NaiveBayes \
-t $training -x 10 > $out_CV.out \
;;
IBk) java -cp /home/daria/tools/weka/weka-3-7-9/weka.jar
weka.classifiers.meta.CostSensitiveClassifier \
-cost-matrix "[0.0 $FN; $FP 0.0]" -W weka.classifiers.lazy.IBk -K 10\
-t $training -x 10 > $out_CV.out \
;;
J48) java -cp /home/daria/tools/weka/weka-3-7-9/weka.jar
weka.classifiers.meta.CostSensitiveClassifier \
-cost-matrix "[0.0 $FN; $FP 0.0]" -W weka.classifiers.trees.J48 \
-t $training -x 10 > $out_CV.out \
;;
RF)  java -cp /home/daria/tools/weka/weka-3-7-9/weka.jar
weka.classifiers.meta.CostSensitiveClassifier \
-cost-matrix "[0.0 $FN; $FP 0.0]" -W weka.classifiers.trees.RandomForest \
-t $training -x 10 > $out_CV.out \
;;
SMO) java -cp /home/daria/tools/weka/weka-3-7-9/weka.jar
```

```
weka.classifiers.meta.CostSensitiveClassifier \
-cost-matrix "[0.0 $FN; $FP 0.0]" -W weka.classifiers.functions.SMO \
-t $training -x 10 > $out_CV.out \
;;
*)   echo "Invalid method"
break
;;
esac
conf_matrix=$(tail -3 $out.out | cut -d "|" -f 1 | tr -s " ");
tp=$(echo $conf_matrix | cut -d " " -f 1)
fn=$(echo $conf_matrix | cut -d " " -f 2)
fp=$(echo $conf_matrix | cut -d " " -f 3)
tn=$(echo $conf_matrix | cut -d " " -f 4)
 sens=$(echo "scale=4; $tp/($tp+$fn)" | bc)
spec=$(echo "scale=4; $tn/($tn+$fp)" | bc)
tot_n=$[$tn+$fp]
tot_p=$[$tp+$fn]
tot=$[$tot_n+$tot_p]
 acc=$(echo "scale=4; ($tp+$tn)/$tot" | bc)
 if [ $[$tp+$fp] -eq 0 ] || [ $[$tn+$fn] -eq 0 ]; then
prec="NaN"
gmean="NaN"
fmeas="NaN"
mcc="NaN"
else
 prec=$(echo "scale=4; $tp/($tp+$fp)" | bc)
 gmean=$(echo "scale=4; sqrt($sens*$spec)" | bc)
fmeas=$(echo "scale=4; 2*($prec*$sens)/($prec+$sens)" | bc)
mcc=$(echo "scale=4; ($tp*$tn-$fp*$fn)/sqrt(($tp+$fp)*($tp+$fn)*($tn+$fp)*($tn+$fn))" |
bc)
fi
echo "$method $FN $FP $tn $fn $tp $fp $tot_n $tot_p $tot $spec $sens $acc $prec $gmean
$fmeas $mcc" >> $summary
 FP=$(echo "scale=2; $FP+0.1" | bc)
counter_FP=$[$counter_FP + 1];
 mv $out.out $folder;
done
FN=$[$FN + 1];
counter_FN=$[$counter_FN+1];
done
done
```

3 A python script to divide the MACCS fingerprints into bite strings: ConvertMACCSInterger2Binary.py

'''
Created on Jul 29, 2010
Simple script to convert MACCS key fingerprints output from MOE into binary vector.
* This program is free software; you can redistribute it and/or modify it under the terms of the GNU Lesser General Public License as published by the Free Software Foundation; either version 2.1 of the License, or (at your option) any later version. All we ask is that proper credit is given for our work, which includes - but is not limited to - adding the above copyright notice to the beginning of your source code files, and to any copyright notice that you may distribute with programs based on this work.
*
* This program is distributed in the hope that it will be useful, but WITHOUT ANY WARRANTY; without even the implied warranty of MERCHANTABILITY or FITNESS FOR A PARTICULAR PURPOSE. See the GNU Lesser General Public License for more details.
@author: ed
'''

```
import os, sys
class ConvertIntegerFPToBinary():
def __init__(self,descriptorFile,outputFile,label):
self.iFile = descriptorFile
self.oFile = outputFile
self.binaryFingerprints = []
self.integerList = []
self.label = label
def populateList(self,maxBitSize):
for i in range(1,maxBitSize+1):
self.integerList.append(str(i))
def convertData(self,maximumBitSize):
self.populateList(maximumBitSize)
inputFile = open(self.iFile,'r')
data = inputFile.readlines()
for i in range(1,len(data)):
splitdata = str(data[i]).replace("\"", "").split()
binaryFingerprint = []
for j in range(len(self.integerList)):
if self.integerList[j] in splitdata:
binaryFingerprint.append(1)
else:
binaryFingerprint.append(0)
binaryFingerprint.append(self.label)
self.binaryFingerprints.append(binaryFingerprint)
return self.binaryFingerprints
def postProcessing(self,fp):
binaryFingerprint = str(fp).replace("[", "").replace("]",
"").replace("'", "")
 return binaryFingerprint
```

```
def writeToFile(self):
outputFile = open(self.oFile,'w')
for i in range(len(self.binaryFingerprints)):
processedFingerprint =
self.postProcessing(str(self.binaryFingerprints[i]))
if i == len(self.binaryFingerprints)-1:
outputFile.write(processedFingerprint)
else:
outputFile.write(processedFingerprint+"\n")
if __name__ == '__main__':
converter = ConvertIntegerFPToBinary(sys.argv[1],sys.argv[2],sys.argv[3])
binaryFingerprints = converter.convertData(166)
converter.writeToFile()
```

4 Parameters obtained for the model 3: NB-6D.txt

=== Run information ===
Scheme: weka.classifiers.meta.FilteredClassifier -F
"weka.filters.unsupervised.attribute.Remove -R 1" -W
weka.classifiers.meta.CostSensitiveClassifier -- -cost-matrix "[0.0 5.0; 3.0 0.0]" -S 1 -W
weka.classifiers.bayes.NaiveBayes --
Relation: 77derivatives-125descriptors-weka.filters.AllFilter-weka.filters.MultiFilter-
Fweka.filters.AllFilter-weka.filters.supervised.attribute.AttributeSelection-
Eweka.attributeSelection.CfsSubsetEval-Sweka.attributeSelection.BestFirst -D 1 -N 5
Instances: 77
Attributes: 8
Working Name
density
lip_don
opr_brigid
PEOE_RPC+
PEOE_VSA+3
SMR
label
Test mode: 10-fold cross-validation
=== Classifier model (full training set) ===
FilteredClassifier using weka.classifiers.meta.CostSensitiveClassifier -cost-matrix "[0.0 5.0;
3.0 0.0]" -S 1 -W weka.classifiers.bayes.NaiveBayes -- on data filtered through
weka.filters.unsupervised.attribute.Remove -R 1

Filtered Header
@relation '77derivatives-125descriptors-weka.filters.AllFilter-weka.filters.MultiFilter-
Fweka.filters.AllFilter-weka.filters.supervised.attribute.AttributeSelection-
Eweka.attributeSelection.CfsSubsetEval-Sweka.attributeSelection.BestFirst -D 1 -N 5-
weka.filters.unsupervised.attribute.Remove-R1'
@attribute density numeric
@attribute lip_don numeric
@attribute opr_brigid numeric
@attribute PEOE_RPC+ numeric
@attribute PEOE_VSA+3 numeric
@attribute SMR numeric
@attribute label {active,inactive}
@data

Classifier Model
CostSensitiveClassifier using reweighted training instances
weka.classifiers.bayes.NaiveBayes

Classifier Model
Naive Bayes Classifier
Class
Attribute active inactive
(0.33) (0.67)

```
================================
density
  mean           0.7122   0.7227
  std. dev.      0.057    0.0348
  weight sum     24.6981  52.3019
  precision      0.0056   0.0056

lip_don
  mean              0     0.45
  std. dev.      0.1667   0.6171
  weight sum     24.6981  52.3019
  precision         1        1

opr_brigid
  mean          15.3412  17.8667
  std. dev.      2.1992   3.4212
  weight sum     24.6981  52.3019
  precision       1.6      1.6

PEOE_RPC+
  mean           0.1455    0.135
  std. dev.      0.0061   0.0172
  weight sum     24.6981  52.3019
  precision      0.0012   0.0012

PEOE_VSA+3
  mean          17.7738  22.2173
  std. dev.      1.4812   7.6963
  weight sum     24.6981  52.3019
  precision      8.8869   8.8869

SMR
  mean           8.8802   9.3651
  std. dev.      0.5826   1.1883
  weight sum     24.6981  52.3019
  precision      0.0894   0.0894

Cost Matrix
 0 5
 3 0
Time taken to build model: 0 seconds

=== Predictions on test data ===
 inst#     actual  predicted error prediction (Working Name)
    1 2:inactive 2:inactive       1 (31)
    2 2:inactive 2:inactive       0.9 (75)
    3 2:inactive 2:inactive       0.744 (48)
    4 2:inactive 2:inactive       1 (6)
    5 2:inactive 2:inactive       1 (26)
    6 2:inactive 2:inactive       1 (13)
    7   1:active   1:active       0.91 (51)
```

8 1:active 1:active 0.914 (**34**)
1 2:inactive 2:inactive 0.751 (**17**)
2 2:inactive 2:inactive 1 (**32**)
3 2:inactive 1:active + 0.952 (**18**)
4 2:inactive 2:inactive 1 (**11**)
5 2:inactive 1:active + 0.693 (**68**)
6 2:inactive 1:active + 0.931 (**74**)
7 1:active 1:active 0.984 (**23**)
8 1:active 1:active 0.9 (**53**)
1 2:inactive 2:inactive 1 (**7**)
2 2:inactive 2:inactive 1 (**58**)
3 2:inactive 2:inactive 1 (**24**)[7]
4 2:inactive 1:active + 0.993 (**77**)
5 2:inactive 2:inactive 0.803 (**70**)
6 2:inactive 2:inactive 1 (**5**)
7 1:active 1:active 0.817 (Piperine)
8 1:active 2:inactive + 1 (**43**)
1 2:inactive 1:active + 0.928 (**57**)
2 2:inactive 2:inactive 0.835 (**20**)
3 2:inactive 2:inactive 1 (**1**)
4 2:inactive 2:inactive 1 (**41**)
5 2:inactive 2:inactive 0.925 (**29**)
6 2:inactive 2:inactive 1 (**9**)
7 1:active 1:active 0.795 (**28**)
8 1:active 1:active 0.518 (**25**)
1 2:inactive 2:inactive 1 (**40**)
2 2:inactive 1:active + 0.935 (**76**)
3 2:inactive 2:inactive 1 (**59**)
4 2:inactive 1:active + 0.952 (**30**)
5 2:inactive 2:inactive 1 (**4**)
6 2:inactive 2:inactive 1 (**39**)
7 1:active 1:active 0.926 (**73**)
8 1:active 1:active 0.943 (**72**)
1 2:inactive 2:inactive 1 (**37**)
2 2:inactive 2:inactive 1 (**16**)
3 2:inactive 2:inactive 1 (**2**)
4 2:inactive 1:active + 0.862 (**66**)
5 2:inactive 2:inactive 1 (**63**)
6 2:inactive 1:active + 0.862 (**69**)
7 1:active 1:active 0.663 (**24**)[7]
8 1:active 1:active 0.93 (**33**)
1 2:inactive 2:inactive 1 (**64**)
2 2:inactive 2:inactive 1 (**8**)
3 2:inactive 2:inactive 1 (**44**)
4 2:inactive 2:inactive 1 (**3**)
5 2:inactive 2:inactive 0.774 (**65**)
6 2:inactive 2:inactive 0.765 (**54**)
7 1:active 1:active 0.846 (**21**)
8 1:active 1:active 0.891 (**47**)
1 2:inactive 1:active + 0.936 (**55**)
2 2:inactive 2:inactive 1 (**14**)

```
    3 2:inactive 2:inactive      1 (42)
    4 2:inactive 2:inactive      1 (61)
    5 2:inactive 2:inactive      0.746 (56)
    6 2:inactive 2:inactive      0.674 (52)
    7   1:active   1:active      0.923 (35)
    1 2:inactive 2:inactive      1 (27)
    2 2:inactive 2:inactive      1 (12)
    3 2:inactive   1:active   +  0.938 (49)
    4 2:inactive 2:inactive      0.722 (50)
    5 2:inactive 2:inactive      0.919 (71)
    6 2:inactive 2:inactive      1 (60)
    7   1:active   1:active      0.97 (22)
    1 2:inactive 2:inactive      0.874 (67)
    2 2:inactive 2:inactive      1 (36)
    3 2:inactive 2:inactive      1 (62)
    4 2:inactive 2:inactive      0.982 (45)
    5 2:inactive 2:inactive      1 (15)
    6 2:inactive 2:inactive      0.54 (46)
    7   1:active   1:active      0.913 (38)

=== Stratified cross-validation ===
=== Summary ===
Correctly Classified Instances          65               84.4156 %
Incorrectly Classified Instances        12               15.5844 %
Kappa statistic                          0.6259
Mean absolute error                      0.2102
Root mean squared error                  0.3853
Relative absolute error                 60.285  %
Root relative squared error             92.756  %
Coverage of cases (0.95 level)          94.8052 %
Mean rel. region size (0.95 level)      73.3766 %
Total Number of Instances               77

=== Detailed Accuracy By Class ===
               TP Rate  FP Rate  Precision  Recall   F-Measure  MCC      ROC Area  PRC Area  Class
               0,941    0,183    0,593      0,941    0,727      0,659    0,833     0,505     active
               0,817    0,059    0,980      0,817    0,891      0,659    0,830     0,932     inactive
Weighted Avg.  0,844    0,086    0,894      0,844    0,855      0,659    0,831     0,838

=== Confusion Matrix ===
  a  b   <-- classified as
 16  1 |  a = active
 11 49 |  b = inactive
```

5 Full composition of 10 trees in model 4: 10trees_RF_6D.txt

=== Run information ===

Scheme: weka.classifiers.meta.FilteredClassifier -F "weka.filters.unsupervised.attribute.Remove -R 1" -W weka.classifiers.meta.CostSensitiveClassifier -- -cost-matrix "[0.0 9.0; 5.0 0.0]" -S 1 -W weka.classifiers.trees.RandomForest -- -I 10 -K 0 -S 1 -num-slots 1
Relation: 77derivatives-125descriptors-weka.filters.AllFilter-weka.filters.MultiFilter-Fweka.filters.AllFilter-weka.filters.supervised.attribute.AttributeSelection-Eweka.attributeSelection.CfsSubsetEval-Sweka.attributeSelection.BestFirst -D 1 -N 5
Instances: 77
Attributes: 8
Working Name
density
lip_don
opr_brigid
PEOE_RPC+
PEOE_VSA+3
SMR
label
Test mode: 10-fold cross-validation

=== Classifier model (full training set) ===

FilteredClassifier using weka.classifiers.meta.CostSensitiveClassifier -cost-matrix "[0.0 9.0; 5.0 0.0]" -S 1 -W weka.classifiers.trees.RandomForest -- -I 10 -K 0 -S 1 -num-slots 1 on data filtered through weka.filters.unsupervised.attribute.Remove -R 1

Filtered Header
@relation '77derivatives-125descriptors-weka.filters.AllFilter-weka.filters.MultiFilter-Fweka.filters.AllFilter-weka.filters.supervised.attribute.AttributeSelection-Eweka.attributeSelection.CfsSubsetEval-Sweka.attributeSelection.BestFirst -D 1 -N 5-weka.filters.unsupervised.attribute.Remove-R1'

@attribute density numeric
@attribute lip_don numeric
@attribute opr_brigid numeric
@attribute PEOE_RPC+ numeric
@attribute PEOE_VSA+3 numeric
@attribute SMR numeric
@attribute label [active,inactive]

@data

Classifier Model
CostSensitiveClassifier using reweighted training instances

weka.classifiers.trees.RandomForest -I 10 -K 0 -S 1 -num-slots 1

Classifier Model
Random forest of 10 trees, each constructed while considering 3 random features.
Out of bag error: 0.2185

All the base classifiers:

RandomTree
==========

```
density < 0.72
|  PEOE_RPC+ < 0.13 : inactive (10/0)
|  PEOE_RPC+ >= 0.13
|  |  density < 0.7
|  |  |  PEOE_RPC+ < 0.13 : active (4/0)
|  |  |  PEOE_RPC+ >= 0.13
|  |  |  |  PEOE_RPC+ < 0.15
|  |  |  |  |  opr_brigid < 13.5 : active (3/0)
|  |  |  |  |  opr_brigid >= 13.5
|  |  |  |  |  |  PEOE_RPC+ < 0.15
|  |  |  |  |  |  |  opr_brigid < 15.5 : inactive (1/0)
|  |  |  |  |  |  |  opr_brigid >= 15.5
|  |  |  |  |  |  |  |  PEOE_RPC+ < 0.14 : inactive (3/0)
|  |  |  |  |  |  |  |  PEOE_RPC+ >= 0.14
|  |  |  |  |  |  |  |  |  PEOE_RPC+ < 0.14 : active (1/0)
|  |  |  |  |  |  |  |  |  PEOE_RPC+ >= 0.14 : inactive (3/0)
|  |  |  |  |  |  PEOE_RPC+ >= 0.15 : active (1/0)
|  |  |  |  PEOE_RPC+ >= 0.15 : inactive (4/0)
|  |  density >= 0.7
|  |  |  opr_brigid < 16.5
|  |  |  |  opr_brigid < 13.5 : active (2/0)
|  |  |  |  opr_brigid >= 13.5
|  |  |  |  |  PEOE_RPC+ < 0.15 : active (1/0)
|  |  |  |  |  PEOE_RPC+ >= 0.15 : inactive (1/0)
|  |  |  opr_brigid >= 16.5 : active (17/0)
density >= 0.72 : inactive (26/0)
```

Size of the tree : 27

RandomTree
==========

```
lip_don < 0.5
|  density < 0.72
|  |  SMR < 10.04
|  |  |  PEOE_RPC+ < 0.15
|  |  |  |  SMR < 9.51 : active (17/0)
|  |  |  |  SMR >= 9.51
```

```
|  |  |  |  density < 0.69 : active (3/0)
|  |  |  |  density >= 0.69
|  |  |  |  |  opr_brigid < 15.5
|  |  |  |  |  |  PEOE_RPC+ < 0.14 : active (1/0)
|  |  |  |  |  |  PEOE_RPC+ >= 0.14 : inactive (1/0)
|  |  |  |  |  opr_brigid >= 15.5 : inactive (1/0)
|  |  |  PEOE_RPC+ >= 0.15
|  |  |  |  SMR < 8.62 : active (4/0)
|  |  |  |  SMR >= 8.62 : inactive (3/0)
|  |  SMR >= 10.04 : inactive (7/0)
|  density >= 0.72
|  |  density < 0.88 : inactive (17/0)
|  |  density >= 0.88 : active (2/0)
lip_don >= 0.5 : inactive (21/0)

Size of the tree : 21


RandomTree
==========

density < 0.72
|  SMR < 9.85
|  |  PEOE_VSA+3 < 25.51
|  |  |  opr_brigid < 17
|  |  |  |  opr_brigid < 11.5 : inactive (1/0)
|  |  |  |  opr_brigid >= 11.5
|  |  |  |  |  opr_brigid < 13.5 : active (8/0)
|  |  |  |  |  opr_brigid >= 13.5
|  |  |  |  |  |  density < 0.7
|  |  |  |  |  |  |  SMR < 9.6
|  |  |  |  |  |  |  |  SMR < 9.51
|  |  |  |  |  |  |  |  |  SMR < 9.45
|  |  |  |  |  |  |  |  |  |  PEOE_RPC+ < 0.15 : inactive (1/0)
|  |  |  |  |  |  |  |  |  |  PEOE_RPC+ >= 0.15 : active (3/0)
|  |  |  |  |  |  |  |  |  SMR >= 9.45
|  |  |  |  |  |  |  |  |  |  PEOE_RPC+ < 0.14 : inactive (1/0)
|  |  |  |  |  |  |  |  |  |  PEOE_RPC+ >= 0.14 : active (2/0)
|  |  |  |  |  |  |  |  SMR >= 9.51
|  |  |  |  |  |  |  |  |  PEOE_RPC+ < 0.14 : active (2/0)
|  |  |  |  |  |  |  |  |  PEOE_RPC+ >= 0.14 : inactive (2/0)
|  |  |  |  |  |  |  SMR >= 9.6 : inactive (1/0)
|  |  |  |  |  |  density >= 0.7 : active (1/0)
|  |  |  opr_brigid >= 17 : active (11/0)
|  |  PEOE_VSA+3 >= 25.51 : inactive (2/0)
|  SMR >= 9.85 : inactive (12/0)
density >= 0.72 : inactive (30/0)

Size of the tree : 27
```

RandomTree
==========

density < 0.72
| SMR < 9.51
| | lip_don < 0.5
| | | SMR < 9.24 : active (15/0)
| | | SMR >= 9.24
| | | | PEOE_RPC+ < 0.14 : inactive (1/0)
| | | | PEOE_RPC+ >= 0.14
| | | | | PEOE_RPC+ < 0.15
| | | | | | PEOE_RPC+ < 0.14 : active (2/0)
| | | | | | PEOE_RPC+ >= 0.14
| | | | | | | PEOE_RPC+ < 0.15 : inactive (1/0)
| | | | | | | PEOE_RPC+ >= 0.15 : active (2/0)
| | | | | PEOE_RPC+ >= 0.15 : inactive (1/0)
| | lip_don >= 0.5 : inactive (5/0)
| SMR >= 9.51
| | density < 0.68 : active (3/0)
| | density >= 0.68 : inactive (17/0)
density >= 0.72 : inactive (30/0)

Size of the tree : 19

RandomTree
==========

density < 0.72
| PEOE_RPC+ < 0.14
| | opr_brigid < 14
| | | lip_don < 0.5 : active (2/0)
| | | lip_don >= 0.5 : inactive (2/0)
| | opr_brigid >= 14 : inactive (13/0)
| PEOE_RPC+ >= 0.14
| | density < 0.7
| | | density < 0.68 : inactive (1/0)
| | | density >= 0.68
| | | | density < 0.69 : active (6/0)
| | | | density >= 0.69
| | | | | opr_brigid < 15.5
| | | | | | PEOE_RPC+ < 0.14 : active (1/0)
| | | | | | PEOE_RPC+ >= 0.14 : inactive (1/0)
| | | | | opr_brigid >= 15.5
| | | | | | PEOE_RPC+ < 0.14 : inactive (1/0)
| | | | | | PEOE_RPC+ >= 0.14
| | | | | | | PEOE_RPC+ < 0.14 : active (4/0)
| | | | | | | PEOE_RPC+ >= 0.14
| | | | | | | | PEOE_RPC+ < 0.15 : inactive (1/0)
| | | | | | | | PEOE_RPC+ >= 0.15
| | | | | | | | | PEOE_RPC+ < 0.15 : active (1/0)

```
|  |  |  |  |  |  |  |  PEOE_RPC+ >= 0.15 : inactive (1/0)
|  |  density >= 0.7 : active (15/0)
density >= 0.72 : inactive (28/0)

Size of the tree : 27


RandomTree
==========

PEOE_RPC+ < 0.13 : inactive (21/0)
PEOE_RPC+ >= 0.13
|  density < 0.72
|  |  SMR < 8.07
|  |  |  density < 0.7 : inactive (3/0)
|  |  |  density >= 0.7
|  |  |  |  density < 0.71 : active (1/0)
|  |  |  |  density >= 0.71 : inactive (1/0)
|  |  SMR >= 8.07
|  |  |  opr_brigid < 17
|  |  |  |  opr_brigid < 13.5 : active (9/0)
|  |  |  |  opr_brigid >= 13.5
|  |  |  |  |  PEOE_RPC+ < 0.14 : inactive (3/0)
|  |  |  |  |  PEOE_RPC+ >= 0.14
|  |  |  |  |  |  density < 0.7
|  |  |  |  |  |  |  PEOE_RPC+ < 0.14 : active (1/0)
|  |  |  |  |  |  |  PEOE_RPC+ >= 0.14 : inactive (2/0)
|  |  |  |  |  |  density >= 0.7
|  |  |  |  |  |  |  SMR < 9.45
|  |  |  |  |  |  |  |  PEOE_RPC+ < 0.15 : active (1/0)
|  |  |  |  |  |  |  |  PEOE_RPC+ >= 0.15
|  |  |  |  |  |  |  |  |  opr_brigid < 15.5 : active (1/0)
|  |  |  |  |  |  |  |  |  opr_brigid >= 15.5 : inactive (1/0)
|  |  |  |  |  |  |  SMR >= 9.45 : active (3/0)
|  |  |  opr_brigid >= 17 : active (10/0)
|  density >= 0.72
|  |  density < 0.88 : inactive (19/0)
|  |  density >= 0.88 : active (1/0)

Size of the tree : 29


RandomTree
==========

PEOE_RPC+ < 0.13 : inactive (29/0)
PEOE_RPC+ >= 0.13
|  density < 0.72
|  |  PEOE_RPC+ < 0.15
|  |  |  SMR < 8.3 : inactive (3/0)
|  |  |  SMR >= 8.3
```

```
|  |  |  |  opr_brigid < 13.5 : active (6/0)
|  |  |  |  opr_brigid >= 13.5
|  |  |  |  |  SMR < 9.51 : active (7/0)
|  |  |  |  |  SMR >= 9.51 : inactive (7/0)
|  |  PEOE_RPC+ >= 0.15 : active (5/0)
|  density >= 0.72
|  |  density < 0.88 : inactive (18/0)
|  |  density >= 0.88 : active (2/0)

Size of the tree : 15


RandomTree
==========

PEOE_RPC+ < 0.13 : inactive (25/0)
PEOE_RPC+ >= 0.13
|  density < 0.72
|  |  SMR < 10.04
|  |  |  density < 0.69 : active (7/0)
|  |  |  density >= 0.69
|  |  |  |  opr_brigid < 17
|  |  |  |  |  SMR < 9.6
|  |  |  |  |  |  density < 0.71
|  |  |  |  |  |  |  PEOE_RPC+ < 0.14 : active (8/0)
|  |  |  |  |  |  |  PEOE_RPC+ >= 0.14
|  |  |  |  |  |  |  |  PEOE_RPC+ < 0.15 : inactive (3/0)
|  |  |  |  |  |  |  |  PEOE_RPC+ >= 0.15
|  |  |  |  |  |  |  |  |  density < 0.7
|  |  |  |  |  |  |  |  |  |  PEOE_RPC+ < 0.15 : active (3/0)
|  |  |  |  |  |  |  |  |  |  PEOE_RPC+ >= 0.15 : inactive (1/0)
|  |  |  |  |  |  |  |  |  density >= 0.7 : active (1/0)
|  |  |  |  |  |  density >= 0.71
|  |  |  |  |  |  |  PEOE_RPC+ < 0.15 : active (1/0)
|  |  |  |  |  |  |  PEOE_RPC+ >= 0.15 : inactive (2/0)
|  |  |  |  |  SMR >= 9.6 : inactive (2/0)
|  |  |  |  opr_brigid >= 17 : active (9/0)
|  |  SMR >= 10.04 : inactive (3/0)
|  density >= 0.72 : inactive (12/0)

Size of the tree : 25


RandomTree
==========

PEOE_VSA+3 < 25.51
|  opr_brigid < 20
|  |  density < 0.69 : inactive (5/0)
|  |  density >= 0.69
|  |  |  SMR < 9.6
```

```
|  |  |  |  PEOE_RPC+ < 0.13 : inactive (3/0)
|  |  |  |  PEOE_RPC+ >= 0.13
|  |  |  |  |  density < 0.74
|  |  |  |  |  |  opr_brigid < 11.5 : inactive (2/0)
|  |  |  |  |  |  opr_brigid >= 11.5
|  |  |  |  |  |  |  SMR < 9.24 : active (23/0)
|  |  |  |  |  |  |  SMR >= 9.24
|  |  |  |  |  |  |  |  PEOE_RPC+ < 0.15
|  |  |  |  |  |  |  |  |  SMR < 9.51 : active (7/0)
|  |  |  |  |  |  |  |  |  SMR >= 9.51
|  |  |  |  |  |  |  |  |  |  PEOE_RPC+ < 0.14 : active (1/0)
|  |  |  |  |  |  |  |  |  |  PEOE_RPC+ >= 0.14 : inactive (1/0)
|  |  |  |  |  |  |  |  PEOE_RPC+ >= 0.15 : inactive (1/0)
|  |  |  |  |  density >= 0.74
|  |  |  |  |  |  density < 0.88 : inactive (4/0)
|  |  |  |  |  |  density >= 0.88 : active (2/0)
|  |  |  SMR >= 9.6 : inactive (3/0)
|  opr_brigid >= 20 : inactive (7/0)
PEOE_VSA+3 >= 25.51 : inactive (18/0)

Size of the tree : 25


RandomTree
==========

density < 0.71
|  SMR < 9.6
|  |  PEOE_RPC+ < 0.14 : active (11/0)
|  |  PEOE_RPC+ >= 0.14
|  |  |  SMR < 9.11
|  |  |  |  density < 0.68 : inactive (1/0)
|  |  |  |  density >= 0.68
|  |  |  |  |  density < 0.71 : active (5/0)
|  |  |  |  |  density >= 0.71
|  |  |  |  |  |  SMR < 8.62 : active (6/0)
|  |  |  |  |  |  SMR >= 8.62
|  |  |  |  |  |  |  PEOE_RPC+ < 0.15 : active (1/0)
|  |  |  |  |  |  |  PEOE_RPC+ >= 0.15 : inactive (1/0)
|  |  |  SMR >= 9.11
|  |  |  |  PEOE_RPC+ < 0.15 : inactive (4/0)
|  |  |  |  PEOE_RPC+ >= 0.15
|  |  |  |  |  PEOE_RPC+ < 0.15 : active (1/0)
|  |  |  |  |  PEOE_RPC+ >= 0.15 : inactive (1/0)
|  SMR >= 9.6 : inactive (11/0)
density >= 0.71 : inactive (35/0)

Size of the tree : 21

Out of bag error: 0.2185
```

Cost Matrix
 0 9
 5 0

Time taken to build model: 0.02 seconds

=== Predictions on test data ===

 inst# actual predicted error prediction (Working Name)
    1 2:inactive 2:inactive   0.9 (**31**)
    2 2:inactive 2:inactive   0.9 (**75**)
    3 2:inactive 2:inactive   0.7 (**48**)
    4 2:inactive 2:inactive   1 (**6**)
    5 2:inactive 2:inactive   0.6 (**26**)
    6 2:inactive 2:inactive   0.7 (**13**)
    7   1:active   1:active   0.9 (**51**)
    8   1:active   1:active   1 (**34**)
    1 2:inactive 2:inactive   0.8 (**17**)
    2 2:inactive 2:inactive   1 (**32**)
    3 2:inactive   1:active   +   0.7 (**18**)
    4 2:inactive 2:inactive   0.6 (**11**)
    5 2:inactive 2:inactive   1 (**68**)
    6 2:inactive 2:inactive   0.7 (**74**)
    7   1:active   1:active   0.8 (**23**)
    8   1:active 2:inactive   +   0.8 (**53**)
    1 2:inactive 2:inactive   1 (**7**)
    2 2:inactive 2:inactive   1 (**58**)
    3 2:inactive 2:inactive   1 (**10**)
    4 2:inactive   1:active   +   1 (**77**)
    5 2:inactive 2:inactive   1 (**70**)
    6 2:inactive 2:inactive   1 (**5**)
    7   1:active 2:inactive   +   1 (Piperine)
    8   1:active 2:inactive   +   0.9 (**43**)
    1 2:inactive   1:active   +   0.9 (**57**)
    2 2:inactive 2:inactive   0.7 (**20**)
    3 2:inactive 2:inactive   1 (**1**)
    4 2:inactive 2:inactive   1 (**41**)
    5 2:inactive 2:inactive   1 (**29**)
    6 2:inactive 2:inactive   1 (**9**)
    7   1:active   1:active   1 (**28**)
    8   1:active   1:active   0.6 (**25**)
    1 2:inactive 2:inactive   1 (**40**)
    2 2:inactive   1:active   +   0.9 (**76**)
    3 2:inactive 2:inactive   0.9 (**59**)
    4 2:inactive   1:active   +   0.5 (**30**)
    5 2:inactive 2:inactive   1 (**4**)
    6 2:inactive   1:active   +   0.5 (**39**)
    7   1:active 2:inactive   +   0.9 (**73**)
    8   1:active   1:active   0.9 (**72**)
    1 2:inactive 2:inactive   1 (**37**)

2 2:inactive 2:inactive 1 (**16**)
3 2:inactive 2:inactive 1 (**2**)
4 2:inactive 2:inactive 0.6 (**66**)
5 2:inactive 2:inactive 1 (**63**)
6 2:inactive 2:inactive 0.6 (**69**)
7 1:active 1:active 0.6 (**24**)[7]
8 1:active 1:active 0.8 (**33**)
1 2:inactive 2:inactive 1 (**64**)
2 2:inactive 2:inactive 1 (**8**)
3 2:inactive 2:inactive 0.9 (**44**)
4 2:inactive 2:inactive 1 (**3**)
5 2:inactive 2:inactive 1 (**65**)
6 2:inactive 2:inactive 1 (**54**)
7 1:active 1:active 0.5 (**21**)
8 1:active 1:active 1 (**47**)
1 2:inactive 1:active + 1 (**55**)
2 2:inactive 2:inactive 0.8 (**14**)
3 2:inactive 2:inactive 1 (**42**)
4 2:inactive 2:inactive 0.7 (**61**)
5 2:inactive 2:inactive 0.7 (**56**)
6 2:inactive 2:inactive 0.7 (**52**)
7 1:active 1:active 1 (**35**)
1 2:inactive 2:inactive 1 (**27**)
2 2:inactive 2:inactive 1 (**12**)
3 2:inactive 1:active + 1 (**49**)
4 2:inactive 2:inactive 1 (**50**)
5 2:inactive 2:inactive 1 (**71**)
6 2:inactive 2:inactive 1 (**60**)
7 1:active 1:active 0.8 (**22**)
1 2:inactive 2:inactive 1 (**67**)
2 2:inactive 2:inactive 1 (**36**)
3 2:inactive 2:inactive 1 (**62**)
4 2:inactive 2:inactive 0.6 (**45**)
5 2:inactive 2:inactive 0.9 (**15**)
6 2:inactive 2:inactive 1 (**46**)
7 1:active 1:active 0.9 (**38**)

=== Stratified cross-validation ===
=== Summary ===

Correctly Classified Instances	65	84.4156 %
Incorrectly Classified Instances	12	15.5844 %
Kappa statistic	0.5823	
Mean absolute error	0.2247	
Root mean squared error	0.3805	
Relative absolute error	64.4284 %	
Root relative squared error	91.6023 %	
Coverage of cases (0.95 level)	94.8052 %	
Mean rel. region size (0.95 level)	73.3766 %	
Total Number of Instances	77	

=== Detailed Accuracy By Class ===

	TP Rate	FP Rate	Precision	Recall	F-Measure	MCC	ROC Area	PRC Area	Class
	0,765	0,133	0,619	0,765	0,684	0,588	0,838	0,550	active
	0,867	0,235	0,929	0,867	0,897	0,588	0,838	0,938	inactive
Weighted Avg.	0,844	0,213	0,860	0,844	0,850	0,588	0,838	0,852	

=== Confusion Matrix ===

a	b	<-- classified as
13	4	a = active
8	52	b = inactive

6 SM Table 1A

143 2D descriptors calculated in MOE (A) and 125 descriptors which underwent feature selection (B).

(A)143 2D descriptors calculated in MOE				
apol	b_rotN	mr	PEOE_VSA_FPOL	SMR_VSA3
a_acc	b_rotR	nmol	PEOE_VSA_FPOS	SMR_VSA4
a_acid	b_single	opr_brigid	PEOE_VSA_FPPOS	SMR_VSA5
a_aro	b_triple	opr_leadlike	PEOE_VSA_HYD	SMR_VSA6
a_base	chi0	opr_nring	PEOE_VSA_NEG	SMR_VSA7
a_count	chi0v	opr_nrot	PEOE_VSA_PNEG	TPSA
a_don	chi0v_C	opr_violation	PEOE_VSA_POL	VAdjEq
a_heavy	chi0_C	PC+	PEOE_VSA_POS	VAdjMa
a_hyd	chi1	PC-	PEOE_VSA_PPOS	VDistEq
a_IC	chi1v	PEOE_PC+	petitjean	VDistMa
a_ICM	chi1v_C	PEOE_PC-	petitjeanSC	vdw_area
a_nB	chi1_C	PEOE_RPC+	radius	vdw_vol
a_nBr	chiral	PEOE_RPC-	rings	vsa_acc
a_nC	chiral_u	PEOE_VSA+0	RPC+	vsa_acid
a_nCl	density	PEOE_VSA+1	RPC-	vsa_base
a_nF	diameter	PEOE_VSA+2	SlogP	vsa_don
a_nH	FCharge	PEOE_VSA+3	SlogP_VSA0	vsa_hyd
a_nI	Kier1	PEOE_VSA+4	SlogP_VSA1	vsa_other
a_nN	Kier2	PEOE_VSA+5	SlogP_VSA2	vsa_pol
a_nO	Kier3	PEOE_VSA+6	SlogP_VSA3	Weight
a_nP	KierA1	PEOE_VSA-0	SlogP_VSA4	weinerPath
a_nS	KierA2	PEOE_VSA-1	SlogP_VSA5	weinerPol
balabanJ	KierA3	PEOE_VSA-2	SlogP_VSA6	zagreb
bpol	KierFlex	PEOE_VSA-3	SlogP_VSA7	
b_1rotN	lip_acc	PEOE_VSA-4	SlogP_VSA8	
b_1rotR	lip_don	PEOE_VSA-5	SlogP_VSA9	
b_ar	lip_druglike	PEOE_VSA-6	SMR	
b_count	lip_violation	PEOE_VSA_FHYD	SMR_VSA0	
b_double	logP(o/w)	PEOE_VSA_FNEG	SMR_VSA1	
b_heavy	logS	PEOE_VSA_FPNEG	SMR_VSA2	

7 SM Table 1B

143 2D descriptors calculated in MOE (A) and 125 descriptors which underwent feature selection (B).

(B) 125 descriptors which underwent feature selection				
apol	b_rotN	logS	PEOE_VSA_FPNEG	SMR
a_acc	b_rotR	mr	PEOE_VSA_FPOL	SMR_VSA0
a_aro	b_single	opr_brigid	PEOE_VSA_FPOS	SMR_VSA1
a_base	chi0	opr_nring	PEOE_VSA_FPPOS	SMR_VSA2
a_count	chi0v	opr_nrot	PEOE_VSA_HYD	SMR_VSA3
a_don	chi0v_C	PEOE_PC+	PEOE_VSA_NEG	SMR_VSA4
a_heavy	chi0_C	PEOE_PC-	PEOE_VSA_PNEG	SMR_VSA5
a_hyd	chi1	PEOE_RPC+	PEOE_VSA_POL	SMR_VSA6
a_IC	chi1v	PEOE_RPC-	PEOE_VSA_POS	SMR_VSA7
a_ICM	chi1v_C	PEOE_VSA+0	PEOE_VSA_PPOS	TPSA
a_nC	chi1_C	PEOE_VSA+1	petitjean	VAdjEq
a_nCl	chiral	PEOE_VSA+2	petitjeanSC	VAdjMa
a_nF	density	PEOE_VSA+3	radius	VDistEq
a_nH	diameter	PEOE_VSA+4	rings	VDistMa
a_nN	FCharge	PEOE_VSA+5	SlogP	vdw_area
a_nO	Kier1	PEOE_VSA+6	SlogP_VSA0	vdw_vol
a_nS	Kier2	PEOE_VSA-0	SlogP_VSA1	vsa_acc
balabanJ	Kier3	PEOE_VSA-1	SlogP_VSA2	vsa_don
bpol	KierA1	PEOE_VSA-2	SlogP_VSA3	vsa_hyd
b_1rotN	KierA2	PEOE_VSA-3	SlogP_VSA4	vsa_other
b_1rotR	KierA3	PEOE_VSA-4	SlogP_VSA5	vsa_pol
b_ar	KierFlex	PEOE_VSA-5	SlogP_VSA6	Weight
b_count	lip_acc	PEOE_VSA-6	SlogP_VSA7	weinerPath
b_double	lip_don	PEOE_VSA_FHYD	SlogP_VSA8	weinerPol
b_heavy	logP(o/w)	PEOE_VSA_FNEG	SlogP_VSA9	zagreb

8 SM Table 2

Summary of MRM transitions of both 23 and 25 including corresponding internal standard (22, 24) are summarized.

MRM transitions	Precursor Ion	Fragmentor	Product Ion	Collision Energy
25	330.2	130	201	18
	330.2	130	115	54
22	302.2	115	201	14
23	302.2	115	201	14
	302.2	115	115	50
24	330.2	140	201	18

9 References

(1) Ribeiro, T. S.; Freire-de-Lima, L.; Previato, J. O.; Mendonca-Previato, L.; Heise, N.; de Lima, M. E. Toxic Effects of Natural Piperine and Its Derivatives on Epimastigotes and Amastigotes of Trypanosoma Cruzi. *Bioorg. Med. Chem. Lett.* **2004**, *14*, 3555-3558.
(2) Mu, L. H.; Wang, B.; Ren, H. Y.; Liu, P.; Guo, D. H.; Wang, F. M.; Bai, L.; Guo, Y. S. Synthesis and Inhibitory Effect of Piperine Derivates on Monoamine Oxidase. *Bioorg. Med. Chem. Lett.* **2012**, *22*, 3343-3348.
(3) Saito, Y.; Ouchi, H.; Takahata, H. Carboxamidation of Carboxylic Acids with 1-Tert-Butoxy-2-Tert-Butoxycarbonyl-1,2-Dihydroisoquinoline (Bbdi) without Bases. *Tetrahedron* **2008**, *64*, 11129-11135.
(4) Paula, V. F. d.; Barbosa, L. C. d. A.; Demuner, A. J.; Piló-Veloso, D.; Picanço, M. C. Synthesis and Insecticidal Activity of New Amide Derivatives of Piperine. *Pest Manage. Sci.* **2000**, *56*, 168-174.
(5) Correa, E. A.; Hogestatt, E. D.; Sterner, O.; Echeverri, F.; Zygmunt, P. M. In Vitro TRPV1 Activity of Piperine Derived Amides. *Bioorg. Med. Chem.* **2010**, *18*, 3299-3306.
(6) Suzuki, H.; Manabe, H.; Inouye, M. Sodium Telluride-Mediated Carbon-Carbon Bond-Forming Reactions. *Nippon Kagaku Kaishi* **1987**, *7*, 1485-1489.
(7) Khom, S.; Strommer, B.; Schöffmann, A.; Hintersteiner, J.; Baburin, I.; Erker, T.; Schwarz, T.; Schwarzer, C.; Zaugg, J.; Hamburger, M.; Hering, S. GABAA Receptor Modulation by Piperine and a Non-TRPV1 Activating Derivative. *Biochem. Pharmacol.* **2013**, *85*, 1827-1836.

7.2 Supporting Information: Identification of Dihydrostilbenes in *Pholidota chinensis* as New Scaffold for $GABA_A$ Receptor Modulators

Supporting Information

Identification of dihydrostilbenes in *Pholidota chinensis* as a new scaffold for $GABA_A$ receptor modulators

Diana C. Rueda[a], Angela Schöffmann[b], Maria De Mieri[a], Melanie Raith[a], Evelyn Jähne[a], Steffen Hering[b], and Matthias Hamburger[a,*]

[a] *Division of Pharmaceutical Biology, University of Basel, Klingelbergstrasse 50, CH-4056 Basel, Switzerland*
[b] *Institute of Pharmacology and Toxicology, University of Vienna, Althanstrasse 14, A-1090 Vienna, Austria*

* Corresponding author. Tel.: +41-61-2671425; fax: +41-61-2671474.
E-mail: matthias.hamburger@unibas.ch

Fig. S1. Diazepam (1 µM) enhanced IGABA through $\alpha_1\beta_2\gamma_{2S}$ $GABA_A$ receptors and was therefore used as positive control for the assay. Currents in the presence of GABA ($EC_{5\text{-}10}$, single bar, control) and during co-application of GABA and diazepam (1 µM, double bar) are shown. At 1 µM diazepam enhanced I_{GABA} up to 231.3 ± 22.6% (n=3).

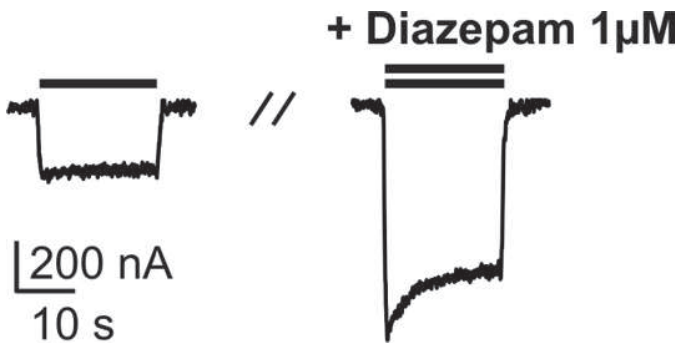

Fig. S2. Analytical HPLC chromatogram of a dichloromethane extract of *P. chinensis*. **A**. UV trace (210-700 nm). **B**. ELSD trace (45°C, N_2 2.8 L/min). Compounds **1**-**3** appear as the major constituents of the extract. Separation was performed with MeOH (solvent A) and water (solvent B), using a gradient from 50% A to 80% A in 40 min, followed by 80% A to 100% A in 5 min. The flow rate was 0.4 mL/min, and 50 μg of extract (in 10 μL of DMSO) were injected.

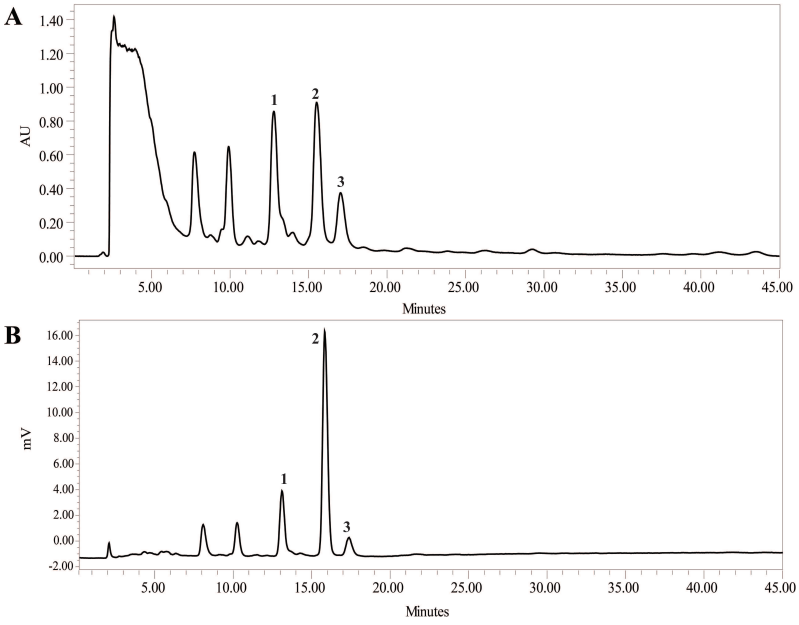

Fig. S3. ^{1}H NMR spectrum of compound **24**

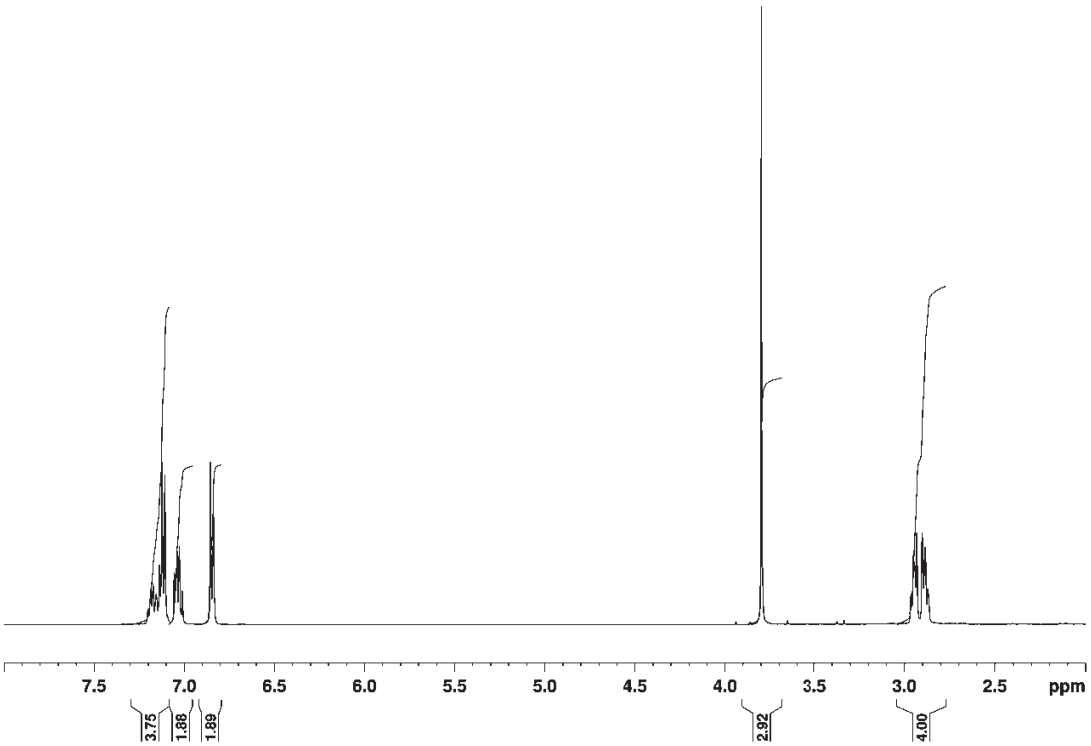

Table S1: NMR spectroscopic data (500.13 MHz, methanol-d_3) for coelonin (**1**)

Molecular formula: $C_{15}H_{14}O_3$; Formula weight: 242.26986; CAS Nr. 82344-82-9

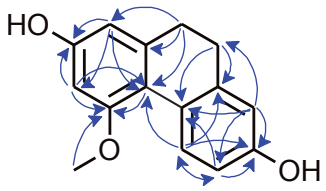

Position	δ_C[a]	δ_H (I, m, *J* in Hz)
1	104.8	6.26 (CH, d, *2.5*)
2	155.4	-
3	100.1	6.30 (CH, d, *2.5*)
4	158.3	-
4a	114.8	-
4b	125.2	-
5	128.6	8.13 (CH, d, *8.4*)
6	112.2	6.62 (CH, dd, *8.3*, *2.7*)
7	154.8	-
8	113.8	6.61 (CH, d, *2.6*)
8a	139.8	-
9	30.1	2.59 (CH_2, s)
10	30.8	2.59 (CH_2, s)
10a	138.7	-
4-OCH_3	54.2	3.67 (CH_3, s)

[a] chemical shifts derived from multiplicity-edited HSQC and HMBC spectra. Blue arrows in structural formula indicate observed HMBC correlations.

Table S2: NMR spectroscopic data (500.13 MHz, methanol-d_3) for batatasin III (**2**)

Molecular formula: $C_{15}H_{16}O_3$; Formula weight: 244.28574; CAS Nr. 56684-87-8

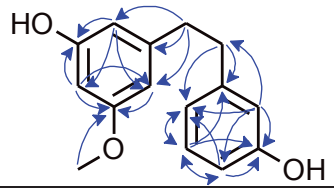

Position	δ_C[a]	δ_H (I, m, *J* in Hz)
1	144.9	-
2	108.1	6.29 (CH, br s)
3	157.6	-
4	98.7	6.23 (CH, m)
5	160.9	-
6	105.5	6.23 (CH, m)
1′	143.3	-
2′	115.3	6.64 (CH, m)
3′	156.7	-
4′	112.4	6.64 (CH, m)
5′	129.0	7.03 (CH, dd, *7.9*, *7.5*)
6′	119.8	6.64 (CH, m)
α	37.0	2.75 (CH_2, m)
β	37.6	2.75 (CH_2, m)
5-OCH_3	54.3	3.63 (CH_3, s)

[a] chemical shifts derived from multiplicity-edited HSQC and HMBC spectra. Blue arrows in structural formula indicate observed HMBC correlations.

Table S3: NMR spectroscopic data (500.13 MHz, methanol-d_3) for pholidotol D (**3**)

Molecular formula: $C_{15}H_{14}O_3$; Formula weight: 242.26986; CAS Nr. 1006380-82-0

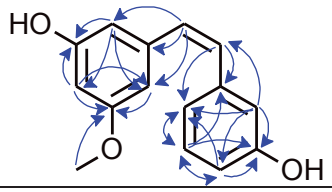

Position	δ_C[a]	δ_H (I, m, *J* in Hz)
1	139.7	-
2	105.8	6.58 (CH, m)
3	157.7	-
4	100.3	6.31 (CH, t, *2.0*)
5	160.8	-
6	103.4	6.58 (CH, m)
1′	138.5	-
2′	112.4	7.00-6.65 (CH, m)
3′	156.0	-
4′	114.4	7.00-6.65 (CH, m)
5′	129.4	7.17 (CH, dd, *7.9*, *7.8*)
6′	117.8	6.69 (CH, dd, *8.2*, *2.2*)
α	128.4	7.00-6.65 (CH, m)
β	128.6	7.00-6.65 (CH, m)
5-OCH_3	54.4	3.76 (CH_3, s)

[a] chemical shifts derived from multiplicity-edited HSQC and HMBC spectra. Blue arrows in structural formula indicate observed HMBC correlations.

7.3 Supporting Information: Identification of Dehydroabietc Acid from *Boswellia thurifera* Resin as a Positive $GABA_A$ Receptor Modulator

Supporting Information

Identification of dehydroabietc acid from *Boswellia thurifera* resin as a positive $GABA_A$ receptor modulator

Diana C. Rueda[a], Melanie Raith[a], Maria De Mieri[a], Angela Schöffmann[b], Steffen Hering[b], and Matthias Hamburger[a,*]

[a] *Division of Pharmaceutical Biology, University of Basel, Klingelbergstrasse 50, CH-4056 Basel, Switzerland*

[b] *Institute of Pharmacology and Toxicology, University of Vienna, Althanstrasse 14, A-1090 Vienna, Austria*

* Corresponding author. Tel.: +41-61-2671425; fax: +41-61-2671474.

E-mail: matthias.hamburger@unibas.ch

S1. Diazepam (1 μM) enhanced I_{GABA} through $\alpha_1\beta_2\gamma_{2S}$ $GABA_A$ receptors and was therefore used as positive control for the assay. Currents in the presence of GABA ($EC_{5\text{-}10}$, single bar, control) and during co-application of GABA and diazepam (1 μM, double bar) are shown. At 1 μM diazepam enhanced I_{GABA} up to 231.3 ± 22.6% (n=3).

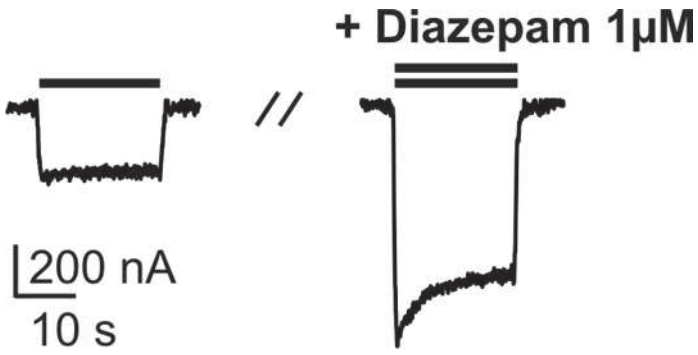

S2. Compounds isolated from *B. thurifera* resin, petroleum ether extract.

	Trivial name	CAS Nr.	MF	Formula weight	Structure
1	Dehydroabietic acid	1740-19-8	$C_{20}H_{28}O_2$	300.44	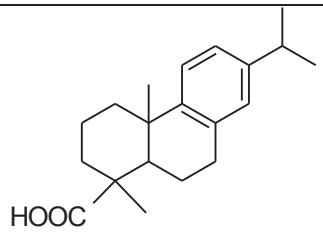
2	Incensole	22419-74-5	$C_{20}H_{34}O_2$	306.48	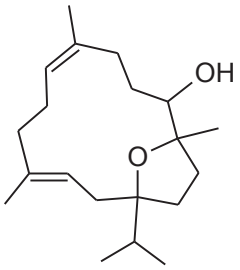
3	AKBA	67416-61-9	$C_{32}H_{48}O_5$	512.72	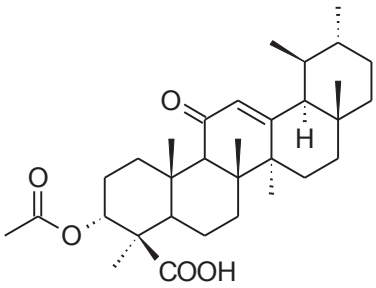

S3. ^{1}H-NMR spectrum (500 MHz in dmso-d_6) of DHA (**1**)

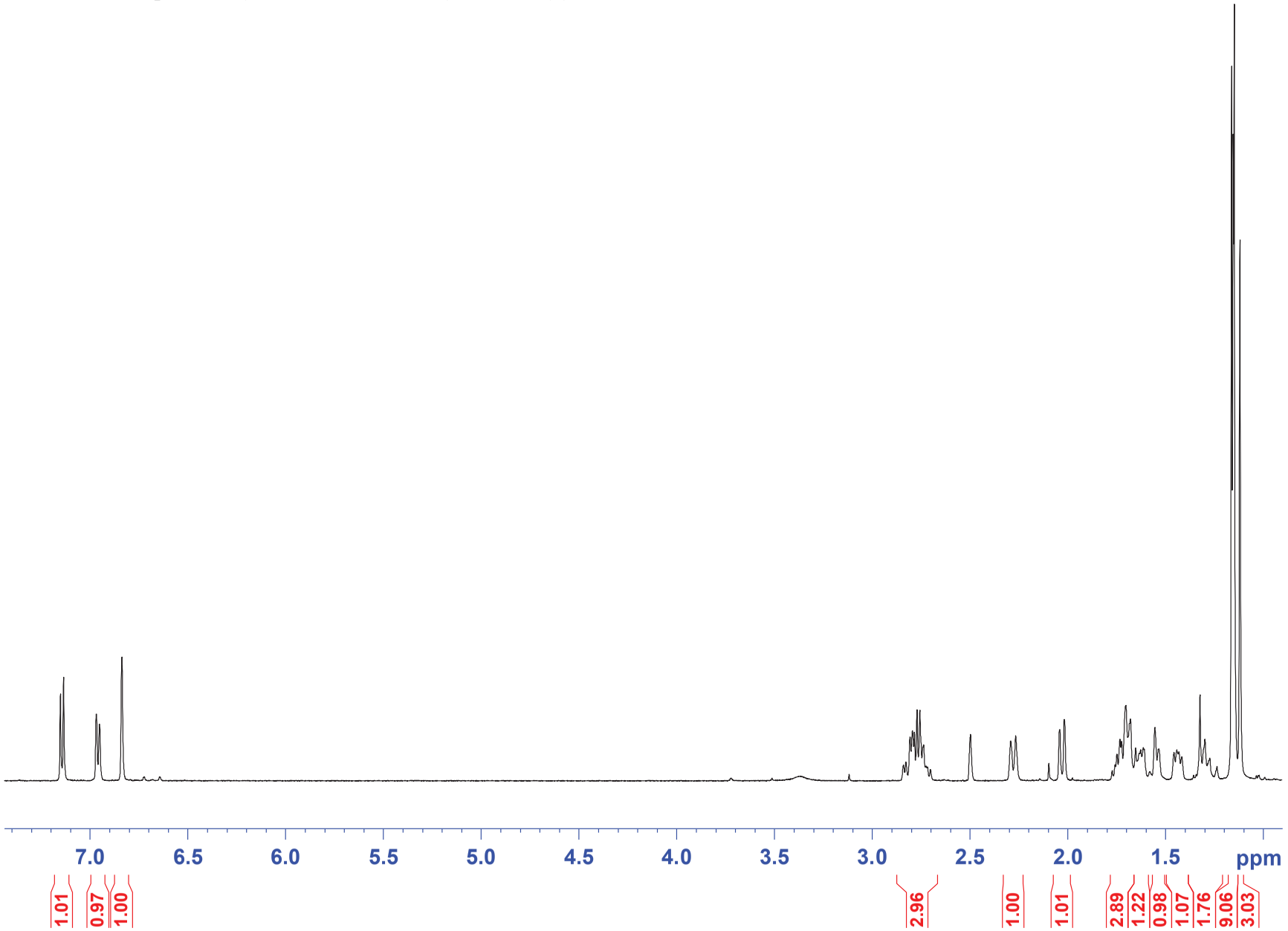

S4. ^{1}H-NMR spectrum (500 MHz in dmso-d_6) of incensole (**2**)

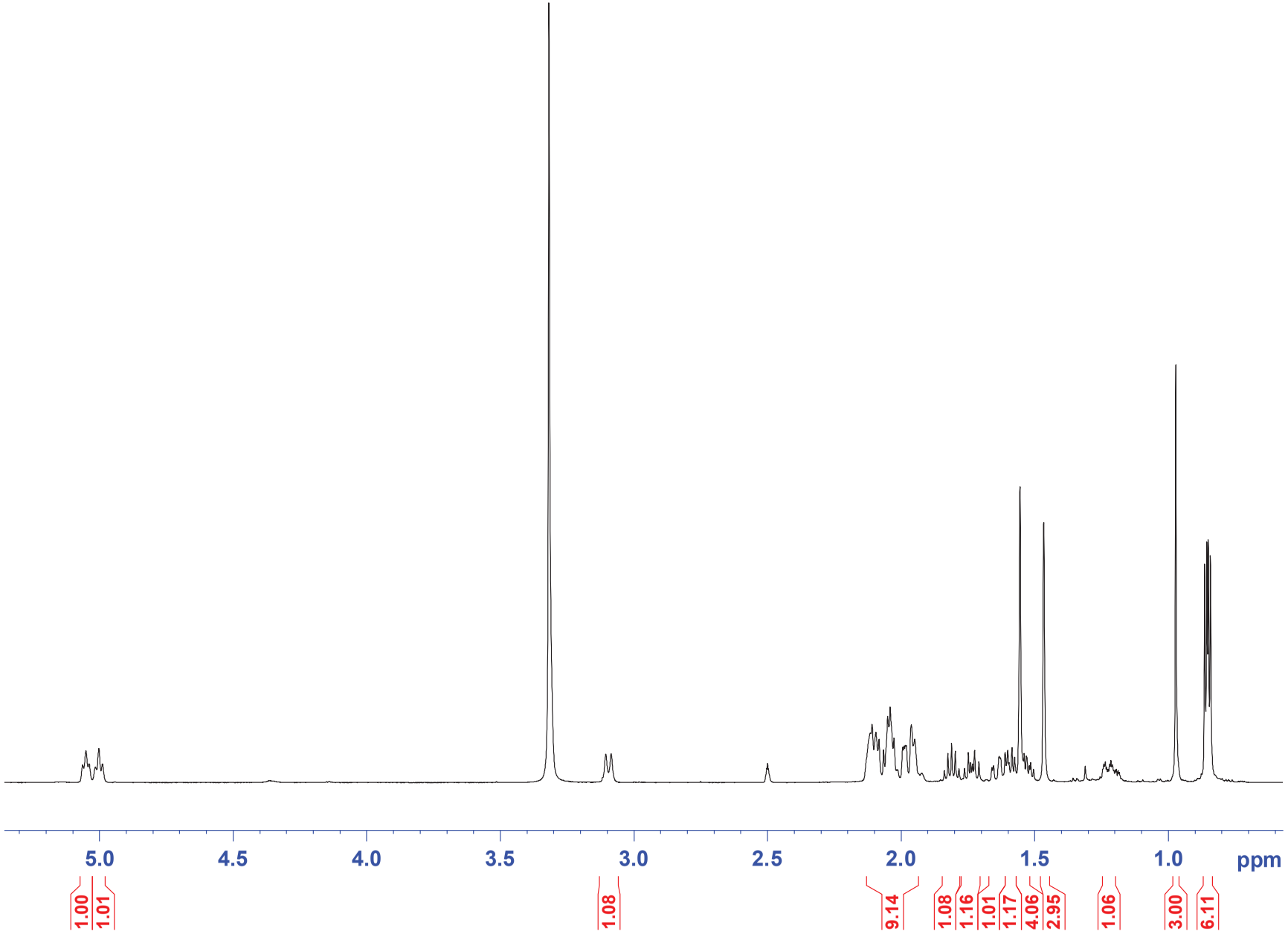

S5. ^{1}H-NMR spectrum (500 MHz in methanol-d_4) of AKBA (**3**)

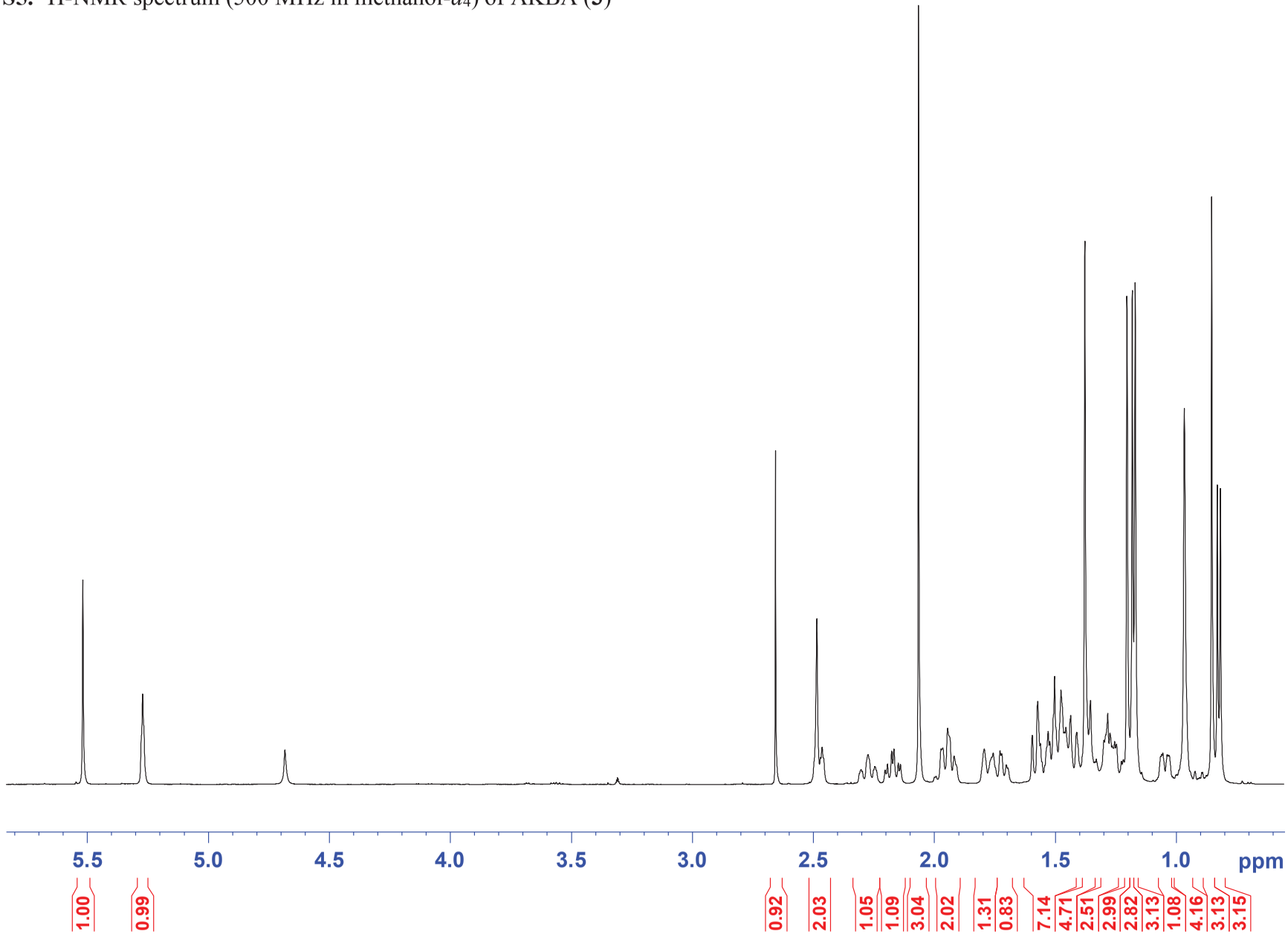

7.4 Supporting Information: Nitrogenated Honokiol Derivatives Allosterically Modulate $GABA_A$ Receptors and Act as Strong Partial Agonists

SUPPLEMENTAL MATERIAL TO:

Nitrogenated honokiol derivatives allosterically modulate GABAA receptors and act as strong partial agonists

Marketa Bernaskova,[†a] Angela Schoeffmann,[‡] Wolfgang Schuehly,[†b,§] Antje Huefner,[†a] Igor Baburin,[‡] Steffen Hering[‡*]

[†]Institute of Pharmaceutical Sciences, [a]Pharmaceutical Chemistry, University of Graz, Schubertstrasse 1, and [b] Department of Pharmacognosy, University of Graz, Universitätsplatz 4, 8010 Graz, Austria;

[§] Institute of Zoology, University of Graz, Universitätsplatz 2, 8010 Graz, Austria

[‡]Department of Pharmacology and Toxicology, University of Vienna, Althanstrasse 14, 1090 Vienna, Austria

***** Author to whom correspondence should be addressed;
Phone: +43-1-4277-55310;
Fax: +43-1-4277-9553;
E-mail: steffen.hering@univie.ac.at

^{1}H-NMR spectra ($CDCl_3$, 400 MHz) of the new compounds 1a, 1, 2a and 2

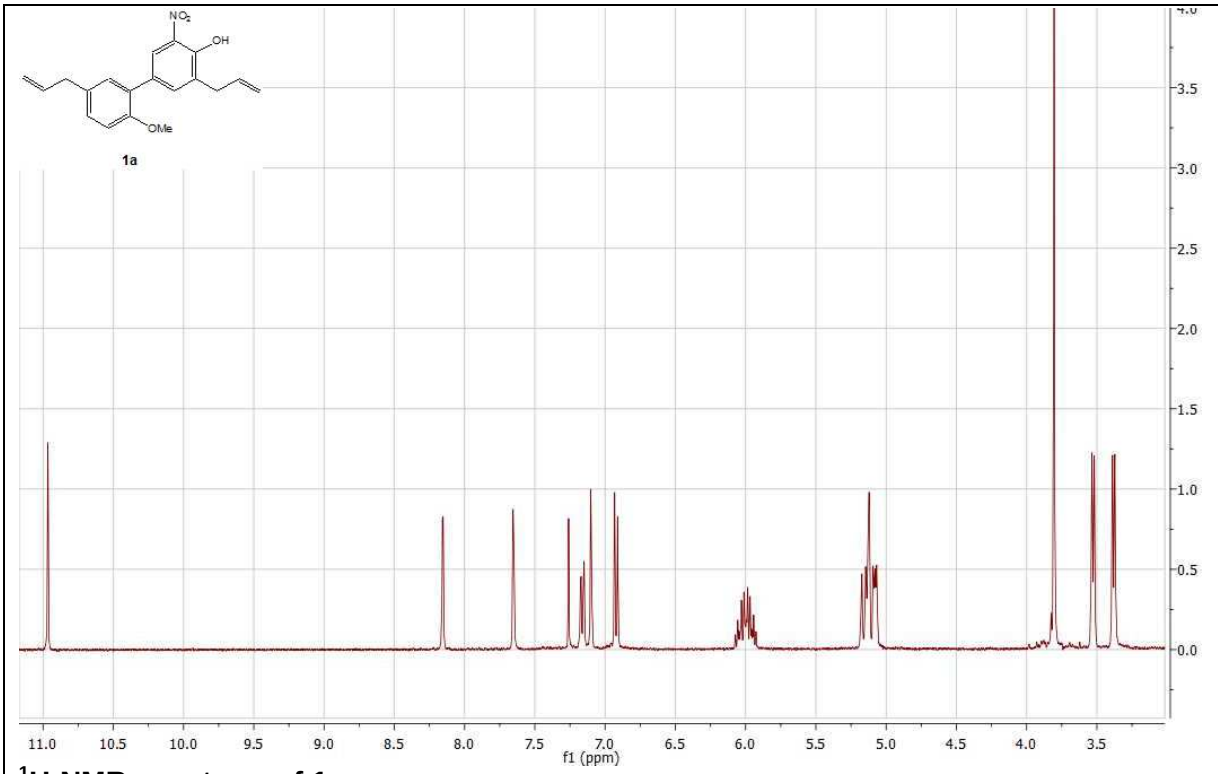

^{1}H-NMR spectrum of 1a

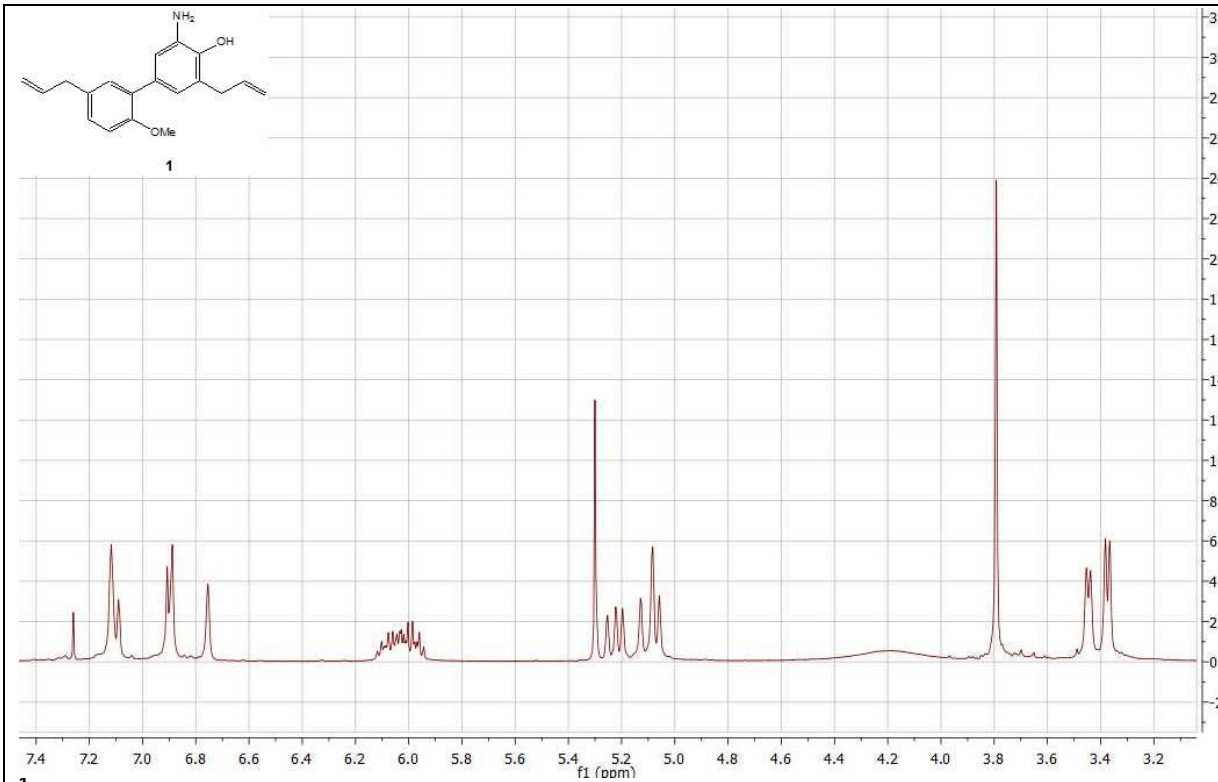

^{1}H-NMR spectrum of 1

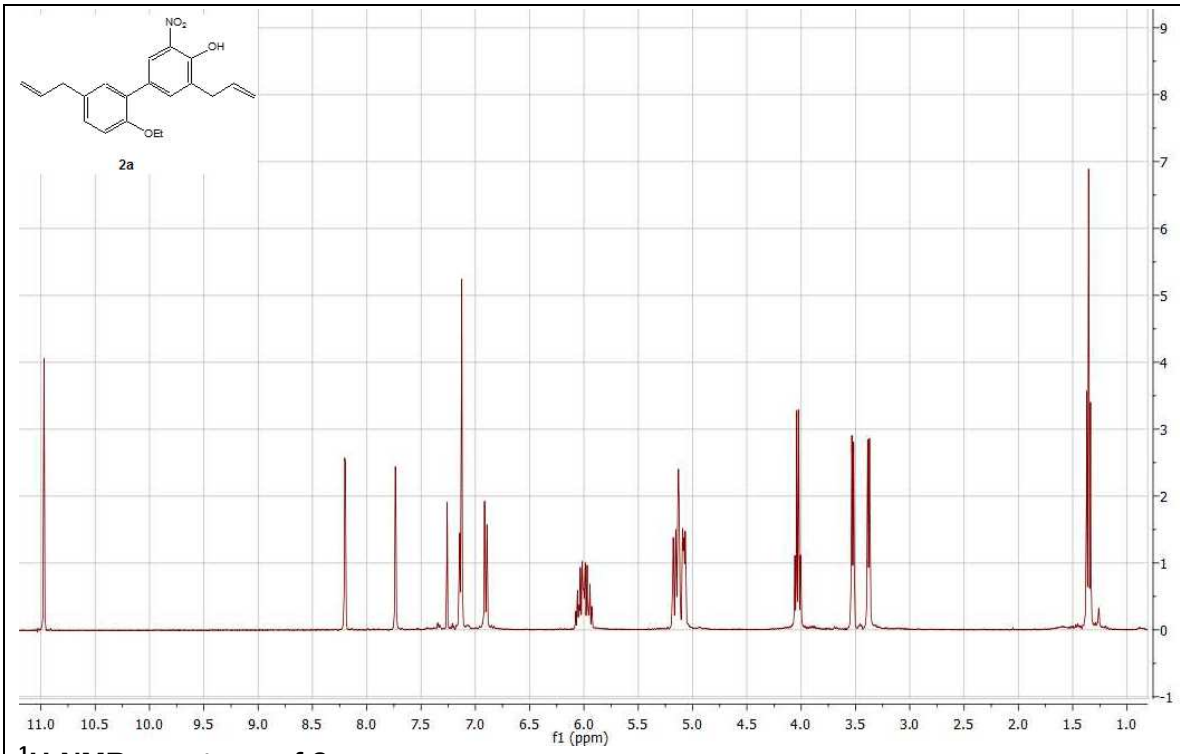

^{1}H-NMR spectrum of 2a

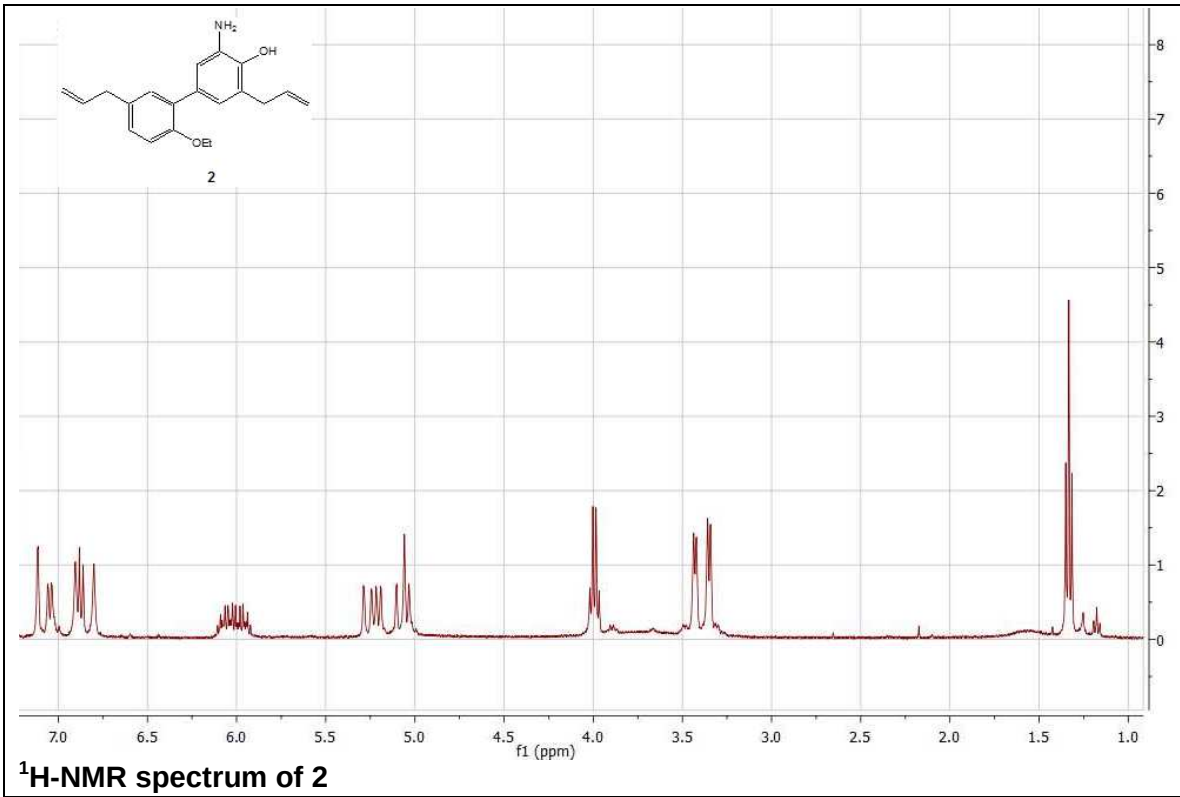

^{1}H-NMR spectrum of 2

8 Curriculum Vitae

Personal Details

Name, Surname	**Angela Johanna Schöffmann**
Date of Birth	January, 3rd 1985
Place of Birth	Klagenfurt
Citizenship	Austria
Proposed Title	Mag. pharm.

Formation

Jan. 2011 – Aug. 2013	Doctoral Studies in Pharmacy, Dept. of Pharmacology and Toxicology, University of Vienna
November 2011	Doctoral Program "Molecular Drug Targets" (FWF1232)
September 2010	Pharmacist's Diploma with Honours, Austrian Chamber of Pharmacists, Vienna
Oct. 2009 – Sept. 2010	Aspirant's Year, Pharmacy "Zur Hl. Brigitta", Vienna
September 2009	Diploma with Honours (Mag. pharm.)
March 2009 – July 2009	Diploma Thesis, Dept. of. Clinical Pharmacy and Diagnostics, University of Vienna, in cooperation with the Institute of Pathophysiology, Medical University of Vienna/Vienna General Hospital (AKH)
Oct. 2004 – Sept. 2009	Diploma Studies in Pharmacy, University of Vienna
June 2004	Matriculation with Honours, BG/BRG St. Martin/Villach

Publications and Congress Proceedings

- Bernaskova M, **Schöffmann A**, Schühly W, Hüfner A, Baburin I, Hering S. Nitrogenated Honokiol Derivatives Allosterically Modulate $GABA_A$ Receptors and Act as Strong Partial Agonists. (Accepted and resubmitted after revision; Medicinal Bioorganic Chemistry (04-Aug-**2015**)

- Wimmer L, Schönbauer D, Pakfeifer P, **Schöffmann A**, Khom S, Hering S, Mihovilovic MD. Developing Piperine towards TRPV1 and $GABA_A$ Receptor Ligands - Synthesis of Piperine Analogs via Heck-Coupling of Conjugated Dienes. Org Biomol Chem. **2015** Jan 28;13(4):990-4. doi: 10.1039/c4ob02242d. Epub 2014 Dec 1
- Rueda DC, Raith M, De Mieri M, **Schöffmann A**, Hering S, Hamburger M. Identification of dehydroabietc acid from Boswellia thurifera resin as a positive $GABA_A$ receptor modulator. Fitoterapia **2014**, 99, 28-34
- **Schöffmann A**, Wimmer L, Goldmann D, Khom S, Hintersteiner J, Baburin I, Schwarz T, Hintersteininger M, Pakfeifer P, Oufir M, Hamburger M, Erker T, Ecker GF, Mihovilovic MD, Hering S. Efficient Modulation of γ-Aminobutyric Acid Type A Receptors by Piperine Derivatives. J Med Chem. **2014** Jul 10;57(13):5602-19. doi: 10.1021/jm5002277. Epub 2014 Jun 27. PMID: 24905252
- Rueda DC, **Schöffmann A**, De Mieri M, Raith M, Jähne EA, Hering S, Hamburger M. Identification of dihydrostilbenes in Pholidota chinensis as a new scaffold for $GABA_A$ receptor modulators. Bioorg Med Chem. **2014**, 22(4):1276-1284. doi: 10.1016/j.bmc.2014.01.008
- Khom S, Strommer B, **Schöffmann A**, Hintersteiner J, Baburin I, Erker T, Schwarz T, Schwarzer C, Zaugg J, Hamburger M, Hering S. $GABA_A$ receptor modulation by piperine and a non-TRPV1 activating derivative. Biochem Pharmacol. **2013**, 85(12):1827-1836. doi: 10.1016/j.bcp.2013.04.017.
- Poster presentation, 9th YSA PhD Symposium; Vienna, June 19 – 20, **2013**
- Poster presentation, Joint Scientific Symposium of the Austrian Societies of Toxicology, Pharmacy, Analytic Chemistry, Forensic Medicine and the CCC; Vienna, March 21 – 22, **2013**
- Poster presentation, "Science Day 2013" organized by the students of the Doctoral Program "Molecular Drug Targets"; Vienna, February 22, **2013**
- Poster presentation and oral presentation, 2nd Annual Retreat of the Doctoral Program "Molecular Drug Targets"; Vienna, December 11 – 12, **2012**
- Poster presentation, 1st Annual Retreat of the Doctoral Program „Molecular Drug Targets"; Vienna, January 19 – 20, **2012**

Teaching and Work Experience

March 2013	Compulsory Practical Course „PR Allgemeine Pharmakologie", course leader
Oct. 2012	Compulsory Practical Course „PR Erste Hilfe f. Pharmazeuten", course assistant

March 2012	Compulsory Practical Course „PR Allgemeine Pharmakologie“, course assistant
Oct. 2011 – Nov. 2012	Supervision of two diploma theses
Oct.2011 – Feb.2012	Compulsory Practical Course „PR Pharmakologie, Pharmakotherapie und Toxikologie 1 und 2“, course leader
March 2011	Compulsory Practical Course „PR Allgemeine Pharmakologie“, course assistant
Sept. 2011 – Nov. 2012	Pharmacist, “St. Richard Apotheke”, Bisamberg
Oct. 2010 – Dec. 2010	Pharmacist, “St. Andreas Apotheke”, Wördern
Sept. 2007 – April 2009	Assistant, Pfizer Corp. Austria, Finance Department, Vienna
July – August 2007	Assistant, Pfizer Corp. Austria, Human Resources Department and Marketing Department, Vienna
July – August 2006	Trainee, Hospital Pharmacy LKH Villach, Villach
February 2005	Trainee, “Feschnig Apotheke”, Klagenfurt

Courses

- MEGRA StartUp: Regulatory Affairs Basics in Modules (2015, MEGRA, Vienna)
- Pharmig Academy: Pharmacovigilance Basics in Modules (2013/14, Pharmig, Vienna)
- Excellence in Pharmacovigilance, European Medicines Agency HQ London, 2012
- Academic Writing in English, Doctoral Centre University of Vienna, 2013
- Introduction to Patents and Inventions, University of Vienna/Patent Office Vienna, 2013
- Patent Searching, Doctoral Centre University of Vienna, 2013
- „In die universitäre Lehre starten - Basisqualifizierung für Einsteiger/innen, Personalwesen und Frauenförderung“, University of Vienna